Illinois U Library

# The American Mineralogist

## *Journal of the Mineralogical Society of America*

Vol. 39 NOVEMBER-DECEMBER, 1954 Nos. 11 and 12

## *Contents*

The system $Al_2O_3$-$SiO_2$-$H_2O$ ........ Rustum Roy and E. F. Osborn 853

Mechanism of "solution" of quartz in pure water at elevated temperatures and pressures ........ A. F. Frederickson and Joseph E. Cox, Jr. 886

Studies of uranium minerals (XV): Schroeckingerite from Argentina and Utah. ........ Cornelius S. Hurlbut, Jr. 901

Geocronite ........ Robert M. Douglass, Michael J. Murphy, and A. Pabst 908

Crystal chemistry of schallerite ........ Duncan McConnell 929

Studies in the mica group; single crystal data on phlogopites, biotites, and manganophyllites ........ A. A. Levinson and E. Wm. Heinrich 937

Multiplicity and disorder in the lattice of ekmanite ........ Bartholomew Nagy 946

An experimental study of the formation and properties of synthetic serpentines and related layer silicate minerals ........ Della M. Roy and Rustum Roy 957

A single crystal temperature controlled oven for an *x*-ray spectrometer ........ R. Lefker, A. deBretteville Jr., and J. S. Dodd 976

Zircons as provenance indicators ........ Michael Wyatt 983

The problem of bond type ........ W. S. Fyfe 991

A new synthetic hydrate of aluminum arsenate ........ Gerald Katz and Horst Kedesdy 1005

Notes and news: Studies of uranium minerals (XVI): An alteration product of ianthinite ........ Judith W. Frondel and Frank Cuttitta 1018

Analyses and indices of refraction of tourmaline from fault gouge near Barstow, San Bernardino County, California ........ Henry Kramer and Robert D. Allen 1020

Derived differential thermal curves ........ A. F. Frederickson 1023

The St. Peter sandstone-Glenwood shale contact ........ W. G. Ernst 1025

Book reviews ........ 1032

New mineral names ........ 1037

Index to volume 39; Title page; Table of contents ........ 1041

EDITOR: WALTER F. HUNT

ASSISTANT EDITOR: LEWIS S. RAMSDELL

BOARD OF ASSOCIATE EDITORS:

MICHAEL FLEISCHER GEORGE TUNELL (1954)

ELBURT F. OSBORN ADOLF PABST (1954–55)

IAN CAMPBELL BRIAN MASON (1954–56)

Published bi-monthly by the Society

# Mineralogical Society of America

ASSOCIATED WITH THE GEOLOGICAL SOCIETY OF AMERICA

*President:* **Sterling B. Hendricks**, U. S. Department of Agriculture, Beltsville, Maryland.
*Vice-President:* **Harry H. Hess**, Princeton University, Princeton, New Jersey.
*Secretary:* **C. S. Hurlbut, Jr.**, Harvard University, Cambridge, Massachusetts.
*Treasurer:* **Earl Ingerson**, U. S. Geological Survey, Washington 25, D. C.
*Editor:* **Walter F. Hunt**, University of Michigan, Ann Arbor, Michigan.
*Councillors:* **George T. Faust**, U. S. Geological Survey, Washington 25, D. C.
**Victor T. Allen**, Institute of Geophysical Technology, St. Louis, Missouri.
**C. Osborne Hutton**, Stanford University, Palo Alto, California.
**Felix Chayes**, Geophysical Laboratory, Washington, D. C.
**J. D. H. Donnay**, The Johns Hopkins University, Baltimore, Maryland.

The enlarged issues of this journal for 1954 are made possible by a grant from the Penrose Fund of the Geological Society of America.

## The American Mineralogist—Journal of the Mineralogical Society of America

A journal containing articles on mineralogy, crystallography, petrography, and allied sciences, is issued every two months. Contributions are invited from everyone.

Office of Publication, Mineralogical Laboratory, Ann Arbor, Mich.

The general conduct of the journal is in the hands of the editor, **Walter F. Hunt**, Ann Arbor, Michigan, to whom all manuscripts should be submitted. To assist the editor the council of the Mineralogical Society has appointed **Lewis S. Ramsdell**, Ann Arbor, Michigan, assistant editor, and the following board of associate editors:

**Ian Campbell**, California Institute of Technology, Pasadena 4, California.
**Michael Fleischer**, U. S. Geological Survey, Washington, D. C.
**Brian H. Mason**, American Museum of Natural History, New York, N. Y.
**Elburt F. Osborn**, Pennsylvania State College, State College, Pa.
**Adolf Pabst**, University of California, Berkeley 4, California.
**George Tunell**, University of California at Los Angeles, California.

It will expedite publication if two copies of each manuscript are submitted to the editor.

Contributors of leading articles are given without charge 100 reprints (without covers) of their article. If additional reprints are desired these can be purchased at the following rates:

| *Pages*<br>*Copies* | *1–4* | *5–8* | *9–12* | *13–16* | *17–20* | *21–24* | *25–28* | *29–32* | *Covers* |
|---|---|---|---|---|---|---|---|---|---|
| 25 | $3.50 | $5.00 | $ 8.00 | $ 9.50 | $11.00 | $13.00 | $15.00 | $16.00 | $4.90 |
| 50 | 3.80 | 5.55 | 8.80 | 10.40 | 12.10 | 14.20 | 16.40 | 17.50 | 5.50 |
| 75 | 4.10 | 6.10 | 9.60 | 11.30 | 13.20 | 15.40 | 17.80 | 19.00 | 6.10 |
| 100 | 4.40 | 6.65 | 10.40 | 12.20 | 14.30 | 16.60 | 19.20 | 20.50 | 6.70 |
| Addl. C's | 1.20 | 2.20 | 3.20 | 3.60 | 4.40 | 4.80 | 5.60 | 6.00 | 2.40 |

Cover Composition $1.55.

Sent to all members and fellows of the Mineralogical Society of America. Subscription price, $4.00 per year (single copies of normal issues, $1.00 plus postage).

Entered as second class matter at the post office at Menasha, Wis., under Act of March 3, 1879. Acceptance for mailing at the special rate of postage provided for in section 1103, Act of Oct. 3, 1917, paragraph 4 section 429 P. L. & R. authorized March 13, 1922.

Notice of change of address, orders, and remittances should be sent to Dr. Earl Ingerson, U. S. Geological Survey, Washington 25, D. C.

Printed by the George Banta Publishing Company, Menasha, Wisconsin
Printed in the United States of America

THE AMERICAN MINERALOGIST

JOURNAL OF THE MINERALOGICAL SOCIETY OF AMERICA

Vol. 39 NOVEMBER–DECEMBER, 1954 Nos. 11 and 12

# THE SYSTEM $Al_2O_3$-$SiO_2$-$H_2O$

Rustum Roy and E. F. Osborn, *College of Mineral Industries, The Pennsylvania State University, State College, Pennsylvania.*

## Abstract

A fundamental approach has been attempted in the study of the temperatures of formation and limits of stability of certain clay minerals and metamorphic rock assemblages. This has been done by studying the phase equilibrium relationships in the system $Al_2O_3$-$SiO_2$-$H_2O$ under conditions of independently controlled temperature and water-vapor pressure. The data from a large number of runs are presented in a series of compatibility triangles for various temperatures and pressures. The equilibrium decomposition temperature of the kaolinite minerals has been placed at 405° C. (at 10,000 psi water pressure) and that of pyrophyllite at 575° C. Two new clay-phases exist in the system and are described in detail, one a pure Al-Si montmorillonite and the other herein named hydralsite, one of the decomposition products of kaolinite. The application of the results to geological and ceramic problems is discussed.

## I. Introduction

Minerals appearing as phases in the system alumina-silica-water (Fig. 2) have been recognized by mineralogists and geologists as being important keys in attempts to decipher the history of rocks. Fenner's study (1913) of the silica minerals, describing the stable and metastable ranges of existence of the various forms of silica, and the investigation of the system $Al_2O_3$-$SiO_2$ by Bowen and Greig (1924), which indicated that mullite, rather than andalusite, sillimanite, or kyanite, is the stable aluminosilicate at high temperatures and atmospheric pressure, were significant milestones in studies contributing to our knowledge of the ternary system. More recently, hydrothermal studies, summarized to 1937 by Morey and Ingerson (1937*a*), have added further data. Among the many later papers may be mentioned especially those by Noll (1944), Ewell and Insley (1935), and Gillingham (1948).

Conditions of temperature, pressure, and composition at which the hydrous aluminosilicates can be synthesized have been of especial interest in previous studies. Data are numerous and conflicting. In Table 1 an attempt is made to summarize the most reliable of these data on stability ranges of ternary compounds. Kaolinite has been synthesized at temperatures as low as 250° C., and up to 400° C. and a montmorillonite probably of the composition near beidellite has been obtained within approximately the same range of temperature where alkali ions have been present. The stability range of kaolinite, particularly the upper temperature limit was not established. Similarly no previous data are at hand to indicate the temperature ranges of stability for pyrophillite and a pure alumina-silica montmorillonite if such a structure exists. The relationship between endellite and halloysite provides another problem, and a definite series of dehydration temperatures of endellite to halloysite with varying pressure should exist.

TABLE 1. SUMMARY OF PREVIOUS DATA ON THE STABILITY RANGE OF ALUMINA-SILICA HYDRATES

| Mineral | Workers | Minimum | | Maximum | | Time Days |
|---|---|---|---|---|---|---|
| | | Temp. °C. | Press. psi. | Temp. °C. | Press. psi. | |
| Kaolinite | Ewell and Insley (1935) | 250 | 600 | 310 | 1450 | 10 |
| | Noll (1944) | 250 | 600 | 400 | 4500 | |
| Dickite | Ewell and Insley (1935) | 345 | 2300 | 365 | 3000 | 10 |
| Nacrite | Permyakov (1936) | 335 | 4500 | | | 6 |
| Beidellite | Ewell and Insley (1935) | 350 | 2500 | 390 | 3900 | 10 |
| Montmorillonite | Noll (1944) | Same range as kaolinite | | | | |
| Pyrophyllite | Noll (1944) | 400 | 4500 | 500 | 8000 | |

The stability ranges of sillimanite and kyanite are unknown. Kyanite has not been synthesized, but possibly sillimanite has. Synthesis of sillimanite has been reported by Morey (1942), Balconi (1941), and Michel-Levy (1950), but in no case was unequivocal evidence presented that the "sillimanite" was not mullite. Andalusite has been reproducibly synthesized by our colleague, D. M. Roy (1953). The suggested range of stability at high water pressures is 450° to 650° C. or higher.

The present study is directed toward finding compatible phases under conditions of divariant equilibrium, and the phase equilibria are described by means of composition triangles, i.e., combinations of three phases which co-exist stably in a particular range of temperature and pressure. The results embody the data relating the starting material, temperature, pressure and time to the product as identified by optical and $x$-ray methods, for some 2,000 runs. The implications of the results in terms of natural mineral association are discussed.

## II. METHOD OF INVESTIGATION

### A. *Equipment*

The hydrothermal equipment used consists of pumps in parallel supplying water under pressure through a system of pressure lines and valves to separate vessels. Each pressure vessel, or bomb, is heated to the desired temperature in an automaticallly controlled furnace, and maintained at a particular pressure independent of that in other bombs in the system. The motor driven pumps with a ball and cone seat are rated for 40,000 psi., but after a few weeks operation with distilled water need constant attention to reach pressures above 20,000 psi. A high-pressure pump (Roy and Osborn, 1952) consisting of a stainless steel chamber in which water is compressed with a stainless steel jack, was constructed, and pressures up to 50,000 psi. can be reached in a few seconds. Much higher pressures are attainable, but are limited by the system of valves and tubing. No leaking occurred in this pump in over one year's continuous and varied operation supplying 20 separate vessels.

The pressure vessels used include the closed type of bomb described by Morey and Ingerson (1937*b*); a modification of this bomb, wherein the plug was drilled and then this connected to the pressure line; and a smaller modification of the "Morey-type" bomb which proved very convenient (Roy and Osborn, 1952*a*). The type of pressure vessel used most extensively was the "test-tube" bomb (see Roy, Roy and Osborn, 1950), a thick-walled test tube of stainless steel or another high-temperature alloy, usually 8 inches long, 1″ outer diameter, $\frac{1}{8}''$ inner diameter, closed at one end and the other attached to the pressure line. The sample is placed in the bottom and the bomb suspended vertically with a thermocouple well near the sample. The top of the bomb extends about two inches above the top of the furnace. For highest temperatures an apparatus similar to that described by Tuttle (1949) was used. In addition, for hastening reaction and decomposition, a "grinding" apparatus (Roy and Osborn, 1952) was used, consisting of rotating Morey type bombs containing several stainless steel rods. The sample is ground at high temperatures and pressures as the bomb rotates.

### B. *Starting Materials*

Standard methods are not available for the preparation of mixtures, and reactivity of alumina-silica mixtures is extremely slow. Mechanical mixtures of the reactive substances, $\gamma$-$Al_2O_3$ (very finely divided, $<.02\mu$ size) and dried silica gel were tried, but even these fine-grained, metastable starting materials were not satisfactory from the standpoint of completely reacting to yield equilibrium phases. More suitable starting materials were co-precipitated alumina-silica gels. The gels were first prepared according to the method described by Ewell and Insley (1935), which consisted of coprecipitating solutions of aluminum nitrate and sodium silicate, adjusting the *pH* to slightly basic with $NH_4OH$, and washing several times after filtering. The gels thus prepared contain sufficient $Na_2O$ to yield sodium-containing minerals such as analcime, and are not suitable for accurate work in the system $Al_2O_3$-$SiO_2$-$H_2O$. Further purification was carried out by electrodialysis in an apparatus similar to that described by Roy (1949), for two to three days in order to remove the alkali. The maximum $Na_2O$ content of the gels thus prepared was of the order of $\frac{1}{2}$ to $\frac{1}{4}$ of one per cent, or less. Mixtures were also prepared from ethylorthosilicate and aluminum nitrate by dissolving in absolute ethyl alcohol and evaporating and heating, thus avoiding $Na_2O$ altogether.

Natural minerals, purified by various methods including electrodialysis and in some cases synthetic minerals prepared in the present study were used as starting materials, particularly for the determination of decomposition temperatures.

### *C. Procedure*

The materials were contained in small platinum or gold envelopes, and in confirmatory runs these were surrounded by another envelope containing more of the same materials acting as a buffer. Temperatures were automatically regulated, and measured with chromel-alumel thermocouples made of calibrated wire, which rarely showed a variation of more than ±1° C. when checked with standards. The bombs were brought up to temperature as rapidly as possible with the pressure turned on. An over-all precision of ±3° C. was attainable under the best conditions, and reproducible with the same type of apparatus. Generally speaking the data presented are accurate to ±10° C. and ±3 per cent of the pressure.

The products were identified largely by *x*-ray diffraction techniques, in combination with petrographic methods and electron microscopy. Most of the products were extremely fine-grained, and the petrographic microscope was not very useful. Phases such as montmorillonite were further identified by expansion characteristics (observed in the *x*-ray diffraction pattern) and differential thermal analysis. *X*-ray data were obtained on North American Philips Geiger-counter spectrometer units. Cu-K$\alpha$ radiation (filtered through Ni) was used in most cases. Such a unit is of great help especially in studying the endellite-halloysite relationship since no tedious experimental procedure is necessary. The sample is simply made into a paste with water and placed on the glass slide. Under ordinary room temperature conditions conversion of endellite to halloysite does not take place in less than ½ hour, and only 5 minutes are essential for identification.

## III. DESCRIPTION OF MINERALS, THEIR SYNTHESIS AND DECOMPOSITION

### *A. Compounds in the System $Al_2O_3$-$SiO_2$*

1. *Sillimanite, Andalusite and Kyanite.* Attempts were made to synthesize these three minerals of the composition $Al_2O_3 \cdot SiO_2$,. using a great variety of starting materials. Hydrothermal runs (nearly 500) were made in the temperature range 110° to 930° C. at pressures of 1,000 to 30,000 psi., starting either with minerals or with gels with ratios of 2:1, 1:1 and 1:2 alumina:silica. In no case were we able to synthesize any of these minerals beyond doubt. Seeding with one of the minerals or all three simultaneously was also tried, but no growth was observed on any seeds. Attempts were made to repeat all previously reported syntheses of sillimanite, by following as closely as possible the described procedures such as those of Balconi (1941) and Michel-Levy (1950). In no case was a product formed which could unequivocally be distinguished from mullite. There has been much interest recently in distinguishing sillimanite from mullite by *x*-ray methods (McAtee and Milligan, 1950, and de Keyser, 1951). In the light of this work, the differences appear to be so small that we consider it impossible to identify positively the broadened patterns obtained from the fine-grained products, especially when admixed with other phases. Relying on optical and thermal evidence only, we were unable to find a single clear case of the formation of sillimanite. Attempts were made to duplicate the synthesis of andalusite as described by Baur (1911, 1912), but we were unable to identify any andalusite in the product. Hydrothermally treating the groundmass of a schist which contained andalusite phenocrysts did not result in certain growth of andalusite. The usual product included a micaceous phase and some needle-like crystals having approximately the correct refractive index for andalusite, but the needles existed in insufficient quantity to identify by *x*-ray diffraction and were not large enough to determine the optical properties accurately. Since these experiments were carried out, Lacy (1951) has reported the synthesis of andalusite by a somewhat similar method, although again the identification based on optical properties of very small crystals is not certain.[1] As mentioned earlier, D. M. Roy has now reproducibly synthesized andalusite.

Several unidentified phases were encountered in these studies. Occasionally the *x*-ray diffraction pattern of a particular phase matched that of andalusite or kyanite fairly well. In the absence of definite duplicate runs and optical evidence, however, synthesis of these minerals is questionable.

---

[1] Lacy, E. D., Personal communication, 1952.

Decomposition through ordinary hydrothermal treatment was slight Several runs giving long exposure at 700° to 900° C. to water at pressures in the range 2,000 to 10,000 psi. caused slight decomposition of kyanite and possibly of sillimanite and andalusite as indicated under the ligh microscope. The products of decomposition were not detected in the $x$-ray diffraction patterns. In the higher temperature runs (800°–900° C. corundum made an anomalous appearance as small hexagons in the decomposition product in several runs. Decomposition of the natura minerals by grinding at lower temperatures was more complete. Andalusite, sillimanite and kyanite were decomposed in the grinding apparatu at temperatures of 350° to 450° C. and water pressures in the range o 2,000 to 5,000 psi. The efficiency of the grinding apparatus (Roy an Osborn, 1952) may be illustrated by the fact that in static runs at 375 C. no evidence for kaolinite was obtained in the $x$-ray pattern after 6 or 90 days, whereas considerable kaolinite is formed in 3 days of grinding. Below 400° C. the decomposition products contained mainly kaolinite, and usually included a mica, suggesting the presence of alkali the natural minerals. The mica may, however, have been present as a original undetected impurity.

2. *Mullite.* The aluminosilicate phase formed in most cases from high alumina mixtures at temperatures above about 425° C. is mullit ($3Al_2O_3 \cdot 2SiO_2$). At lower temperatures the hydrates, diaspore, kaolinite and aluminum montmorillonite, are stable in the presence of high pressure water. Mullite was identified in most cases by $x$-ray diffractio patterns since the crystals were too small to identify optically. Th difficulty in distinguishing between the $x$-ray diffraction patterns of mullite and sillimanite makes it possible that in some cases the patter ascribed to mullite was actually that of sillimanite.

Mullite was decomposed through long runs in the grinding apparatu at temperatures of 330° and 450° C. (water pressures 2,000 and 10,000 psi.), and the products included kaolinite, pyrophyllite, and possibl hydralsite. No recognizable decomposition was effected through ordinar hydrothermal treatment at higher temperatures up to 900° C. for tw weeks.

### *B. Compounds in the System $Al_2O_3$-$H_2O$*

The system $Al_2O_3$-$H_2O$ has been described by Laubengayer and Weis (1943) and by Ervin and Osborn (1951). A schematic representation c the relations among the compounds is shown in Fig. 1. The only crystalline phases stable under hydrothermal conditions are gibbsite, boehmite

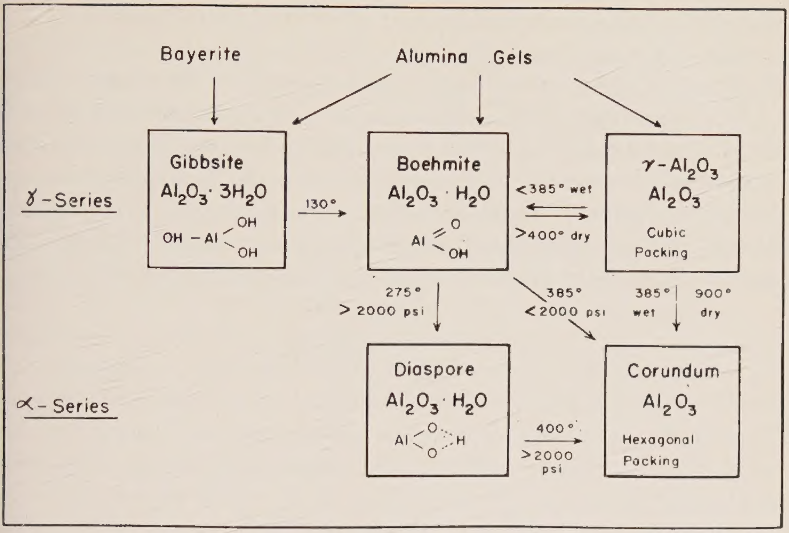

FIG. 1. Schematic representation of relationships among phases in the system $Al_2O_3$-$H_2O$.

diaspore and corundum. Under such conditions gibbsite is formed stably below 130° C. Boehmite[2] exists stably between 130° and 275° C. at pressures greater than 2,000 psi., and up to 385° C. at lower pressures. Diaspore is apparently formed only under pressures greater than 2,000 psi., and at temperatures between 275° and 415° C.; in most cases "seeding" is necessary for the growth of this crystalline phase. Otherwise boehmite will be formed metastably. However, diaspore was synthesized under very high water pressures by Ervin and Osborn (1951), and we have recently synthesized crystals, without seeding, at pressures as low as 20,000 psi. Crystals 1 to 2 mm. in length have been obtained. Corundum or α-$Al_2O_3$, is the stable phase above 410° C., and almost invariably grows as euhedral hexagonal prisms.

### C. *Ternary Compounds*

1. *Endellite and Halloysite.* The ternary phase of highest water content (see Fig. 2) is endellite ($Al_2O_3 \cdot 2SiO_2 \cdot 4H_2O$),[3] and this on partial dehydration yields halloysite ($Al_2O_3 \cdot 2SiO_2 \cdot 2H_2O$). Bates, Swineford and Hilde-

---

[2] A typographical error in the paper of Ervin and Osborn for the refractive indices of synthetic boehmite has been noted. These should be: $\alpha = 1.649 \pm 0.001$, $\beta = 1.659 \pm 0.002$, $\gamma = 1.665 \pm 0.002$.

[3] Throughout this paper the terms "endellite" and "halloysite" are used to designate the phases of nominal composition $Al_2O_3 \cdot 2SiO_2 \cdot 4H_2O$ and $Al_2O_3 \cdot 2SiO_2 \cdot 2H_2O$, respectively. Other workers (see for example Brindley, 1951) have chosen to refer to the first as "halloysite" and to the second as "metahalloysite."

brand (1950) have demonstrated that endellite and halloysite have a tubular habit. Acceptance of this view leads to the deduction that halloysite cannot be formed except by dehydration of endellite. The tubes of endellite are believed to develop as a consequence of the "misfit" between the silica and gibbsite layers in the structure and because of the separation of the layers one from the other by a layer of water molecules. When this interlayer water is removed, halloysite is formed as the layers collapse and meet, setting up new bonds which apparently cannot be broken again to permit the re-entry of water. Thus, once endellite has been dehydrated

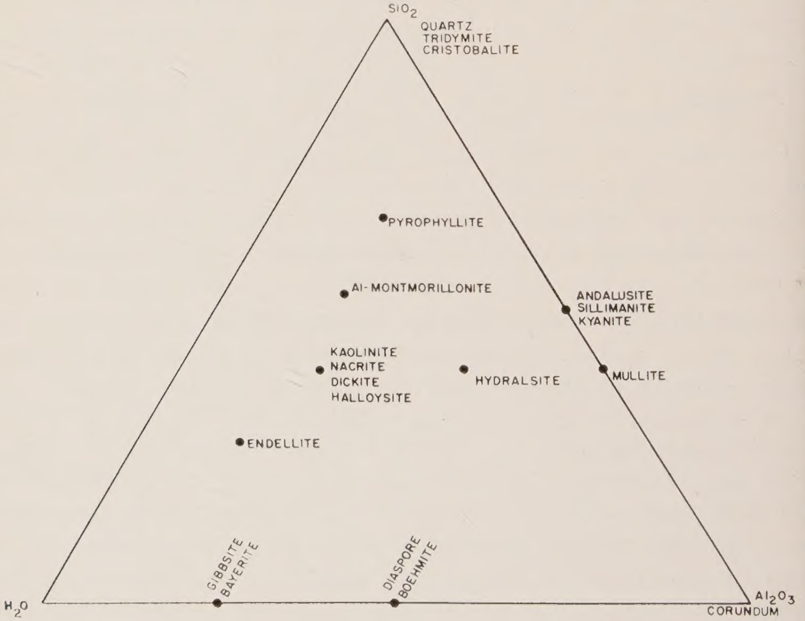

FIG. 2. Crystalline phases in the system $Al_2O_3$-$SiO_2$-$H_2O$.

to yield halloysite, rehydration back to endellite will not take place. This is borne out by all the experimental evidence to date. We have not yet synthesized endellite (and therefore halloysite). Runs of duration from one month to three months, and "grinding" runs have been made starting with gels, at temperatures from 100° upwards to 400° C. When any crystalline structure has appeared it has been that of kaolinite, but generally at the low temperatures virtually no reaction takes place. Halloysite and kaolinite from several localities were treated under various conditions, usually the same conditions as above, and the wet sample was examined for any sign of the formation of endellite. In no case has endellite appeared.

Brindley and Goodyear (1948) have stated that halloysite has an 001 spacing of 7.4 or 7.5kX. Such a spacing was encountered in several of our runs and it was at first considered feasible that the 7.4 Å reflection—characteristic of a hydrate with more than 2 $H_2O$—represented the true value for halloysite. This would have meant that halloysite and kaolinite are not polymorphs. However, a study of the spacings of halloysite dehydrated at temperatures from 100° C. to 450° C. shows that after the attainment of equilibrium the spacing is constant at 7.17 Å. Apparently in the work of Brindley (1951, p. 52) and also in our runs which yielded a structure with a 7.4 Å spacing, dehydration was not carried to equilibrium at the temperatures used. In hydrothermal runs at temperatures and pressures in the region near the equilibrium decomposition curve, endellite may dehydrate only partially to yield the 7.4 Å phase. However, we have found that the spacing of halloysite derived by decomposition of endellite under temperature and pressure conditions existing to the right of Curve II (Fig. 6) is invariably 7.17 Å. Moreover, halloysites dehydrated at 110° C., 300° C. and 400° C. would not rehydrate to the 7.4 Å phase, even under high water pressures at appropriate temperatures. While the above shows that halloysite is a true polymorph of kaolinite with a 7.17 Å spacing, it also does suggest that the interlayering proposed by Brindley and Goodyear has some unique stability, since no other intermediate spacings have been consistently found.

2. *Kaolinite, Nacrite and Dickite* ($Al_2O_3 \cdot 2SiO_2 \cdot 2H_2O$). Kaolinite, or a mineral of the kaolin group was synthesized from coprecipitated $Al_2O_3$-$SiO_2$ gels between 150° and 405° C., under varying water pressures. Identification was made by $x$-ray diffraction, and in some cases the crystals were well enough formed to show distinctive shapes under the electron microscope. No distinction was made between kaolinite, nacrite or dickite in the products of reaction. These products are extremely fine-grained, yielding diffuse $x$-ray diffraction patterns from which a clear verdict with respect to which of the three phases is present cannot readily be obtained. For the same reason, members of the kaolin group (such as the fire clay minerals) (Brindley & Robinson, 1947) are not distinguished. The product therefore is referred to as kaolinite. In many runs, the pattern obtained was more similar to nacrite or dickite than to kaolinite, but no trends could be found indicating that certain temperature-pressure ranges favored formation of nacrite or dickite. From the natural occurrences it might be expected that nacrite and dickite would form at higher temperatures. However, even at 400° C. and 10,000 psi., only 5° C. below the stability limit of the three minerals as determined by decomposition studies, the $x$-ray diffraction pattern of the synthesized structure agrees more closely with that of kaolinite than

TABLE 2. *X*-RAY AND ELECTRON DIFFRACTION DATA ON PHASES

| HYDRALSITE | | | | PYROPHYLLITE | | | | |
|---|---|---|---|---|---|---|---|---|
| *X*-ray | | Electron | | Natural (API) | | Synthetic (F-228) | | |
| "*d*" (Å) | $I/I_0$ | "*d*" (Å) | *hk*0* | "*d*" (Å) | $I/I_0$ | *hkl*† | "*d*" (Å) | $I/I_0$ |
| 8.91 | 80 | | | 8.97 | 30 | 002 | 9.32 | 90 |
| 4.448 | 60 | 4.45 | 100 | | | ? | 4.94 | 15 |
| 3.414 | 100 | 2.57 | 110 | 4.53 | 40 | 020, 004 | 4.634 | 20 |
| 2.430 | 50 | 2.225 | 200 | | | | 4.439 | 100 |
| 2.362 | 40 | 1.682 | 210 | 4.12 | 20 | 111 | | |
| | | | | | | $11\bar{2}$ | 4.280 | 30 |
| 2.074 | 20 | 1.483 | 300 | | | 021 | 4.077 | 30 |
| 2.044 | 10 | 1.285 | 220 | 3.85 | 5 | $11\bar{3}$ | | |
| | | | | | | 022 | 3.786 | 5 |
| 1.845 | 20 | 1.234 | 310 | 3.34 | 25 | 113 | 3.420 | 15 |
| 1.810 | 10 | 1.113 | 400 | | | ? | 3.186 | 5 |
| 1.768 | 20 | 1.021 | 320 | 3.037 | 80 | 006 | 3.084 | 90 |
| 1.471 | 5 | .9706 | 410 | 2.524 | 20 | 200 | 2.571 | 40 |
| 1.450 | 10 | .8902 | 500 | | | $13\bar{2}$ | 2.543 | 60 |
| 1.405 | 10 | .8565 | 330 | 2.400 | 30 | 204 | 2.424 | 70 |
| | | | | | | 132 | | |
| 1.3804 | 10 | .8410 | 420 | 2.287 | 20 | 008 | 2.309 | 5 |
| 1.3360 | 5 | .7988 | 510 | 2.142 | 15 | $20\bar{6}$ | 2.166 | 20 |
| | | | | | | 134 | | |
| 1.2765 | 5 | .7418 | 600 | 2.071 | 10 | 204 | 2.078 | 40 |
| 1.2343 | 20 | .7316 | 430 | 2.044 | 10 | | | |
| | | .7126 | 520 | 1.881 | 5 | | | |
| | | .6787 | 610 | 1.828 | 30 | 0010 | 1.843 | 20 |
| | | .6424 | 440 | | | | | |
| | | $a_{\text{hex}}=4.450$ | | $a_0=5.14$ | | $a_0=5.13$ | | |
| | | $a_{\text{orth}}=5.138$ | | $b_0=8.90$ | | $b_0=8.88$ | | |
| | | $b_{\text{orth}}=8.90$ | | $c_0=18.55$ | | $d_{001}=18.50$ | | |

* This is indexed on 120° hexagonal axes.

† *API* Indices common to natural and synthetic pyrophyllite.

of nacrite or dickite. Other factors than temperature appear to be responsible for the formation in nature of nacrite and dickite instead of kaolinite.

Decomposition runs were made on several natural minerals. Three different samples of kaolinite were studied to check on the variations within the same mineral species: Florida kaolinite, Langley kaolinite, and kaolinite from Banda, India. The last is an extremely pure kaolinite which under the electron microscope is seen to consist only of well-formed hexagons. Halloysite samples used were from Eureka, Utah, and Bedford, Indiana. The dickite used was from Pottsville, Pa., and the nacrite from Brand, Saxony (obtained through the courtesy of Dr. C. Frondel). All these minerals were found to decompose at the same temperature, within experimental error, this being 405° C. at 10,000 psi. water pressure. Varying the pressure from 2500 to 25,000 psi. did not alter the decomposition temperature by more than 10° C. from this value. The main difference in decomposition behavior is the rate of decomposition, with the larger particles of dickite and nacrite requiring longer periods of time to effect significant decomposition (see Table 3). Differences in the thermodynamic constants among these four phases must be slight.

The first phase forming on hydrothermal decomposition of kaolinite, nacrite, dickite, and halloysite is so-called "hydralsite" which is described below. Mullite and pyrophyllite or mullite and cristobalite are formed at higher temperatures, usually not much below 500° C.[4]

3. *Hydralsite.* On the hydrothermal decomposition of kaolinite, nacrite, dickite and halloysite, or when 1:2 $Al_2O_3$:$SiO_2$ gels are heated under water pressure at temperatures greater than 405° C., a hydrous aluminosilicate phase appears which does not occur as a mineral nor has it been encountered in other investigations. *X*-ray and electron diffraction data and an electron micrograph of this phase appear in Table 2 and Fig. 3*a*. In a previous publication (Roy and Osborn, 1952), we referred to this structure as "X-phase" for lack of a better name. Inasmuch as this is a term applicable to any unknown phase, whereas the approximate composition and many of the properties of this compound are known, some other designation is needed. The term "hydralsite," a contraction of hydro-aluminosilicate, is used herein for convenience for want of anything better. This term would be equally applicable to any of the ternary phases, but confusion should not result inasmuch as the others all have mineral names.

Hydralsite contains less $H_2O$ and has a higher $Al_2O_3$:$SiO_2$ ratio than kaolinite. Its precise composition is not known, but evidence suggests a composition in the neighborhood of $2Al_2O_3 \cdot 2SiO_2 \cdot H_2O$ or conceivably $Al_2O_3 \cdot SiO_2 \cdot H_2O$. That this phase is a monohydrate is not established beyond question because of the inevitable uncertainty regarding purity of samples used in water loss determinations and because the $Al_2O_3$:$SiO_2$ ratio is not definitely known. The weight loss (at 1,000° C. for 50 hours) of hydralsite, prepared from kaolinite and dried to constant weight at 110° C., was 5.61 per cent. Another sample, prepared from a 1:1 $Al_2O_3$

[4] Earlier workers have reported the formation of pyrophyllite at temperatures just above the stability limit of kaolinite. There is little doubt that hydralsite was here mistaken for pyrophyllite.

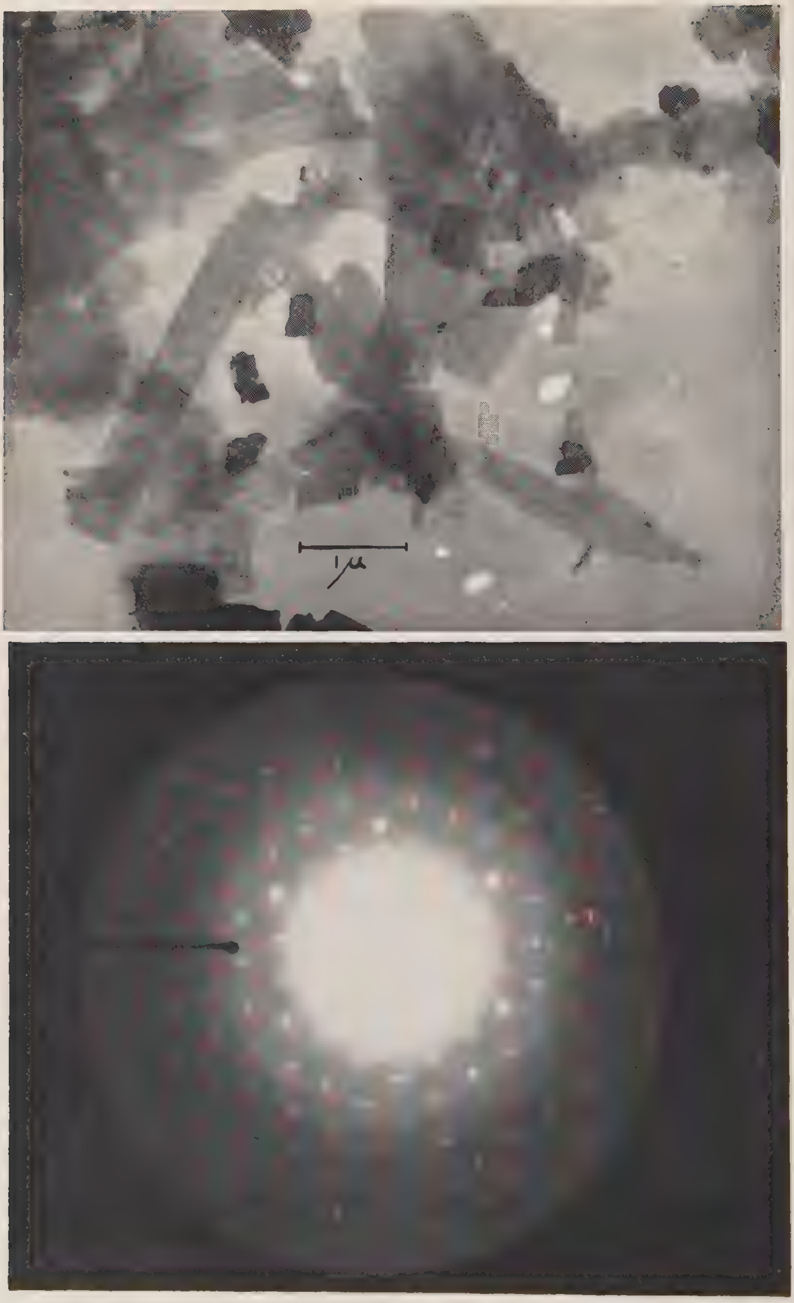

FIG. 3. Hydralsite prepared from 1:1 $Al_2O_3$:$SiO_2$ gel: (*a*) Electron micrograph. (*b*) Single crystal electron diffraction pattern.

:$SiO_2$ nitrate-ethyl silicate mixture, showed a weight loss of 6.03 per cent. The weight loss corresponds approximately to the water content of $2Al_2O_3 \cdot 2SiO_2 \cdot H_2O$, which is 5.27%. The $Al_2O_3$:$SiO_2$ ratio is considered to be higher than that in kaolinite on the basis of the following facts: (1) On the complete conversion of kaolinite, hydralsite is invariably accompanied by a small amount of pyrophyllite, no other phase being present in sufficient amounts to be identified (see Table 5). Were the $Al_2O_3$:$SiO_2$ ratio in hydralsite and kaolinite the same, either hydralsite alone should be the decomposition product or a higher alumina phase such as mullite as well as pyrophyllite should be present (due to nonequilibrium conditions) with hydralsite in the mixture. Similarly, if the $Al_2O_3$:$SiO_2$ ratio were lower than in kaolinite, some other higher alumina phase must be present. (2) Starting with a 1:1 $Al_2O_3$:$SiO_2$ gel or nitrate-ethyl-silicate mixture, the product contains no detectable pyrophyllite or other phase than hydralsite, and under the electron microscope appears more homogeneous and better crystallized. This does not necessarily prove, however, that the $Al_2O_3$:$SiO_2$ ratio is 1:1 because in our experience some $Al_2O_3$ or $SiO_2$ or both may remain in an apparently "amorphous" state and not be readily detected, at least at lower temperatures.

Hydralsite bears a resemblance to paragonite and pyrophyllite in its *x*-ray diffraction pattern, but as may be seen from Table 2, the basal spacing is distinctly different from that of pyrophyllite (8.91 Å for hydralsite as compared with 9.0 Å for pyrophyllite). Moreover, the strongest reflection for pyrophyllite, at 3.04 Å, is completely absent in the pattern for hydralsite. Single crystal electron diffraction patterns[5] (Fig. 3*b*) yield directly the *a* and *b* parameters: $a=5.14$, $b=8.90$. The pseudo-hexagonal nature of the *a*-*b* projection can be seen immediately from the photograph (Fig. 3*b*). Careful measurement shows that the cell is not triclinic like kaolinite, the *a* and *b* axes intersecting at 90° within the precision of measurement (one part in one thousand in favorable cases). The basal spacing (equal to $c \sin \beta$) as obtained from *x*-ray diffraction is 8.91 Å.

From the data available certain speculations can be made regarding the structure of hydralsite. A formula of $Al_2O_3 \cdot SiO_2 \cdot H_2O$ can be fitted into a structural scheme wherein a disilicic tetrahedral layer is formed by aluminum replacement, the charge being balanced by the introduction of more hydroxyl ions in place of oxygen (Fig. 4*a*). However, such a formula requires a weight loss on ignition of about 10% which is far greater than that found. The formula $2Al_2O_3 \cdot 2SiO_2 \cdot H_2O$ would be in better accord with all the *compositional* data. A structure compatible with this may be obtained by replacement of more than $\frac{1}{4}$ of the tetrahedral Si by Al, and the balance of charge being made up by a possible filling of more than $\frac{2}{3}$rds of the octahedral positions by Al. Under such conditions any exact stoichiometric ratios for the hydralsite phase would be unlikely, as is seen in Fig. 4 (*b*) and (*c*).

---

[5] These patterns were initially obtained through the assistance of Dr. A. F. Moodie (of the CSIRO, Melbourne, Australia), and we are also greatly indebted to Dr. Moodie for advice and guidance in obtaining and interpreting single crystal electron diffraction patterns. These patterns are similar in type to those published by Finch (1937), Cowley (1952, 1953), and Brown and Clark (1952).

POSSIBLE STRUCTURES FOR HYDRALSITE

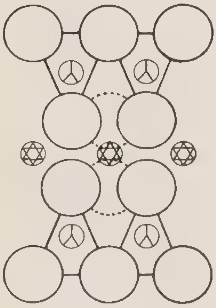

| 1st. Model | 2nd. Model | 3rd. Model |
|---|---|---|
| 6 O | 6 O | 6 O |
| 2 Si, 2Al | 2Si, 2Al | 2-1/2 Si, $\frac{3}{2}$ Al |
| 2 O, 4 OH | 4 O, 2 OH | 4 O, 2 OH |
| 4 Al | 5-1/3 Al | 5 Al |
| 2 O, 4 OH | 4 O, 2 OH | 4 O, 2 OH |
| 2 Si, 2Al | 2Si, 2Al | 2-1/2 Si, $\frac{3}{2}$ Al |
| 6 O | 6 O | 6 O |
| $Si_4Al_8O_{16}(OH)_8$ | $Si_4Al_{\frac{28}{3}}O_{20}(OH)_4$ | $Si_5Al_8O_{20}(OH)_4$ |
| (a) | (b) | (c) |

FIG. 4. Schematic representation of possible structures for hydralsite based on a mica-type arrangement, with complete "internal" balance as suggested by low base exchange capacity.

The index of refraction of hydralsite is not distinctly different from that of pyrophyllite, being of the order of 1.600. The differential thermal analysis pattern of hydralsite resembles that of mica or pyrophyllite rather than that of a clay mineral. A broad endothermic peak, which may be accentuated by increasing the rate of temperature rise to 12° C. per minute, occurs with the maximum at 550° C. (see Fig. 5*a*). The infrared absorption for hydralsite is indicated in Fig. 5*b*.

The hydralsite structure persists to high temperatures when heated in air. A recognizable *x*-ray diffraction powder pattern is still obtained after heating hydralsite for 30 hours at 900° C.

The surface area of a sample made from other minerals as starting materials was about 57 $m^2/g$. The base exchange capacity is quite low, also indicative of a "balanced" structure. A value of only 1 m.eq./100 gms. was obtained on the same sample.[6]

Hydralsite is formed invariably under the conditions given, but no consistent maximum stability limit or temperature of decomposition could be obtained. Pyrophyllite and mullite are the products of its decomposition, as determined in these studies, and in addition andalusite as found by D. M. Roy (1953). Once formed it has never been converted to kaolinite or montmorillonite. An interesting observation in connection with studies in the system $MgO$-$Al_2O_3$-$SiO_2$-$H_2O$ (Roy and Roy, 1952) is that hydralsite is still formed in the presence of $Mg^{2+}$, at temperatures between the upper stability temperature of Mg-montmorillonite and the lower temperature of formation of pyrophyllite.

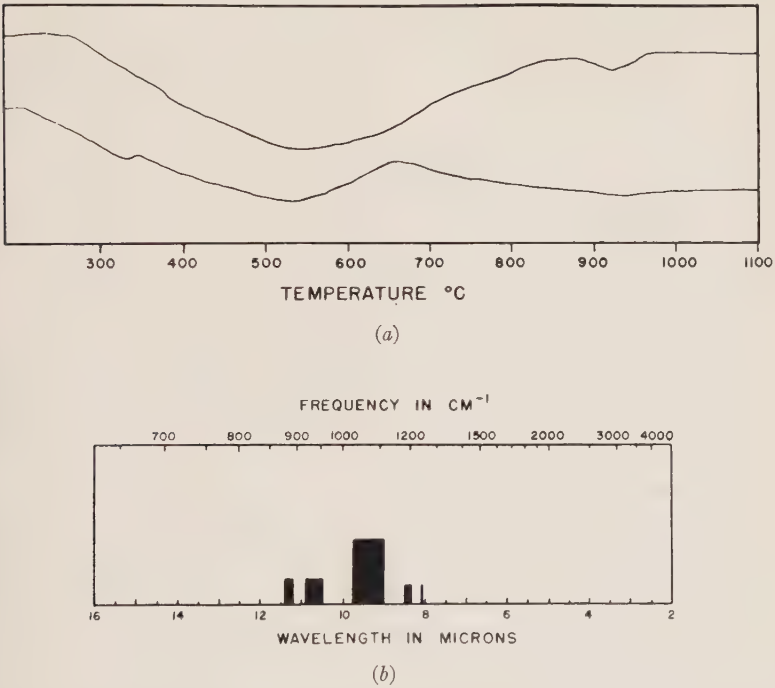

Fig. 5. (*a*) Two differential thermal analysis curves of hydralsite. The material used for the upper curve was prepared from a 1:1 $Al_2O_3$-$SiO_2$ gel; that for the lower curve from kaolinite. Heating rate used: 12° C./min. (*b*) Infra-red absorption spectrum for hydralsite shown as a block diagram.

While the double layer structures (kaolinite, etc.) are not stable above 405° C., the triple layer structures, pyrophyllite and montmorillonite,

---

[6] We are indebted to Mr. T. D. Oulton of the Filtrol Corp., Los Angeles, for the measurements of surface area and base exchange capacity.

persist as stable phases to higher temperatures. Therefore, the former (double layer structures) must decompose to yield the latter (triple layer structures) when heated under equilibrium conditions. This involves a major rearrangement of atoms, including the complete removal of one gibbsite sheet. In this process an intermediate, metastable phase might be expected to form. Hydralsite may be such a phase, appearing invariably on the decomposition of double layer structures. Our inability to obtain consistent decomposition temperatures for hydralsite is also suggestive of metastability. The non-occurrence of hydralsite in nature may possibly be explained both on the basis of this probable metastability and on the fact that the ubiquitous alkali ions would facilitate the transformation to micas and montmorillonites.

4. *Aluminum montmorillonite.* This phase is obtained from 1:4 $Al_2O_3$:$SiO_2$ gels (which have been carefully electrodialyzed to remove any impurity ions) between the lowest temperature used, 200°, and 420° C. under varying $H_2O$ pressure. This structure represents a pure aluminum end member[7] of the montmorillonites (beidellites). The $x$-ray diffraction pattern (Table 3) corresponds closely to that of natural montmorillonite and the structure swells to a basal spacing of 14 Å with ethylene glycol. This diminished "expansibility" is noteworthy; no explanation has been found for it.

The question of the possible existence of such a phase, namely a pure hydrated aluminum silicate with the montmorillonite structure, has previously attracted the attention of mineralogists. Ross and Hendricks (1945) suggest the possibility of such an end member of the beidellite series, where the exchangeable base may be $Al(OH)_2^+$. Hoffman, Endell, and Wilm (1933) in their earliest work had also suggested a typical formula, where only Al and Si cations were present. The formula of Ross and Hendricks (1945) gives a composition ratio of very nearly $Al_2O_3$:$2SiO_2$. Substitution in the tetrahedral layer of $Al^{3+}$ for $Si^{4+}$ was assumed to be extensive ($Al_{.83}Si_{3.17}$) in order to reach the formula ($Al_2O_3$:$2SiO_2$). This was probably done to accommodate the experimental results of Ewell and Insley. However, the latter authors had at least 2 to 3 per cent soda in their mixtures, which would occupy the base exchange position. Thus we have found that with nonelectrodialyzed gels

---

[7] Chemical and spectroscopic analyses of mixtures used in synthesis of aluminum montmorillonite and of the phase itself showed the presence of no other oxides than $Al_2O_3$ and $SiO_2$ in quantities greater than a few tenths of one per cent, total impurities not exceeding 0.5 per cent. Whether or not even the one or two tenths of a per cent of alkali actually are essential to the structure cannot easily be proved. However, the amounts of alkali present cannot alone balance the excess charge caused by substitution in the tetrahedral layer and the basic picture is therefore unchanged.

TABLE 3. X-RAY DATA ON AL-MONTMORILLONITE

(Run #5454, 390° C., 25,000 psi)

| $2\theta$ | $d$ (Å) | $I/I_0$ | hkl |
|---|---|---|---|
| 8.00 | 11.05 | 100 | 001 |
| 16.40 | 5.405 | 3 | 002 |
| 19.90 | 4.462 | 2.5 | 110, 020 |
| 28.15 | 3.170 | 37 | |
| 45.55 | 1.991 | 1.5 | |
| 49.05 | 1.857 | 1 | 006 (?) |
| | Expanded With Ethylene Glycol | | |
| 6.57 | 13.43 | 100 | 001 |
| | Dried at 110° C. | | |
| 8.9 | 9.94 | 100 | 001 |

prepared in the manner described by Ewell and Insley, when the composition is 1:4 $Al_2O_3:SiO_2$, analcime is obtained in a wide composition range, and only at lower silica concentrations do the clay phases form, since there are no sodium minerals with such compositions.

We may ascribe to the mineral an ideal formula such as $(Al(OH)_2)_{.33}Al_2(Si_{3.67}Al_{0.33}O_{10})(OH)_2$ where the $(Al(OH)_2)^+$ is the exchangeable base. The ideal composition then approaches an alumina:silica ratio of 1:3. It is more than likely, however, that the structure can exist over a range of compositions. This structure does not form above about 420° C., where pyrophyllite is the stable phase. No lower decomposition temperature has been found, and this phase is presumably stable down to atmospheric temperature and pressure. Its natural analogue is of course the high alumina beidellite with mainly $Na^+$ ions in the base exchange positions.

5. *Pyrophyllite* ($Al_2O_3 \cdot 4SiO_2 \cdot H_2O$). Pyrophyllite is a stable phase above 420° C. under varying water pressures, in all alumina-silica mixtures high in silica. Pyrophyllite is obtained as the only crystalline phase from 1:4 $Al_2O_3:SiO_2$ gels at equilibrium. The substance forms with considerable difficulty in our experience and is invariably fine-grained. It was identified by its *x*-ray diffraction pattern which is essentially identical with that of natural pyrophyllite. The close correspondence is illustrated for a typical sample in Table 2.

The difficulty in synthesizing pyrophyllite may be ascribed to the fact that in the co-precipitated gels the alumina and silica are intimately mixed, and on heating, the $Al^{3+}$ ions tend to go into fourfold coordination in the silica network, this being especially true for the high silica gels from which pyrophyllite forms. Pyrophyllite has $Al^{3+}$ only in sixfold coordination. There is a great resistance to this required rearrangement, so much so that several anhydrous aluminosilicate minerals having aluminum in octahedral coordination have never been synthesized, e.g., kyanite, jadeite, and pyrope. Kaolinite, which also has aluminum in octahedral coordination, forms with relative ease as compared to pyrophyllite. This difference in rate of growth of kaolinite and pyrophyllite may be ascribed to the lower temperature range of stability of kaolinite where six-fold coordination of aluminum is favored and to the fact that kaolinite is synthesized in a general higher alumina compositional range. The additional hydroxyl ions in kaolinite would also be a factor in promoting octahedral coordination for aluminum.

## IV. PHASE RELATIONS

*A. Binary Systems.* The three bounding binary systems have been previously investigated. The system $Al_2O$-$H_2O$ was studied by Ervin and Osborn (1951) over a wide range of temperature and water pressure. An interesting feature of their proposed equilibrium diagram for the system is the pressure "bottom" for the stability region of diaspore. This phase is believed to be stable only at water pressures greater than 2,000 psi and in the temperature range of 275° to 415° C. Repeated runs at water pressure below 2,000 psi failed to produce diaspore[8] whereas at higher pressures diaspore grows readily. Since this work was published, we have made longer runs to obtain additional information of diaspore stability. Both alumina gel and gamma alumina were used as starting materials, both seeded with diaspore crystals. Data obtained on representative runs are listed in Table 4. These data on two-week runs along with evidence obtained in connection with a study of the system $Al_2O_3$-$Ga_2O_3$-$H_2O$ (Hill, Roy, and Osborn, 1952) support the conclusion that diaspore is stable only above 2,000 psi. water pressure and 275° C.

[8] Laubengayer and Weisz (1943) report the growth of diaspore at 305° C. with "about 0.7" degree of filling of the bomb (their run 17*a*), and it is implied that under these conditions the pressure would be that of the saturated vapor pressure of water, about 1,325 psi. Actually, 0.7 degree of filling at room temperature is very critical with respect to complete filling with liquid water at 305° C., as shown by data of Kennedy (1950) and by extrapolation of curves of van Niewenburg and Blumendahl (1932). With precisely 0.7 degree of filling, the pressure at 305° C. is approximately 2,100 psi. A few tenths of a milliliter in excess of that required for 0.7 degree of filling in bomb used by Laubengayer and Weisz would cause a sharp increase in this pressure. Moreover, a temperature increase of a few degrees over 305° C., to be expected with normal variations in temperature under their experimental conditions, would produce a similar marked increase in pressure over the nominal 2,100 psi. The data of Laubengayer and Weisz are thus consistent with those of Ervin and Osborn (1951), rather than being at variance with them.

TABLE 4. REPRESENTATIVE RUNS OF ALUMINA GEL AND GAMMA ALUMINA, SEEDED WITH DIASPORE

| Temperature ° C. | Water pressure psi. | Time, days | Result |
|---|---|---|---|
| 270 | 32,000 | 15 | Boehmite |
| 295 | 32,000 | 14 | Large amount of diaspore plus boehmite |
| 302 | 1,280 | 14 | Boehmite |

In the system $SiO_2$-$H_2O$, no binary compounds were found or are known to exist. The form of $SiO_2$ most commonly present in the product of a hydrothermal run where gels are starting materials is cristobalite, and only prolonged heating, especially at higher temperatures will produce the stable modification, quartz, This of course indicates a degree of metastability in such runs; but inasmuch as we have been able to crystallize quartz under similar conditions without affecting the over-all equilibria, it is considered that the equilibria must be essentially identical with quartz substituting for cristobalite.

No additional work has been done in the "dry" system $Al_2O_3$-$SiO_2$, and our present concept of the system is that presented by Bowen and Greig (1924), with the eutectic temperature modification as proposed by Schairer.[9] In addition to information on the compound mullite, which occurs in the condensed system $Al_2O_3$-$SiO_2$, it was hoped that the present study would reveal some further information on the problem of the stability of compounds andalusite, sillimanite and kyanite. This has been discussed in connection with the individual minerals and their synthesis.

## *B. The Ternary System*

1. *General Statement.* A summary of significant phase equilibrium data for the system $Al_2O_3$-$SiO_2$-$H_2O$ is given in Table 5. These are representative runs selected from more than two thousand, chosen to illustrate the type of data actually obtained for each run. Our interpretation of the phase equilibrium relations in the system $Al_2O_3$-$SiO_2$-$H_2O$ is represented by a series of composition triangles (Fig. 6), showing the phases in equilibrium for a given composition within certain temperature and water pressure limits. The triangles drawn here apply for a pressure of about

---

[9] A later temperature figure of 1,585° C. for the eutectic was suggested by Schairer (See Osborn, 1952) as probably being more nearly correct.

TABLE 5. REPRESENTATIVE RUNS FOR THE SYSTEM $Al_2O_3$-$SiO_2$-$H_2O$

| Run No. | Starting Material | Temp. (° C.) | Water Pres. psi. | Time (days) | Products* |
|---|---|---|---|---|---|
| | | | *CURVE II* | | |
| 3277 | Endellite | 125 | 34 | 22 | end. |
| 3174 | Endellite | 132 | 250 | 13 | end.+l. hall. |
| 3249 | Endellite N. C. | 143 | 200 | 2 | l. end.+hall. |
| 3270 | Endellite | 145 | 100 | 2.5 | l. end.+hall. |
| 3247 | Endellite | 150 | 150 | 2 | hall.+l. end. |
| 3237 | Endellite | 160 | 250 | 1 | hall. |
| 3274 | Endellite | 150 | 75 | 2 | hall.+int. |
| 3307 | Endellite | 155 | 78 | 11 | hall.+end. |
| 3335 | Endellite N. C. | 165 | 100 | 8 | hall. |
| 3336 | Endellite Ind. | 165 | 100 | 8 | hall.+end. |
| 3212 | Endellite | 160 | 10,000 | 3 | end. |
| 3531 | Endellite | 172 | 100 | 1 | hall. |
| 3215 | Endellite | 170 | 10,000 | 2 | end. |
| 3357 | Endellite Ind. | 175 | 5,000 | 2 | hall.+int.+l. end. |
| 3380 | Endellite Ind. | 180 | 10,000 | 2 | end.+l. hall. |
| 3382 | Endellite Ind. | 184 | 10,000 | 3 | end.+l. hall. |
| 3391 | Endellite N. C. | 190 | 10,000 | 6 | end.+hall. |
| 3521 | Endellite N. C. | 190 | 182 | 4 | hall. |
| 3404 | Endellite | 195 | 15,000 | 3 | hall.+some end. |
| 3418 | Endellite | 200 | 10,000 | 4 | hall. |
| 3423 | Endellite | 205 | 10,000 | 2 | hall.+possibly v. l. end. |
| 3495 | Endellite | 210 | 4,000 | 1 | hall.+l. end. |
| 3485 | Endellite | 225 | 400 | 2 | hall. |
| 3517 | Endellite (suspension) | 250 | 5,000 | 1 | hall. |
| 3500 | Endellite | 288 | 3,500 | 1 | hall. |
| 3507 | Endellite Utah | 274 | 6,000 | 1 | hall. |
| 3503 | Endellite N. C. | 310 | 3,500 | 1 | hall. |
| | | | *CURVE IV* | | |
| 3286 | kaolinite | 395 | 5,000 | 2 | kaolinite |
| 3160 | kaolinite | 400 | 250 | 14 | kaolinite−v.l. decomp. |
| 3152 | kaolinite | 403 | 1,000 | 2 | kaolinite−v. l. decomp. |
| 1713 | kaolinite | 405 | 20,000 | 3 | kaolinite−slight change |
| 3306 | kaolinite | 411 | 5,000 | 4 | kaolinite+l. hyd. |
| 3189 | kaolinite | 408 | 15,000 | 2 | kaolinite+v. l. decomp. |
| 3463 | kaolinite | 415 | 10,000 | 28 | hyd.+l. kaol. |
| 3101 | Banda kaol. | 400 | 8,000 | 6 | kaolinite, possibly trace of decomposition no detectable hyd. |
| 3102 | Langley kaol. | 400 | 8,000 | 6 | |
| 3103 | Florida kaol. | 400 | 8,000 | 6 | |

* Abbreviations used: and.=andalusite; crist.=cristobalite; cor.=corundum; end.=endellite; hall.=halloysite; hyd.=hydralsite; kaol.=kaolinite; ky.=kyanite; mont.=montmorillonite; mull.=mullite; pyroph.=pyrophyllite; sill.=sillimanite; N. C.=North Carolina; Ind.=Indiana; l.=little; v.=very; int.=intermediate.

| Run No. | Starting Material | Temp. (° C.) | Water Pres. psi. | Time (days) | Products* |
|---|---|---|---|---|---|
| 3128 | Banda kaol. | 404 | 10,000 | 6 | clearly observable decomposition kaol.+hyd. |
| 3129 | Langley kaol. | 404 | 10,000 | 6 | |
| 3130 | Florida kaol. | 404 | 10,000 | 6 | |
| 3107 | Banda kaol. | 407 | 8,000 | 8 | hyd.+kaol. |
| 3108 | Langley kaol. | 407 | 8,000 | 8 | hyd. |
| 3109 | Florida kaol. | 407 | 8,000 | 8 | hyd.+l. kaol. |
| 3166 | nacrite | 408 | 250 | 9 | nacrite |
| 3186 | nacrite | 408 | 15,000 | 2 | nacrite |
| 3305 | nacrite | 411 | 5,000 | 4 | nacrite, slight decomp., optical only. |
| 3203 | nacrite | 410 | 10,000 | 3 | |
| 3318 | nacrite | 420 | 5,000 | 9 | nacrite-decomp.; anomalous $x$-ray |
| 3464 | nacrite | 415 | 10,000 | 28 | mostly hyd. |
| 3072 | dickite | 397 | 5,000 | 5 | dickite—intensity change |
| 3047 | dickite | 400 | 15,000 | 12 | dickite—v. l. change |
| 3202 | dickite | 410 | 10,000 | 3 | dickite—mottling visible |
| 3465 | dickite | 415 | 10,000 | 28 | hydralsite+dickite |
| 3071 | halloysite | 397 | 5,000 | 5 | halloysite, v. l. decomp. |
| 3188 | halloysite | 408 | 15,000 | 2 | halloysite |
| 3208 | halloysite | 414 | 10,000 | 2 | halloysite+l.hyd.+l.monty |
| 3017 | halloysite | 428 | 9,000 | 6 | pyroph(?)+hyd. |
| 3309 | 1:2 n.e.d. gel | 155 | 80 | 11 | kaolinite |
| 3177 | 1:2 e.d. gel | 195 | 250 | 69 | kaolinite |
| 3190 | 1:2 e.d. gel | 408 | 15,000 | 2 | kaolinite |
| 3201 | 1:2 e.d. gel | 410 | 10,000 | 3 | kaolinite |
| 3209 | 1:2 e.d. gel | 414 | 10,000 | 2 | hydralsite |
| 3018 | 1:2 e.d. gel | 428 | 9,000 | 6 | hydralsite |
| 5453 | 1:2 e.d. gel | 417 | 25,000 | 9 | monty+hydralsite |
| 5443 | 1:2 organic-nit. | 390 | 30,000 | 7 | kaolinite |
| 5452 | 1:2 organic-nit. | 417 | 25,000 | 9 | hydralsite+pyroph. |
| | | | *CURVE VI* | | |
| 3110 | 1:4 e.d. gel | 407 | 8,000 | 9 | mont. |
| 3098 | 1:4 e.d. gel | 417 | 10,000 | 5 | mont. |
| 3121 | 1:4 e.d. gel | 423 | 10,000 | 9 | mont.+pyroph |
| 1734 | 1:4 e.d. gel | 430 | 5,000 | 7 | pyroph (broadened peaks) |
| 3170 | 1:4 e.d. gel | 440 | 10,000 | 30 | pyroph |
| | | | *CURVE VII* | | |
| 3018 | 1:2 e.d. gel | 428 | 9,000 | 6 | hydralsite |
| 1757 | 1:2 e.d. gel | 448 | 8,000 | 10 | prophy+hyd. |
| 3171 | 1:2 e.d. gel | 440 | 10,000 | 30 | hydralsite+cor. ? |
| 3516 | 1:2 e.d. gel | 475 | 10,000 | 6 | pyroph+hyd. |
| 1581 | 1:2 e.d. gel | 485 | 8,000 | 12 | pyroph+mullite |
| 1799 | 1:2 e.d. gel | 515 | 8,000 | 7 | pyroph+mullite |
| F-284 | 1:1 organic-nit. mixt. | 435 | 5,000 | 8 | hydralsite |
| F-267 | 2:3 organic-nit. mixt. | 445 | 6,000 | 13 | hyd.+1. pyroph |
| F-239 | 1:2 organic-nit. mixt. | 440 | 10,000 | 17 | hyd.+pyroph |
| F-242 | 1:3 organic-nit. mixt. | 440 | 10,000 | 16 | hyd.+pyroph |

| Run No. | Starting Material | Temp. (° C.) | Water Pres. psi. | Time (days) | Products* |
|---|---|---|---|---|---|
| 3172 | 1:1 e.d. gel | 440 | 10,000 | 30 | hydralsite |
| 3138 | 1:1 gel | 481 | 12,000 | 8 | hydralsite |
| 3025 | kaolinite e.d. | 435 | 10,000 | 7 | hydralsite |
| 3515 | kaolinite e.d. | 475 | 10,000 | 6 | hyd.+pyroph+cor. ? |
| 3522 | kaolinite e.d. | 495 | 10,000 | 13 | mainly hydralsite |
| 3449 | kaolinite e.d. | 530 | 5,000 | 30 | mull.+l. hyd. |
| 3514 | hydralsite | 475 | 10,000 | 6 | hydralsite+pyroph. |
| 3523 | hydralsite | 495 | 10,000 | 13 | hydralsite+l. pyroph +quartz (?) |
| 3450 | hydralsite | 530 | 5,000 | 30 | mull.+pyroph.+hydralsit |
| | | *CURVE VIII* | | | |
| 3095 | pyroph. | 555 | 10,000 | 1½ | pyroph. |
| 3104 | pyroph. | 562 | 10,000 | 4 | pyroph. |
| 3125 | pyroph. | 567 | 1,000 | 2 | mottled (pyroph. *x*-ray) |
| 3224 | pyroph. | 568 | 250 | 4 | pyroph. good |
| 3115 | pyroph. | 567 | 10,000 | 3 | attack (pyroph. *x*-ray) |
| 3134 | pyroph. | 573 | 1,000 | 4 | mottling, needles seen (p roph. *x*-ray) |
| 3149 | pyroph. | 578 | 1,000 | 4 | mottled pyroph. |
| 3140 | pyroph. | 578 | 10,000 | 3 | pyroph.+qtz.+mull. |
| 3253 | pyroph. | 581 | 250 | 6 | qtz.+pyroph. |
| 5188 | 1:4 e.d. gel | 525 | 20,000 | 7 | pyroph. |
| 3282 | 1:4 e.d. gel | 555 | 5,000 | 17 | pyroph. |
| 5176 | 1:4 e.d. gel | 555 | 15,000 | 10 | pyroph+? ? |
| 1707 | 1:4 e.d. gel | 565 | 4,000 | 4 | crist. mostly |
| 1774 | 1:4 e.d. gel | 582 | 8,000 | 3 | crist.+mullite |
| 3325 | kaolinite | 530 | 6,000 | 25 | mullite+cor.+pyroph. |
| 3329 | kaolinite | 565 | 5,000 | 20 | mullite+crist. |
| 3327 | 1:2 e.d. gel | 530 | 6,000 | 25 | pyroph.+mull.+cor. ? |
| 3330 | 1:2 e.d. gel | 565 | 5,000 | 20 | mullite+crist. |
| | | *DECOMPOSITION BY GRINDING* | | | |
| G 666 | sillimanite | 340 | 3,000 | 8 | sill.+kaol.+mica |
| G 674 | mull. | 330 | 2,400 | 35 | kaol.+? |
| G 675 | mull. | 450 | 3,700 | 35 | kaol.+pyroph.+hyd. ? |
| G 669 | andalusite | 360 | 3,000 | 6 | and.+kaol.+mica |
| G 665 | kyanite | 347 | 5,000 | 4 | kaol.+ky. |
| G 662 | kyanite | 375 | 5,000 | 26 | ky.+and.+kaol. |
| G 678 | kyanite | 425 | 4,500 | 32 | kaol. or nacrite |
| G 667 | kyanite | 438 | 10,000 | 6 | kaol. ?+ky.+mica |
| G 670 | kyanite | 510 | 13,500 | 3 | amorphous+mica |
| G 672 | kyanite | 515 | 14,000 | 11 | ky.+mica |
| | | *MISCELLANEOUS* | | | |
| 1719 | 1 kaol.+1 diaspore | 415 | 20,000 | 3 | diaspore+hyd. |
| 3119 | pyroph. | 195 | 250 | 69 | pyroph.+kaol. |
| 3033 | pyroph. | 225 | 200 | 18 | definite attack (mic.) n kaol. in *x*-ray. |

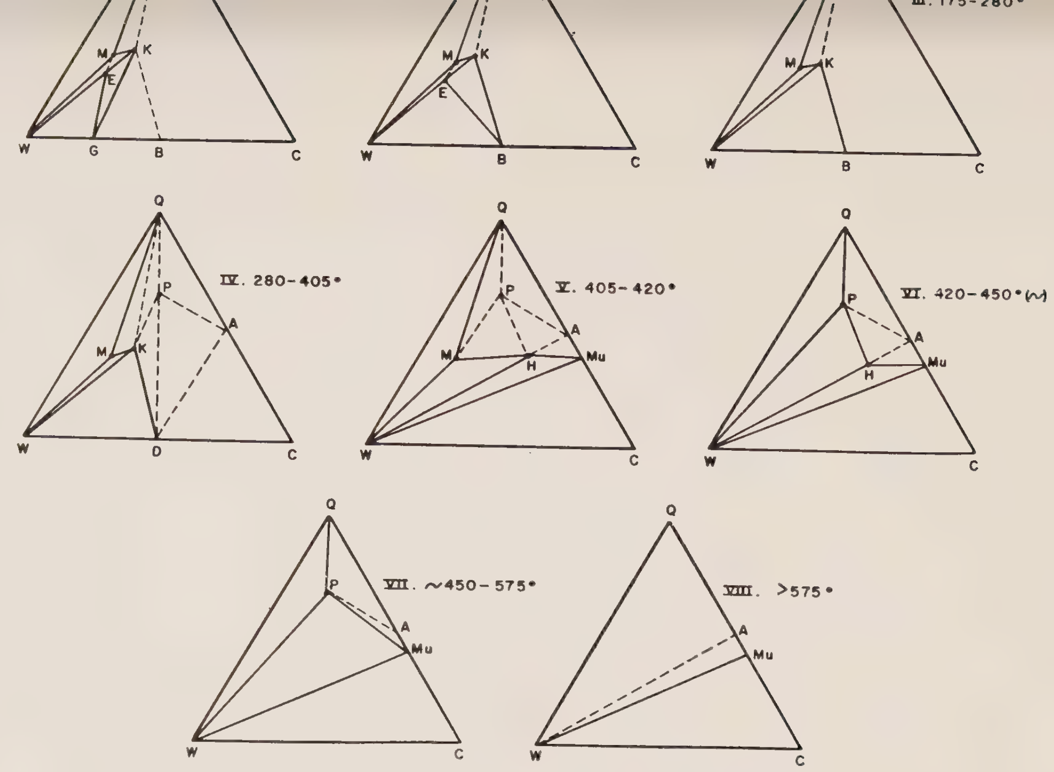

FIG. 6. Triangles showing compatible phases in the system $Al_2O_3$-$SiO_2$-$H_2O$ for various temperature ranges, illustrated for a pressure of about 10,000 psi. Triangles bounded by solid lines have been experimentally determined. Dashed lines indicate probable relationships. $A$ = andalusite, $B$ = boehmite, $C$ = corundum, $D$ = diaspore, $E$ = endellite, $G$ = gibbsite, $H$ = hydralsite, $K$ = kaolinite, nacrite, dickite, or halloysite, $M$ = Al-montmorillonite, $Mu$ = mullite, $P$ = pyrophyllite, $Q$ = quartz, $W$ = water.

10,000 psi, and except for the transition, endellite = halloysite + $H_2O$, increase in pressure (up to 20,000) or decrease down to about 2,000 ps would produce only a very small change in the equilibria. The equilibri determined in the present study apply only to triangles having $H_2O$ a an apex, *i.e.*, where an aqueous phase exists. Various attempts were mad to study phase equilibrium relations in composition having too little $H_2$ to give a water solution as one phase at equilibrium. Sealed platinun tubes, for example, were used, with the mixture inside and water pressur applied outside. With such small amounts of water present, reaction i extremely slow, and no useful data were obtained. The equilibria whic have been definitely established are therefore those involving water a one of the three phases.

The equilibrium data may also be expressed by a series of pressure temperature curves, as shown in Fig. 7. The curves represent conditio of univariant equilibrium, and the areas between the curves represe divariant equilibria, with three phases coexisting over a range of pressu and temperature for ternary mixtures. The triangles of Fig. 6 descri

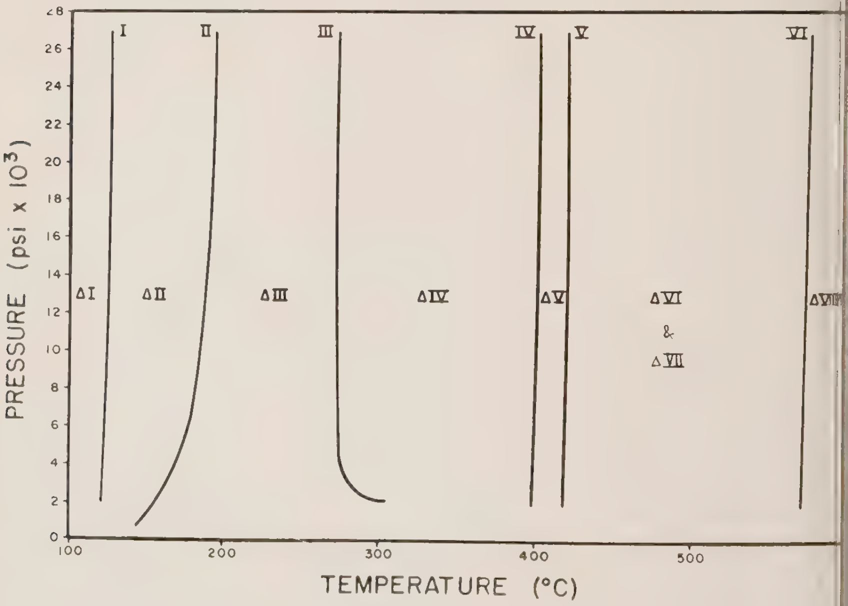

FIG. 7. Univariant curves for the system $Al_2O_3$-$SiO_2$-$H_2O$. The triangle numbers areas between curves refer to triangles in Fig. 6. Reactions taking place along the curv are as follows: I, Gibbsite⇆boehmite + $H_2O$; II, Endellite → halloysite + $H_2O$; III, boehn it⇆diaspore; IV, diaspore⇆corundum + $H_2O$, and kaolinite⇆hydralsite + pyrophylli + montmorillonite; V, montmorillonite⇆pyrophyllite + hydralsite + $H_2O$; VI, pyroph lite⇆mullite (or andalusite) + quartz + $H_2O$.

the latter equilibria. Univariant curves are almost vertical at pressures between 5,000 and 25,000 psi in this system, and in view of the error limits no attempt has been made to show "true" slopes.

2. *Discussion of Triangles.* Triangle I (Fig. 6) applies to temperatures below 130° C., the estimated decomposition temperature of gibbsite (Ervin and Osborn, 1951). Stable structures in equilibrium with the water phase in this temperature range are: quartz, montmorillonite, gibbsite, and either kaolinite or endellite. Whether tubular endellite or platy kaolinite will form depends on factors incompletely understood, except that endellite should not form if water pressures are lower than those at which endellite dehydrates to form halloysite. At the lower water vapor pressures, therefore, kaolinite is the stable phase, but it is not clear at present which of the two structures has the lower free energy at higher pressures. Hence, in Triangle I (Fig. 6), both endellite and kaolinite are shown as possible phases in equilibrium with a water phase, and a dashed line is shown joining montmorillonite and endellite. The pairs of crystalline phases coexisting in equilibrium with the aqueous phase at temperatures below 130° C., are therefore: quartz+montmorillonite, montmorillonite+endellite or kaolinite, and gibbsite+endellite or kaolinite. If insufficient water is present for the existence of an aqueous phase, other stable assemblages as indicated by the dashed lines are: quartz+montmorillonite+kaolinite and gibbsite+kaolinite+boehmite.

Halloysite is not shown as a stable phase inasmuch as it forms only through the dehydration of endellite. Various workers have concerned themselves with the decomposition of endellite, among them MacEwan (1946, 1948), Brindley and Goodyear (1948), and Sand (1952). Brindley and Goodyear presented data which would indicate that endellite, halloysite, and an aqueous phase coexist with two degrees of freedom. Assuming that the system halloysite-water is binary, with endellite being an intermediate compound in the system, this is not possible if equilibrium is presumed. Sand (1952) showed that endellite was stable up to 100° C. in the presence of water vapor pressures greater than the saturated vapor pressure. We extended these studies to 400° C. and 30,000 psi. water pressure. The experimental data indicate that endellite is stable up to about 175° C. at the saturated vapor pressure, but above this temperature, pressure has very little effect and endellite is not stable even at the highest pressures used (30,000 psi.). This was not the expected result, for it was thought that endellite would be stable as long as liquid water were present, *i.e.*, below the critical temperature and at pressures greater than the saturated vapor pressures. One criterion only, however, was used to judge the progress of the reaction. The sample after reaction was extracted wet, and immediately made up into a slide for examination by

$x$-ray diffraction, the elapsed time being 5 to 10 minutes. If the pattern showed the presence of endellite, it was concluded that endellite does not dehydrate under those conditions, even though halloysite was also found to be present. If the sample contained largely halloysite mixed with minor amounts of endellite, the run was repeated. In these experiments two different samples of endellite were run simultaneously, one from Eureka, Utah, and the other from Bedford, Indiana. It is not easy to understand the fact that in most of the runs the product contained halloysite. There are, of course, several operations during which part of the sample may dehydrate, e.g., in the removal from the bottle and partial drying to introduce the sample into the very small platinum envelopes, during the introduction into the long test-tube type bombs which are initially dry, and in the process of removing the sample and obtaining its $x$-ray pattern. Furthermore, small pockets of air may form in the envelope, permitting dehydration of endellite crystals near the air pockets before attainment of equilibrium. To discount this possibility the runs were repeated using a finely dispersed sample of endellite in the Morey type vessels. No different results were noted. If one considers that there is an exchange between the liquid and vapor water molecules, especially prior to the establishment of equilibrium, then should any of these exchanging water molecules originate from between the layers of the alumina-silica sheets in endellite, we can picture a possible irreversible collapse of the structure. The water layer in endellite may be considered essentially "solid" or "liquid," and not structureless, like vapor. That the water between the layers in endellite is essentially the same as unbound water is borne out experimentally by both our data and those of Sand (1950) inasmuch as the decomposition curve of endellite follows so closely, if not coincides with the vaporization curve of water.

The fact that endellite once formed, persists up to at least 175° C., would indicate that other factors besides composition must play a deciding role in its formation; for kaolinite also forms at these temperatures and in the presence of an abundance of water. The influence of *pH*, presence of other ions, and especially "structural control" depending on the parent mineral are all possibly important factors in determining whether kaolinite or endellite forms. Sand (1952) has shown that there is evidence for at least the last named factor. If during the formation of the clay minerals the system is saturated with water, either endellite or kaolinite may form (below at least 175° C.), but it is not clear which is the more stable. If the system is not saturated with water, endellite is unstable and should not form. Halloysite, as mentioned in an earlier section, forms only as a dehydration product of endellite.

Triangle II (Fig. 6), representing equilibrium relations between 130°

and 175° C. differs from Triangle I in the substitution of boehmite for gibbsite as the stable alumina hydrate.

Triangle III describes the relations in the range of about 175° C. to 280° C.[10] The assemblages kaolinite+boehmite+water, kaolinite+montmorillonite+water, and montmorillonite+quartz+water are stable. We have been able to synthesize kaolinite throughout this temperature range. Halloysite will also form, presumably as a metastable phase, if endellite is used as a starting material. Triangle III is applicable for water pressures in the range of 2,000 to at least 30,000 psi. If, however, pressures are less than 2,000 psi., then the relations shown in this triangle prevail up to about 385° C.[10]

Above 280° C.[11] and 2,000 psi water pressure, diaspore replaces boehmite as the stable alumina hydrate as shown in Triangle IV. The assemblages, diaspore+kaolinite+water, kaolinite+montmorillonite+water, and montmorillonite+quartz+water are stable. We still have no positive data for the equilibria in which an aqueous solution is not one of the three phases. However, natural associations of diaspore with pyrophyllite and with andalusite suggest the joins shown as dashed lines.

With increasing temperature, kaolinite and diaspore are no longer stable,[11] and relations between 405° and 420° C. are shown in Triangle V. The crystalline material which we here designate as "hydralsite" replaces kaolinite in the phase assemblages appearing in the system, and diaspore is replaced by corundum. Mullite is formed from high-alumina mixtures, and therefore the join, mullite-water is presumed to exist under stable equilibrium conditions. Joins involving hydralsite, however, may be metastable, although they appear reproducibly just above the decomposition temperature of kaolinite.

Above 420° C. aluminum montmorillonite is no longer stable, and relations are as described in Triangle VI. Pyrophyllite forms in high-silica mixtures, and hydralsite from compositions lower in silica. The upper limit of stability of hydralsite is not well-established, as has been previously discussed, but it persists to 450° C. or higher.

---

[10] The boehmite-diaspore transformation temperature varies from 275° C. at 20,000 psi. to 300° C. at 2,500 psi. water pressure (Ervin and Osborn 1951). Other reaction temperatures, such as diaspore$\rightleftarrows$corundum+water, boehmite$\rightleftarrows$corundum+water, and pyrophyllite$\rightleftarrows$mullite+quartz+water, are also a function of pressure, although at higher pressures the effect of pressure on temperature of reaction is usually small. A single temperature is given in order to simplify the discussion.

[11] The decomposition temperature of kaolinite is 405° C. at 10,000 psi. and is not greatly affected by pressure; the decomposition temperature of diaspore increases from 385° C. at 2,000 psi. of 415° C. at 20,000 psi. Therefore, at lower water pressures diaspore disappears as a stable phase at a lower temperature than kaolinite, and the reverse is true at higher pressures. For the sake of brevity, triangles are not shown for these two cases. At 10,000 psi., kaolinite and diaspore cease to be stable at approximately the same temperature.

Triangle VII indicates the relations where hydralsite is no longer obtained, and the assemblage pyrophyllite+mullite+water appears. The join shown as a dashed line connecting pyrophyllite with andalusite, sillimanite, or kyanite is probable, although we have no direct evidence for the stability of these three minerals in the temperature range indicated.[12]

Triangle VIII represents the relations above 575° C., where pyrophyllite is no longer stable, and the triangles mullite+corundum+water and mullite+quartz+water are stable. A dashed line indicating a possible join between sillimanite, andalusite or kyanite and water is drawn. As suggested previously, the difficulty in distinguishing sillimanite from mullite makes it possible that some of the equilibria we have shown as involving mullite may actually involve sillimanite.

## V. Discussion and Conclusions

1. The dehydration of endellite, which approximately follows the vapor pressure curve of $H_2O$ at lowest temperatures (below 100° C.) and increases to about 175° C. at 5,000 psi., suggests a temperature limit for the formation of this phase in nature. Recently it has been recognized that many of the clays previously described as "kaolin" contain significant amounts of endellite or halloysite, whereas others are nearly all kaolinite. We were unable to synthesize endellite in the present study, which may be partly a result of extremely slow reaction at such temperatures. The phase which was synthesized at higher temperatures, however, was a kaolinite, having characteristic hexagonal platy structure recognizable under the electron microscope, but never the tubular crystals of halloysite (or endellite).

Whereas we have not been able to synthesize the minerals endellite and halloysite, an upper stability temperature of about 175° C. has been indicated for endellite, at water pressures which would be attained near the surface in nature. Kaolinite would alternatively be formed within the same temperature range when the vapor pressure of water is insufficient to form endellite. The structural relationship between endellite and halloysite suggests that halloysite is only formed as a dehydration product of endellite and therefore endellite must always be formed first.

In nature, endellite and kaolinite may both form under apparently similar temperature and water vapor pressure conditions. In such instances it is not clear which is the more stable. Where the water vapor pressure is sufficiently high for endellite to form, the free energies of the two structures are probably very similar, and a factor such as arrangement of atoms in a previous structure becomes controlling. Sand (1952) has shown that in the North Carolina pegmatite area endellite is formed from the rapid weathering of feldspars, whereas the product always formed by weathering of primary or secondary micas is kaolinite. But within such environmental limitations endellite could only be formed when there is sufficient $H_2O$ present, within the pressure and temperature range indicated above.

---

[12] D. M. Roy (1953) has since shown that andalusite forms between 450° and 650° C.

2. An upper stability temperature of about 405° C. has been established for kaolinite, halloysite, nacrite and dickite, and this may be applied to natural occurrences. Much kaolinite is formed through weathering at low temperatures, but the upper temperature limit may also be applied to kaolinite formed by hydrothermal action and to nacrite and dickite, which commonly have a hydrothermal origin. Their presence or transformation may provide a fairly reliable temperature index in a metamorphic sequence. These temperatures would apply for burial of 1–5 miles.

3. The significance of the upper stability temperature for aluminum montmorillonite (420° C.) is less clear, since widespread solid solution occurs among the various natural montmorillonite minerals. For relatively pure "beidellites," i.e., montmorillonites consisting largely of alumina and silica, the upper temperature limit may be applied approximately. Systematic addition of other components is necessary to determine stability relations for a number of montmorillonites, and the results of the present study provide a framework for such additional work. The addition of MgO, for example has been shown (Roy and Roy, 1952) to increase the upper stability temperature of montmorillonite.

4. The absence of a phase corresponding to hydralsite in natural deposits may be a result of the presence of numerous cations which could enter the structure and convert it to various types of mica, which could form stably in the corresponding temperature range.

5. Pyrophyllite would be expected to crystallize only in the temperature range of 420° to 575° C. when excess $H_2O$ is present, i.e., sufficient water present for assemblages shown in the triangles (Fig. 6) to form. It is no doubt a stable phase, however, at much lower temperature (see Triangle IV) and will form if insufficient water is present to convert the mixture to higher hydrates. Whereas pyrophyllite is not a very common mineral—and the range 420° to 575° may be sufficient to include most of its associations—the occurrence of diaspore with pyrophyllite in some natural deposits suggests a temperature of formation of these deposits in the range of 275° to 405° C.

6. The failure to synthesize sillimanite, andalusite and kyanite has

been discussed in some detail. Sillimanite may have been synthesized in this study but the very fine-grained material could not be distinguished from mullite, and thus the relations are expressed in terms of equilibria involving mullite. Andalusite, sillimanite and kyanite have been decomposed hydrothermally at temperatures below 450° C., which indicates that they are not stable below this temperature in the presence of excess water. This is to be expected from the equilibrium relations established, wherein alumina-silica hydrates are stable. Andalusite, sillimanite and kyanite may be stable in this temperature range, but only where there is a deficiency of water with respect to that required to form the stable hydrates. In Fig. 6 it is seen that the composition $Al_2O_3 \cdot SiO_2$ (andalusite sillimanite and kyanite) is located behind the joins which describe equilibria involving $H_2O$ as one component. It is therefore possible that these phases may be stable with a deficiency of $H_2O$ at temperatures up to 575° C. Such a proposed relationship is indicated by dashed lines ir Triangles IV to VII.

7. The problem of the mullitization of kaolinite is of fundamenta importance to ceramists, and has been studied very extensively. Th results of the present work provide an answer to the *equilibrium* progress of the mullitization of kaolinite. Kaolinite decomposes finally at 405° C. (and obviously very much lower at the very low partial pressures of water obtaining under ordinary conditions of firing) and if sufficient water is present to cause recrystallization forms a little pyrophyllite along with hydralsite. On heating to about 500° C. pyrophyllite and mullite are formed, and above 575° C. kaolinite is completely "mullitized" to mullite and cristobalite. This therefore indicates the possibility of actually "firing" a ceramic body hydrothermally at less than 600° C. and obtaining the same phase assemblage as is obtained by firing dry at very much higher temperatures.

Data obtained under equilibrium conditions will usually not correspond to those obtained by various other methods. In the study of clays and hydrous oxides both differential thermal analysis and "dehydration isobars" are used. While these methods, especially the former, can serve as excellent tools for the characterization of a wide variety of phases, they can lead to quite erroneous results if used for other purposes such as the detection of other phases in a system and the determination of either the equilibrium constant or certain other thermodynamic parameters of a phase or reaction. Thus, it is well-known that by the use of dehydration isobars of several trihydrates of group III oxides no evidence is found for the existence of "monohydrates" which have been well-established. Differential thermal analysis would similarly indicate no other "peaks" or stepwise decomposition in these trihydrates. These methods are dynamic non-equilibrium methods in most cases, as may also be inferred from the frequent circumstance that the product of dehydration is "amorphous." And while they can provide a great deal of useful data on a particular process under specified conditions, these data will only in rare cases correspond to equilibrium, reproducible data. A relevant example in the recent literature is the study by Stone (1952) of the decomposition of the kaolinite group minerals. It is claimed that the reaction studied is

(1) $$Al_2Si_2O_5(OH)_4 = Al_2O_3 + 2SiO_2 + 2H_2O.$$

Such a reaction could probably never be made to take place under any conditions whatsoever, and certainly no evidence is presented for assuming that the reaction is other than

(2) Kaolinite = dehydrated kaolinite (not heated above 1,000° C.) + water.

Several erroneous conclusions are reached such as "in the steam (15 psi.) atmosphere it (kaolinite) will not decompose until about 475° C." We have shown that at even 1,000 atmospheres of steam the decomposition temperature is about 410° C. A decomposition temperature (under very low partial pressures of water vapor) of 465° C. is arrived at for diaspore (formula incorrectly given as $Al(OH)_3$ p. 94) whereas it has been shown not to exceed 400° C. at 10,000 psi. water pressures. A significantly (100° C.) higher decomposition temperature was assigned to dickite as compared to kaolinite, whereas we have shown that at equilibrium there is no significant difference in the equilibrium decomposition temperatures. These examples serve to illustrate the differences which may be obtained between equilibrium and non-equilibrium conditions. While from the former it is possible to predict something about the latter, the opposite is not always as sure a process. Thus the data from the present study would indicate that *DTA* curves of dickite would approach more and more closely those of kaolinite as the particle shape and size were made more and more equal. They also indicate that kaolinite may be decomposed below 400° C. under very low partial pressures of water. Under equilibrium conditions we also know that the first products of decomposition of kaolinite are hydralsite and pyrophyllite.

8. The data obtained herein suggest that mullite should not be as rare a mineral as has been supposed. While we have very little positive data on the stability of andalusite, sillimanite and kyanite, the data suggest that mullite should be formed whenever a relatively pure alumina rich aluminosilicate rock is heated above 575° C. at relatively low pressures. Such conditions prevail at the contacts of lava flows (or near-surface extrusive rocks), and certain clays and it is not inconceivable that mullite should occur in such localities. The phase called hydralsite herein, may also possibly be found in localities where relatively pure alumino-

silicate rocks have been metamorphosed. In this connection, it is interesting to note that the mineral zunyite has a composition quite similar to that proposed for hydralsite, and occurs in such an assemblage as mentioned above. The essential $Cl^-$ ion present in zunyite however, precludes a similarity in structure.

## ACKNOWLEDGMENTS

We wish to acknowledge the assistance of Dr. D. M. Roy in preparing the manuscript and checking the $x$-ray data in addition to making available her more recent data, and of V. G. Hill, K. C. Tu and R. H. Insley in a part of the laboratory work. This study was conducted as a part of an investigation into the stability relations of metamorphic mineral assemblages, sponsored by the geophysics branch of the Office of Naval Research, and first appeared as *Tech. Report No. 2, Contract N60Nr-26909*, dated Aug. 1, 1949.

## REFERENCES

BALCONI, M. (1941), Synthesis of sillimanite: *Rend. Soc. Min. Ital.*, **1,** 77.

BAUR, E. (1911), Hydrothermal silicates: *Zeit. Electrochem.*, **17,** 739. (1912), *Zeit. Anorg Chem.*, **72,** 119.

BATES, T. F., HILDEBRAND, F. A., AND SWINEFORD, ADA (1950), Morphology and structure of endellite and halloysite: *Am. Mineral.*, **35,** 463–484.

BOWEN, N. L., AND GREIG, J. W. (1924), The system $Al_2O_3$-$SiO_2$: *J. Am. Ceram. Soc.*, **7,** 238–254 and 410.

BRINDLEY, G. W. (1951), *X*-ray identification and structures of clay minerals: Min. Soc., London.

BRINDLEY, G. W., AND GOODYEAR, J. (1948), Dehydration of halloysite in relation to humidity: *Mineral. Mag.*, **28,** 407–422.

BRINDLEY, G. W., AND ROBINSON, K. (1946), Randomness in kaolin clays: *Trans. Farad. Soc.*, **42B,** 198–205.

BRINDLEY, G. W., AND ROBINSON, K. (1947), Fireclay: *Trans. Brit. Ceram. Soc.*, **46,** 49–62.

BRINDLEY, G. W., ROBINSON, K., AND GOODYEAR, J. (1948), Dehydration of halloysite in relation to pressure and temperature: *Mineral. Mag.*, **28,** 423–428.

BROWN, J. F., AND CLARK, D. (1952), The use of the three-stage electron microscope in crystal-structure analysis: *Acta Cryst.*, **5,** 615–619.

COWLEY, J. M., REES, A. L. G., AND SPINK, J. A. (1951), Secondary elastic scattering in electron diffraction: *Proc. Phys. Soc.*, **64,** 609–619.

ERVIN, GUY, AND OSBORN, E. F. (1951), The System $Al_2O_3$-$H_2O$: *J. Geol.*, **59,** 381–394.

EWELL, R. H., AND INSLEY, H. (1935), Hydrothermal synthesis of kaolinite, dickite, beidellite and nontronite: *J. Res Natl. Bur. Stand.*, **15,** 173.

FENNER, C. N. (1913), The stability relations of the silica minerals: *Am. J. Sci.*, 4th Ser., **36,** 331–384.

FINCH, G. I., AND WILMAN, H. (1937), Ergebn. exakt. *Naturwiss.*, **16,** 353.

GILLINGHAM, T. E. (1948), The solubility and transfer of silica and other non-volatiles in steam: *Econ. Geol.* **43,** 241.

HILL, V. G., ROY, R., AND OSBORN, E. F. (1952), The system alumina-gallia-water: *J. Am. Ceram. Soc.*, **35,** 135–142.

HOFMANN, V., ENDELL, K., AND WILM, K. (1933), Kristallstruktur und innerkristalline Quellung von Montmorillonit: *Z. Krist. (A)*, **104,** 265–293.

KENNEDY, G. C. (1950), Pressure-volume-temperature relations in water at elevated temperatures and pressures: *Am. J. Sci.*, **248,** 540–564.

DE KEYSER, W. L. (1951), Contribution to the study of sillimanite and mullite by *x*-rays: *Trans. Brit. Ceram. Sic.*, **50,** 349–364.

LACY, E. D. (1951), Minerals and magmas: Studies at high temperatures and pressures: *Nature*, **168,** 537.

LAUBENGAYER, A. W., AND WEISZ, R. S. (1943), A hydrothermal study of equilibria in the system alumina-water: *J. Am. Chem. Soc.*, **65,** 247–250.

MACEWAN, D. M. C. (1946), Halloysite organic complexes: *Nature*, **157,** 159.

——— (1948), Organic complexes of halloysite and montmorillonite: *Trans. Farad. Soc.*, **44,** 349–367.

MCATEE, J. L., AND MILLIGAN, W. O. (1950), *X*-ray diffraction examination of synthetic mullite: *Texas Jour. Sci.*, **2,** 200–205.

MICHEL-LEVY, M. C. (1950), Reproduction artificielle de la sillimanite: *Compt. Rend.*, **230,** 2213.

MOREY, G. W. (1942), Solubility of solids in water vapor: *Proc. Am. Soc. Testing Materials*, **42,** 986.

MOREY, G. W., AND INGERSON, E. (1937*a*), The pneumatolytic and hydrothermal alteration and synthesis of silicates: *Econ. Geol.*, **32,** 607–761.

———, ——— (1937*b*), A bomb for hydrothermal experimentation: *Am. Mineral.*, **22,** 1121.

NOLL, W. (1944), New investigations in water-silicate systems: *Kolloid Zeits.*, **107,** 181.

OSBORN, E. F. (1952), Andrew Carnegie, geochemistry and refractories: *Regional Tech. Meetings, Am. Iron and Steel Inst.*, Fig. 5, p. 110.

PERMYAKOV, V. M. (1936), The hydrothermal synthesis of kaolin: *Akad. V. I. Vernadskomu K. Pyat. Nauch. Dey.*, **1,** 563–580.

ROSS, C. S., AND HENDRICKS, S. B. (1945), Minerals of the montmolrilonite group: *U.S.G.S. Prof. Paper*, **205-B,** 23–79.

ROY, D. M. (1953), The hydrothermal synthesis of andalusite, *Am. Mineral.*, **39,** 140–143.

———, AND ROY, R. (1952), The system $MgO$-$Al_2O_3$-$SiO_2$-$H_2O$: *Bull. Geol. Soc. Am.*, **63,** 1293 (Abstract).

ROY, R. (1949), Decomposition and re-synthesis of the micas: *J. Am. Ceram. Soc.*, **32,** 202.

———, AND FRANCIS, E. E. (1953), On the distinction of sillimanite from mullite by infrared techniques: *Am. Mineral.*, **38,** 725.

———, AND OSBORN, E. F. (1952*a*), Some simple aids in the hydrothermal investigation of mineral systems: *Econ. Geol.*, **47,** 717–721.

———, ——— (1952*b*), Studies in the system alumina-silica-water, problems of clay and laterite genesis symposium: *Am. Inst. Min. Metal. Eng.*, 76–80.

ROY, R., ROY, D. M., AND OSBORN, E. F. (1950), Compositional and stability relationships among the lithium alumino-silicates; eucryptite, spodumene and petalite: *J. Am. Ceram. Soc.*, **33,**152–159.

SAND, L. B. (1952), Mineralogy and petrology of the residual kaolin of the southern Appalachian region: Ph.D. Dissertation, Pennsylvania State College.

STONE, R. L. (1952), Differential thermal analysis of kaolin group minerals under controlled partial pressures of $H_2O$: *J. Am. Ceram. Soc.*, **35,** 90–99.

TUTTLE, O. F. (1948), A new hydrothermal quenching apparatus: *Am. J. Sci.*, **246,** 628.

VAN NIEUWENBURG, C. J., AND BLUMENDAHL, N. B. (1932), The isotherms of water from 350°–480° and for pressures up to 600 kg/cm$^2$: *Rec. Trav. Chim.*, **51,** 708–741.

*Manuscript received Sept. 17, 1953.*

# MECHANISM OF "SOLUTION" OF QUARTZ IN PURE WATER AT ELEVATED TEMPERATURES AND PRESSURES*

A. F. Frederickson and Joseph E. Cox, Jr., *Washington University, St. Louis, Missouri.*

## Abstract

The solubilities of quartz in pure water at elevated temperatures and pressure are given. Water, under these conditions, differentially etches or corrodes the quartz and gives a solution or suspension that is not homogeneous. It is concluded that silica "dissolves" or disintegrates to give a colloidal suspension.

Quartz crystals contain discontinuities on a different scale. A cementing material of the same composition but of different physical properties from the bulk of the crystal is postulated to exist which holds the various lineage and mosaic elements together. The cementing material is thought to be preferentially removed during etching to produce some of the features observed. Some geological consequences of this argument are given.

A model is suggested to account for both the disintegration and regrowth of quartz.

## Introduction

Conflict still exists in geological and chemical literature over the state in which "dissolved" silica exists in natural waters. Experiments can be cited which indicate that the silica occurs largely as a colloidal dispersion, yet other work seems to point just as clearly toward true solutions.

The physical state in which silica exists in water is of particular interest to geologists in that it has a direct bearing on ideas concerning the breakdown and eventual rebuilding of important rock-forming minerals. Ideas concerning the mechanism of growth of minerals are also involved.

The experiments described in this paper were designed to determine if quartz, when attacked by water, dissolved into individual ions or whether the mechanism of decomposition or disintegration was more complex.

## Equipment

The solubility tests were carried out in two 195 cc. capacity stainless steel bombs, designed by the senior author at Washington University (Fig. 1). The steel used for the body of the bomb was a 100NT-2 alloy developed for jet-turbine blade use in the laboratories of the Massachusetts Institute of Technology under the direction of Nickolas J. Grant (Grant, Frederickson and Taylor, 1948). The other parts were made of various alloy steels possessing different coefficients of expansion so that the parts would shrink free on cooling thus ensuring easy opening

---

* Contribution number 171 of the Department of Geology, Washington University, St. Louis, Missouri.

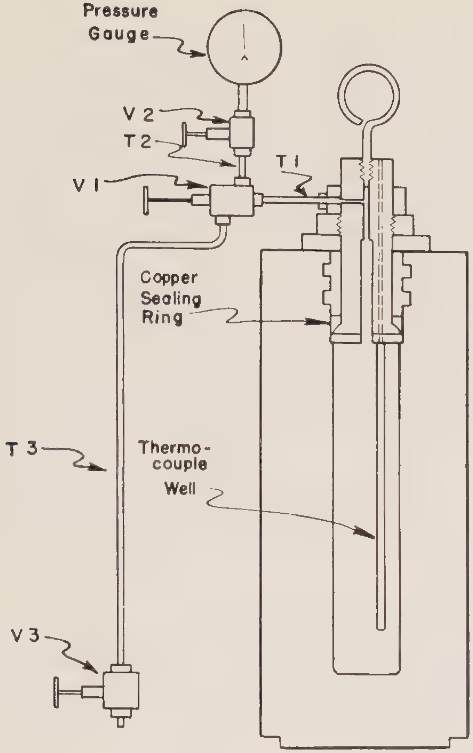

DIAGRAM OF HYDROTHERMAL BOMB
SHOWING TUBE AND VALVE ARRANGEMENT

FIG. 1. Valve V-1 is an offset tee-valve with two connections on the pressure side—one connecting to the bomb head, the other to the isolation valve and pressure gauge. V-2 is the isolation valve, and V-3 the sampling valve for withdrawal of the test solution. By evacuating tube T-3 then closing V-3, valve V-1 can be opened so as to fill T-3 with a known amount of solution. When V-1 is again closed, the test solution is withdrawn into an evacuated flask.

of the bomb. The bombs are designed to give high tensile strength at high temperatures and pressures. Contamination by corrosion within the bomb chamber was eliminated by preheating and quenching the empty bombs so that a durable and inert oxide surface was produced. No metals were detected in a spectrographic check on the solution from the bombs at 370° C., the maximum temperature used in the tests.

The bombs were heated in electric furnaces, which when closed produced a uniform heating throughout the bomb chamber. Temperature was controlled to within one degree Centigrade by a Leeds-Northrup controller-recorder, using calibrated chromel-alumel thermocouples. Pressure was produced by the expansion of water with increasing temperature, and controlled by the initial degree of filling of the bomb. Measurements of pressure were made on 4½″ Bourdon-type Ashcroft Laboratory Test Gauges (10,000 psi range) attached to the bombs by isolation valves as shown in Fig. 1. The Bourdon tube of the gauge and the adjoining pressure tubing (T-2, Fig. 1) were vacuum filled with distilled water to eliminate trapped air bubbles, and the isolation valve closed before attachment to the rest of the assembly. In this way pressure in the bomb could be brought to bear on the gauge when desired by opening the isolation valve. The compressibility of the water in the Bourdon tube under these test conditions was considered negligible.

Volume of the system was determined by vacuum filling with distilled water at 20° C. Pressure tubing and valves, suitable for use up to 6,00 psi, were used. The valve and tube arrangement was such that a sma amount of solution could be withdrawn during a test without coolin or opening the bomb. (See Fig. 1 and appended explanation.)

## PROCEDURE

"Solubility" was determined at two levels in the bomb. One series of tests was made by removing the test solution from the top of the bom chamber (see Fig. 1). A second series was made in which material from near the bottom of the bomb was sampled through a 5 inch tube welded on to the withdrawal opening of the bomb head. The source crystal of quartz was suspended by a platinum wire about half way between th two points of sampling. The bomb was in an upright position and was not rocked or disturbed during these experiments.

All tests were made at 300 bars pressure. The temperature range covered was from 200° to 370° C. Under these conditions of supercritical pressure and subcritical temperature for water, no gaseous phase existed in the system. The bomb was filled to 88% of capacity with distilled water ($pH=7$) at 20° C., so that when the temperature was raised to 200° C. a pressure of 300 bars would be produced in the bomb. After a previously determined time for establishment of equilibrium under the conditions of each test,[1] withdrawals of aliquots of solution were made. At the temperature and pressure of the first test, three samplings depleted the bomb of enough solution so that the temperature could be raised to 260° C. and the desired pressure of 300 bars maintained. This also provided

[1] In most runs approximately 100 hours elasped between samplings. This is as much as 3 to 4 times longer than it is necessary for the establishment of equilibrium particularly a the higher temperature where equilibrium is reached in a few hours.

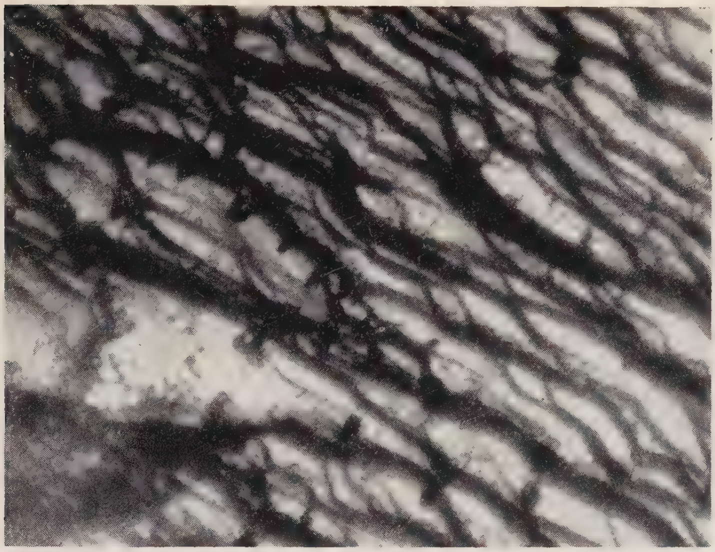

FIG. 2. Regrowth of quartz on the nutrient crystal. Magnification: 80×.

The surface of the water-etched quartz crystal has a "shingle" appearance as if it were made up of a series of smaller sheet-like units. The size of the sheets can be seen in the large, irregular protruding fragment in the lower left hand portion of the figure. The small irregular specks along the upper edges of the shingles are quartz that has regrown onto the parent crystal. The black streaks are shadows of the much larger, well-formed quartz crystals which seem to grow most often in the "valleys" between the shingles.

After the last withdrawal was made, the bomb was allowed to cool to room temperature before it was opened. We believe that the smaller quartz crystals along the edges of the shingles grew spontaneously when the bomb was first removed from the furnace. This is equivalent to an air quench. The larger crystals are believed to have developed during the longer cooling period between the time of the air quench and time of opening.

extra portions of test solution as a check. By withdrawing appropriate amounts of solution for each test, the temperature could be raised in steps of approximately 50° and the entire range from 200° to 370° C. covered without opening the bomb.[2] Each aliquot of solution was placed in weighed aluminum foil cups, evaporated and re-weighed to determine the weight of the residue. From this weight and the calculated amount of test solution in the sampling tube at the temperature and pressure of the run, solubility values in parts $SiO_2$ per hundred parts of water were determined.

---

[2] It might be suspected that the temporary pressure drop within the bomb caused by removal of test samples would result in nucleation and formation of particles of colloidal dimensions in the remaining solution. Exploratory runs were made without removing any of the solution, so that the pressure, once established, never fell below 300 bars. The results duplicated those given by the successive withdrawal technique, indicating that in the latter case (1) large nuclei had not been formed immediately on reduction of pressure, or (2) that if formed, they did not survive the temperature increase which followed each withdrawal. This point has a decided bearing on the interpretation of our solubility results, where it becomes necessary to explain a wide difference in solubility between the top and bottom of the bomb, and where the generation and segregation of colloidal sized particles seems to be the most logical answer.

This technique permits the operator to actually isolate a portion of the system while it is under the test temperature with only a very small drop in pressure. It is believed that this technique gives more reliable data than quenching methods which give low solubility results because some of the quartz grows back onto the parent crystal before it can be removed from the bomb (Fig. 2).

## RESULTS

### 1. *Apparent Solubility Curves*

The solubility values are plotted in Fig. 3. The upper curve represent material taken from the bottom of the bomb; the lower curve gives th values for the top of the bomb. The middle curve is drawn through th averages of the two sets of values and indicates the solubility in the bom

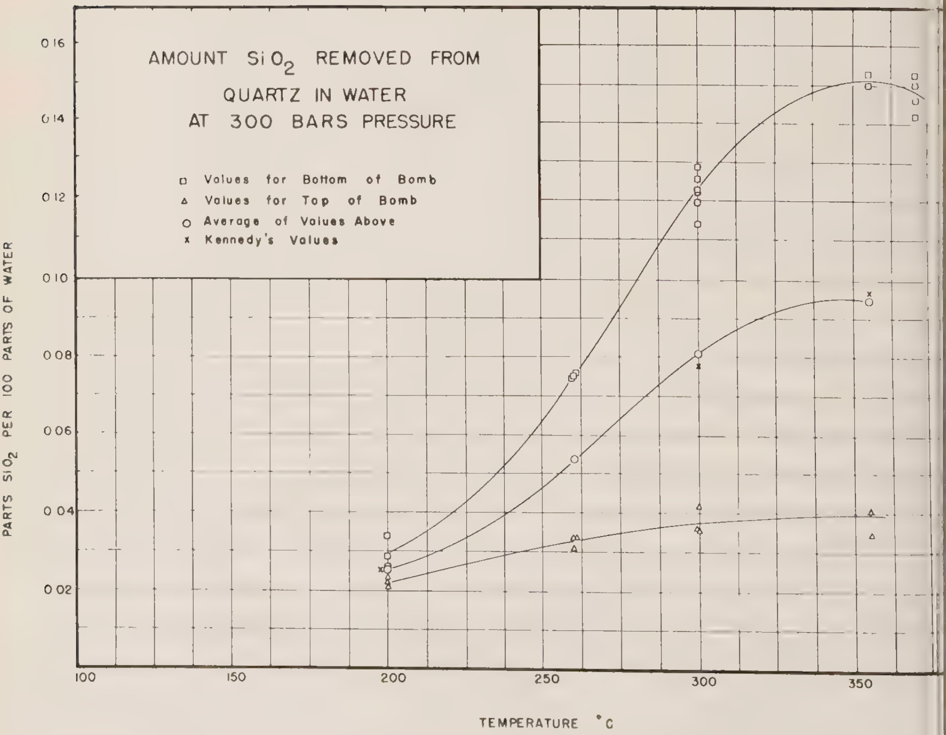

FIG. 3. "Solubility" of quartz in water at elevated temperatures and pressures.

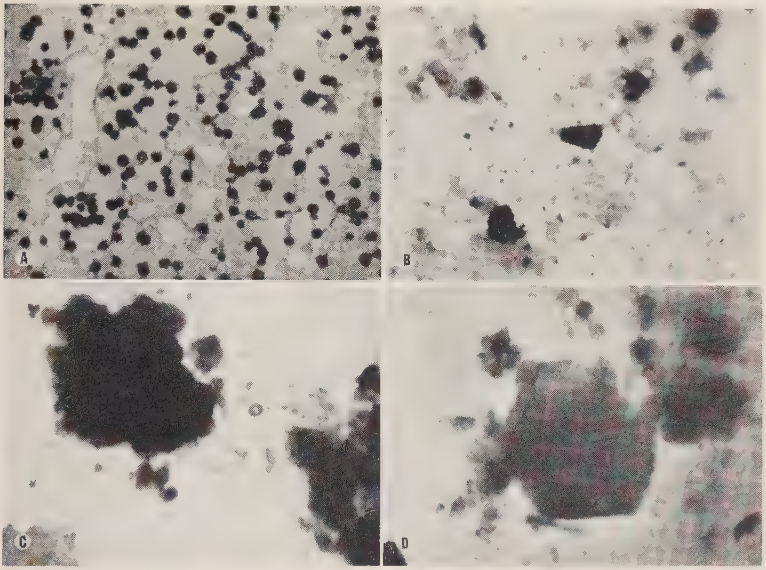

FIG. 4. Electron micrographs of withdrawal products. (From the bottom of the bomb.)

*A*. Mag.: 2,700×. The black spots are believed to be reaggregated silica gel. The gel phase forms a background film which shrinks and cracks on drying. The black spots have a rude polygonal outline which, in many cases, is hexagonal. The uniformity in particle size is remarkable.

*B*. Mag.: 2,700×. A desiccated gel forms the background. The truncated triangular fragment in the center of the micrograph is thought to be a fragment of the parent crystal.

A photographic emulsion cannot record the range in densities that actually exist in the specimen being examined. By varying the printing technique, it is possible to obtain a print that shows quite different apparent results. This fragment did not behave like some others when various tests were applied to it, consequently we believe it to be a solid fragment of the crystal.

*C*. Mag.: 7,000×. Here we see that some of the clumps are aggregates of the gel material. The edges of the clumps are very ragged. Different printing techniques reveal that the clumps are various thicknesses of the gel films and fragments. These clumps are very porous and look much like the first stages of aggregation of many aluminum hydroxide precipitates.

*D*. Mag.: 8,000×. Here is a relatively well formed hexagonal platelet of quartz. It is made up of tiny gel fragments. Each gel fragment is very thin. They often roll up into elongate tube-like particles.

This specimen is an enlargement (made in the electron microscope) of one of the tiny clumps shown in *A*. Apparently all the clumps shown in *A* actually are tiny quartz crystals "in the making."

taken as a whole. For comparison, some points obtained by G. C. Kennedy (1950) using a different technique have been plotted as x's. Note that the averages of the solubility values for top and bottom of the bomb closely correspond to Kennedy's values (1950).

### 2. *Electron Micrographs of Products*

The products of the decomposition of quartz were examined under an electron microscope. The photomicrographs in Fig. 4 illustrate the range of particle sizes which occur in the solution at room temperature and pressure. The larger masses are re-aggregates and seem to be made up of many chunks of various sizes, most of which are essentially equidimensional. Where some of these fragments have remained dispersed as in photo *A*, they show remarkable uniformity in size and shape, and many have outlines that look suspiciously hexagonal. These crystals are probably aggregates of still smaller particles. Their maximum dimension is 0.27 microns (2,700 Å), whereas the dimension of the average particle in the bomb was calculated to be of the order of 0.08 micron (800 Å). Near these crystals, and extending from them, can be seen traces of a very fine-grained $SiO_2$ residue left as the droplet of water containing it evaporated.

In photo *D*, the incomplete hexagonal crystal which is taking shape has borders that give a good idea of the size and shape of its building blocks. The length across this aggregate is approximately 2.5 microns. Similar aggregations of various sized particles may be seen in the other photos.

Photos *B* and *C* are typical of the quartz residue in various states of aggregation. The more finely divided material has come out of solution or suspension to produce a patchy film which forms the background in these photomicrographs, and the larger fragments have grouped themselves in clusters.

### 3. *Electron Micrographic and Petrographic Studies of Quartz Surfaces*

Beyond the evidence given by the two solubility curves (Fig. 3) that "dissolved" quartz exists in different sizes, it is not experimentally possible at present to make a direct determination under test conditions of the actual state of aggregation of the larger sizes in the bomb. A good indirect means of learning something of the suspended particles is to study in detail the surface of the parent quartz crystal which furnished all the $SiO_2$ to the system. Both the electron and petrographic microscope can be used for this purpose.

Collodian molds or replicas were made for examination under the electron microscope. The replicas were shadowed with chromium according to standard procedure and photographed. Some of the results are shown in Figs. 5 and 6. The electron micrographs clearly show that the solution action has been preferential even when material is dissolved along the same crystallographic direction.

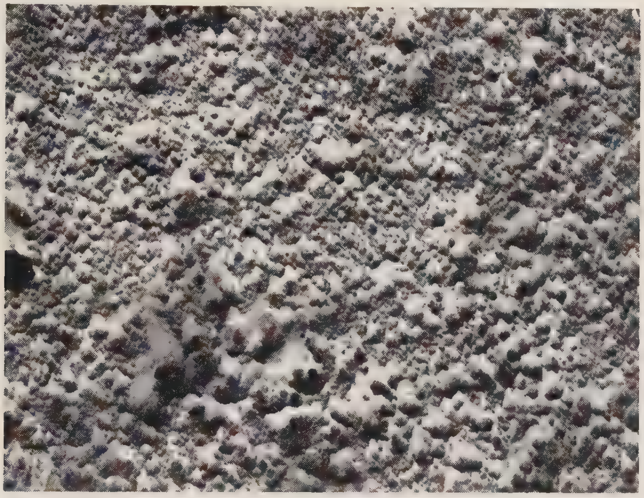

FIG. 5. Electron micrograph of a quartz surface. Chromium-shadowed negative collodian replica. Mag.: 12,000×.

The circular elevations on the surface of a water-etched quartz surface are interpreted to represent the ends of resistant rods. The much larger rods or mosaic units shown in Fig. 7*D* must therefore be made up of smaller units. The similarity in diameter between these circular elevations and the rods shown in electron micrographs of albite (Fig. 6, *Am. Mineral.*, **39,** 747, 1954), is striking.

With suitable illumination techniques (Frederickson, 1953*a*), a considerable amount of detail can be seen on hydrothermally etched quartz crystals. Quartz seems to consist of an aggregate of bundles or elongated fragments (Fig. 7, *A*, *B* and *C*) which, in turn, are made up of smaller elongated units or rods (Fig. 7*D*).

## EVALUATION OF RESULTS AND DISCUSSION

The wide difference in solubility values between the top and bottom of the bomb seems best explained by the segregation of $SiO_2$ particles—much too large to be considered truly dissolved—from the bulk of the solution and their gradual settling to the lower part of the bomb. The curve for material taken from the top of the bomb is not to be interpreted as truly dissolved silica alone, but includes a considerable amount of colloidally dispersed silica of smaller particle size than that at the bottom of the bomb.

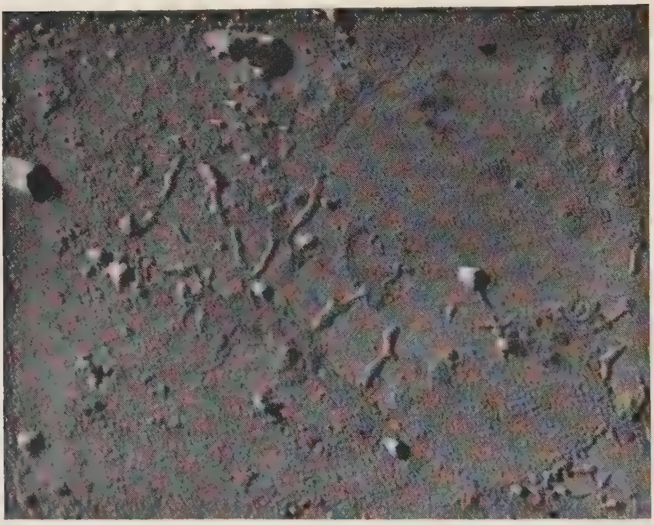

FIG. 6. Electron micrograph of a quartz surface. Chromium-shadowed, negative collodian replica. Mag.: 12,000×.

The first stages of etching appears to be a removal of a rather uniform layer. The uppe right hand quarter of the micrograph shows a plateau-like surface that has irregular outlines and a few deep furrows and pits. The shadows around the edges of the plateau are quite regular indicating an approximate equal depth of removal of material from the surface. Apparently the attacking solution vigorously corrodes loci of weakness whenever they are encountered to produce pits of various shapes. (The pits here appear as tiny elevations with white shadows because this is a negative replica.)

Something of the nature of the average particle size of "dissolved" quartz in the bomb is given in the following table:

AVERAGES OF CERTAIN CHARACTERISTICS OF "DISSOLVED" QUARTZ

| Temperature ° C. | Average Weight in gm/particle | Average Volume Cm$^3$ | Average Number $SiO_2$ units/particle |
|---|---|---|---|
| 200 | $1.4\times10^{-18}$ | $5.2\times10^{-19}$ | $1.4\times10^{4}$ |
| 260 | $1.5\times10^{-18}$ | $5.5\times10^{-19}$ | $1.5\times10^{4}$ |
| 300 | $1.7\times10^{-18}$ | $6.5\times10^{-19}$ | $1.7\times10^{4}$ |
| 355 | $2.1\times10^{-18}$ | $7.7\times10^{-19}$ | $2.1\times10^{4}$ |

Calculations for the above data are based on an equation used in sedimentation equilibrium studies which relates concentration and depth of suspension in a column of water to particle density and volume (Getman, F. H., and Daniels, F.; (1947) Outlines of Physical Chemistry).

These tests verify the long standing idea that silica does not exist in dilute water solutions in the form of simple ions. The tests also show that at equilibrium under constant temperature-pressure conditions, the silica removed from quartz exists as particles of widely different size; segregation of these particles is demonstrated, and it is suspected that a diffuse stratification of sizes occurs throughout the bomb chamber.

Here two questions arise:

(1) What is the origin of the colloidal sized particles in the bomb—are they flocculates from a true solution of $SiO_2$ or are they small crystalline fragments removed from the source crystal?

(2) What determines the solubility limit at a given temperature and pressure, and what sort of equilibrium is reached for a silicate mineral such as quartz?

The study of the surface features of the parent quartz crystals showed that along the edges of the stubby to elongated pencil-shaped units that make up the bulk of the crystal, important discontinuities (Fig. 7, *A* and *B*) exist. In addition, when closely examined, quartz appears to have a regular mosaic structure (Frederickson, 1953) the smallest units of which are rod-shaped and are about 0.0009 mm. thick. The length to width ratio averages between 30:1 and 40:1. The rods are laid side-by-side to form sheets or "shingles" so commonly observed on etched quartz surfaces. The sheets are relatively coherent, therefore the rods must be "cemented" or otherwise held together by silica of some kind. Although the larger elongated units are relatively well oriented on a small scale, they show considerable misorientation on a large one. The visible lines produced by this misorientation are called lineages and can be seen in all natural (and synthetically prepared) crystals. Because the crystal, as a whole, has considerable strength, these units must be strongly cemented together. It also follows that this cement that binds the units together must have slightly different properties from the bulk of $SiO_2$ in the units. If two dendrites or lineage elements start out with a uniform orientation and develop a lineage, the cement must contain a number of bonds at angles different from what is normally found. The cementing material may therefore be considered to exist in a strained or slightly disordered condition and consequently will be more soluble than the units it binds together.

We believe that the equilibrium existing in the bomb can be represented by the following equation:

$$\text{PARENT CRYSTAL} \rightleftarrows \text{Solid fragments} + \text{silicate ions} \rightleftarrows \text{solid fragments and/or colloidal dispersion}$$

Under conditions of elevated temperature, the water in the bomb dissociates to form an increased number of hydrogen ions (*I.C.T.*, p. 152,

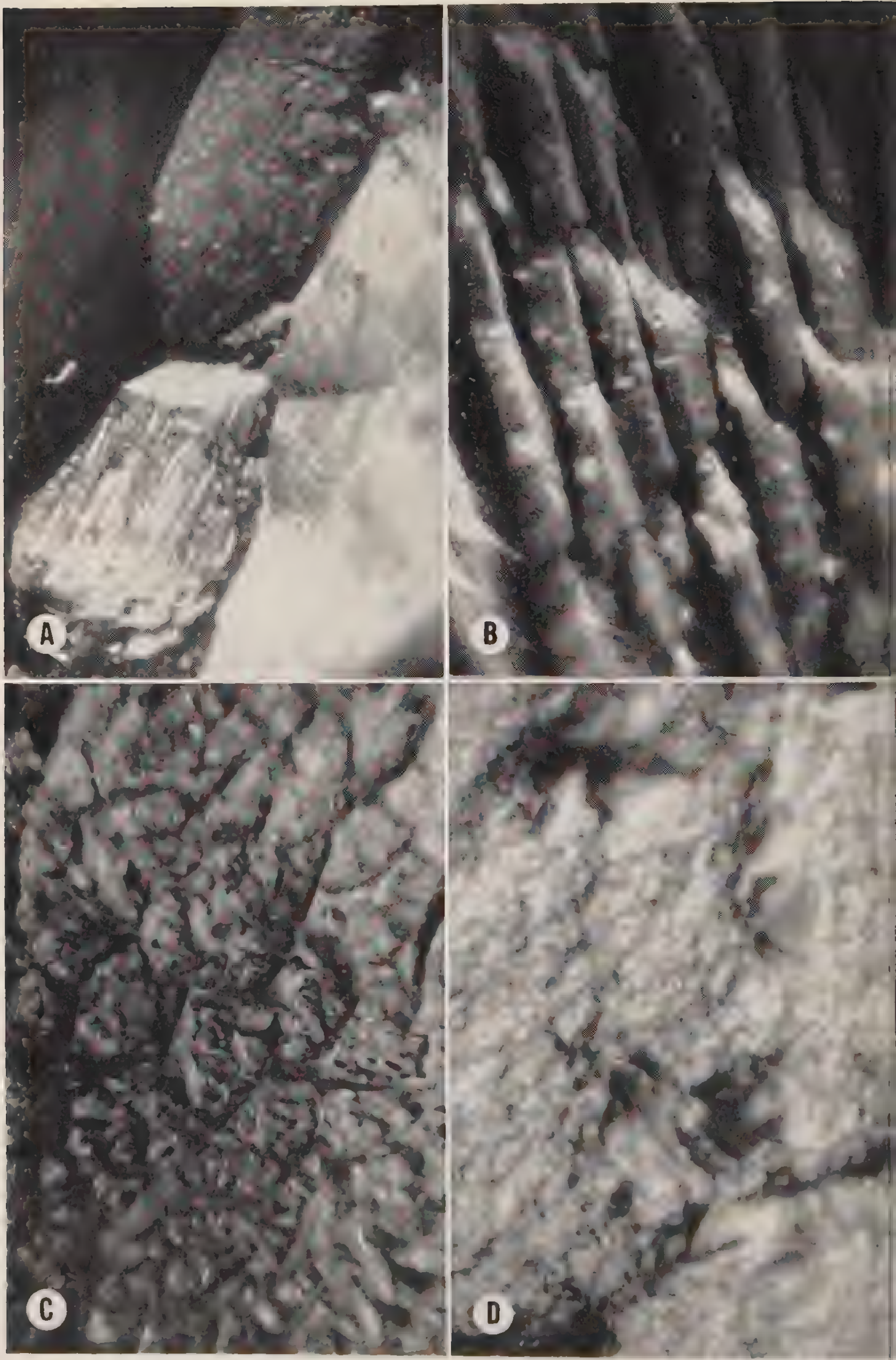
A
B
C
D

1929) which attack the weakest oxygen bonds[3] in the parent crystal. The weakest bonds in the crystal are found along the lineages and other discontinuities; i.e. in the material we have called the "cement." This results in the formation of silicate ions and the removal of some of the mosaic chunks of quartz from the parent crystal. These chunks enter the solution and, if large enough, settle toward the bottom of the bomb.

The silicate ions do not remain simple but rapidly polymerize to form long, complex ions better termed a silicate polyelectrolyte (Katchalsky, 1950, 1951).

The equilibrium between the solid fragments and the polymerized silicate ions is determined by the temperature of the system which, in turn, controls the number of hydrogens ions available to attack O-O bonds and form new OH bonds.

---

[3] It is a relatively simple matter to imagine how water attacks and dissolves crystals like the feldspars and pyroxenes which contain relatively weak bonds between oxygen and large cations, but in the case of quartz where only O-O or Si-O bonds exist, some reason for the preferential attack of certain of the O-O bonds must be found.

FIG. 7. Photomicrographs of various structures observed on quartz surfaces.

*A*. Mag.: 180×. Irregular shaped masses of quartz separated by important lineage surfaces. Note that these masses are rounded and certainly do not represent any crystallographic surface. These surfaces, then, must be relatively unstable. Deep pits, striations and other irregularities indicate that on this relatively large scale quartz is far from being a homogeneous crystal even though it may show, on a hand specimen scale, relatively perfect crystallographic outlines.

*B*. Mag.: 225×. These are relatively large rods that apparently are made up of the sheets shown in Fig. 2 except that the sheets are broken up by a large number of lineages which are more or less perfectly aligned to give this rod-cluster effect. Here again we see that quartz is very inhomogeneous and that it should not be surprising that it is selectively etched by suitable solvents.

*C*. Mag.: 90×. Water etched irregularities on the surface of quartz crystal which looked perfectly transparent and clear. Spectrographic analyses of these crystals indicated that the amount of contamination was relatively small. Because the whole crystal shows these and the other irregular etch effects shown above, it is highly improbable that substitutions for Si play an important role in the production of weak zones within the crystal which permit it to be selectively etched.

*D*. Mag.: 150×. A quartz oscillator plate, which had been acid etched with HF, was then ground, polished and placed in the bomb for approximately 15 hours. Here we see the very deep pits produced by the HF etch as well as a mottled, rough surface. Within the deep pits can be seen the sheet or shingle structure shown in Fig. 2. Here we see that the sheets are actually made up of a series of small rods held together by some sort of silica cement. The diameter of these rods is very uniform.

The intersections or surfaces of contact of the rods and other irregularities shown in these photomicrographs must be places of weakness in the crystal which can be selectively etched with suitable solvents. Not only is the crystal relatively porous, but when attacked by corrosive solvents (water, for example, under the proper conditions) the quartz crystal may become a veritible molecular sieve. Is it along zones such as these that various cations move when these crystals are part of a metamorphic or other rock?

Although this model has its defects, we think it is essentially correc because it better accounts for our experimental results than any other It also offers a more rational explanation of certain problems concernin crystal growth. For example, a large patent literature (Stericker an Hazel, 1950) exists on the role played by silica adhesives in system where it is desired to cement some material (such as phosphors) to glas (television tubes). This analogy has a direct application to the problem at hand.

The silica is introduced into the system in the form of sodium silicate The cementing process can be described in two steps:

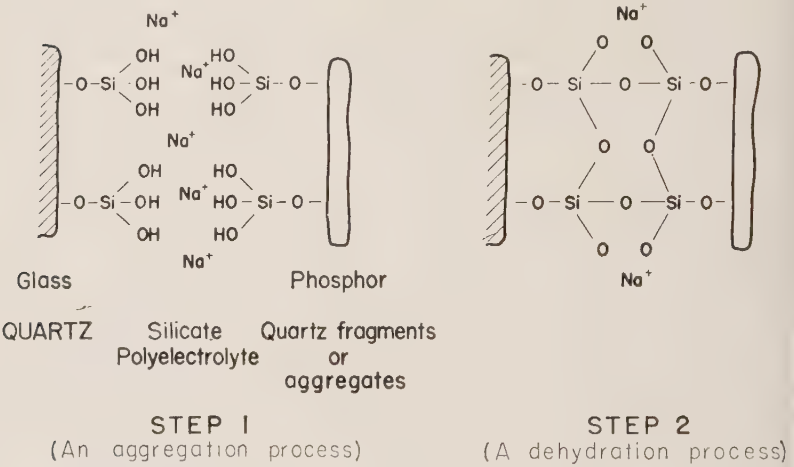

FIG. 8

The silicate in the diagram is simplified to show only one $Si^{+4}$ ion wherea it actually may contain from 5 to 20 or more. Step 1 involves oxyge bond formation by electron sharing between one of the oxygen ions c the silicate and an oxygen on the glass surface. The same reaction occur between the sodium silicate and the phosphor. The role played by th sodium ions is to bring these two phases, which now possess identica surface charges, into close approach. As soon as the phases are clos enough together (flocculation), oxygen-bond formation can again occu as is illustrated in Step 2. This essentially is a dehydration process whic releases hydrogen ions which may combine or be shared with oxygen ion to form water. If this reaction is correct (the process works on an industrial scale) we can see why the hydrogen-ion concentration of the startin system is so critical.

Now substitute the words *QUARTZ*, *Silicate polyelectrolyte*, and *quart* *fragments* for those shown in Step 1 of the above diagram and we have the situation which is believed to prevail in the bomb during decomposition of quartz. In the bomb, however, H ions take the place of Na.

The decomposition of quartz results when the hydrogen ions of the water attack the cement to remove mosaic or larger units from the parent crystal. The silicate fragments are in turn attacked by the hydrogen ions and further decompose until the available hydrogen ions are utilized by the silicate polymers and oxygen ions on the surface of the crystalline fragments. Both the fragments (Fig. 4, *A*) and the silicate-polymer (gel) phases (Fig. 4, *A* and *B*) can be directly observed in the electron micrographs of the "solution" siphoned from the bomb. The gel phase results from a more or less complete random polymerization of the silicate when the temperature of the "solution" is rapidly lowered after isolation and extraction from the bomb.

## Application of this Model to Quartz Synthesis Problems

Quartz can be hydrothermally synthesized from a wide range of solutions, the most promising of which are restricted to sodium hydroxide and carbonate. Although very large crystals (up to several pounds) can be made, they are not always as perfect as is desired. The above model suggests that the reverse of the disintegration process might not yield the best crystals. Any crystal fragment may act as a site for development of twins, lineages or other defects. Silicate solutions would therefore appear to be better nutrients than solid quartz maintained in a chamber at a higher temperature than the growing crystal.

If the silicate in solution actually is in the form of large polymers or polyelectrolytes, the initial *pH* and Na-content of the solution will be critical. The degree of openness of the coiled polymers is determined by their degree of ionization and the number of positive ions on the outside of the coil. Addition of positive ions to the coil will cause it to expand or straighten out due to repulsion of the large positive ions along the chain. It is highly probable that optimum crystal growth only occurs when the coiled polymers have the correct surface charge and configuration: they must have a certain degree of openness or uncoiling before they can polymerize to form a *regular* crystal network. If tightly coiled units are dumped onto a crystal surface, it is possible that they might act as sites for the complex twinning often observed.

According to this concept then, twinning, so-called spontaneous nucleation, blue-needle formation and several other kinds of defects are primarily due to sudden changes in the hydrogen-ion concentration of the system induced either by introduction of gasses or sudden temperature changes.

## Physical State of Silica in Natural Dilute Solutions

From a geological point of view, it is important to know whether or not silica in natural waters, under atmospheric conditions, exists as individual simple ions or colloidal complexes. Roy (1945) has recently argued that silica exists as individual ions and not as colloids in natural waters. His best supporting evidence is that during molybdate titrations, silica, in the assumed form of $SiO_3^=$ ions, is precipitated stoichiometrically and that the titration data check gravimetric determinations. Recent work in our laboratories on sodium silicate (Frederickson and Feng, 1953) indicates that, in dilute solution, this material behaves like a large polyelectrolyte and not as a simple ion. This may account for the checks between the titration and gravimetric work without proving that the silicate exists as simple ions.

## Acknowledgments

This work was done as part of a U. S. Army Signal Corps research contract (*No. DA-36-039 sc5513*). Their support and encouragement is gratefully acknowledged.

## References

Frederickson, A. F. (1953*a*), A method of effectively increasing the resolving power of a microscope to reveal unsuspected detail in thin section: *Am. Mineral.*, **38,** 815–826.

Frederickson, A. F. (1953), Mosaic structure in quartz: *Am. Mineral.*, in press.

Frederickson, A. F., and Feng, P. (1953), The polyelectrolytic nature of some silicate solutions. In preparation.

Getman, F. H., and Daniels, F. (1947), Outlines of Physical Chemistry. 7th Ed. John Wiley and Sons, New York, N. Y.

Grant, N. J., Frederickson, A. F., and Taylor, M. E. (1948), Heat resistant alloys from 1200° to 1800° F.: *Iron Age,* **161,** No. 12, 73–78; No. 15, 75-81; and No. 16, 84–93.

I.C.T. International Critical Tables (1929), vol. VI, p. 152. McGraw Hill Book Co., Inc., New York, N. Y.

Kennedy, G. C. (1950), A portion of the system silica-water: *Econ. Geol.*, **45,** 629–653.

Roy, C. J. (1945), Silica in natural waters: *Am. Jour. Sci.*, **243,** 393–403.

Stericker, W., and Hazel, F. (1950), The adhesion of phosphors on cathode ray screens: *J. Phys. and Colloid Chem.*, **54,** 1045.

*Manuscript received Oct. 13, 1953*

# STUDIES OF URANIUM MINERALS (XV): SCHROECKINGERITE FROM ARGENTINA AND UTAH*

Cornelius S. Hurlbut, Jr., *Harvard University, Cambridge, Massachusetts*

## Abstract

Schroeckingerite crystals have been found at Moab, Utah, and San Isidro, Argentina. They are orthorhombic pseudohexagonal, flattened on {001} with additional forms {010}, {110}, {014}, {012}, {011}, {021}, {041}, {118}, {114}, {112}, {111}. Unit cell dimensions are; $a_0=9.69$ Å, $b_0=16.83$, $c_0=14.26$ ($a_0{:}b_0{:}c_0=0.5758{:}1{:}0.8473$). Space group *Cmmm*. Z=4. Optically biaxial (−), $X=c$, $Y=b$. Argentina: $nX=1.492$, $nY=1.543$, $nZ=1.544$. $2V=10°$. $G=2.550$. Utah: $nX=1.490$, $nY=1.537$, $nZ=1.538$. $2V=18°$. $G=2.544$. Calculated $G=2.547$. Dehydrated over $H_2SO_4$, schroeckingerite goes to $NaCa_3UO_2(CO_3)_3SO_4F \cdot 4H_2O$ and becomes hexagonal with unit cell dimensions: $a_0=9.72$ Å, $c_0=11.03$ ($a{:}b=1{:}1.1348$). Z=2. Optically uniaxial (−). $nO=1.581$, $nE=1.532$. Measured $G=2.86$, calculated $G=2.874$.

## Introduction

Schroeckingerite [$NaCa_3UO_2(CO_3)_3SO_4F \cdot 10H_2O$] from two widely separated localities arrived almost simultaneously at the Harvard Mineralogical Museum early in 1953. One specimen from the Shinarump No. 3 Mine, Seven Mile Canyon near Moab, Utah, was sent by Professor J. W. Gruner. The other material, from Mina "La Soberania" San Isidro, Mendoza Province, Argentina, had been acquired by the late Mr. Samuel Gordon and was generously given to Harvard by Mrs. Gordon. Schroeckingerite has previously been described from three other localities: 1. Joachimsthal, Bohemia, by Schrauf (1873); 2. Wamsutter, Wyoming, by Larsen and Gonyer (1937), and called by them *dakeite;* 3. Yavapai County, Arizona, by Axelrod *et al.* (1951). Schroeckingerite from all these localities is reported to be in minute scales aggregated into globular groups (Joachimsthal), pisolites (Wyoming) and rosettes (Arizona). The only mention of individual crystals was by Schrauf who described six-sided scales.

## Morphology

The Argentine schroeckingerite collected by Mr. Gordon had been carefully separated by him so that the mineral association is unknown. It is in minute scales, some aggregated into rosettes, but others are isolated transparent crystals many of which show a hexagonal outline. The maximum dimension of individual crystals is one millimeter and the thickness rarely exceeds 0.02 millimeter. Five crystals, thicker than the others, had been mounted on pins by Mr. Gordon for goniometric measurement. The largest of these was about 1 millimeter in diameter and 0.2 millimeter thick and showed many crystal faces. Examination of the thin hexagonal plates showed that many of them also had truncating faces.

---

* Contribution No. 348 of the Department of Mineralogy and Petrography, Harvard University, Cambridge, Massachusetts.

The schroeckingerite from Utah occurs associated with gypsum in seams in a shale. Much of it is in crusts but there are many isolated crystals with hexagonal outline showing truncating faces. All but the thinnest crystals are aggregates of superimposed crystals in nearly parallel position. When viewed through the microscope, the nonparallelism of the aggregated individuals appears as though the smaller crystals, when compared to the major crystal, had been rotated slightly about the *c* axis and that the (001) planes were parallel (Fig. 1). With the optical goniometer one can see that there is also a nonparallelism of the plates amounting to as much as three degrees. Aggregates similar to these are found also on some of the Argentine crystals.

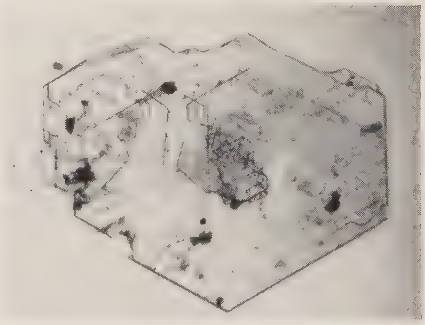

FIG. 1. Schroeckingerite, Moab, Utah. ×50.

Eighteen crystals from Argentina and twenty crystals from Utah were mounted for measurement on the two-circle goniometer with the largest face (001) polar. Of these, eleven gave no reflections except from the polar face, but the others all showed two or more measurable faces. Similar form development was shown at the top and bottom of the crystals. There were no observed systematic differences in the angular measurements of the crystals from the two localities. On many crystals curved faces made it impossible to read some rho values closer than two degrees.

All the faces are arranged in vertical zones at 60° or nearly 60° to one another (Fig 2). There is no regularity in the divergence from 60°, for on some crystals all zones fall within a few minutes of 60°, whereas on others the zones may be $58\frac{1}{2}°$ to $61\frac{1}{2}°$ apart but without systematic ar-

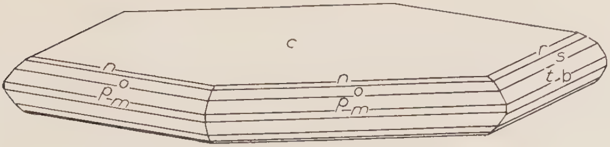

Fig. 2. Schroeckingerite, Argentina.

rangement. This may be due in part to the slight disorientation of the superimposed plates.

From the morphology alone one might conclude that schroekingerite is hexagonal, but from other evidence it appears to be orthorhombic with a striking pseudohexagonal symmetry. All the faces fall in the *hkl* and 0*kl* zones, and with the poor angular readings, it is impossible to tell in which zone a face lies. Consequently, in the measured values of Table 1, the forms of the two zones having similar rho readings are grouped together and the phi readings are given as though all forms belonged in the 0*kl* zone. The principal forms are shown in Fig. 2. This drawing is a fair representation of the largest Argentine crystal but appears many times thicker than the average plate.

Table 1. Schroeckingerite—Two-Circle Measurement

| Forms | Mean | | Range | | No. of Faces |
|---|---|---|---|---|---|
| | φ | ρ | φ | ρ | |
| *c* 001 | — | 0°00′ | — — | — — | 27 |
| *b* 010, *m* 110 | 0°06′ | 90 05 | 1°20′—1°10′ | 89°45′—90°25′ | 22 |
| *n* 114, *h* 118 | 0 06 | 11 51 | 1 20 —1 10 | 11 38 —12 18 | 3 |
| *r* 012, *n* 114 | 0 06 | 23 09 | 1 20 —1 10 | 22 15 —23 58 | 7 |
| *s* 011, *o* 112 | 0 06 | 41 02 | 1 20 —1 10 | 39 50 —42 55 | 43 |
| *t* 021, *p* 111 | 0 06 | 59 34 | 1 20 —1 10 | 58 05 —61 35 | 18 |
| *u* 041, or 221 | 0 06 | 73 30 | 1 20 —1 10 | 73°30′ | 1 |

Because of the wide range in the angles measured for any given form as well as the inability to distinguish forms in one zone from those in another, it is felt that axial ratios calculated from the mean values would be much less accurate than those derived from the *x*-ray measurements of the unit cell. The axial ratios and calculated angles in Table 2 are, therefore, based on unit cell measurements.

## Unit Cell and Space Group

Rotation and Weissenberg *x*-ray photographs using copper radiation and nickel filter were taken of schroeckingerite rotating about the *c*

Table 2. Angle Table for Schroekingerite*

Orthorhombic; dipyramidal—$2/m\ 2/m\ 2/m$

$a:b:c=0.5758:1:0.8473 \qquad p_0:q_0:r_0=1.4715:0.8473:1$

$q_1:r_1:p_1=0.5758:0.6769:1 \quad r_2:p_2:q_2=1.1802:1.7367:1$

| Forms | $\phi$ | $\rho=C$ | $\phi_1$ | $\rho_1=A$ | $\phi_2$ | $\rho_2=B$ |
|---|---|---|---|---|---|---|
| *c* 001 | | 0°00′ | 0°00′ | 90°00′ | 90°00′ | 90°00′ |
| *b* 010 | 0°00′ | 90°00′ | 90°00′ | 90°00′ | | 0°00′ |
| *m* 110 | 60°04′ | 90°00′ | 90°00′ | 29°56′ | 0°00′ | 60°04′ |
| *f* 014 | 0°00′ | 11°57½′ | 11°57½′ | 90°00′ | 90°00′ | 78°02½′ |
| *r* 012 | 0°00′ | 22°57½′ | 22°57½′ | 90°00′ | 90°00′ | 67°02½′ |
| *s* 011 | 0°00′ | 40°16½′ | 40°16½′ | 90°00′ | 90°00′ | 49°43½′ |
| *t* 021 | 0°00′ | 59°27½′ | 59°27½′ | 90°00′ | 90°00′ | 30°32½′ |
| *u* 041 | 0°00′ | 74°33½′ | 73°33½′ | 90°00′ | 90°00′ | 16°26½′ |
| *h* 118 | 60°04′ | 11°59′ | 6°03′ | 79°36½′ | 79°34½′ | 84°03′ |
| *n* 114 | 60°04′ | 23°00′ | 11°57½′ | 68°25′ | 69°48′ | 77°46′ |
| *o* 112 | 60°04′ | 40°20′ | 22°57½′ | 55°53′ | 53°39½′ | 71°09½′ |
| *p* 111 | 60°04′ | 59°30½′ | 40°16½′ | 41°41½′ | 34°12′ | 64°32′ |

* Angles in Table 2 calculated by Miss Mary E. Mrose.

and the *a* axes. The corresponding photographs of crystals from Utah and Argentina proved to be identical. Even by selecting the smallest and apparently most perfect crystals, it was necessary to take photographs of several crystals before satisfactory results were obtained. The slightly disoriented superimposed crystals give rise to spurious spots and complicate the interpretation of the photographs.

A rotation photograph and zero, first, second, and third layer-line Weissenberg photographs were taken rotating around *c*, and a rotation, zero, first and second layer-line Weisenberg photographs were taken rotating around *a*. From measurements of these photographs $a_0=9.69$ Å, $b_0=16.83$, $c_0=14.26$, giving the ratios $a_0:b_0:c_0=0.5758:1:0.8473$.

The extinctions on the Weissenberg photographs show that schroeckingerite has a *C* centered lattice with space group either $C_{2v}^{11}-Cmm$ or $D_{2h}^{19}-Cmmm$. The crystals are too small to determine whether or not they are piezoelectric and thus give a unique solution. However, if the crystal class is orthorhombic-dipyramidal as indicated by the morphology, the space group is *Cmmm*.

The chemical formula for schroeckingerite determined by Jaffe, Sherwood and Peterson (1948) from an analysis of material from Wyoming was found to be $NaCa_3UO_2(CO_3)_3SO_4F\cdot 10H_2O$. The same formula was arrived at independently by Axelrod *et al.* (1951) from an analysis of schroeckingerite from Arizona. Assuming this formula to be correct, the molecular weight is $M=888.56$. From the unit cell volume, $2322A^3$, and the average measured specific gravity, 2.547, the molecular weight of the cell contents is calculated as $M_0=3568$. These figures show that there are 4 formula weights of schroeckingerite per unit cell.

## PHYSICAL AND OPTICAL PROPERTIES

Schroeckingerite from both Argentina and Utah have physical properties similar to those of the mineral as described from other localities. The chief difference lies in the specific gravity. The specific gravity of schroeckingerite from Argentina (G=2.550) and Utah (G=2.544), as determined by suspension in a mixture of bromoform and acetone, is slightly higher than that from Wyoming (G=2.51) and Arizona (G=2.5). These higher values are undoubtedly the result of using single crystals rather than aggregates as found in Wyoming and Arizona.

The optical properties of schroekingerite from the two new localities, with those of the Wyoming material given for comparison, are summarized in Table 3.

TABLE 3. OPTICAL PROPERTIES OF SCHROECKINGERITE

| | Argentina<br>*n*Na | | Utah<br>*n*Na | | Wyoming<br>*n* |
|---|---|---|---|---|---|
| $X=c$ very pale yellow | 1.492 | ±0.001 | 1.490 | ±0.001 | 1.489±0.002 |
| $Y=b$ yellowish green | 1.543 | | 1.537 | | 1.542±0.001 |
| $Z=a$ yellowish green | 1.544 | | 1.538 | | 1.542±0.001 |
| | 2V=10° | | 2V=18° | | 2V=5° |
| Opt. | (−) | | (−) | | (−) |
| Measured specific gravity | 2.550 | | 2.544 | | 2.5 |
| Calculated specific gravity | 2.547 | | | | |

A real difference of about 0.001 exists in the refractive index between *n*Y and *n*Z in crystals from Argentina and Utah. A check of the Wyoming schroeckingerite during the present study showed that *n*Z−*n*Y is less, not greater than 0.0005. The water content of the crystals has a marked effect on refractive index. Crystals from Argentina placed over water at room temperature for 24 hours show a change of *n*Y from 1.543 to 1.541. No change was shown in the crystals from Utah treated in the same manner.

## DEHYDRATION

Schroeckingerite from the two new localities was placed in a desiccator over concentrated sulfuric acid at room temperature. After 48 hours the appearance had completely changed. The clear, transparent crystals had become cloudy and the formerly brilliant basal planes gave poor reflections. With this relatively mild treatment schroeckingerite had lost $6H_2O$ and changed to: $NaCa_3UO_2(CO_3)_3SO_4F \cdot 4H_2O$.

That such a lower hydrate exists might have been predicted from the dehydration curves published by Nováček (1939). His curves showed that schroeckingerite from Wyoming and Joachimsthal lost approximately 12 per cent of its weight on heating between 76° C. and 79° C. Since the mineral contains 20.28 per cent water, this represents 6 of the $10H_2O$ originally present. Insufficient material from either Utah or Argentina is available to run similar dehydration experiments. However, abundant schroeckingerite from Wyoming was at hand and 400 milligrams of this material was placed in a desiccator over concentrated sulfuric acid. After 6 days it lost 11.7 per cent of its original weight; thereafter no further weight loss took place. Since no great effort was made to purify this sample, it is assumed that the 0.5 per cent short of the theoretical 12.2 per cent loss is the result of impurities.

Rotation and Weissenberg $x$-ray photographs of dehydrated schroeckingerite were taken rotating about both the $a$ and $c$ axes. Although these were poor, good measurements could be made along the axial directions of the 0-layer Weissenberg photographs which gave the following unit cell dimensions: $a_0 = 9.72$ Å (an increase of 0.03), $b_0 = 16.83$ (unchanged), $c_0 = 11.03$ (a decrease of 3.23). The ratio of $a_0 : b_0 = 9.72 : 9.72\sqrt{3}$ is the exact ratio of a hexagonal lattice. The dehydrated schroeckingerite is, therefore, hexagonal with $a_0 = 9.72$ Å and $c_0 = 11.03$; $a_0 : c_0 = 1 : 1.1348$.

Using the above dimensions, the volume for the hexagonal unit cell is calculated as 902Å$^3$. The specific gravity, measured by suspending crystals in a mixture of bromoform and acetone, is 2.86. Using these figures the molecular weight of schroeckingerite with $4H_2O$ instead of $10H_2O$ is $M = 781$. There are thus two formula weights in the hexagonal unit cell.

Accompanying dehydration there is a marked increase in the indices of refraction. Equally striking is the uniaxial character of the mineral with the complete disappearance of the optic angle. The optical properties are summarized in Table 4.

TABLE 4. OPTICAL PROPERTIES OF DEHYDRATED SCHROECKINGERITE

| | $n$Na | |
|---|---|---|
| $O$ pale yellow | $1.581 \pm 0.001$ | Uniaxial (−) |
| $E$ colorless | $1.532 \pm 0.002$ | |
| Measured $G = 2.86$ | | Calculated $G = 2.874$ |

Dehydrated schroeckingerite standing in air for two days at room temperature showed only a slight decrease in refractive index. The same crystals placed over water at room temperature for one day showed a complete return to the initial optical properties. These crystals did not, however, become clear and transparent but retained the cloudy appearance they assumed on dehydration.

The fluorescence of dehydrated schroeckingerite, although striking, is less brilliant than before dehydration.

## REFERENCES

AXELROD, J. M., GRIMALDI, F. S., MILTON, C., AND MURATA, K. J., The uranium minerals from the Hillside Mine, Yavapai County, Arizona: *Am. Mineral.*, **36**, 1–22 (1951).

JAFFE, H. W., SHERWOOD, A. M., AND PETERSON, M. J., New data on schroeckingerite: *Am. Mineral.*, **33**, 152–157 (1948).

LARSEN, E. S., JR., AND GONYER, F. A., Dakeite, a new uranium mineral from Wyoming: *Am. Mineral.*, **22**, 561–563 (1937).

NOVÁČEK, R., The identity of dakeite and schroeckingerite: *Am. Mineral.*, **24**, 317–323 (1939).

SCHRAUF, A., Schroeckingerite, ein neus mineral von Joachimsthal: *Min. Mitt., Heft* **II,** 137–138 (1873).

*Manuscript received Aug. 11, 1953*

# GEOCRONITE

ROBERT M. DOUGLASS,* *University of California, Berkeley, Calif.*,
MICHAEL J. MURPHY, *c.s.c.*, *University of Notre Dame, Notre Dame, Ind.*, AND A. PABST, *University of California, Berkeley, Calif.*

## ABSTRACT

*X*-ray examination of geocronite from several localities shows that it is monoclinic, probable space group $C_{2h}^2-P2_1/m$, with cell dimensions varying slightly near $a_0$ 9.0, $b_0$ 31.9, $c_0$ 8.5, $\beta$ 118°. Geocronite is isostructural with jordanite and presumably constitutes the intermediate member of a series with varying proportions of antimony and arsenic, and possibly other compositional variation. Jordanite is the arsenic end-member of this series, the antimony end-member not being certainly known. As with jordanite there is uncertainty as to the cell content of geocronite and no simple formula can be assigned with assurance. Polished-surface observations indicate that geocronite, jordanite, and boulangerite are not distinguishable from one another with certainty by these methods alone and suggest that in a number of respects previous descriptions may be unreliable.

## HISTORY

Geocronite was named by Svanberg (1841). It has usually been assigned the formula $Pb_5(Sb, As)_2S_8$. Goniometric measurements have been reported by Kerndt (1845) and by D'Achiardi (1901) who considered it to be orthorhombic. Lamellar twinning has been repeatedly noted, D'Achiardi (1901), Ramdohr (1950) and Schröder (1941). Geocronite has been recognized as monoclinic by Hiller (1938), by Ramdohr and Ödman (1939) and by Ramdohr (1950). The powder *x*-ray diffraction pattern of geocronite has been reported by Hiller (1938) and by Harcourt (1942), these authors being substantially in agreement. No single-crystal *x*-ray study on geocronite is known to the writers. The close relationship of geocronite to jordanite was recognized by Solly (1900) from the morphology, especially the twin lamellae, and by Ramdohr and Ödman (1939) who stated that Hiller was to show the structural similarity by *x*-ray investigation.

## MATERIAL AND ACKNOWLEDGMENTS

The present study arose from the examination of a specimen of a sulfosalt from the 600 level of the Silver King mine, Park City, Utah, sent to the senior author (A.P.) for identification, by Mr. Rodney B. Sprague in 1950. Another specimen from this locality showing a small amount of the same mineral was later received from Mr. Everett O. Bracken. The sulfosalt, which was finally shown to be geocronite, occurs in the first and richer specimen as coatings of striated lead-gray crystals on galena, associated with quartz and a bit of pyrite. The galena crystals are in clusters with individual crystals over half a centimeter in diameter. The geocronite crusts reach a thickness of three millimeters or more in places. In the later stages of the study, specimens of geocronite from other localities, including material from the type locality, Sala, Sweden, and jordanite were obtained for comparison. Dr. George Switzer kindly lent 4 specimens from the collections of the United States National Museum and Mr. John B. Jago of San Francisco lent 2 specimens from his personal collection.

---

* Present address, P.O. Box 1663, Los Alamos, New Mexico.

Altogether a dozen or more different specimens of geocronite, of supposed geocronite, or of jordanite from ten localities, were examined. Among these the following are of special interest:

1. Geocronite, 600 level, Silver King mine, Park City, Utah, gift of Mr. Rodney B. Sprague and Mr. Everett O. Bracken;
2. Geocronite, Sala, Sweden, *U.S.N.M. C 830;*
3. Geocronite, Custer Co., Idaho, *U.S.N.M. 106120;*
4. Boulangerite and galena, labelled "Geocronite, Sala, studied by Max Short," *U.S.N.M. 84328;*
5. Geocronite, labelled "boulangerite," Defiance mine, Cerro Gordo, California, *UC spec. No. 100,* gift of Dr. H. W. Gould;
6. Geocronite, 2800′ level, Livingston mine, Mackay, Idaho, gift of Anaconda Copper Mining Company;
7. "Jordanite," Hope mine, Bonner County, Idaho, from J. B. Nichols Collection, purchased from Minerals Unlimited;
8. Jordanite with sphalerite and pyrite, Wiesloch, Baden, Germany, purchased from Ward's.

As suggested by this list, boulangerite and geocronite may readily be mistaken for each other though their *x*-ray diffraction patterns are distinctive. In addition to the case listed above another specimen in the collections of the University of California labelled geocronite was found to be boulangerite and Berry (1940) has reported a similar mislabelling of material from near Deer Lodge, Montana.

Funds for the analysis of geocronite, which was carried out by Dr. R. Klemen of Vienna, and for the spectrographic examinations were provided by a grant from the Committee on Research of the University of California. Professor Leonard G. Berry of Queen's University has critically examined the manuscript, and Professor Charles Meyer of the University of California has examined the section on polished-surface observations. The writers are most grateful to all who have given or lent materials and to those who have aided our work in various ways.

## Unit Cell and Space Group

Specimens from Park City, Utah, Custer Co., Idaho, and from Sala, Sweden, numbers 1 to 3 in the list above, were studied by means of single-crystal diffraction patterns using the rotation, Laue, Weissenberg and precession methods. Over 50 exposures were made. Geocronite proves to be monoclinic with cell dimensions very close to those of jordanite.

The cell dimensions of the three geocronites are set forth in Table 1. These are such that there also exists another monoclinic cell of nearly the same dimensions, as well as a pseudo-orthorhombic cell of double the volume. The relations are shown in Fig. 1. The lattice is also not far from being pseudohexagonal. Were the $\beta$ angles closer to 120° there would exist three possible monoclinic cells of nearly the same dimensions. Table 1 includes the constants of the monoclinic cells with slightly larger $a_0$ and also the angle $(100\wedge\bar{1}02)$ whose difference from 90° is a measure of the departure of the pseudo-orthorhombic cell from orthogonality.

Table 1. Cell Dimensions of Geocronite and Jordanite

| | Geocronite Park City, Utah | Geocronite Sala, Sweden *USNM C*830 | Geocronite Custer County, Idaho *USNM* 106120 | Jordanite Binnenthal, Switzerland (Berry, 1940) |
|---|---|---|---|---|
| Dimensions of cell with smallest possible $a_0$ and $c_0$: | | | | |
| $a_0$ | 8.96±0.03 Å | 9.00±0.02 | 8.96±0.03 | 8.87* |
| $b_0$ | 31.85±0.05 | 31.94±0.03 | 31.92±0.06 | 31.65±0.03 (kX)† |
| $c_0$ | 8.48±0.03 | 8.52±0.02 | 8.48±0.02 | 8.40±0.02† |
| $\beta$ | 118°00′±10′ | 118°00′±10′ | 118°00′±10′ | 118°6′* |
| $(\bar{1}02\wedge 100)$ | 90°14′ | 90°27′ | 90°14′ | 90°5′* |
| Dimensions of cell with same $c_0$ and $b_0$ as above and slightly longer $a_0$: | | | | |
| $a_0$ (alt.) | 8.99 | 9.04 | 8.99 | 8.89±0.03† |
| | 118°23′ | 118°31′ | 118°23′ | 118°21′±30′† |
| Angle for cell with smallest possible $a_0$ and $c_0$ corresponding to pseudo-cell which is strictly orthorhombic metrically, i.e., with $(\bar{1}02\wedge 100)=90°00'$. | | | | |
| | 118°15′ | 118°15′ | 118°15′ | 118°16′ |

* Values calculated from Berry's figures.

† Values given by Berry in Peacock and Berry (1940), presumably in kX units.

The only systematic extinction observed in the $x$-ray patterns is the absence of $0k0$ with $k$ odd. This would allow the space groups $C_{2h}^2 - P2_1/m$ or $C_2^2 - P2_1$. We incline towards the former group as more probable in view of the relations of geocronite to jordanite and what seems to us the lack of conclusive evidence of polarity of the 2-fold axis. (See discussion of morphology.)

Table 1 also lists data for jordanite obtained by Berry (Peacock and

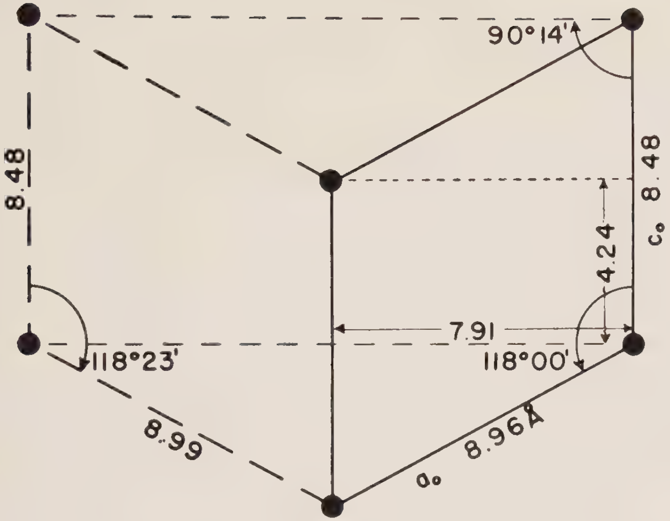

FIG. 1. A portion of the $x0z$ plane of the direct lattice of geocronite showing the relations of several choices of unit cell.

Berry, 1940). It appears that the cell which he chose is not that with shortest possible $a_0$. The axial elements of the two similar cells for jordanite may be compared with the axial elements given for this mineral by Baumhauer (1891) as transformed by Berry:

$a_0:b_0:c_0$ 0.281 :1:0.265 118°21′ (Berry)
$a:b:c$ 0.2795:1:0.2655 117°49½′ (Baumhauer-Berry)
$a_0:b_0:c_0$ 0.280 :1:0.2655 118° 6½′ (alternative)

It seems reasonable to suppose that jordanite and geocronite are isostructural. Substitution within the series is attended by changes in cell dimensions. These may be such that a direction chosen as $a_0$, the next to the shortest translation in the *ac* plane, for one member of the series is structurally equivalent to a translation direction in another member of the series which is not the next to the shortest in the *ac* plane. Accordingly it may be that Berry's $a_0$ is equivalent to our $a_0$ even though Berry's is not the next to the shortest translation in the *ac* plane.

Without reference to the structure or to suitable single-crystal patterns of Binnenthal jordanite, this point cannot be resolved. We have, however, assured ourselves that the orientations chosen for the three geocronites described in Table 1 are equivalent. Geocronite is not only metrically but also symmetrically pseudo-orthorhombic. All the principal spots in an $h0l$ pattern show intensities conforming to the plane point group $2l$. Among the weaker spots, however, it is possible to discern that

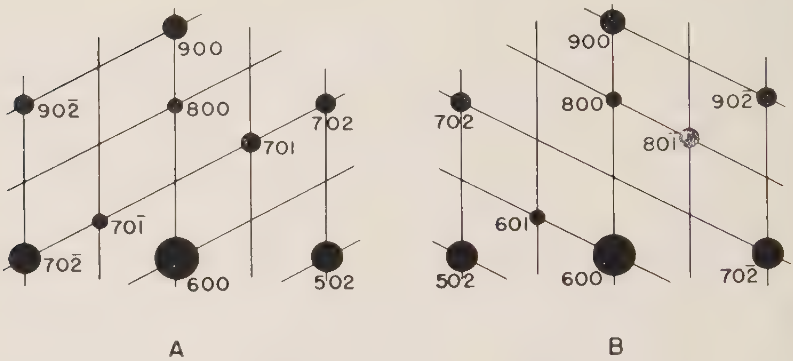

FIG. 2. A portion of the reciprocal lattice of geocronite. *A*. Indexed according to the cell with shortest possible $a_0$ and $c_0$. *B*. Indexed according to a cell with slightly longer $a_0$ as shown in Fig. 1. Sizes of circles are intended to suggest different intensities.

the symmetry is only 2 regardless of the closeness of approach of the pseudo-orthorhombic lattice to orthogonality. In order to tie the orientation chosen for geocronite to structural features as expressed in the diffraction pattern, a portion of the reciprocal lattice plane *h*0*l* is shown in Fig. 2. Fig. 2*A* shows the indexing of a group of points in accord with the cell bounded by the smallest possible $a_0$ and $c_0$. Fig. 2*B* shows the indexing of the same points in accord with the same $c_0$ but with another $a_0$ only slightly different in length. It may be seen that the indexing of pairs of points similarly situated on opposites side of the $a^*$ line is interchanged in these two settings so that these points offer no means of discriminating between them. There are points, 701 and $70\bar{1}$ of Fig. 2*A*, whose indexing is peculiar to a certain setting and can be used to define the same.

Yet another feature of the lattice of geocronite merits mention. In the pseudo-orthorhombic reciprocal lattice all planes in the series 1*kl*, 2*kl*, etc., with *h* even and those in the series *hk*1, *hk*2, etc., with *l* even show the symmetry 2*l*. Only the odd-numbered planes in these series show the lower symmetry *l* proper to a monoclinic crystal. Moreover these odd-numbered planes contain only very weak spots. The effect of these relations is apparent in the fragment of the reciprocal lattice shown in Fig. 2. There is then a pseudo-orthorhombic sub-cell (indicated in Fig. 1) having half the *a* and *c* dimensions of the B-centered pseudo-orthorhombic cell mentioned above and having orthorhombic symmetry. This would have half the volume of the correct monoclinic cell.*

* The true cell and various pseudocells of geocronite are analogous to those described for boulangerite by Berry (1940). Berry took the "orthorhombic" pseudocell to be orthogonal leaving a choice of two dimensionally identical monoclinic cells. He did not consider the problem of discriminating between these two.

An atomic arrangement in an orthorhombic space group with a cell of these dimensions ($a_0$ 7.91, $b_0$ 31.85, $c_0$ 4.24 for the Utah geocronite, for example) would represent the structure of geocronite to a first approximation. The case is somewhat similar to that of pyrrhotite, or at least of certain pyrrhotites, in which the commonly accepted structure is that of an hexagonal subcell, the true structure requiring a larger monoclinic cell for its description. Bertaut (1953) has shown that this larger cell is connected with a systematic distribution of vacancies in Fe positions. Though the structure of geocronite probably also involves vacancies in atomic positions (see discussion of cell content) it is not suggested that these necessarily determine differences between the true structure and an approximate structure conforming to the higher symmetry of the orthorhombic subcell.

## Composition and Cell Content

All of the geocronites and jordanites studied except specimens 2 and 6 (geocronite from Sala, *USNM C-830* and geocronite from Mackay, Idaho) were examined spectrographically by Mr. George M. Gordon in the Division of Mineral Technology, University of California, Berkeley. In all cases antimony and arsenic were found to be the only important metals, in addition to lead. The jordanite from Wiesloch showed the expected preponderance of arsenic over antimony, though the latter was

Table 2. Some Analyses of Geocronite and Jordanite

| | *A* | *B* | *C* |
|---|---|---|---|
| Pb | 67.52 wt.% | 68.90 | 68.72 |
| As | 3.65 | 4.54 | 12.39 |
| Sb | 11.48 | 9.27 | |
| S | 17.45 | 17.13 | 18.31 |
| Total | 100.10 | 99.84 | 99.42 |
| Density | 6.46±0.05 | | 6.44 |

A. Geocronite, Silver King mine, Park City, Utah. Dr. R. Klemen, *analyst*. Density by Berman balance.

B. Geocronite, Sala, Sweden. C. Guillemain, *analyst*. Guillemain (1900).

C. Jordanite, Binnenthal, Switzerland. H. Jackson, *analyst*. Solly (1900). Density from Berry in Peacock and Berry (1940).

The figures given are in each case the means of two closely agreeing analyses, except for sulfur in *A* for which only a single determination was reported. One of the pair of jordanite analyses reported by Guillemain was used as the basis for cell content estimates by Richmond (Palache, Richmond and Winchell, 1938), whereas the average for the two given above was used by Palache and Fisher (1940) and both were used by Fisher (1940).

estimated to be present to the extent of several per cent so that this would probably be a more highly antimonian jordanite than any for which analyses are recorded by Doelter or Dana. The geocronites examined were all found to have about 10% Sb and 3–5% As, corresponding to the composition of most geocronites hitherto analyzed. Specimen 7, labelled jordanite, from the Hope mine, Bonner County, Idaho, was found to have about the same proportions of Sb and As as the geocronites. (The relations of these materials will again be referred to in the discussion of the powder patterns.)

A chemical analysis of the geocronite from the Silver King mine, Park City, Utah, was kindly carried out by Dr. R. Klemen of Vienna, on about one and a quarter grams of carefully purified material. The results of this analysis together with an analysis of geocronite from the type locality and one of jordanite are given in Table 2. The antimony content of the newly analyzed geocronite from Park City, Utah, is substantially higher than that previously found for any geocronite in which arsenic was also reported. According to The System of Mineralogy (1944) "the validity of [an arsenic-free variety]—is not yet established."

TABLE 3. CELL CONTENTS OF GEOCRONITE AND JORDANITE

| | *A*<br>Geocronite<br>Park City,<br>Utah | | *B*<br>Geocronite<br>Sala,<br>Sweden | | *C*<br>Jordanite<br>Binnenthal,<br>Switzerland |
|---|---|---|---|---|---|
| $a_0$ | 8.96 Å | | 9.00 | | 8.908* |
| $b_0$ | 31.85 | | 31.94 | | 31.714 |
| $c_0$ | 8.48 | | 8.52 | | 8.417 |
| $\beta$ | 118°00′ | | 118°00′ | | 118°21′ |
| Density | 6.46 | | 6.45 (assumed) | | 6.44 |
| Cell Vol. | 2,136.73 Å$^3$ | | 2,162.48 | | 2,092.67 |
| Cell wt. | 13,803.27×10$^{-24}$ grs. | | 13,948.03 | | 13,476.78 |
| Number of atoms in cell corresponding to analyses in table 2.† | | | | | |
| Pb | 27.09 | | 27.94 | | 26.92 |
| As | 4.05 | 11.89 | 5.09 | 11.49 | 13.42 |
| Sb | 7.84 | | 6.40 | | |
| S | 45.25 | | 44.89 | | 46.36 |

* Berry's cell dimensions, presumably in kX units, have been converted to Å units by multiplying by 1.00202. The values given have been carried to one more decimal place than our own figures because it seemed best to avoid possibly excessive "rounding" on the data of others.

† Using atomic weights for 1942, Pb 207.21, As 74.91, Sb 121.76 and S 32.06, and weight of the unit of atomic weight 1.6602×10$^{-24}$ grs. for consistency with dimensions in Angstrom units.

In Table 3 are presented the results of cell content calculations for the geocronites and jordanite whose analyses are given in Table 2. Unfortunately Guillemain failed to state the density of the geocronite from Sala which he analyzed. The density 6.45 has been assumed for this material because nearly all good density determinations on geocronite are near this figure and it seems reasonable in view of the densities for the other minerals included in Table 2.

There has been much uncertainty as to the proper formulas for geocronite and jordanite. In later years several attempts have been made to idealize the cell content of jordanite in formulas. These have been summarized by Berry (Peacock and Berry, 1940) as follows:

$$\begin{array}{rl} \mathrm{Pb_{27}As_{14}S_{48}} & \text{(Berry)} \\ \left.\begin{array}{r} \mathrm{Pb_{14}As_7S_{24}} = \frac{1}{2}(\mathrm{Pb_{28}As_{14}S_{48}}) \\ \mathrm{Pb_{13}As_7S_{23}} = \frac{1}{2}(\mathrm{Pb_{26}As_{14}S_{46}}) \end{array}\right\} & \text{(Richmond)} \\ \mathrm{Pb_{14}As_7S_{23}} = \frac{1}{2}(\mathrm{Pb_{28}As_{14}S_{46}}) & \text{(Fisher).} \end{array}$$

Berry also pointed out that "in terms of the generally accepted formula the cell content is nearly given by:

$$\mathrm{Pb_{28}As_{14}S_{49}} = 7[4\mathrm{PbS} \cdot \mathrm{As_2S_3}].\text{"}$$

In The System of Mineralogy (1944) the formula of geocronite is written $\mathrm{Pb_5(Sb, As)_2S_8}$, which might be taken to correspond to an ideal cell content $\mathrm{Pb_{30}(Sb, As)_{12}S_{48}}$, with integral subscripts close to those of the jordanite formulations just quoted.

This confused picture is not clarified by consideration of the new analysis or the results of calculations presented in Table 3. To the extent that the cell content calculations yield values less than those required by the formulas, one might ascribe the discrepancies to low determinations of density. Thus assumption of a density of 6.66 for Binnenthal jordanite would raise the calculated cell content to Pb 27.84, As 13.88, S 48.05, very close to the values chosen in the first of Richmond's formulations. Tempting though such manipulation may be, it seems unwarranted in the present case. It appears certain that geocronite and jordanite are isostructural. Referred to any of the formulas for jordanite given above, the geocronites are highly deficient in sulfur, whereas the lead content of one fits nicely the formula of Berry and that of the other the formula of Fisher. Berry (letter to Pabst, Dec. 2, 1953) points out that the "new analysis strongly suggests $27\mathrm{PbS} \cdot 6\mathrm{(Sb,As)_2S_3}$ for geocronite." This would necessitate a defect structure since neither of the permitted space groups for geocronite offer odd-fold positions. It may be that the numbers of positions for each kind of atom provided by the structure differ from those corresponding to any formula yet proposed.

TABLE 4. INDEXED POWDER PATTERN OF GEOCRONITE, SPECIMEN 1, SILVER KING MINE, PARK CITY, UTAH

| *hkl* | $d_{\text{calc.}}$ | $d_{\text{obs.}}$ | *I* | *hkl* | $d_{\text{calc.}}$ | $d_{\text{obs.}}$ | *I* |
|---|---|---|---|---|---|---|---|
| 120 | 7.08 | 6.91 | 1d | 240 | 3.54 | 3.54 | 10 |
| 021 | 6.77 | 6.74 | 1 | 032 | 3.53 | | |
| $\bar{1}21$ | 6.75 | | | $\bar{2}32$ | 3.52 | | |
| 130 | 6.34 | 6.36 | 2– | 042 | 3.38 | 3.39 | 8 |
| 031 | 6.12 | 6.12 | 2– | $\bar{2}42$ | 3.38 | | |
| $\bar{1}31$ | 6.10 | | | 052 | 3.23 | 3.18 | 8B |
| 041 | 5.45 | 5.49 | 2+ | $\bar{2}52$ | 3.22 | | |
| $\bar{1}41$ | 5.44 | | | 0·10·0 | 3.18 | | |
| 150 | 4.96 | 4.95 | 1–d | 260 | 3.17 | | |
| $\bar{1}51$ | 4.84 | 4.84 | 1d | 062 | 3.059 | 3.06 | 9 |
| 101 | 4.48 | 4.46 | 4 | $\bar{2}62$ | 3.052 | | |
| $\bar{2}01$ | 4.46 | | | 270 | 2.985 | 2.98 | 7 |
| 111 | 4.44 | | | 072 | 2.891 | 2.89 | 9 |
| 061 | 4.33 | 4.33 | 1–? | $\bar{2}72$ | 2.884 | | |
| $\bar{1}61$ | 4.32 | | | 280 | 2.806 | 2.80 | 5d |
| $\bar{1}12$ | 4.20 | 4.21 | 1+ | 132 | 2.796 | | |
| 131 | 4.13 | 4.13 | 1+ | $\bar{3}32$ | 2.784 | | |
| $\bar{2}31$ | 4.12 | | | 191 | 2.779 | | |
| 200 | 3.95 | 3.93 | 2– | 082 | 2.727 | 2.72 | 5 |
| 170 | 3.94 | | | 142 | 2.723 | | |
| 210 | 3.92 | | | $\bar{2}82$ | 2.722 | | |
| 071 | 3.89 | | | $\bar{3}42$ | 2.712 | | |
| 220 | 3.84 | 3.83 | 4– | 152 | 2.638 | 2.63 | 2 |
| 012 | 3.72 | 3.71 | 6 | 300 | 2.637 | | |
| 230 | 3.71 | | | $\bar{3}52$ | 2.628 | | |
| $\bar{2}12$ | 3.70 | | | 310 | 2.628 | | |
| 022 | 3.64 | 3.64 | 2 | | | | |
| $\bar{2}22$ | | | | | | | |

## POWDER PATTERN

Powder patterns of all the geocronites examined proved to be nearly identical. By calculating the first 134 lines compatible with the space group it is possible to account for the first 24 lines of the powder pattern of Utah geocronite. Table 4 shows the indexing of all lines in a pattern of Utah geocronite corresponding to a spacing of 2.53 Å or more. Only those calculated lines considered to correspond to observed lines are included. Coincidences are numerous due to the large cell and indexing was assured only by comparison with fully indexed single-crystal patterns. Under these circumstances more extended indexing of the powder patterns was not attempted.

In Table 5 a more extended portion of the powder pattern of the Utah

TABLE 5. COMPARISON OF POWDER PATTERNS OF GEOCRONITE AND JORDANITE

| Specimen 1 Geocronite Park City, Utah | | Specimen 7 "Jordanite" Hope mine, Idaho | | Specimen 8 Jordanite Wiesloch, Baden | | Geocronite Falun, Sweden (Hiller, 1938) | | Jordanite Silesia (Harcourt, 1942) | |
|---|---|---|---|---|---|---|---|---|---|
| *I* | *d* | *I* | *d* | *I* | *d* | *I* | *d* | *I* | *d* |
| 1d | 6.91 Å | 1d | 7.05 Å | 1− | 7.25 Å | | | | |
| 1 | 6.74 | | | 1+ | 6.71 | | | | |
| 2− | 6.36 | 1 | 6.30 | | | | | | |
| 2− | 6.12 | | | 1 | 6.03 | | | | |
| 2+ | 5.49 | | | | | | | | |
| 1-d | 4.95 | | | 1d | 4.87 | | | | |
| 1d | 4.84 | | | | | | | | |
| 4 | 4.46 | 2− | 4.42 | 2 | 4.40 | | | | |
| 1−? | 4.33 | | | | | | | | |
| 1+ | 4.21 | | | 2 | 4.17 | | | | |
| 1+ | 4.13 | | | | | | | | |
| | | | | 1 | 4.01 | | | | |
| 2− | 3.93 | 1 | 3.90 | | | m | 3.89 | | |
| 4− | 3.83 | 2 | 3.84 | | | | | | |
| | | | | 3 | 3.78 | | | | |
| 6 | 3.71 | 5 | 3.70 | 4 | 3.65 | m | 3.71 | | |
| 2 | 3.64 | | | 1 | 3.58 | | | | |
| 10 | 3.54 | 8 | 3.53 | 6 | 3.47 | m-st | 3.54 | 1.0 | 3.49 |
| 8 | 3.39 | 7B | 3.39 | 7 | 3.34 | m-st | 3.40 | 1.0 | 3.31 |
| 8B | 3.18 | 10 | 3.19 | 8 | 3.15 | st | 3.19 | 1.0 | 3.15 |
| | | 5 | 3.12 | | | | | | |
| 9 | 3.06 | 5 | 3.05 | 8 | 3.06 | m | 3.07 | 1.0 | 3.01 |
| 7 | 2.98 | 5− | 2.98 | 9 | 2.97 | m | 2.99 | | |
| | | 5+ | 2.96 | | | | | | |
| 9 | 2.89 | 7 | 2.89 | 4− | 2.87 | st | 2.90 | 1.0 | 2.87 |
| 5d | 2.80 | 3d | 2.80 | 5 | 2.78 | m | 2.84 | 0.5 | 2.75 |
| 5 | 2.72 | 4 | 2.72 | | | m | 2.74 | | |
| 2 | 2.63 | 1d | 2.64 | 1 | 2.63 | v w | 2.64 | | |
| 1 | 2.59 | | | | | | | | |
| 1− | 2.55 | | | | | | | | |
| 2-B | 2.49 | 1+ | 2.49 | | | m | 2.46 | 0.3 | 2.48 |
| 1 | 2.44 | | | | | | | | |
| 3− | 2.39 | 3 | 2.39 | 3+ | 2.39 | | | 0.3 | 2.36 |
| 1+ | 2.33 | | | | | | | | |
| 1− | 2.29 | | | | | | | | |
| 9 | 2.235 | 10 | 2.245 | 10 | 2.238 | v st | 2.24 | 3.0 | 2.22 |
| 6 | 2.122 | 4+ | 2.122 | 6 | 2.110 | m | 2.12 | 2.0 | 2.10 |
| 3 | 2.086 | 4+ | 2.094 | | | w | 2.087 | | |
| 4+ | 2.052 | 3d | 2.047 | | | | | | |
| 4− | 2.030 | | | 3 | 2.025 | m | 2.033 | | |
| | | | | 1 | 1.999 | | | 0.5 | 2.01 |
| 3+ | 1.973 | 2− | 1.981 | | | m | 1.971 | | |
| 5 | 1.984 | 3 | 1.949 | | | m-st | 1.947 | 0.5 | 1.93 |
| 2 | 1.918 | 6− | 1.908 | 4 | 1.912 | v w | 1.910 | | |
| 4 | 1.889 | | | | | v w | 1.886 | | |
| | | | | 4 | 1.870 | | | | |
| 3 | 1.850 | 9B | 1.836 | | | | | | |
| 8 | 1.831 | | | 8 | 1.829 | st | 1.830 | 2.0 | 1.815 |
| 1 | 1.791 | 4 | 1.786 | 2 | 1.784 | | | | |
| 7 | 1.765 | 6 | 1.765 | 5 | 1.755 | sr | 1.763 | 1.0 | 1.745 |
| 4 | 1.744 | 3 | 1.729 | 1 | 1.735 | m-st | 1.730 | | |
| 3 | 1.694 | 2d | 1.705 | 3 | 1.705 | m | 1.696 | | |
| 2 | 1.677 | | | 2 | 1.681 | v w | 1.677 | | |
| 2 | 1.651 | 5 | 1.627 | | | | | | |
| 1 | 1.618 | | | | | | | | |
| 3 | 1.597 | 2+ | 1.598 | | | v w | 1.595 | | |
| 1d | 1.565 | | | 3d | 1.575 | | | | |
| | | | | 1 | 1.497 | | | | |
| 3 | 1.489 | | | | | w | 1.485 | | |
| 4d | 1.469 | 4B | 1.481 | 3 | 1.477 | | | | |
| | | | | 3+ | 1.462 | w | 1.467 | | |
| 4 | 1.448 | 3− | 1.447 | 2+ | 1.440 | w | 1.448 | | |
| 2 | 1.428 | 1 | 1.433 | 2d | 1.417 | w | 1.428 | | |
| 4 | 1.409 | 3− | 1.410 | 2d | 1.403 | w | 1.408 | | |
| plus about 20 more lines in each pattern. | | | | | | plus 16 more lines. | | | |

geocronite is tabulated together with earlier published patterns of geocronite and jordanite and with patterns obtained from the two specimens labelled jordanite which were examined in the course of this study. As may be seen from the table these do differ from the geocronite pattern but are not identical to each other. Hiller (1938) gave his powder-pattern results for geocronite in terms of angle and $\sin^2$ values for Fe radiation. These have been converted to spacings for presentation in Table 5. *ASTM* card 2-1144 gives a composite record of Hiller's geocronite pattern and one reported by Harcourt (1942). In Table 5 lines are tabulated only to *d* 1.41, the limit of this card. Harcourt's jordanite pattern is recorded on *ASTM* card 2-1149.

## MORPHOLOGY

Goniometric measurements on geocronite have been published only by Kerndt (1845) and by D'Achiardi (1901). Both measured crystals from Val di Castello, near Pietrasanta, Tuscany. The measurements

TABLE 6. SUMMARY OF SOME GEOCRONITE SETTINGS BASED ON ANGLES REPORTED BY KERNDT

| *Author* | *Year* | *Indices*<br>pinacoid | <br>prism | <br>dipyramid | *a*:*b*:*c* |
|---|---|---|---|---|---|
| Kerndt*<br>as corrected by<br>Goldschmidt | 1845<br>1890 | {100} | {120} | {111} | 0.290 :1:0.503 |
| Goldschmidt<br>Goldschmidt | 1890<br>1897 | {001} | {011} | {212} | 1.006 :1:0.58 |
| Groth† | 1882 | | | | 0.58 :1:0.48 circa |
| Dana | 1892 | {100} | {110} | {211} | 0.5805:1:0.5028 |

* The axial ratios given by Kerndt, "$a:b:c=1:0.269197:0.468949$," are difficult to interpret and probably in error.

† Probably a slightly erroneous statement of ratios corresponding to the setting later used by Dana.

The transformations for the settings given above are:

| | Kerndt (Gdt. 1890) | Goldschmidt 1890 | Dana 1892 |
|---|---|---|---|
| Kerndt | | 002/010/200 | $200/010/00\bar{1}$ |
| Goldschmidt | 00½/010/½00 | | 001/010/½00 |
| Dana | ½00/010/001 | 002/010/100 | |

of Kerndt were the basis of crystallographic descriptions of geocronite in many well-known texts. The work of Kerndt is subject to several uncertainties which were discussed by Goldschmidt (1890). The results of Kerndt and the more important descriptions based thereon are summarized and correlated in Table 6.

Whereas Kerndt reported only three forms D'Achiardi found a great number. Inspection of the drawings published by these authors leaves no doubt that D'Achiardi used a setting corresponding to that adopted by Goldschmidt (1890 and 1897). It is not possible, however, to give a transformation between the setting of D'Achiardi and previous settings.

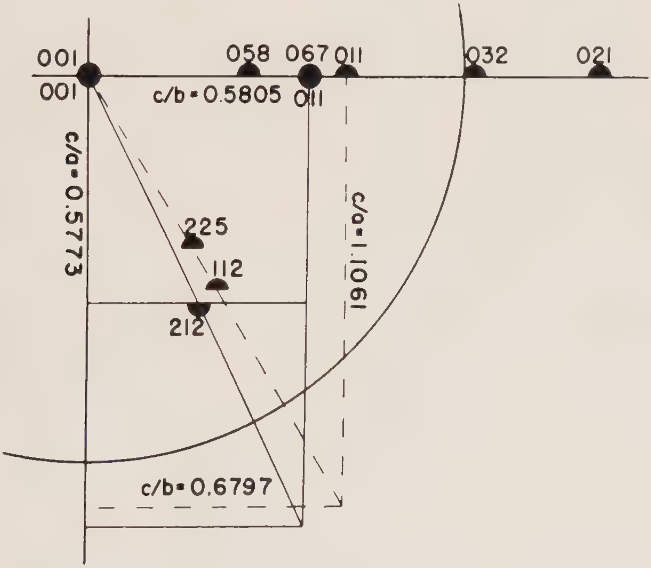

FIG. 3. One quadrant of a gnomonic projection of geocronite. Upper semicircles and projection elements written above dashed lines according to D'Achiardi (1900). Lower semicircles and projection elements written below full lines according to Goldschmidt (1890, 1897) from angles of Kerndt (1845).

Though $\rho_{067}$ of D'Achiardi, 30° 12′, is close to $\rho_{011}$ of Goldschmidt, 30° 07′, this is insufficient to establish a transformation since no certain correlation can be found between the "pyramidal" forms reported by D'Achiardi and the single such form reported by Kerndt. This is illustrated in Fig. 3 by superposition of gnomonic projections corresponding to the Kerndt-Goldschmidt and the D'Achiardi settings.

The difficulty just explained was circumvented in the 7th edition of The System of Mineralogy, 1944 (vol. 1, pages 395–396). The axial ratios given there, $a:b:c=0.5028:1:0.5805$, correspond to those in the

6th edition derived from Kerndt's measurements with *a* and *c* interchanged. A note contains the statement "Elements from Kerndt's angles, on Val di Castello crystals in the orientation of D'Achiardi (1901) with the unit of Dana (1892). The angles of D'Achiardi are not in close agreement with those of Kerndt. Transformation Kerndt to D'Achiardi 001/010/100." The transformation is misleading. It ought to result in correspondence of the newly transformed axial ratios given above with those of D'Achiardi, 0.6145:10.6797. The so-called "transformation" must be taken to indicate merely the correspondence of axial directions and not of unit distances. Possibly such a relation could be more appropriately symbolized by Z/Y/X.

D'Achiardi (1901) reported differences in the terminations at either end of the axis normal to the large face which he designated (001) and referred geocronite to the orthorhombic pyramidal class. The crystals we measured show a development obviously similar to that of Val di Castello crystals. Such crystals rarely show identical development at the positive and negative ends of the *b* axis normal to the large face because they are most frequently attached in such a way that only one of these faces is developed. Under these circumstances it is difficult to check on the polar character of this axis. Such observations as we have made indicate lack of complete correspondence between *hkl* and $h\bar{k}l$ faces but no systematic variations. The minor departures from ideal $2/m$ symmetry observed might well be attributed to accidents of growth. Since our work has shown that geocronite is isostructural with jordanite

TABLE 7. STANDARD ANGLE TABLE FOR GEOCRONITE BASED ON STRUCTURAL CELL DETERMINED FOR SPECIMEN 1

Monoclinic; prismatic—$2/m$
$a:b:c=0.2813:1:0.2662$; $\beta$ 118°00′; $p_0:q_0:r_0=0.9463:0.2350:1$
$r_2:p_2:q_2=4.2546:4.0257:1$; $\mu$ 62°00′; $p_0'$ 1.0717, $q_0'$ 0.2662, $x_0'$ 0.5317

| | *Forms:* | $\phi$ | $\rho$ | $\phi_2$ | $\rho_2=B$ | C | A |
|---|---|---|---|---|---|---|---|
| | 001 | 90°00′ | 28°00′ | 62°00′ | 90°00′ | — | 62°00′ |
| *b* | 010 | 0 00 | 90 00 | — | 0 00 | 90°00′ | 90 00 |
| *a* | 100 | 90 00 | 90 00 | 0 00 | 90 00 | 62 00 | — |
| | 170 | 29 54 | 90 00 | 0 00 | 29 54 | 76 28 | 60 06 |
| $\epsilon$ | 110 | 76 03 | 90 00 | 0 00 | 76 03 | 62 58 | 13 57 |
| | 101 | −90 00 | 28 22 | 118 22 | 90 00 | 56 22 | 118 22 |
| | 011 | 63 24 | 30 44 | 62 00 | 76 46 | 13 14 | 62 48 |
| | 111 | −63 26 | 31 07 | 118 22 | 76 49 | 57 23 | 62 27 |

(Letter designations are given for those forms surely corresponding to the similarly lettered forms in the angle table for jordanite in The System of Mineralogy, 7th ed. Vol. I, p. 398, 1944.)

which is recognized as having the symmetry 2/*m*, we are inclined to consider that geocronite has this symmetry as well, and this has influenced our choice of probable space group.

An angle table calculated for geocronite with elements based on the structural cell is reproduced as Table 7. All forms listed in the angle table were observed, but numerous other forms were observed in each of the zones [001], [100] and [101] represented in the table. In certain parts of these zones faces may be so closely spaced that signals overlap on the reflecting goniometer and a continuum of reflections is seen. It is not possible to assign an order of prominence of the forms with any assurance but {010} which is common to the three zones mentioned is generally the most prominent form. The form {170} is included in the angle table only because its $\rho_2$ value is close to that of D'Achiardi's {067} and of the single prismatic form {*g*} recorded by Kerndt.

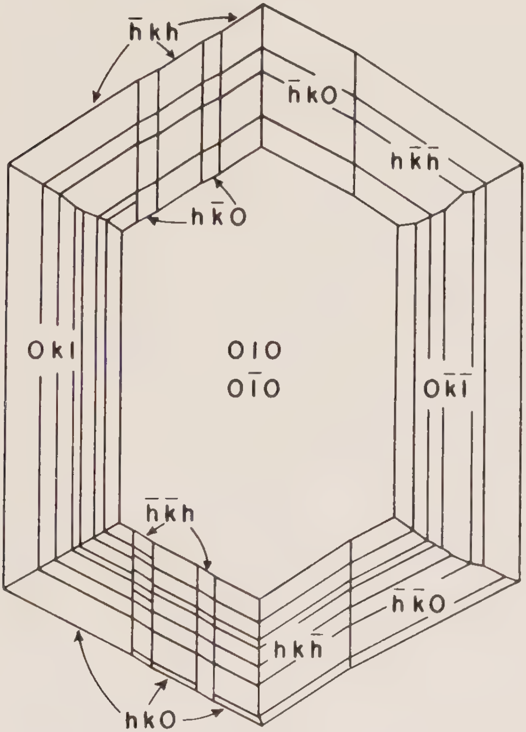

Fig. 4. Idealized sketch of a twinned crystal of geocronite.

The habit of geocronite corresponds closely to that of jordanite. The similarity of the crystals is apparent in a comparison of the angle tables.* An idealized drawing of one crystal of geocronite from Park City, Utah, is shown in Fig. 4. The over-all appearance is that of an orthorhombic crystal with pronounced development of one pinacoid, one series of cozonal prisms and one series of cozonal dipyramids. Where twin boundaries traverse (010), which is in common for the two parts of the twin, they are not discernible and hence are not shown in the drawing. Though the material available to us lacks fully developed crystals a little variation in habit is discernible. In general {010} is a little less prominent than in the drawing and the development of the three zones having this form in common varies somewhat, the [001] zone being least conspicuous in some instances. One crystal, however, shows a large (010) face and prominent development of a zone of faces not traversed by twin striations as pictured by Kerndt (1845) and D'Achiardi (1901). Figure 4 gives the interpretation of such a crystal taking into account the monoclinic character and the twinning.

Most of the crystals are twinned in such a way that nearly coincident zones appear in certain sectants. $\phi_2$ differences measured for such pairs of zones were somewhat erratic, ranging from $3\frac{1}{2}$ to $6\frac{1}{2}$ degrees, usually close to 5 degrees. Such a development might arise from repeated twinning on either {001} or {101}, the ideal $\phi_2$ differences being 5° 38′ and 5° 16′ respectively. From lattice dimensions either twinning seems probable. The index of the twin is unity in both cases and the obliquity 3° 49′ and 3° 34′ respectively (Donnay, 1940). Goniometric measurement will not distinguish the two cases with certainty or even eliminate the possibility that both kinds of twinning occur since the $\rho_2$ angles in the zones [100] and [101] differ by only a few minutes. Fortunately it was possible to discern twinning in zero-layer Weissenberg patterns on the *b* axis for crystals from specimens 1, 2, and 3. In each case {001} twinning only was observed. This does not exclude the possibility of the occurrence of {$\bar{1}$01} twinning as well, or of a combination of the two. For jordanite twinning reported by Palache is described in the System of Mineralogy (1944) in terms of the cell found by Berry as "(*a*) On {001}, most common and often lamellar; (*b*) on {$\bar{2}$01}, common; (*c*) on {$\bar{1}$01}, rare; (*d*) on {101}, very rare." The correspondence of the {001} or {$\bar{1}$01} twinning of jordanite to {001} twinning in geocronite is subject to the uncertainty connected with the existence of two nearly identical line lattices in these minerals as set forth in the discussion of Table 1.

We have observed what appeared to be cleavage parallel to {100} and have checked its orientation by means of single-crystal patterns in fragments from specimens 1, 2 and 3. This is not at all conspicuous. It is uncertain whether it corresponds to the better cleavage reported by Kerndt (1845) and mentioned as "{011} distinct" in The System of Mineralogy (1944). In any case the lack of {010} cleavage in geocronite, whereas jordanite is reported to have "very perfect" {010} cleavage, furnishes one of the few sharp differences between these closely related minerals.

---

* Note: The values $r_2$ and $\rho_2$ in the angle table for jordanite in the System of Mineralogy, 7th edition, vol. I, p. 398, 1944, should be interchanged.

## Polished-surface Observations [R. M. D.]

Polished sections of specimens of geocronite, jordanite and boulangerite were studied using with few modifications the techniques set forth by Short (1940). Geocronite and jordanite were examined because of their close relation to each other, and boulangerite because of its frequently being mistaken for geocronite and vice versa. The identification of all specimens was confirmed by *x*-ray powder patterns, and numbers 1, 3, 5, 7 and 8 were examined spectrographically in addition.

In spite of uncertainty of identification of many of the materials described as one of these three minerals in the literature, the results of the present polished-surface study are in fairly good agreement with those descriptions with the notable exception of the behavior of these three minerals toward nitric acid. All of the authors cited below reported strongly positive reactions with this reagent whereas the tests are all reported herein as negative. This discrepancy is apparently due principally to the care with which the acid is applied to the surface rather than to misidentification of materials, although the latter might be partly responsible. If the drop is applied so as to avoid overlapping onto cracks or intergrown grains of other minerals, no reaction ensues; with many specimens this may necessitate very careful application of quite small drops. If such overlapping occurs rapid blackening accompanied by effervescence usually results. If this reaction is not too rapid it can be seen to originate at the cracks or inclusions, passing as a wave across the surface with iridescent concentric rings preceding the blackening and effervescence. Frequently the entire surface covered by the acid is thus affected, although occasionally the reaction may stop short. To demonstrate that failure to react is not due merely to an unclean surface (in spite of careful polishing) or to the relatively small area of the mineral in contact with the reagent, the surface may be scratched gently with a needle immediately prior to application of the drop. Moreover if a needle be introduced into the drop after application there results a "positive" reaction closely simulating that described above. These observations suggest that some extraneous electrolytic effect is responsible for the reported "positive" reactions with nitric acid, and further emphasize the necessity of great care in making and interpreting etch tests in general.

Although presence of lamellar twinning is suggestive of geocronite or possibly jordanite, and slightly stronger anisotropism is suggestive of boulangerite, it remains doubtful whether or not these three minerals can be distinguished with certainty by polished-surface observations alone.

GEOCRONITE: Murdoch (1916) performed etch tests on one specimen from one locality (not given) and considered the determination only "fairly reliable"; no confirmatory data as to the identification of the specimen are mentioned. Davy and Farnham (1920) gave no sources of data. Schneiderhöhn and Ramdohr (1931) and Ramdohr (1950) referred to Murdoch for etch behavior and gave no further sources of data. Short (1940) stated (p. 2) that "over 20 per cent of [Murdoch's] minerals were mislabelled"; furthermore a specimen labelled "geocronite, Sala, studied by Max Short" (no. 4 of this paper) was found in the present study to be a mixture of boulangerite and galena. Anderson (1946) based his identification solely on polished-surface observations as described by Short. Uytenbogaardt (1951) referred to Murdoch, to Short and to Schneiderhöhn and Ramdohr.

Five specimens of geocronite were examined in the present study—numbers 1, 2, 3, 5 and 6.

*Hardness*—Talmage hardness ∼B, but harder than galena as indicated by lightly drawing a needle across geocronite-galena contacts (nos. 1, 2 & 3): the scratches are decidedly deeper and wider in galena. Difference in relief owing to difference in polishing hardness is not discernible by movement of "Becke-like" line. (This is contrary to Schneiderhöhn and Ramdohr, 1931, and to Ramdohr, 1950, who reported polishing hardness definitely lower than galena although variable. Uytenbogaardt, 1951, gave "H<galena" [after Schneiderhöhn and Ramdohr?].)

*Cleavage*—Not apparent in polished sections. (Short, 1940, stated that geocronite "has at least one good cleavage.")

*Color*—Galena white, but where in contact with galena (nos. 1, 2, & 3) a faint but definite greenish, bluish-green, or olive tinge is seen.

*Polarization*—Anisotropism, but color effects weak: light gray to dark gray, bluish gray, or steel blue; or creamy tan to brownish gray. (The polarization colors in any given section are subject to considerable variability depending especially on the angular departure from perpendicularity of the planes of polarization of the nicol prisms, and on the light source.) Reflection pleochroism weak. Fine lamellar twinning and rare coarser twinning on another law may be revealed under crossed nicols. Twinning in any given section is frequently not apparent, however, and thus lamellar twinning as a diagnostic (suggested by Schneiderhöhn and Ramdohr, 1931, and by Ramdohr, 1950) may be unreliable.

*Etch reactions*

$HNO_3$ (1 part concentrated nitric acid, sp. gr. 1.42:1 part water by volume)—Negative. (Descriptions in the literature give rapid blackening with effervescence—see opening discussion.)

$HNO_3$ conc.—Negative, although on long standing a very faint brown tarnish may remain which does not wash off.

HCl (1 pt. conc. hydrochloric acid, sp. gr. 1.19:1 pt. water by vol.) and HCl conc.—Essentially negative, although on long standing a very faint tan tarnish may remain which does not wash off; fumes may tarnish also. (Short, 1940, classed the reaction with HCl (1:1), as positive. Murdoch, 1916, reported "instantly bright brown" with concentrated HCl.)

Aqua regia (3 pts. conc. HCl:1 pt. conc. $HNO_3$ by vol.)—Fumes may tarnish light yellowish brown, not washing off; little or no effect under drop. (Murdock, 1916, reported "rapidly tarnishes iridescent.")

KCN (20% by wt. in water), $FeCl_3$ (20%), KOH (40%) and $HgCl_2$ (5%)—Negative.

JORDANITE: Murdoch (1916) performed etch tests on one specimen from one locality (not given) and considered the determination "doubtful." Davy and Farnham (1920) and Short (1940) described the mineral but gave no information as to reliability of identification of the specimens, the number examined, or their localities. Schneiderhöhn and Ramdohr (1931) and Ramdohr (1950) referred to Murdoch regarding etch behavior. Anderson (1946) based his identification solely on polished-surface observations as described by Short. Uytenbogaardt (1951) referred to Anderson and to Schneiderhöhn and Ramdohr.

Two specimens of jordanite were examined in the present study—numbers 7 and 8 of this paper; number 7 is from the same locality as material described by Anderson (1946).

*Hardness*—Talmage hardness B to C. (Schneiderhöhn and Ramdohr, 1931, and Ramdohr, 1950, stated polishing hardness slightly greater than that of galena.)

*Cleavage*—Not apparent in polished section.

*Color*—Galena white.

*Polarization*—Anisotropism weak to moderate; colors from light to dark gray. (Anderson, 1946, reported "distinctive but rather weak anisotropism," Schneiderhöhn and Ramdohr, 1931, and Ramdohr, 1950, strong anisotropism.) Twinning not apparent. (Schneiderhöhn and Ramdohr and Ramdohr reported both lamellar twinning and rarer, less well developed twinning on another law in material from Binnenthal.)

*Etch reactions*

$HNO_3$—Negative. (Descriptions in the literature give reaction slow in starting, then staining gray to brown; Short, 1940, reported reaction accompanied by slow effervescence—see opening discussion.)

$HNO_3$ conc., HCl and HCl conc.—Negative, or very faint brown stain may remain after rinsing.

Aqua regia—Negative or faint brown stain; fumes may tarnish also.

KCN, $FeCl_3$, KOH and $HgCl_2$—Negative.

BOULANGERITE: Murdoch (1916) performed etch tests on two specimens from two localities (not given), but gave no confirmatory data. Davy and Farnham (1920) and Short (1940) described the etch behavior but gave no information as to reliability of identification of the specimens, the number examined, or their localities. Schneiderhöhn and Ramdohr (1931) and Ramdohr (1950) referred to Murdoch regarding etch behavior. Berry (1940), Hawley (1941) and Chace (1948) confirmed the identification of the materials they examined by *x*-ray patterns and by density determinations. Anderson (1946) based his identification solely on polished-surface observations as described by Short. Uytenbogaardt (1951) referred to Short, to Berry, to Hawley, to Chace and to Schneiderhöhn and Ramdohr.

Six specimens of boulangerite were examined in the present study—number 4 of this paper (studied by Max Short as geocronite), two from Oberlahr, Germany (cf. Berry, 1940, numbers 5 and/or 19), one from Cleveland mine, Stevens County, Washington (cf. Berry number 11), and two from Lower California, Mexico (one of which was mislabelled "geocronite").

*Hardness*—Talmage hardness B and C; harder than associated galena (no. 4) (by scratching across contact). (Schneiderhöhn and Ramdohr, 1931, and Ramdohr, 1950, stated hardness very similar to galena, a trace less.)

*Cleavage*—Not apparent in polished section.

*Color*—Galena white, but when in contact with galena (no. 4) shows a faint bluish-green tinge.

*Polarization*—Anisotropism moderate to strong; colors light tan or gray to steel blue. Twinning not apparent.

*Etch reactions*

$HNO_3$—Negative. (Descriptions in the literature give blackening with effervescence—see opening discussion.)

$HNO_3$ conc., HCl and HCl conc.—Negative, or very faint brown stain may remain after rinsing.

Aqua regia—Fumes may tarnish light brown, not washing off. (Murdoch, 1916, reported blackening with effervescence.)

KCN, $FeCl_3$, KOH and $HgCl_2$—Negative. (Chace, 1948, reported slight brown to iridescent stain with KOH. Hawley, 1941, reported negative or in some places possibly stains faint gray or brown with KOH and faint brown color at edge of drop with $HgCl_2$. It is suspected that these observers have encountered the difficulty in using these reagents which is discussed by Short, 1940, p. 98).

## REFERENCES

ANDERSON, A. L. (1946), Lead-silver mineralization in the Clark Fork district, Bonner County, Idaho: *Econ. Geol.*, **41,** 105–123.

BAUMHAUER, H. (1891), Über das Krystallsystem des Jordanits: *Ak. Berlin, Ber.*, 915–925.

BERRY, L. G. (1940), Studies of mineral sulpho-salts: III—Boulangerite and "epiboulangerite": *Toronto Univ. Studies, Geol. ser.*, **44,** 5–19.

BERTAUT, E. F. (1953), Contribution a l'Etude des Structures Lacunaires: La Pyrrhotine: *Acta Cryst.*, **6,** 557–561.

CHACE, F. M. (1948), Tin-silver veins of Oruro, Bolivia. Part 2: *Econ. Geol.*, **43,** 435–470.

D'ACHIARDI, G. (1901), Geocronite di Val di Castello presso Pietrasanta (Toscana): *Att. soc. tosc., Mem.*, **18,** 35–48.

DANA, E. S. (1892), The System of Mineralogy. Sixth edition, John Wiley & Sons, New York.

DAVY, W. M., AND FARNHAM, C. M. (1920), Microscopic Examination of the Ore Minerals. McGraw-Hill, New York.

DONNAY, J. D. H. (1940), Width of albite-twinning lamellae: *Am. Mineral.*, **25,** 578–586.

FISHER, D. J. (1940), Discussion of "the formula of jordanite": *Am. Mineral.*, **25,** 297–298.

GOLDSCHMIDT, V. (1890), Index der Krystallformen der Mineralien. Vol. 2. Springer, Berlin. 77–78.

GOLDSCHMIDT, V. (1897), Krystallographische Winkeltabellen. Springer, Berlin. 156.

GROTH, P. (1882), Tabellarische Übersicht der Mineralien. Vieweg, Braunschweig. 29.

GUILLEMAIN, C. (1898), Beiträge zur Kenntnis der natürlichen Sulfosalze: Inaug. Diss., Breslau, 35–37.

HARCOURT, G. A. (1942), Tables for the identification of ore minerals by *x*-ray powder patterns: *Am. Mineral.*, **27,** 63–113.

HAWLEY, J. E. (1941), Boulangerite from Montgay Township, Abitibi County, Quebec: *Toronto Univ. Studies, Geol. ser.*, **46,** 25–32.

HILLER, J. E. (1938), Röntgenographische Bestimmungsmethoden und Untersuchung der Bleispiessglanze: *Zeit. Krist.*, **100,** 128–156.

KERNDT, T. (1845), Ueber die Kristallform und die chemische Zusammensetzung des Geokronits von Val di Castello in Toscana: *Ann. Phys.*, **65,** 302–307.

MURDOCH, J. (1916), Microscopical Determination of the Opaque Minerals. John Wiley & Sons, New York.

PALACHE, C., BERMAN, H., AND FRONDEL, C. (1944), The System of Mineralogy. Seventh edition, Vol. I, John Wiley & Sons, New York.

PALACHE, C., AND FISHER, D. J. (1940), Gratonite—a new mineral from Cerro de Pasco, Peru: *Am. Mineral.*, **25,** 255–265.

PALACHE, C., RICHMOND, W. E., AND WINCHELL, H. (1938), Crystallographic studies of the sulphosalts: baumhauerite, meneghinite, jordanite, diaphorite, freieslebenite: *Am. Mineral.*, **23,** 821–836.

PEACOCK, M. A., AND BERRY, L. G. (1940), Röntgenographic observations on ore minerals: *Toronto Univ. Studies, Geol. ser.*, **44,** 47–69.

RAMDOHR, P., AND ÖDMAN, O. (1939), Falkmanit, ein neues Bleispiessglanzerz, und sein

Vorkommen, besonders in Boliden und Grube Bayerland. (Mit einem Beitrag zur Kenntnis des Geokronits.): *Jb. Min.*, *Beil. Bd.* **A 75,** 315–350.

Ramdohr, P. (1950), Die Erzmineralien und ihre Verwachsungen. Akademie Verlag, Berlin.

Schneiderhöhn, H., and Ramdohr, P. (1931), Lehrbuch der Erzmikroskopie. Zweiter Band, Borntraeger, Berlin.

Schröder, A. (1941), Datensammlung der Mineralien der türkischen Republik: *Maden Tetkik ve Arama Enstitüsü Mecmuasi*, 208–221. [*M. A.*, **10,** 123].

Short, M. N. (1940), Microscopic Determination of the Ore Minerals: *U. S. Geol. Sur., Bull.* **914,** 1–314.

Solly, R. H. (1900), Sulpharsenites of lead from the Binnenthal: *Mineral. Mag.*, **12,** 282–297.

Svanberg, L. F. (1841), Undersökning af Geokronit och Hydrofit, tvenne inom Sverige förekommande nya mineralier: *Ak. Stockholm, Handl.*, **1839,** 184–187.

Uytenbogaardt, W. (1951), Tables for Microscopic Identification of Ore Minerals. Princeton Univ. Press, Princeton, N. J.

*Manuscript received Dec. 18, 1953*

# CRYSTAL CHEMISTRY OF SCHALLERITE

DUNCAN MCCONNELL, *College of Engineering, The Ohio State University, Columbus, Ohio.*

## ABSTRACT

Crystallographic data obtained from precession and powder diffraction photographs indicate that schallerite is hexagonal. For a specimen containing 6.37 per cent $As_2O_3$, $a_0 = 13.36$ and $c_0 = 14.24$ Å.

If the combining ratio with oxygen is known for each oxide, the number of oxygen atoms in the unit cell can be calculated from the chemical analysis, specific gravity and dimensions of the unit cell. Knowledge of the number of oxygen atoms, in turn, permits calculation of the number of positively charged atoms, thus leading to the structural formula. The method is illustrated by calculations on schallerite.

A fundamental difficulty arises from the recent assumption of a phyllosilicate structure for schallerite: either the number of tetrahedral cations is significantly deficient or the number of oxygen atoms is excessive or both.

## INTRODUCTION

Investigations on schallerite were carried out without knowledge of concurrent studies on manganpyrosmalite, friedelite and schallerite by Frondel and Bauer (1953). These authors concluded that these three minerals are phyllosilicates in which arsenic occurs in tetrahedral coordination in isomorphic substitution for silicon. However, the only mineral that they considered in detail chemically contained merely 0.13 per cent $As_2O_5$. Thus the question of the manner of occurrence of arsenic in the structure does not appear to have been conclusively resolved by their results.

Whereas the writer's crystallographic measurements essentially confirm the measurements reported by Frondel and Bauer (1953), their conclusion concerning the phyllosilicate structure of schallerite contains a fundamental incompatibility which they did not adequately consider.

Gossner and Mussgnug (1931) investigated pyrosmalite by Laue and rotation methods, and although they discuss the dimensional relation to mica and chlorite, they do not indicate a structural relation to phyllosilicates. These authors were unable to obtain a complete structural analysis, but they concluded that the structural formula for pyrosmalite is $4[(Mn, Fe)_4(OH, Cl)_6Si_3O_7]$, and obtained $a_0 = 13.44$ and $c_0 = 7.20$ for the hexagonal unit cell of space group $C\bar{3}m$.

Although the present work will not further resolve the structure of schallerite, a novel method for deriving the structural formula of such complex silicates will be demonstrated.

## ACKNOWLEDGMENTS

The writer is indebted to Dr. W. T. Schaller and Professor Wm. J. McCaughey for reading the unrevised manuscript and for pertinent comments. Professor Preston M. Harris of the chemistry department also read the manuscript and contributed several precession photographs which were used as a basis for indexing the powder photograph. Professor Dana J. Demorest of the metallurgy department analyzed the schallerite sample for arsenic.

Samples of pyrosmalite (*R 3555*) and friedelite (*R 9080*) from the type localities were supplied by the U. S. National Museum through the kindness of Dr. George Switzer. The sample of schallerite was supplied by the late L. H. Bauer who was Chief Chemist of the New Jersey Zinc Company.

## CRYSTALLOGRAPHIC MEASUREMENTS

Powder diffraction data are given in Table 1 for schallerite which contains 6.37 per cent $As_2O_3$ (analysis by D. J. Demorest). Table 2 contains the summary information from a precession photograph that was used to index the powder photograph.

The dimensions for the hexagonal unit cell compare with those obtained by Frondel and Bauer (1953), as follows:

| | *Present Results* | *Results of F. & B.* |
|---|---|---|
| $a_0$ | 13.36 | 13.43 |
| $c_0$ | 14.24 | 14.31 |

The differences probably are to be attributed to differences in the arsenic contents of the samples. Inasmuch as their sample probably more closely corresponded with the type 1 (high arsenic) schallerite for which Bauer and Berman (1928) reported physical and chemical data, the unit cell dimensions obtained by Frondel and Bauer (1953) will be used in subsequent crystal chemical calculations in preference to the measurements obtained by the writer. The agreement is sufficiently good to eliminate the existence of any significant differences.

## CALCULATION OF THE STRUCTURAL FORMULA

Before proceeding with a calculation of the structural formula of schallerite, it is necessary to demonstrate that the formula for manganpyrosmalite proposed by Frondel and Bauer, i.e. $2[(Mn, Fe)_8(Si_6O_{15})\ (OH, Cl)_{10}]$, is not compatible with the silicate sheet proposed by Strunz (1949) and apparently accepted by them. Although the periodicity of the sheet, when taken as [210] of the mica structure, is approximately correct, it is clearly indicated in Fig. 1 that this layer unit contains 14 silicon atoms

TABLE 1. POWDER DIFFRACTION PATTERN OF SCHALLERITE

(Radiation: $\lambda\mathrm{FeK}_{\alpha}=1.937$ Å; Camera radius$=57.3$ mm.)

| Line Number | Estimated Intensity | Interplanar Spacing | Experimental $\sin^2\theta$ | $hk.l$ | Calculated $\sin^2\theta$ |
|---|---|---|---|---|---|
| 1 | 1 | 7.025 | .0190 | 00.2 | .0185 |
| 2 | 4 | 3.547 | .0743 | 00.4 | .0740 |
| 3 | ½ | 3.411 | .0802 | 10.4 | .0810 |
| 4 | ½ | 3.313 | .0855 | 22.0 | .0841 |
| 5 | 3 | 2.825 | .1175 | 40.1 | .1166 |
| 6 | 6 | 2.673 | .1311 | 40.2 | .1305 |
| 7 | 5 | 2.466 | .1540 | 40.3 | .1537 |
| 8 | ½ | 2.370 | .1668 | 00.6 | .1664 |
| 9 | ½ | 2.309 | .1759 | 32.3 | .1748 |
| 10 | 1 | 2.222 | .1901 | 33.0 | .1892 |
| 11 | ½ | 2.105 | .2109 | 33.2 | .2078 |
| 12 | ½ | 2.087 | .2146 | 42.2 | .2148 |
| 13 | 5 | 2.022 | .2291 | 40.5 | .2277 |
| 14 | 4 | 1.975 | .2789 | 40.6 | .2785 |
| 15 | 10 | 1.688 | .3364 | 44.0 | .3362 |
| 16 | 2 | 1.6275 | .3535 | 44.2 | .3547 |
| 17 | 6 | 1.5108 | .4063 | 40.8 | .4079 |
| 18 | ½ | 1.4420 | .4512 | 44.5 | .4518 |
|  |  |  |  | 80.1 | .4521 |
| 19 | 1 | 1.4256 | .4616 | 00.10 | .4622 |
| 20 | 1 | 1.4176 | .4669 | 80.2 | .4668 |
| 21 | 3 | 1.3906 | .4852 | 33.8 | .4850 |
|  |  |  |  | 40.9 | .4865 |
| 22 | 2 | 1.3687 | .5000 | 54.4 | .5013 |
|  |  |  |  | 44.6 | .5026 |
| 23 | ½ | 1.3546 | .5113 | 72.3 | .5109 |
|  |  |  |  | 21.10 | .5113 |
| 24 | ½ | 1.3432 | .5288 | 61.7 | .5279 |
|  |  |  |  | 81.2 | .5299 |
|  |  |  |  | 55.1 | .5300 |
| 25 | 2 | 1.2913 | .5453 | 55.2 | .5439 |
|  |  |  |  | 22.10 | .5463 |
| 26 | 2 | 1.2796 | .5557 | 81.3 | .5530 |
|  |  |  |  | 43.8 | .5551 |
|  |  |  |  | 73.1 | .5580 |
| 27 | ½ | 1.2580 | .5928 | 82.1 | .5930 |

rather than 12. Thus the supposition of Gossner and Mussgnug (1931), that pyrosmalite is not structurally related to mica, is valid if it is assumed that manganpyrosmalite and pyrosmalite are isostructural. Frondel and Bauer (1953) state that the powder patterns are identical so there is no reason to question this isostructural relation.

TABLE 2. RELATIVE INTENSITIES (UNCORRECTED) FROM PRECESSION PHOTOGRAPH ($h0.l$)

(Radiation $MoK_\alpha$)

| $l$ \ $h$ | 0 | 1 | 4 | 8 | 9 | 12 |
|---|---|---|---|---|---|---|
| 0 | — | | | | v. wk | str. |
| 1 | — | | med.* | med.* | v. wk. | abs. |
| 2 | med.* | v. wk. | str.* | str.* | | med. |
| 3 | abs. | | med.* | str. | | abs. |
| 4 | str.* | wk.* | wk. | wk. | | med. |
| 5 | abs. | | med.* | med. | | abs. |
| 6 | med.* | | wk.* | wk. | | wk. |
| 7 | abs. | | med. | med. | | abs. |
| 8 | wk. | | med.* | wk. | | abs.? |
| 9 | abs. | | med.* | med. | | abs. |
| 10 | med.* | | wk. | v. wk. | | med. |
| 11 | abs. | | v. wk. | v. wk. | | abs. |
| 12 | wk. | | wk. | wk. | | med. |
| 14 | med. | | | | | med. |

* Starred reflections were identified on the powder diffraction pattern (Table 1).

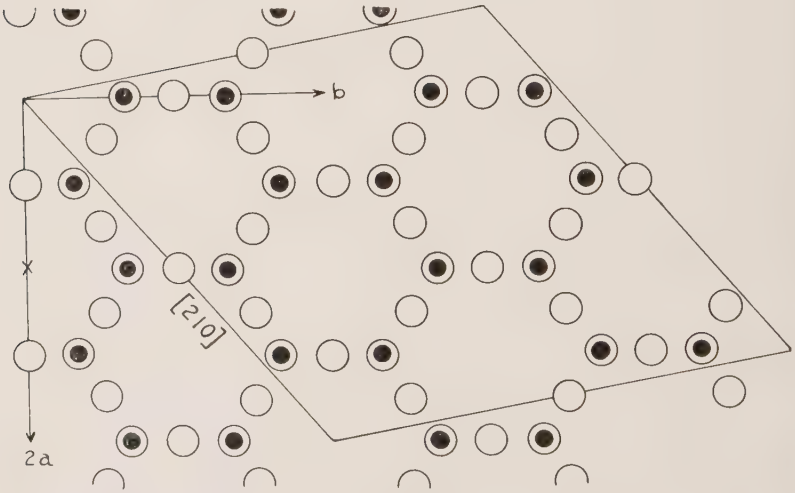

FIG. 1. Tetrahedral silicate layer of phyllosilicates showing a hexagonal periodicity of about 13.4 Å in the orthogonal direction [210] (Strunz, 1949). Any hexagonal sheet with such dimensions will contain 14 silicon atoms (solid circles) rather than 12. The $a$ and $b$ periodicities are for the unit cell of muscovite, assuming that $b_0 = a_0\sqrt{3}$.

Table 3. Calculation of the Number of Oxygen Atoms

| Oxides* | Weight Per cents | Weight Ratios $\Sigma=4535$ | Oxygen Ratios | Weights of Oxygen Atoms |
|---|---|---|---|---|
| $SiO_2$ | 31.44 | 1423.8 | .5328 | 758.6 |
| MnO | 44.70 | 2024.2 | .2256 | 456.7 |
| MgO | 2.19 | 99.2 | .3968 | 39.4 |
| FeO | 2.12 | 96.1 | .2227 | 21.4 |
| CaO | .36 | 16.3 | .2853 | 4.7 |
| ZnO | .54 | 24.5 | .1966 | 4.8 |
| $As_2O_3$ | 12.24 | 554.3 | .2426 | 134.5 |
| $H_2O$ | 6.55 | 296.6 | .8879 | 263.4 |
| | 100.14 | 4535.0 | | 1683.5 |

* Analysis by L. H. Bauer (Bauer and Berman, 1928). The analysis includes 0.08 per cent of Cl which has been disregarded for the purpose of these calculations.

From the writer's investigation of schallerite and the data provided by Gossner and Mussgnug (1931) and by Frondel and Bauer (1953), the interpretations contained in the latter work are quite acceptable with respect to the stacking of structural units in the *c* direction. Nevertheless, if this premise is correct, it follows that none of these polymorphs are phyllosilicates if pyrosmalite is not.

In order to resolve the problem further it is necessary to make an assumption which has almost universal applicability, that is, the number of oxygen atoms (including hydroxyl, chlorine and fluorine) within the unit cell is an integer. The particular integer may be known from pertinent structural analogies or may require determination in situations where the structural information is inadequate, as is the case with schallerite.

Assuming that the lattice dimensions, specific gravity and chemical composition are known, it is possible to calculate the number of oxygen atoms in the unit cell by means of the following equation:

$$n_0 = \frac{D \cdot V(C_1p_1 + C_2p_2 + C_3p_3 + \cdots)}{26.56\Sigma_c}$$

where

$n_0$ = number of oxygens per unit cell
$D$ = experimental specific gravity
$V$ = volume of the unit cell in cubic Å
$\Sigma_c$ = summation of weight percentages of oxides
$C_1, C_2 \cdots$ weight percentages of oxides
$p_1, p_2 \cdots$ atomic weight ratios of oxygen to molecular weights of oxides, i.e. 32/60.06 for $SiO_2$.

The detailed calculations are given in Table 3 in conformity with lattice dimensions given by Frondel and Bauer, and the specific gravity and analysis given by Berman and Bauer (1928). The molecular weight for the unit cell was computed in the usual manner as

$$(MW\cdot Z) = \frac{3.368\cdot \sin 60^\circ \cdot 13.43^2 \cdot 14.31}{1.66} = 4535.$$

This calculation yields a total oxygen weight of 1683.5 atomic units or 105.2 oxygen atoms, whereas Frondel and Bauer (1953) assumed 30 oxygens on the basis of a Si:O ratio of 2:5 and calculated an additional 21.2 hydroxyl and chlorine ions. They calculate a total for large anions as 51.2 but conclude that the correct number is 50 (their Table 2, p. 757) for the unit cell of manganpyrosmalite which is approximately half as large as schallerite.

Because odd orders of 00.*l* are absent (Table 1) the number of oxygens must contain the factor 2. Table 2 demonstrates a pronounced pseudosymmetry tending toward a quartering in the *a* direction, that is, $h=4n$ for all except a few weak reflections. Were this smaller $a_0$ dimension real, the number of oxygens would necessarily contain the factor 32 but more likely a factor of 8 is indicated for reasons which will appear subsequently. The integer 104 is within about one per cent of the calculated value and tentatively can be accepted as correct, at the same time noting that this is twice the value obtained by Gossner and Mussgnug (1931) for the unit cell of pyrosmalite.

On the basis of 104 oxygen atoms, the number of cations (including hydrogen atoms of hydroxyl ions) in the unit cell can be calculated by methods previously described in detail (McConnell, 1951). The calculations are given in Table 4 and are summarized as follows:

| | Si | (Mn, Mg, Fe, etc.) | As | H | O |
|---|---|---|---|---|---|
| Analytical | 23.5 | 32.5 | 5.5 | 32.6 | 105.2 |
| Theoretical | 24 | 40 | | 32 | 104 |

and for pyrosmalite (Gossner and Mussgnug, 1931):

| | | | | | |
|---|---|---|---|---|---|
| Theoretical | 12 | 16 | | 24 | 52 |

An obvious ambiguity arises concerning the arsenic. If added to the silicon the total becomes 29, which is reasonably close to the 28 required for the phyllosilicate structure (Strunz, 1949). It must be recalled, however, that manganpyrosmalite and pyrosmalite contain a number of silicon atoms which is inconsistent with Strunz's proposal.

Although the sum of the metallic cations is exactly 38 (rather than 40) this number is highly improbable because it does not contain the factor

TABLE 4. CALCULATION OF THE NUMBER OF CATIONS IN THE UNIT CELL

| Oxides* | Weight Per cents | Molecular Ratios | Cation Ratios | Ratios of Charges | Charges of Cations $\Sigma=208$ | Cations in Unit Cell | |
|---|---|---|---|---|---|---|---|
| $SiO_2$ | 31.44 | .5235 | .5235 | 2.094 | 93.8 | 23.5 | |
| MnO | 44.70 | .6302 | .6302 | 1.261 | 56.5 | 28.2 | 38.0 |
| MgO | 2.19 | .0543 | .0543 | .109 | 4.9 | 2.5 | |
| FeO | 2.12 | .0295 | .0295 | .059 | 2.6 | 1.3 | |
| CaO | .36 | .0064 | .0064 | .013 | 0.6 | 0.3 | |
| ZnO | .54 | .0048 | .0048 | .010 | 0.4 | 0.2 | |
| $As_2O_3$ | 12.24 | .0619 | .1238 | .371 | 16.6 | 5.5 | |
| $H_2O$ | 6.55 | .3637 | .7274 | .727 | 32.6 | 32.6 | |
| | 100.14 | | | | 208.0 | | |

* See note for Table 3.

8. Pyrosmalite contains only 16 rather than 20 metallic cations and the vacancies are compensated by 24 rather than 16 hydrogen atoms. The structural formula for type 1 schallerite therefore becomes

$$8[((Mn, Mg, Fe)_{4.0}As_{0.7})Si_3O_9(OH)_4]$$

which simplifies to $8[R''_5Si_3O_9(OH)_4]$ when trivalent atoms are absent.

It remains necessary to consider Bauer's analysis of type 2 schallerite (Bauer and Berman, 1928). If the total number of oxygen atoms (including 0.60 per cent of chlorine) is taken as 104, similar calculations yield the following results:

| | *Analytical* | | *Theoretical* |
|---|---|---|---|
| Si | 23.8 | | 24 |
| Mn, Fe, Mg | 31.7 | 36.4 | 40 |
| As | 3.3 | | |
| Al | 1.4 | | |
| H | 35.3 | | 32 |

Again it is necessary to conclude that the number of hydroxyl ions is not fixed but exceeds 32 when the number of divalent and trivalent metallic cations is insufficient to produce electrical neutrality. Here, as was the case for type 1 schallerite, the calculated number of silicon atoms is slightly less than the theoretical requirement. In light of the suggestion of Wickman (1951) that arsenic with valences of both 3 and 5 occurs in dixenite, it is possible that a very small amount of arsenic occurs in tetrahedral coordination.

The general structural formula for schallerite must account for more than 32 hydroxyl ions as well as less than 40 metallic cations, thus:

$$8[[R^{\cdot\cdot}{}_{(5-x-y)}R^{\cdot\cdot\cdot}{}_{x}]Si_3O_9[O_4H_{(4+2y-x)}]].$$

In conclusion it must be commented that the mutual consistency of these calculations indicates the excellence of the experimental data given by Bauer, Berman and Frondel. While the writer obtained the conclusion that schallerite is not consistent with a phyllosilicate structure prior to the appearance of the published results on schallerite (Frondel and Bauer, 1953), all of the crystal chemical calculations have been revised in order to obtain a greater consistency by using unit cell dimensions made on material more nearly comparable to that on which the chemical analysis and specific gravity had been determined.

There is a major discrepancy between Strunz's proposal and the crystal chemical calculations for manganpyrosmalite which Frondel and Bauer (1953) did not recognize. However, the stacking of structural units, as postulated by these authors, is confirmed by the writer's independent investigations of schallerite.

An alternative explanation is obtained by assuming that the two missing silicon atoms required for the phyllosilicate sheet of pyrosmalite and manganpyrosmalite are compensated by statistical substitution of $H_4$, as proposed by the writer for the tetrahedral layer of the montmorillonite structure (McConnell, 1950) and for ortho-antigorite (McConnell, 1954). Under these circumstances it would presumably follow that the arsenic (and aluminum in type 2) occurs in tetrahedral coordination in schallerite. Contrary evidence exists, however. It is highly improbable that both pyrosmalite and manganpyrosmalite should be deficient by two silicon atoms, whereas schallerite shows a very small deficiency, if any. Under any circumstances, it is concluded that the structure contains 104 rather than 100 large anions (O+OH+Cl).

## References

Bauer, L. H., and Berman, Harry (1928), Friedelite, schallerite, and related minerals: *Am. Mineral.*, **13,** 341–348.

Frondel, Clifford, and Bauer, L. H. (1953), Manganpyrosmalite and its polymorphic relation to friedelite and schallerite: *Am. Mineral.*, **38,** 755–760.

Gossner, B., and Mussgnug, F. (1931), Die molekulare Einheit von Pyrosmalith: *Zeits. Krist.*, **76A,** 525–528.

McConnell, Duncan (1950), The crystal chemistry of montmorillonite: *Am. Mineral.*, **35,** 166–172.

——— (1951), The crystal chemistry of montmorillonite. II—Calculation of the structural formula: *Clay Minerals Bull.* (London) **1,** 179–188.

——— (1954), Ortho-antigorite and the tetrahedral configuration of hydroxyl ions: *Am. Mineral.*, **39,** 830–831.

Strunz, H. (1949), Mineralogische Tabellen, p. 222.

Wickman, F. E. (1951), From the notes of the late K. Johansson. VII—A revised chemical analysis of dixenite from Långban: *Geol. Fören. Förhandl.*, **73,** 637–638.

*Manuscript received Nov. 16, 1953*

# STUDIES IN THE MICA GROUP; SINGLE CRYSTAL DATA ON PHLOGOPITES, BIOTITES AND MANGANOPHYLLITES

A. A. LEVINSON AND E. WM. HEINRICH, *Department of Mineralogy, The Ohio State University, Columbus, Ohio, and Department of Mineralogy, University of Michigan, Ann Arbor, Michigan.*

## ABSTRACT

Weissenberg studies of about 250 specimens of phlogopite, biotite and manganophyllite, of which 63 have been chemically analyzed, indicate: (1) in phlogopites there is no discernible relationship between structure and either composition or paragenesis; (2) in biotites there is no relationship between structure and composition, but geologic environment may be a factor in determining the polymorphic type; (3) the optic plane of all 2-layer polymorphs is normal to (010), as is also the case for the biotite variety, anomite; and (4) 1-layer polymorphs nearly always have the optic plane parallel with (010), which corresponds with the orientation of the biotite variety, meroxene.

## INTRODUCTION

Systematic variations between composition and the various polymorphs in the muscovite-lepidolite series have been demonstrated by Levinson (1953). On the basis of these results it seemed desirable to investigate the biotite-phlogopite series in a similar manner in the hope of gaining insight into causes of the complex polymorphism known to exist in these micas. The only other Weissenberg study of these micas known to the writers is in the work of Hendricks and Jefferson (1939), predominantly on unanalyzed specimens.

We have obtained over 60 analyzed specimens of biotite, phlogopite and manganophyllite (which we consider as manganoan phlogopite), most of which have been described by several investigators. In addition we have studied a suite of approximately 200 unanalyzed biotites and phlogopites from geologically well-studied occurrences. All specimens were studied by means of the Weissenberg method using copper radiation. In most cases only zero level, *a*-axis photographs were taken, as these are sufficient to determine the layer periodicity. In many cases, however, upper level photographs were taken, which confirmed the structure identification based on the zero level, *a*-axis photographs. In agreement with Hendricks and Jefferson (1939, p. 762), the 3-layer polymorph is considered to be hexagonal (actually trigonal) as a limiting case, even though some specimens are not truly uniaxial. Orientation of the flakes was secured by optical methods in those cases in which 2V was approximately 10° or greater. Laue photographs and percussion figures were

---

Contribution from The Department of Mineralogy and Petrography, University of Michigan, No. 185.

TABLE 1. STRUCTURES OF ANALYZED PHLOGOPITES

| Number | Reference | Structure | Occurrence | FeO | $Fe_2O_3$ | MgO | $TiO_2$ | F |
|---|---|---|---|---|---|---|---|---|
| 1054 | Jakob (1938) | ? Very diffuse scattering | from Morawitza, Czechoslovakia | 0.64 | 1.05 | 26.77 | 0.10 | 0.00 |
| 1055 | Jakob (1931) No. 55 | 1-layer (mod. scattering) | mica peridotite, Italy | 2.52 | 0.00 | 25.45 | 2.80 | 0.00 |
| 1056 | Jakob and Parga-Pondal (1932) No. 73 | 1-layer | Burgess, Ontario[1] | 1.24 | 0.73 | 26.45 | 1.15 | 1.00 |
| 1057 | No. 70 | 1-layer | Rossie, N. Y.[2] | 4.79 | 0.00 | 22.30 | 4.07 | 0.12 |
| 1058 | No. 69 | 1-layer | Hull, Quebec[1] | 2.49 | 0.71 | 24.60 | 1.74 | 2.04 |
| 1059 | No. 68 | 1-layer | Burgess, Ontario[1] | 0.30 | 0.00 | 27.32 | 0.39 | 6.74 |
| 1060 | No. 67 | 1-layer | Burgess, Ontario[1] | 1.50 | 0.00 | 26.14 | 0.86 | 2.37 |
| 1061 | No. 66 | 1-layer | Isolo, Madagascar[3] | 3.28 | 0.00 | 25.29 | 2.19 | 1.15 |
| 1062 | No. 65 | 2-layer (mod. scattering) | Ampandrandara, Madagascar[3] | 2.96 | 1.18 | 23.40 | 1.69 | 0.68 |
| 1063 | No. 64 | 1-layer | Mandridano, Madag.[3] | 2.09 | 0.00 | 24.48 | 1.64 | 0.08 |
| 1064 | No. 63 | 2-layer | Saharakara, Madag.[3] | 2.79 | 1.68 | 23.78 | 1.11 | 0.56 |
| 1065 | No. 62 | 1-layer | Ambatoabo, Madag.[3] | 1.42 | 0.66 | 24.80 | 0.86 | 0.86 |
| 1066 | Jakob (1928) No. 19 | 1-layer (heavy scattering) | Simplon Tunnel, Switzerland | 0.00 | 1.71 | 24.79 | 0.39 | 0.00 |
| 1067 | Jakob (1928) No. 20 | 1-layer | dolomite-Tessin | 0.00 | 1.31 | 25.81 | 0.83 | 0.00 |
| 1068 | Jakob (1928) No. 22 | 1-layer | contact metamorphic S. W. Africa | 2.72 | 0.97 | 25.05 | 0.66 | 0.58 |
| 1069 | Jakob (1928) No. 23 | 1-layer | pneumatolytic, Vesuvius, Italy | 0.58 | 1.92 | 28.18 | 1.27 | — |
| 1071 | Jakob—not published | 1-layer | Skräbböle, Pargas, Finland[4] | 0.71 | 1.01 | 27.80 | 0.12 | 2.11 |
| 1072 | Jakob—not published | 1-layer | Pargas, Finland[4] | 5.59 | 1.54 | 22.00 | 1.41 | 2.80 |
| 1073 | Jakob—not published | 1-layer | Patteby, Pargas, Finland[4] | 1.47 | 1.29 | 26.16 | 0.33 | 1.87 |
| 1074 | Jakob—not published | 1-layer | Ontala, Pargas,[4] Finland | 1.68 | 1.87 | 25.91 | 0.68 | 1.30 |
| 1075 | Jakob—not published | 1-layer | Skräbböle, Pargas, Finland[4] | 0.59 | 1.75 | 27.22 | 0.10 | 0.48 |
| 949 | Dana (1892) Anal. 12 p. 633 | 1-layer | Rossie, N. Y.[2] | 7.62 | 1.12 | 21.47 | 1.16 | 4.00 |
| 1135 | Pagliani (1940) | 1-layer | marble, Italy | 1.55 | 2.65 | 27.62 | 2.83 | — |
| 1139 | Hutton and Seeyle (1947) | 1-layer | marble, New Zealand | 2.38 | 0.43 | 22.95 | 0.82 | 0.62 |
| 1252 | Pieruccini (1950) | 1-layer | pneumatolytic, Mt. Somma, Italy | 7.89 | tr. | 15.66 | 0.33 | 2.57 |
| 1261 | (a) (b) (c)<br>Mauguin (1928) | 1-layer<br>3-layer | Ambatoabo, Madagascar.[3] | 2.30 | n.d. | 24.42 | 0.74 | n.d. |
| 730 | Prider (1939) | 1-layer | leucite lamproite,[5] West. Australia | 3.75 | 2.18 | 19.66 | 8.97 | 0.66 |
| 1325 | Cross (1897) | 1-layer | in wyomingite,[5] Leucite Hills, Wyo. | 0.90 | 2.73 | 22.40 | 2.09 | 2.46 |

---

(1) The Quebec and Ontario phlogopites occur in pegmatitic bodies associated with pyroxenite and marble.

(2) The occurrences near Rossie, St. Lawrence, N. Y., are in marble.

(3) The Madagascar deposits are similar to the Canadian type.

(4) The occurrences at Pargas are in marble.

(5) Of pyrogenic origin.

used in the majority of the cases; for the most part the percussion figure method was found to be unreliable.

This study is a part of the research program, "Natural Mica Studies," sponsored by the U. S. Army Signal Corps, Squier Signal Laboratory, Ft. Monmouth, New Jersey, under the general supervision of Dr. S. Benedict Levin and administered as *Project M-978* of the Engineering Research Institute, University of Michigan (Heinrich, *et al.*, 1953). The writers are indebted to Dr. Levin for his general assistance, to Professor Duncan McConnell for critically reading the manuscript, and to the following for gifts and loan of specimens: Prof. C. Frondel, Dr. A. F. Hallimond, Prof. C. O. Hutton, Prof. J. Jakob, Dr. Y. Kawano, Prof. C. Mauguin, Dr. and Mrs. A. Miyashiro, Prof. G. P. Pagliani, Prof. R. L. Parker, Prof. R. T. Prider, Prof. R. Pieruccini, Dr. F. T. Seeyle, Dr. K. Sugiura, Dr. G. Switzer, Dr. S. van Biljon, Prof. H. Winchell and Dr. H. Yamada.

## *X*-RAY STUDIES OF PHLOGOPITE

The structures of approximately 80 phlogopite crystals from about 50 different specimens (28 chemically analyzed) were identified. All but five have crystallized with the 1-layer monoclinic structure. Of these five, three have crystallized as the 2-layer monoclinic polymorph, whereas the remaining two have crystallized with the 3-layer structure.

2-layer phlogopites:
  No. 1062 (*a* and *b*)—Madagascar; see Table 1 for analysis and reference.
  No. 1064 (*a* and *b*)—Madagascar; see Table 1 for analysis and reference.
  No. 1220 (*a*) —Hull, Quebec; not analyzed.
3-layer phlogopites:
  No. 1261 (*b* and *c*)—Madagascar; see Table 1 for analysis and reference.
  No. 1227 (*a*) —Labelle Co., Quebec; not analyzed.

It is noteworthy that three of the non 1-layer types are from Madagascar, but four other specimens of Madagascar phlogopite crystallized with the common 1-layer monoclinic structure (Table 1). The analyzed specimen (No. 1261) from Prof. Mauguin consisted of two thin cleavage fragments; specimens No. 1261 (*b* and *c*) *x*-rayed from one of these have the 3-layer structure, whereas No. 1261 (*a*) from the second fragment has the 1-layer structure. The optical properties of the *x*-rayed crystals are similar (all essentially uniaxial), and there is probably little difference in their composition. This appears to be analogous to the association of 1- and 3-layer lepidolites as described by Levinson (1953). The specimens of known composition that have crystallized as the 2- and 3-layer forms do not appear to be markedly different, chemically, from the 1-layer types. In fact, the compositions of all the Madagascar varieties are practically identical. Optically, however, the 2-layer varieties differ in having their optic planes normal to (010); all 1-layer forms have their optic planes parallel with (010).

These findings are in qualitative agreement with those of Hendricks and Jefferson (1939), who found 14 phlogopites with the 1-layer monoclinic structure and one each with the 2- and 3-layer forms. No new polymorphs of phlogopite have been found in our investigations. Crystals reported by Pieruccini (1950) to be triclinic on the basis of goniometric measurements were isolated from a type specimen supplied by him. Weissenberg photographs indicate that the structure is the common 1-layer monoclinic form (Table 1). However, written communication with Professor Pieruccini indicated that two distinct varieties of phlogopite are to be found in his specimens, and it is possible, therefore, that we did not *x*-ray the crystals he believes to be triclinic.

The unanalyzed specimens are from widely scattered localities but are predominantly from pegmatites in Canada, and from marbles or contact metamorphic deposits in New York and to a lesser extent in Montana and Finland.

## RELATION OF CHEMISTRY, STRUCTURE AND PARAGENESIS

On the basis of the data in Table 1 an attempt was made to correlate polymorphism with chemistry and paragenesis in phlogopite but the results were negative. The fact that all three polymorphic modifications of phlogopite occur among the Madagascar specimens, may well rule out the possibility of temperature or pressure as a major factor in determining lattice type.

## *X*-RAY STUDIES OF MANGANOPHYLLITE

The only *x*-ray work reported for manganophyllite has been that of Hendricks and Jefferson (1939), who note a manganophyllite from Rajsberg, Sweden, with a 2-layer monoclinic structure. We have found that all the Swedish manganophyllites described by Jakob (1925) have the 1-layer monoclinic structure. Of the six unanalyzed specimens studied, only one from Franklin, N. J. (No. 1358) has a 2-layer structure; we found no examples of the 3-layer structure. The Swedish manganophyllites that have a very small 2V (particularly Jakob, 1925, Nos. 1 and 5, which are from Varmland) appear to approach the 3-layer hexagonal structure, owing to an intimate "twinning" on (001) of thin sheets, similar to that described for uniaxial lepidolites (Levinson, 1953). From the chemical analyses of these micas there is no correlation between composition and polymorphism. Manganophyllites with the 1-layer form show extreme ranges in Fe and Mn (for example, $Fe_2O_3=0.00$ to 16.94%, see Table 2).

TABLE 2. STRUCTURES OF ANALYZED MANGOPHYLLITES

| Michigan Number | Reference: Jakob (1925) | FeO | $Fe_2O_3$ | MgO | MnO | $Mn_2O_3$ | $TiO_2$ |
|---|---|---|---|---|---|---|---|
| 1076 | No. 8 | 0.00 | 16.94 | 26.79 | 4.52 | 0.00 | 0.00 |
| 1077 | No. 7 | 2.54 | 0.00 | 29.22 | Tr. | Tr. | 0.00 |
| 1078 | No. 6 | 0.00 | 3.95 | 22.60 | 0.00 | 8.30 | Tr. |
| 1079 | No. 5 | 0.00 | 4.68 | 21.18 | 9.25 | 2.96 | 0.00 |
| 1080 | No. 4 | 0.00 | 2.97 | 24.80 | 0.00 | 5.77 | 0.55 |
| 1081 | No. 3 | 0.00 | 2.68 | 26.65 | 0.00 | 4.07 | 0.41 |
| 1082 | No. 2 | 0.00 | 0.91 | 29.28 | 0.00 | 3.92 | 0.00 |
| 1083 | No. 1 | 0.00 | 2.81 | 27.87 | 0.00 | 4.93 | 0.22 |

All have the 1-layer structure and are from Långban and Varmland, Sweden, but apparently are of several different paragenetic types.

The most significant observation concerning the optical properties of the studied manganophyllites is the fact that several of Jakob's (1925) specimens (Numbers 3, 4, and 6) have the optic plane normal to (010). Nearly all micas crystallizing as the 1-layer polymorph have the optic plane parallel with (010). The orientations of these micas were determined by *x*-ray methods; the cause of the anomalies has not been determined.

## *X*-RAY STUDIES OF BIOTITE

The results of the *x*-ray studies of analyzed biotites are in Table 3. Among the biotites there is a significantly larger number of specimens with multiple layer periodicities. During this study, however, neither the 6- nor 24-layer triclinic biotites described by Hendricks and Jefferson (1939) have been found. Zero-level Weissenberg photographs taken about one of the pseudo *a*-axes of the 2-layer monoclinic polymorph appear to be identical with the zero-level, *a*-axis photograph of the 6-layer triclinic biotite illustrated by Hendricks and Jefferson (1939, p. 745). Likewise, zero-level pseudo *a*-axis photographs of the 1-layer monoclinic polymorph strongly resemble zero-level, *b*-axis photographs of the 6-layer monoclinic polymorph reported only in lepidolites. Therefore extreme caution had to be exercised in deciding the structure of these micas from zero-level photographs. Diffuse scattering, particularly among the biotites, also made structure determinations difficult in several instances.

The structures of several uncommon biotite varieties (not analyzed) also were determined (Table 4).

## RELATIONSHIP BETWEEN CHEMISTRY, STRUCTURE AND PARAGENESIS

As is the case of the phlogopites, attempts to correlate structure with

TABLE 3. STRUCTURES OF ANALYZED BIOTITES

| Number | Reference | Structure | Paragenesis | FeO | $Fe_2O_3$ | MgO | $TiO_2$ |
|---|---|---|---|---|---|---|---|
| 728 | Glass (1935) | 3-layer | pegmatite, Amelia, Va. | 26.72 | 2.87 | n.d. | 3.60 |
| 729 | Stevens (1946) | 1-layer | pegmatite, Ridgeway, Va. | 8.96 | 3.31 | 16.15 | 1.11 |
| 797 | Grout (1924) No. 1 | 1-layer (+3-layer ?) | basic segreg. in Kekequabic granite, Minn. | 7.72 | 7.44 | 16.55 | 1.67 |
| 798 | Grout (1924) No. 2 | 3-layer (mod. scattering) | Vermillion granite, Minn. | 14.80 | 4.05 | 10.21 | 2.23 |
| 799 | Grout (1924) No. 3 | 2-layer | granite, Mora, Minn. | 23.23 | 3.03 | 9.24 | 3.32 |
| 800 | Grout (1924) No. 4 | 1-layer | granite, Rockville, Minn. | 23.75 | 1.14 | 6.16 | 2.73 |
| 801 | Grout (1924) No. 5 | 1-layer | peridotite, base Duluth gabbro, Minn. | 12.96 | 8.63 | n.d. | 4.34 |
| 994 | van Biljon (1940) | 2-layer | granite, Namaqualand, S. Af. | 13.58 | 4.23 | 12.16 | 3.89 |
| 960 | Pagliani (1949) | 2-layer | mica schist, Beura, Italy | 9.10 | 5.10 | 10.44 | 0.56 |
| 1001 | Inoue (1950) | 1-layer | nepheline syenite* | 19.9 | 4.53 | 6.26 | 1.10 |
| 1002 | Inoue (1950) | 1-layer (very heavy scatt.) | nepheline syenite* | 21.94 | 8.53 | 5.32 | 1.97 |
| 1003 | Inoue (1950) | 1-layer | nepheline syenite* | 21.02 | 12.45 | 4.19 | 1.04 |
| 1004 | Inoue (1950) | 1-layer (mod. scattering) | cancrinite syenite pegmatite* | 16.03 | 20.22 | 1.37 | 0.70 |
| 1010 | Kawano (1933) | 1-layer | metamorphosed xenolith, Minederayama, Japan | 16.38 | 3.28 | 8.99 | 2.45 |
| 1011 | Kawano (1942) | 1-layer | lepidomelane-quartz-fels, Minederayama, Japan | 23.27 | 7.81 | 4.32 | 2.42 |
| 1084 | Jakob (1931) No. 57 | 2-layer (weak scattering) | 2-mica pegmatite, Monti di Daro, Bellinzona, Switz. | 10.47 | 4.09 | 13.19 | 2.06 |
| 1085 | Jakob (1931) No. 58 | 2-layer | 2-mica pegmatite, Monti di Daro, Bellinzona, Switz. | 9.72 | 2.24 | 14.22 | 1.64 |
| 1086 | Jakob (1931) No. 59 | (3-layer ?) | 2-mica pegmatite, Claro, Tessin, Switz. | 16.26 | 4.03 | 8.46 | 3.16 |
| 1087 | Jakob (1931) No. 60 | 2-layer (weak scattering) | 2-mica pegmatite Claro, Tessin, Switz. | 16.85 | 4.08 | 8.06 | 2.71 |
| 1088 | Jakob (1931) No. 61 | 1-layer | lamprophyre, Gotthard, Switz. | 15.84 | 5.03 | 11.17 | 1.95 |
| 1089 | Jakob (1937) | 1-layer | feldspar pegmatite, Derome, Halland, Sweden | 28.61 | 0.00 | 6.72 | 1.99 |
| 1117 | Coats and Fahey (1944) | 1-layer (mod. scattering) | (siderophyllite) pegmatite, Brooks Mtn., Alaska | 30.16 | Tr. | 0.22 | 0.02 |
| 1140 | C. O. Hutton (not published) | 2-layer | from sands derived from granitic rocks, Calif. | 14.49 | 9.30 | 5.80 | 3.47 |
| 1145 | Hallimond (1947) | 1-layer | marble, Tiree, Hebrides, Gr. Brit. | 6.8 | 1.1 | 18.7 | 1.9 |
| 1257 | Hutton and Seeyle (1947) | 2-layer | pegmatite-like lens in gneiss, Old Pt., Charles Sound, New Zealand | 14.41 | 3.92 | 11.11 | 3.02 |
| 1262 | Mauguin (1928) | 1-layer (heavy scattering) | from Tschebarkul, Ural Mtns., U.S.S.R. | 12.77 | 7.09 | 13.30 | 1.61 |
| 1350 | Yamada and Sugiura (1950) | 1-layer (weak scattering) | pegmatite, Motomiya, Korea | 3.49 | 0.67 | 24.24 | 0.64 |

*Fuku-Shinzan, Korea

TABLE 4. STRUCTURES OF BIOTITE VARIETIES

| Number | Varietal name | Locality | Structure |
|---|---|---|---|
| 732(*a*) | waddoite | Isle of Waddo | 1-layer |
| 746(*a*) | lepidomelane (pterolite) | Brevig, Norway | 2-layer |
| 752(*a*) | meroxene | Mt. Vesuvius | 1-layer |
| 753(*a*) | meroxene (colorless) | Mt. Vesuvius | 3-layer |
| 759(*a*) | meroxene | Mendham, N. J. | 1-layer |
| 754(*a*) | calciobiotite | Italy | 1-layer |
| 770(*a*) | annite | Rockport, Mass. | 1-layer |
| 1116(*a*) | annite | Rockport, Mass. | 1-layer |
| 775(*a*) | siderophyllite | Pikes Peak, Colo. | 1-layer |
| 1117(*a*) | siderophyllite | Brooks Mt., Alaska | 1-layer (mod. scattering) |
| 783(*a*) | cryophyllite | Rockport, Mass. | 1-layer |
| 1112(*a*) | monrepite | Vibora, Finland | 1-layer |
| 1113(*a*) | eukamptite | Presburg, Hungary | 1-layer |
| 1114(*a*) | bastonite | Bastogne, Belgium | 2-layer |

chemistry have been unsuccessful and for the most part structural-paragenesis correlations are likewise not evident. However, some generalizations are available with regard to the geographic and geologic distribution of various polymorphs in selected pegmatite districts.

About 80 biotite specimens from about 15 pegmatite deposits in the southeastern United States were studied. Fifty have crystallized as the 2-layer monoclinic polymorph, 15 as the 3-layer hexagonal polymorph, but only one as the 1-layer monoclinic polymorph. Diffuse scattering, which is characteristic of biotites from this area, and the presence of mixed structures prevented accurate structural determination of the remainder. The results of studies from other scattered pegmatite districts are:

Southern Norway—predominantly 1-layer monoclinic forms, but 2-layer forms common.
Canada: Bancroft and Wilberforce Districts—predominantly 1-layer forms.
Colorado: Guffey District—predominantly 1-layer forms.

Geological environment may play an important role in guiding the crystallization of biotite micas. Pegmatites of the southeastern United States (North Carolina, particularly) are chiefly of quartz dioritic or granodioritic composition, whereas those of the Bancroft area, for example, are nepheline syenitic. It seems possible that biotites crystallizing from magmas of such widely different compositions might have structures related to their particular crystallization environments or source magmas, but further investigation is required to test this hypothesis. As mentioned above, these factors do not themselves uniquely account for the layer types. It was hoped that a knowledge of the temperature of crystallization of these micas might be useful and for this reason a suite of biotite phenocrysts from hypabyssal acid dike rocks from the Guffey District, Colorado, was studied. However, both 1- and 2-layer polymorphs were found in these biotites.

## POSITION OF OPTIC PLANE

Among the studied 2-layer biotites and phlogopites the position of the optic plane is invariably normal to (010). In this respect the 2-layer octophyllite type micas are similar to the 2-layer muscovite types, which have been shown by Hendricks and Jefferson (1939) and Levinson (1953) to have their optic planes normal to (010). All the investigated dark colored micas that have crystallized as the 1-layer polymorph, with the exception of the three anomalous manganophyllites described above, have their optic planes parallel with (010). Hendricks and Jefferson (1939) also observed a 1-layer phlogopite similarly anomalous, i.e., with its optic plane normal to (010).

There has been considerable discussion as to the origin and abundance of the biotite varieties, meroxene (optic plane parallel with (010)) and anomite (optic plane normal to (010)). It has been noted that anomite is relatively rare, whereas meroxene is more common (Winchell and Winchell, 1951). These observations appear to be correct, i.e., the 2-layer polymorph with optic plane normal to (010) (anomite) is less common than 1-layer forms, but it is by no means rare. The cause of this difference in optic orientation is inherent in the various polymorphs, so that the term anomite is synonymous with 2-layer biotite and meroxene with 1-layer biotite. Since the structural characteristics are more fundamental than the optical characteristics, the varietal terms anomite and meroxene probably should be discarded. Furthermore, most of the older descriptions of anomite and meroxene were based on orientation by means of the longest ray of percussion figures. In this study, after the position of (010) has been determined by $x$-ray method, we found that the percussion orientation method was unreliable in about one-third of the trials.

## REFERENCES

COATS, R. R. AND FAHEY, J. J. (1944), Siderophyllite from Brooks Mountain, Alaska: *Am. Mineral.*, **29**, 373–377.

CROSS, W. (1897), Igneous rocks of the Leucite Hills and Pilot Butte, Wyoming: *Am. Journ. Sci.*, ser. 4, **4**, 115–141.

DANA, E. S. (1892), *The System of Mineralogy*: 6th ed., New York.

GLASS, J. J. (1935), The pegmatite minerals from near Amelia, Virginia: *Am. Mineral.*, **20**, 748.

GROUT, F. F. (1924), Notes on biotite: *Am. Mineral.*, **9,** 159–165.

HALLIMOND, A. F. (1947), Pyroxenes, amphibole and mica from the Tiree Marble: *Mineral. Mag.*, **28,** 230–243.

HEINRICH, E. WM., LEVINSON, A. A., LEVANDOWSKI, D. W., and HEWITT, C. H. (1953), Studies in the natural history of micas. Final Rpt., *Project* **M978,** *Univ. Mich. Eng. Res. Inst.*, 241 pp.

HENDRICKS, S. B., AND JEFFERSON, M. E. (1939), Polymorphism of the micas: *Am. Mineral.*, **24,** 729–771.

HUTTON, C. O., AND SEEYLE, F. T. (1947), Contributions to the mineralogy of New Zealand, Part 3: *Trans. Roy. Soc. New Zealand*, **76,** 481–491.

INOUE, T. (1950), Amphiboles and biotites from Fukushinzan alkaline complex, Korea: *Jour. Geol. Soc. Japan*, **56,** 71–77.

JAKOB, J. (1925), Beiträge zur chemischen Konstitution der Glimmer. I Mitteilung: Die schwedischen Manganophylle: *Zeit. Krist.*, **61,** 155–163.

——— (1928), Beiträge zur chemischen Konstitution der Glimmer. IV Mitteilung: Die Phlogopite. I. Teil; *Zeit. Krist.*, **69,** 217–225.

——— (1931), Beiträge zur chemischen Konstitution der Glimmer. IX Mitteilung; Über den Bau der Biotite in weitern Sinn: *Zeit. Krist.*, **79,** 367–378.

——— (1937), Über das Auftreten von dreiwertigem Titan in Biotiten: *Schweiz. Min. Pet. Mitt.*, **17,** 149–153.

——— (1938), Magnesiaglimmer von Morawitza; *Schweiz. Min. Pet. Mitt.*, **18,** 473–474.

——— AND PARGA-PONDAL, I. (1932), Beiträge zur chemischen Konstitution der Glimmer. X Mitteilung: Über die Rolle des Titans in den Phlogopiten: *Zeit. Krist.*, **82,** 271–284.

KAWANO, Y. (1933), Chemical studies of the orbicular rock from Minederayama: *Proc. Imp. Acad. Tokyo*, **9,** 613–616.

——— (1942), Chemical studies of lepidomelane in garnet-lepidomelane-quartzfels from Yuksikou iron mine, Manchuria: *Jour. Jap. Assoc. Min., Petrol. and Econ. Geol.*, **27,** 283–290.

LEVINSON, A. A. (1953), Studies in the mica group; Relationship between polymorphism and composition in the muscovite-lepidolite series: *Am. Mineral.*, **38,** 88–107.

MAUGUIN, C. (1928), Étude des micas au moyen des rayons X: *Bull. Soc. Fr. Min.*, **51,** 326–327.

PAGLIANI, G. (1940), Flogopite e titanolivina di Monte Braccio (Val Malenco): *Atti. Soc. Ital. Sci. Nat. Mus. Civ. Milano*, **79,** 20–22.

——— (1949), La tourmalina di Beura: *Atti. Soc. Ital. Sci. Nat. Mus. Civ. Milano*, **88,** 191–198.

PIERUCCINI, R. (1950), La mica di un blocco pneumatolitico del Monte Somma ed i minerali che l'accompagnano: *Atti. Soc. Toscana Sci. Nat. Mem.*, **57,** ser. A, 145–175.

PRIDER, R. T. (1939), Some minerals from the leucite-rich rocks of the West Kimberly area, Western Australia: *Mineral. Mag.*, **25,** 373–387.

STEVENS, R. E. (1946), A system for calculating analyses of micas and related minerals to end members: *U. S. Geol. Survey, Bull.* **950,** 118.

VAN BILJON, S. (1940), The Kuboos batholith, Namaqualand, South Africa: *Trans. Geol. Soc. South Africa,* **42,** 167.

WINCHELL, A. N., AND WINCHELL, H. (1951), *Elements of Optical Mineralogy, Part II, Descriptions of Minerals:* 4th ed., New York.

YAMADA, H., AND SUGIURA, K. (1950), On hydrated biotite in Motomiya clay: *Jour. Jap. Assoc. Min., Petrol. and Econ. Geol.*, **34,** 122–128.

*Manuscript received November 15, 1953*

# MULTIPLICITY AND DISORDER IN THE LATTICE OF EKMANITE

Bartholomew Nagy,* *Pennsylvania State University, State College, Pennsylvania.*

Abstract

Chemical evidence indicates that ekmanite, a flaky hydrous-iron-manganese silicate mineral, is related to the layer lattice silicates. The results of single crystal $x$-ray studies suggest that ekmanite possesses a structure that is essentially a packing of talc-type sheets and interleaved cations and that the orthohexagonal cell is a multiple of a sub-unit of the following dimensions: $a=5.54$ Å, $b=9.60$ Å, and $c=12.08$ Å. The distribution of diffuse reflections indicates the presence of a disordered lattice related to random and *irregular* shifts of the talc-type units.

An $x$-ray investigation was undertaken in an attempt to determine the mineralogical position of ekmanite. It is expected that the study of rare, hydrous-silicate minerals like ekmanite may result in data that can be significant with respect to the entire layer lattice silicate group.

Ekmanite was first described from its occurrence at Grythytte, Sweden, by Igelström, as reported by Dana (1892). It was found to be a flaky, massive or asbestiform mineral that has a color varying between light green and black, and resembles the common types of chlorites in its megascopic appearance. Ekmanite was reported to be associated with the magnetite iron ore.

Jakob (1923) reexamined ekmanite samples from the same locality and came to the conclusion that the mineral is related to the friedelite-pyrosmalite group. Jakob emphasized the fact that the ekmanite crystals very commonly show perfect basal cleavage planes, and noted that the mineral is apparently optically uniaxial. This agrees with the results of Hamberg, as reported by Dana, who also concluded that ekmanite is uniaxial. This conclusion was confirmed by the results of the optical investigation performed during the present study.

## Investigation of the Chemical Relationship Between Ekmanite and the Layer Lattice Silicates

Chemical analyses of ekmanite obtained from the literature and differential thermal analysis curves prepared during the present study were compared with those of known sheet structure minerals and it was concluded that the available data seemed to suggest the existence of a chemical relationship between ekmanite and the layer lattice silicates.

There are only a few chemical analyses available of ekmanite. The chemical data show that this mineral is essentially an iron-manganese hydrous-silicate that usually also contains a small percentage of alumina and magnesia. Table 1 shows seven chemical analyses of ekmanite; the first six of these analyses were given by Igelström and the seventh by Jakob; Igelström's analyses were obtained from Dana. A chemical analysis of stilpnomelane was also included in Table 1, in order to enable one to compare the chemical composition of this mineral with the chemical data of ekmanite.

---

* Present address: Stanolind Oil and Gas Company, P.O. Box 591, Tulsa 2, Oklahoma.

TABLE 1. CHEMICAL ANALYSES OF EKMANITE AND STILPNOMELANE

| | *Ekmanite* | | | | | | | *Stilpnomelane* |
|---|---|---|---|---|---|---|---|---|
| | 1 | 2 | 3 | 4 | 5 | 6 | 7 | 8 |
| $SiO_2$ | 34.30 | 36.42 | 40.30 | 37.07 | 37.69 | 36.82 | 39.41 | 45.61 |
| $Al_2O_3$ | tr | 1.07 | 5.08 | 5.85 | — | 3.63 | 8.36 | 5.00 |
| $Fe_2O_3$ | 4.97 | 4.79 | 3.60 | — | — | — | 14.06 | — |
| FeO | 35.78 | 24.27 | 25.54 | 38.20 | 36.07 | 31.09 | 13.54 | 37.70 |
| MnO | 11.45 | 21.56 | 7.13 | 6.32 | 14.74 | 9.29 | 5.15 | — |
| MgO | 2.99 | tr | 7.64 | | | 7.53 | 3.69 | 3.00 |
| CaO | — | tr | — | 2.73 | — | tr | 4.51 | — |
| $H_2O$ | 10.51 | 9.91 | 10.74 | 9.71 | 11.50 | 10.71 | 9.42 | 9.14 |
| $CO_2$ | — | — | — | — | — | — | 1.94 | — |
| | 100.00 | 98.02 | 100.03 | 99.88 | 100.00 | 99.07 | 100.08 | 100.45 |

Analyses 1–6 and 8 were reported by Igelström and listed by Dana (1892).
Analysis 7 was given by Jakob (1923).

An approximate chemical formula was calculated from the average of these seven analyses. It may be written in the following oxide form:

$$(Fe, Mn, Mg)\,O \cdot SiO_2 \cdot H_2O.$$

The molecular ratio between silica and the oxides of the other cations is approximately 1:1. An arbitrary step was taken during the calculations that consisted of grouping the silica and alumina together, and including ferric iron in the total sum of the ferrous, manganese and magnesium oxides. Due to the relatively low amounts of alumina and ferric iron present in most of the chemical analyses, the fundamental 1:1 ratio between silica and the metallic oxides does not appear to be seriously affected even if a different grouping of the oxides were to be chosen.

The chemical composition of ekmanite was compared with that of other hydrous silicate minerals. The ratio between the silicon ion and the other cations present in ekmanite is approximately the same as in biotite. It is lower than that of talc, stilpnomelane and also tremolite, but it is higher than the ratio present in chrysotile and chlorite.

Another approach that was followed during the investigation of the relationship between ekmanite and other hydrated silicate minerals involved the comparison of the differential thermal analysis curves. The *DTA* patterns of ekmanite are characterized by a double exothermic peak between approximately 250–450° C. and another weaker exothermic reaction at approximately 770° C. There is only one endothermic peak present on the differential thermal analysis patterns; this peak occurs around 140° C.

The ekmanite *DTA* curves resemble those of stilpnomelane. In Fig. 1 an ekmanite differential thermal analysis pattern is shown together with that of a mineral that appeared to be stilpnomelane and one of clinochlore. All of the *DTA* runs were made at the heating rate of 600° C. per hour, using platinum crucible sample holders and a continuously recording potentiometer unit. The differential thermal analysis patterns were recorded on a chart on which one set of coordinates were curved lines. The patterns were replotted, however, on a rectangular coordinate system in order to facilitate their observation. Furthermore, it was also thought that it might be easier to compare these re-plotted curves with the *DTA* patterns of other hydrous silicates present in the literature which are usually plotted on rectangular coordinate system.

The high temperature endothermic reaction that occurs with clay minerals was absent on the ekmanite differential thermal analysis patterns. One of the *DTA* runs performed on stilpnomelane showed an endothermic peak at approximately 660° C., but it was impossible to reproduce this peak. The *DTA* curve of stilpnomelane shown in Fig. 1 represents a pattern which seemed to be characteristic and reproducible. Gruner (1937) reported that stilpnomelane loses water around 500° C.; this temperature, however, is very close to the upper limit of the temperature at which the exothermic reaction occurs. Hutton (1938) reported that this water loss of stilpnomelane occurs around 350° C. This temperature coincides with the temperature of the exothermic reaction caused by the oxidation of ferrous iron and consequently the development of the strong exothermic peak of the differential thermal analysis patterns may interfere with the development of an endothermic peak.

The exothermic peaks present on the ekmanite and stilpnomelane *DTA* patterns below 500° C. may be due to the oxidation of the ferrous iron. This possibility is based on the results of experiments performed with ferrous and sodium oxalate. These two (chemically pure) materials were run in the differential thermal analysis unit in order to note the approximate temperature at which the exothermic reaction due to the oxidation of the ferrous iron takes place. The differential thermal analysis of sodium oxalate served as a control on the ferrous oxalate run; if the exothermic

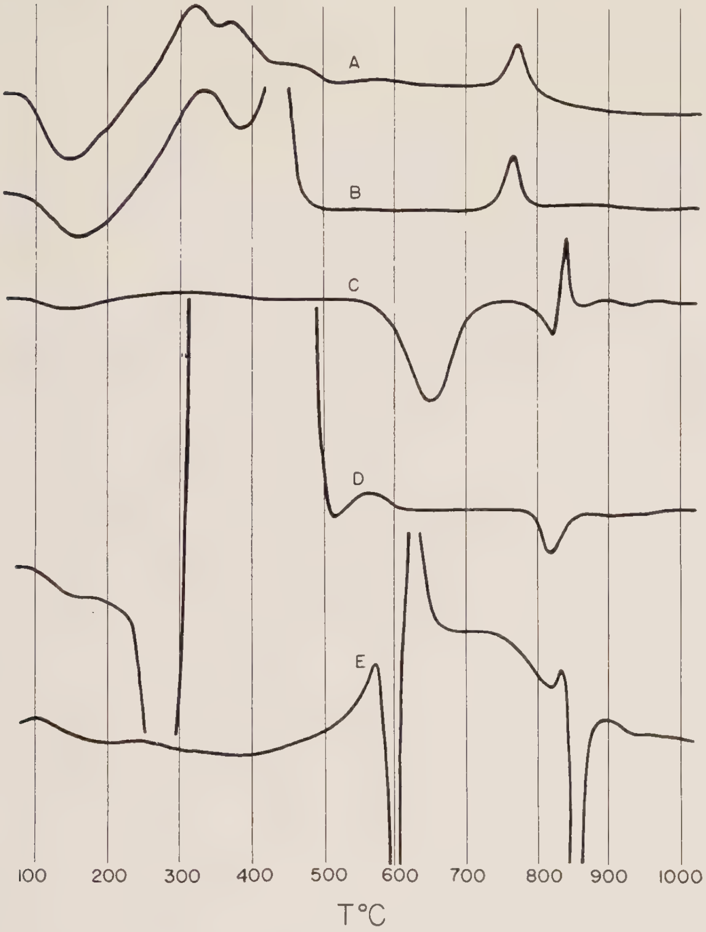

FIG. 1. Differential thermal analysis patterns of (*A*) ekmanite, (*B*) stilpnomelane, (*C*) clinochlore, (*D*) ferrous oxalate and (*E*) sodium oxalate.

reaction in question were not caused by the oxidation of ferrous iron, one might expect it to occur in both ferrous and sodium oxalate *DTA* patterns. The differential thermal analysis curves of ferrous and sodium oxalate are shown in Fig. 1. The exothermic reaction between approximately 300 and 500° C. occurred only in the case of ferrous oxalate. This strengthens the possibility that the similar reactions which occurred during the heating of ekmanite and stilpnomelane might also be caused by the oxidation of ferrous iron. These reactions, however, may not be due entirely to the oxidation of ferrous iron but may also be the result of the oxidation of manganese that is expected to occur in the same temperature range. One may draw an analogy between the exothermic reactions of ekmanite or stilpnomelane and ferrous oxalate only if the bond strengths between the ferrous iron and the surrounding ions are similar in both materials. Such a relationship is anticipated due to the fact that in the stilpnomelane structure (Gruner, 1944) iron is located between the talc-type layers and between the Si-O double sheets.

According to Gruner the crystal structure of stilpnomelane consists of a talc-type unit together with ions located between the basal planes of this unit. Although the chemical composition of ekmanite is somewhat different from that of stilpnomelane, *x*-ray investigations showed that the two minerals may be closely related.

## SINGLE CRYSTAL *X*-RAY INVESTIGATION OF EKMANITE

In order to determine the cell dimensions and symmetry of ekmanite Laue photographs, rotation, oscillation, Weissenberg diagrams and powder patterns were taken. The material employed was obtained from a specimen from Brunsjö (near Grythytte), Sweden; some of the flakes present in this sample were large enough for single crystal *x*-ray studies. Because of the presence of a greenish-gray coating that often covered the particles, the sample was examined under a binocular microscope in order to detect the presence of any visible impurity and in order to be able to discard all impure flakes. The flakes selected for the single crystal *x*-ray studies showed excellent basal cleavage planes. Poor development of the crystals around the edges prevented the appearance of other faces, with the exception of a distorted, apparently pyramidal face that was present on some of the particles.

Unfiltered molybdenum radiation was used for the Laue diagrams. The Weissenberg photographs were taken with iron and the rotation diagrams with both iron and molybdenum radiation. Iron radiation proved to be a suitable choice for the last two methods because of the ferriferous nature of ekmanite and the large cell dimensions.

The Laue photographs taken normal to the basal plane show both diffuse streaks and spots. Those spots which do not lie along the strong, diffuse streaks may be connected with very weak streaks. A three-fold axis was detected normal to the basal plane together with three vertical mirror planes intersecting each other at the center of the diagram at 120° angles. These features can be seen on Fig. 2 which is a reproduction of a Laue diagram taken with the *x*-ray beam normal to the basal plane. The symmetry elements present on the photographs indicate that the Laue symmetry of ekmanite is $D_{3h}$.

The first rotation diagrams were taken with Mo radiation and the photographs were exposed for twelve hours. Photographs taken by rotating the crystal about an axis which was later found to be the orthohexagonal *b* axis show five well developed layer lines together with a few very weak and diffuse spots at approximately 1/3 and 2/3 height between the zero and what appeared to be the first layer line. The identity period between the zero and the first layer lines was found to be 3.2 Å; such a value is low by analogy with other chemically similar minerals. In order to detect the true identity period between the zero and the first layer lines the rotation diagrams were retaken with FeK$_\alpha$ radiation and an exposure of 48 hours. The resultant photograph reveals a different periodicity. The identity period appears to be much larger than the previously observed value; it was found to be 38.40 Å and the strong line at 3.2 Å position is preceded by 11 more layer lines. The rotation diagrams are characterized by the strong 0 and 12th layers and by the large number of closely spaced, comparatively weak reflections of the intermediate layer lines. Most of the reflections appear to be diffuse streaks rather than sharp spots. It is important to note that "streaky" reflections are present on all of the layer lines; and since the rotation axis is the orthohexagonal *b* axis, one may conclude that such reflections are not restricted to planes

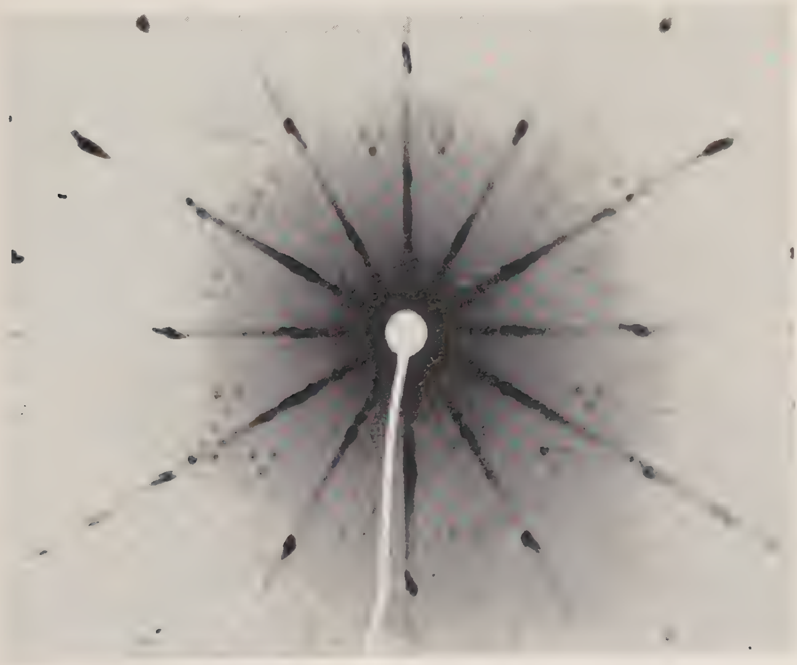

FIG. 2. Laue photograph of ekmanite taken with the *x*-ray beam normal to the basal plane. Unfiltered Mo radiation.

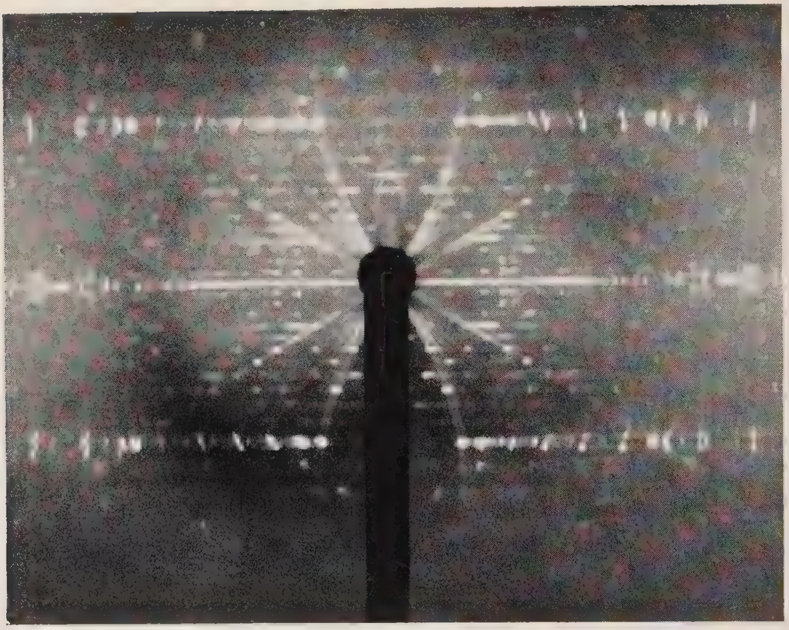

FIG. 3. Rotation diagram of ekmanite taken with rotation around the *b* axis. Fe $K_\alpha$ radiation. Most of the weak, diffuse reflections were lost when a reversed (negative) print was made from the original rotation photograph; a positive print of the *x*-ray film, that is shown above, is in good agreement with the original pattern.

of only certain *k* indices but that *diffuse streaks occur for every value of k.* An example of this distribution is shown in Fig. 3.

The Weissenberg method resulted in photographs showing "streaky" reflections. Normal beam equatorial Weissenberg photographs show that the 00*l* reflections are the least "streaky" in character and that all of the *h*0*l* reflections are spread out along continuous curves. Indices can be assigned to reflections on the basis of an orthohexagonal unit cell. The dimensions of this cell and of the corresponding hexagonal unit are the following:

| *Orthohexagonal cell* | *Hexagonal cell* |
|---|---|
| $a=66.52$ Å ($12\times 5.54$ Å) | $a_1=38.40$ Å |
| $b=38.40$ Å ($4\times 9.60$ Å) | $a_2=38.40$ Å |
| $c=96.62$ Å ($8\times 12.08$ Å) | $c=96.62$ Å |

The multiplicity of the sub-unit along the three axes is expected to vary in different samples. This may be similar to the polymorphous forms of mica which show such a variation along the *c* axis, as reported by Hendricks and Jefferson (1939).

The agreement between the calculated and observed interplanar spac-

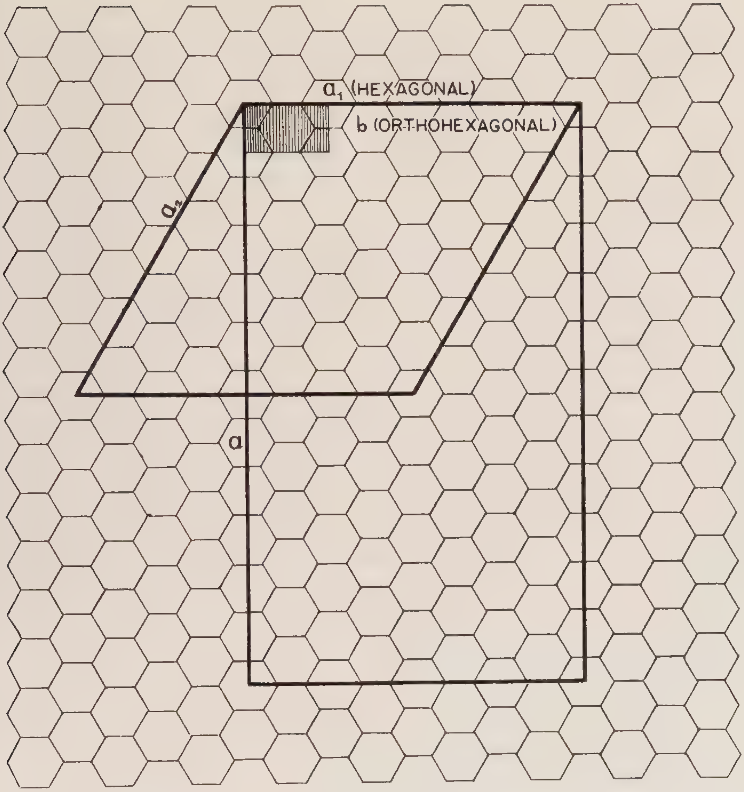

FIG. 4. A possible relationship between the hexagonal $a_1$ and $a_2$ and orthohexagonal *a* and *b* cell dimensions of ekmanite and a hexagonal network of atoms similar to the silicon-oxygen hexagons of the layer lattice silicates. The shaded area shows the approximate dimensions of the 00*l* section of the unit cell of talc.

ings confirms: (1) the unit cell dimensions, (2) the multiplicity along the axes, and (3) the right choice of axes. The hexagonal unit is based on a rhombic section in the $a_1$ and $a_2$ plane. The length of these two axes is the twelfth multiple of 3.2 Å, which is approximately the length of one of the edges of a silicon-oxygen hexagon that characterizes the layer lattice silicates. One possible relationship between the length of the hexagonal $a_1$ and $a_2$ and orthohexagonal *a* and *b* cell dimensions and such a hexagonal pattern of atoms is shown in Fig. 4. The *ab* plane of a talc-type unit is shown by the shaded area on the diagram. One may observe the apparent relationship between the talc-type and the ekmanite *a* and *b* unit cell dimensions and the fact that the ekmanite *a* axis is an approximately twelfth multiple of the talc-type *a* axis, and that the *b* axis is a fourth multiple of that of the talc-type sub-unit.

The multiplicity along the $c$ axis is also significant. The distribution of the $00l$, $h0l$, $hkl$ reflections on the rotation and Weissenberg photographs indicate a $c$ unit cell dimension which is fundamentally an 8th multiple of a 12.08 Å sub-unit. The 008 ($d_{008}=12.08$ Å) reflection is the strongest one present on the ekmanite powder photographs; $00l$ reflections were $l=n8$ also appear as very prominent and strong reflections.

Consideration of some of the prominent features of the $x$-ray diagrams led to some tentative conclusions about the basic structural pattern of ekmanite. A structural analysis was not attempted due to the fact that certain reflections could not be indexed with sufficient certainty because of their diffuse, "streaky" character and closely spaced distribution. The following facts, however, appear to be significant: (1) the apparent 8 fold multiplicity of the 12.08 Å sub-unit along the $c$ axis, (2) the relationship between the orthohexagonal $a$ and $b$ axes and a hexagonal network of atoms, and also the apparent relationship between a talc-type sub-unit and the ekmanite $a$ and $b$ unit cell dimensions, and (3) the analogy in both interplanar spacing and intensity between the 008 reflection ($d_{008}=12.08$ Å) and the corresponding $00l$ reflection of certain layer lattice silicates, especially stilpnomelane ($d=12.1$ Å). The chemical composition, differential thermal analysis data and morphology of ekmanite may also be significant. These data seem to suggest that ekmanite possesses a structure which is essentially a packing of talc-type sheets and interleaved cations with possible variations in the sub-units resulting in the super-lattice. This talc-type sub-unit present in the ekmanite lattice appears to have the following dimensions: $a=5.54$ Å, $b=9.60$ Å and $c=12.08$ Å.

Another aspect of the $x$-ray investigations involves the disorder present in the ekmanite lattice. The diffuse streaks of the Laue photographs have been referred to by some authors as "asterism." This phenomenon has been studied by several investigators, including Hendricks and Jefferson, who have examined this effect in the case of the micas, and also by Hutton and Fankuchen (1938), who have made a comparison between the Laue photographs of stilpnomelane and other layer lattice silicates. Hendricks and Jefferson suggested that the diffuse streaks present on the Laue patterns correspond to continuous curves on the Weissenberg diagrams and that both of them can be explained in terms of reflections showing continuous variation in the $l$ index but possessing constant $h$ and $k$ indices. The $x$-ray patterns of most of the layer lattice silicates show such continuous curves only when $k\neq 3n$. When $k=3n$ reflections are sharp spots that suggest a random displacement of the mica layers along the $b$ axis by $nb/3$ increments, where $n$ is an integer. Random shifts of the structural layers are not restricted to the micas only; they may also be observed with other layer lattice silicates. Brindley, Oughton and Robinson (1950) have shown rotation photographs of chlorites taken of ordered and disordered single crystals. The disordered sample yielded a rotation photograph on which the diffuse streaks appeared when $k \neq 3n$ and sharp spots when $k = 3n$. All of the reflections were sharp spots when the sample had an ordered lattice.

The rotation photograph of ekmanite is different because diffuse streaks occur for every value of $k$, as is shown in Fig. 3. Accordingly, equatorial Weissenberg photographs taken about the $b$ axis show continuous diffuse streaks for all of the $h0l$ reflections. These results suggest that the displacement of the ekmanite structural layers is different from those of the micas of Hendricks and Jefferson and also from the disordered chlorites of Brindley, Oughton and Robinson. The displacement does not leave the reflections undisturbed where $k = 3n$ and, therefore, it cannot be attributed to random shifts of $nb/3$ along the $b$ axis. A random and *irregular* shift of the structural layers along the $a$ and $b$ axes may account for the pattern; this would indicate, however, a different type of disorder than the one that is commonly present in the mica and chlorite structures.

Figure 5 shows three dimensional drawings of the reciprocal lattice of a hypothetical crystal. When the lattice has a perfect order (*A*) all of the

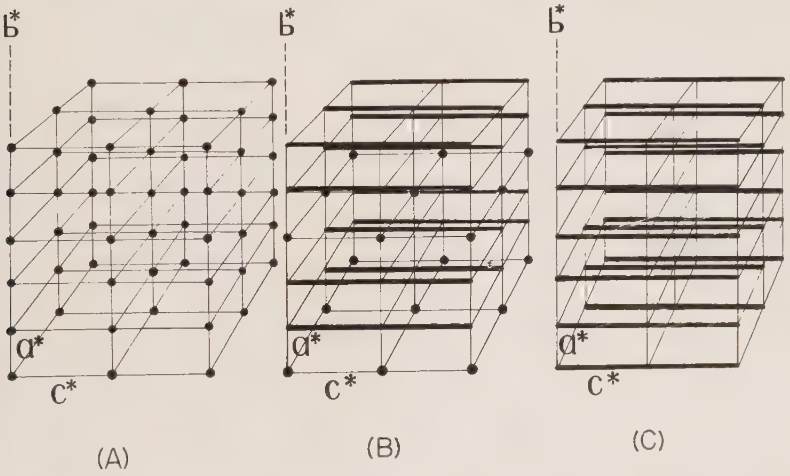

Fig. 5. Three dimensional representations of the reciprocal lattice of a hypothetical crystal: (*A*) in perfect order, (*B*) affected by a random displacement of the structural layers by $nb/3$ increments along the $b$ axis, and (*C*) affected by random and irregular displacement of the structural elements along the $a$ and $b$ axes. The diagram shown in (*C*) is an exaggerated representation (because it portrays complete disorder) of the effect of random disorder that appears to be present in the ekmanite lattice.

reciprocal lattice points appear as points. A random and regular shift along one axis results in a reciprocal lattice that is essentially a combination of points and straight lines; in case of the displacement by $nb/3$ increments ($B$) points are found only on those reciprocal lattice planes where $k=3n$. A random and irregular shift of the structural layers along two axes will cause the reciprocal lattice to consist entirely of straight lines ($C$). The rotation and Weissenberg photographs show related features that may be explained in terms of these examples.

## CONCLUSIONS

The results of single crystal $x$-ray studies and chemical evidence suggest that the lattice of ekmanite is based on talc-type units. Similarity between the structure of ekmanite and of layer lattice silicates of the stilpnomelane type may be anticipated. The multiplicity along all three axes results in a super-lattice that also shows signs of disorder related to random and irregular displacements of the structural layers along the $a$ and $b$ axes. The multiplicity along the $a$, $b$ and $c$ directions may vary with different samples similar to the polymorphous forms of mica which show such a variation along the $c$ axis. Accordingly a variation of the symmetry of different crystals of ekmanite is anticipated.

## ACKNOWLEDGMENT

The author is greatly indebted to Professor W. R. Büssem for his interest and advice.

## REFERENCES

BRINDLEY, G. W., OUGHTON, B. M., AND ROBINSON, K. (1950), Polymorphism of the chlorites. I. Ordered structures: *Acta Cryst.*, **3,** 408–416.

DANA, E. S. (1892), Descriptive Mineralogy, John Wiley & Sons, New York, Sixth Edition.

GRUNER, J. W. (1937), Composition and structure of stilpnomelane: *Am. Mineral.*, **22,** 912–925.

GRUNER, J. W. (1944), The structure of stilpnomelane reexamined: *Am. Mineral.*, **29,** 291–298.

HENDRICKS, S. B., AND JEFFERSON, M. E. (1939), Polymorphism of the micas: *Am. Mineral.*, **24,** 729–771.

HUTTON, C. O., AND FANKUCHEN, I. (1938), The stilpnomelane group of minerals: *Mineral. Mag.*, **25,** 172–206.

JAKOB, J. (1923), Zur Kenntnis der Ekmannit-Minerale I.: *Schweiz. Min. Petr. Mitt.*, **3,** 237–239.

*Manuscript received July 23, 1953*

# AN EXPERIMENTAL STUDY OF THE FORMATION AND PROPERTIES OF SYNTHETIC SERPENTINES AND RELATED LAYER SILICATE MINERALS

Della M. Roy and Rustum Roy*

## Abstract

The hypothesis that the formation of tubular crystals of chrysotile is the result of misfit of the alternate brucite and silica layers, is tested by means of chemical substitution. Increasing the size of the tetrahedral layer by substituting $Ge^{4+}$ for $Si^{4+}$ results in the formation of hexagonal platy crystals of the serpentine phase, $Mg_6Ge_4O_{10}(OH)_4$. Decreasing the size of the octahedral layer and at the same time increasing the size of the tetrahedral layer is accomplished by partial substitution of $Al^{3+}$ into the structure to form platy aluminian serpentine, $Mg_5AlAlSi_3O_{10}(OH)_4$. The replacement of $Mg^{2+}$ by the similar-sized $Ni^{2+}$ ion yields a serpentine $Ni_6Si_4O_{10}(OH)_4$ which is either tubular or platy, depending on other factors. Another serpentine phase synthesized, $Ni_6Ge_4O_{10}(OH)_4$, forms hexagonal platy crystals. Other substitutions using the following ions: $Mn^{2+}$, $Zn^{2+}$, $Co^{2+}$, $Fe^{3+}$, $Cr^{3+}$, and $Ga^{3+}$, fail to yield a serpentine type structure.

A number of other hydrosilicate type structures have been synthesized, and comparisons are made of the phase equilibrium relations determined to be present among phases in the systems, $MgO$-$SiO_2$-$H_2O$, $NiO$-$SiO_2$-$H_2O$ and $MgO$-$GeO_2$-$H_2O$.

## I. Introduction

One of the mineralogical problems which has attracted considerable attention in recent years concerns the structure, morphology and synthesis of the serpentine minerals chrysotile and antigorite. The structure of chrysotile, although known in outline, has been the subject of much debate, the choice between a kaolinite type sheet structure and an amphibole chain structure being relatively difficult and not resolved till relatively recent times. Acceptance of the sheet structure makes possible the consideration of the curving of these sheets, first suggested by L. Pauling (1930), as the means of compensating for any slight strain among the layers. The diffraction effects (both *x*-ray and electron) to be expected from curved sheets were studied both theoretically and experimentally by Fock and Kolpinsky (1940). Comprehensive work by Aruja (1945) and Whittaker (1952) greatly enlarged our understanding of these minerals. Most recently on the basis of direct observation in the electron microscope numerous investigators have shown these chrysotile crystals not only to be curved but to actually occur as cylindrical or tubular crystals. (See Bates, Sand and Mink, 1950; Noll, 1950; Hillier, 1949; and Turkevitch and Hillier, 1949.) Whereas previous investigators have relied on physical proofs for the concept of the tubular crystals being caused by the misfit of layers, a "chemical" method for adducing evidence to this same end may be devised on the basis of synthesizing a series of such structures containing ions of slightly different size. At the same time interesting data may be obtained on the formation and stability of various structures containing different ions.

---

* College of Mineral Industries, The Pennsylvania State University, Contribution No. 53–9.

In earlier work Bowen and Tuttle showed electron micrographs of synthetic chrysotile ($Mg_6Si_4O_{10}(OH)_4$) with apparently tubular habit although they did not recognize these as "tubes," while Bates, Sand and Mink (1950), Hillier (1949), and Noll (1950) have demonstrated the tubular habit of natural chrysotile using the electron microscope. Tu (1949) claimed that he had prepared "antigorite" with a platy habit from magnesia-silica mixtures containing small amounts of $Al_2O_3$, and Roy (1952) and Yoder (1952) presented evidence for solid solution with 2 Al replacing Mg+Si in chrysotile, giving rise to a phase with platy hexagonal habit -probably the same phase as Tu's "antigorite." Since the inception of this work, Noll prepared synthetic Ni-serpentines in the presence of $Na^+$ and $Cl^-$ ions, and showed these to be tubular. Van Eyk Voorthuysen (1952) had also reported the preparation of synthetic Ni-serpentine but did not describe its morphology. The present work was carried out in an attempt to obtain comparative data on several synthetic serpentines with respect to morphology.

Incidental to the work on morphology, by studying a few compositions in each of the systems investigated it was possible to obtain information on the existence, properties and stability range of other phases which form in these systems. A comparison of the stability of the various analogous phases (isomorphs) can provide useful geochemical data.

## II. Experimental

In the present study the phases were prepared by now well-established hydrothermal techniques (Roy and Osborn, 1952; Roy, Roy, and Osborn, 1950). For such preparations it is very desirable if not essential to start with the components in a very finely divided and if possible "amorphous" form. To this end mixtures were prepared by one or more of the following techniques: (*a*) as coprecipitated gels; (*b*) by mixing alcohol soluble salts or compounds in solution and evaporating; or (*c*) mixing finely divided salts which would decompose easily, such as hydroxides and carbonates by wet grinding in agate mortars. All chemicals used were of reagent grade purity. Such mixtures are wrapped in gold or platinum foil and treated at the appropriate temperature and pressure. The temperature range was from 150° C.–900° C. and the pressure range from 500 psi-30,000 psi. Runs varied in length from $\frac{1}{2}$ day to 60 days. More complete details of the experimental technique are omitted here since they have been given in earlier papers (Roy and Osborn, 1952; Roy, Roy, and Osborn, 1950). Some 250 runs were made to obtain these data. After hydrothermal treatment, the products were identified largely by their optical properties and *x*-ray diffraction patterns—all the products being so examined. Either Norelco 90° Geiger-counter "diffractometers" or a GE XRD-3 165° diffractometer were used, with filtered Cu or Fe radiation. The petrographic microscope proved to be of limited use with such fine-grained material, and most of the material was studied under the electron microscope (RCA Model EMU). Latterly, some work was done with single crystal electron diffraction patterns to determine unit cell dimensions. Where *x*-ray data are listed, they were obtained on the high angle instrument, although in some cases only the few low-angle spacings were obtained. Instead of using calibrants in the latter cases, the instrument zero was checked and the low-angle spacings read directly. Under such conditions reliable data are obtained for calibrating materials. Reproducibility in most cases was better than .01° $\theta$. The frequently large discrepancies between 001 and higher order reflections were absent.

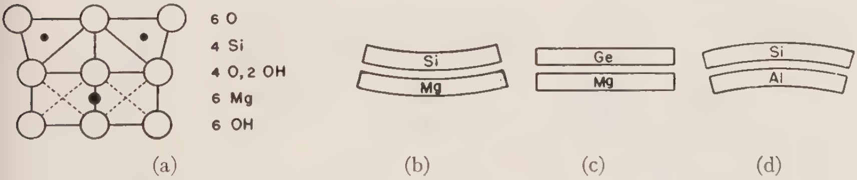

(a) (b) (c) (d)

Fig. 1. Schematic representation of serpentine-type structures. (*a*) Chrysotile structure; (*b*) Chrysotile structure, silica and brucite layers, showing curvature due to larger size of brucite layer; (*c*) Magnesia-germania serpentine layers, not curved; (*d*) Gibbsite and silica layers in halloysite, curved in opposite direction from serpentine.

## III. Results

### A. Relation Between Morphology and Composition:

1. *Misfit due to composition.* In Fig. 1 (*a*) we represent (according to the scheme used by Pauling): the structure of magnesium chrysotile and in Fig. 1 (*b*) the structure is illustrated very schematically as two sheets (one of brucite and one of silica) of slightly different length. Due to the "misfit" between these layers there is a tendency to curvature with the brucite layer on the outside. This curving tendency is the apparent cause for the tubular nature of chrysotile and endellite ($Al_2O_3 \cdot 2SiO_2 \cdot 4H_2O$).* It is desirable to obtain further information to show whether this is indeed the case. In order to obtain a closer fit of the layers, we can change the size of either the brucite or silica layers, eliminating any tend-

---

* A detailed illustrated treatment of the "misfit" idea has been given by Bates, Hildebrand, and Swineford (1950).

ency to curvature due to misfit. In Fig. 1 (*c*) the size of the silica layer is increased by the replacement of $Si^{4+}$ by $Ge^{4+}$, to show an approximate fit. (A quantitative figure is not available directly for the expected size of the "$GeO_2$" layer.) Whereas complete replacement of 3 $Mg^{2+}$ in the brucite layer by $2Al^{3+}$ (to produce endellite, Fig. 1 (*d*) gives the opposite type of misfit with the silica layer on the outside, partial substitution should cause a condition of good fit for some compositions. Roy (1952) has shown there is no substitution of $2Al^{3+}$ for $3Mg^{2+}$ in the octahedral position *only*, but that substitution takes place, on the other hand, when the equivalent amount of $Al^{3+}$ enters the tetrahedral position simultaneously. This makes $Al^{3+}$ doubly effective, since it contracts the brucite layer and expands the silica layer simultaneously; and hence, only a

TABLE 1. MORPHOLOGY OF SERPENTINES

| Starting Material Composition | Temp. ° C. | Press. (psi) | Time (hrs.) | Electron Microscope Observations |
|---|---|---|---|---|
| 3 $MgO \cdot 2\ SiO_2$† | 392 | 10,000 | 408 | long fibrous "jointed" tubes, curved |
| 3 $MgO \cdot 2\ SiO_2$† | 230 | 5,000 | 648 | short stubby tubes |
| 3 $MgO \cdot 2\ GeO_2$† | 500 | 10,000 | 92 | hexag. plates, thin and thick |
| 3 $MgO \cdot 2\ GeO_2$† | 450 | 20,000 | 120 | hexag. plates, some thick |
| 3 $NiO \cdot 2\ SiO_2 + NaCl$‡ | 325 | 5,000 | 48 | good tubes |
| 3 $NiO \cdot 2\ SiO_2 + NaCl$‡ | 325 | 5,000 | 172 | v.* fine plates, few tubes |
| 3 $NiO \cdot 2\ SiO_2 + NaCl$‡ | 445 | 10,000 | 22 | good tubes, some plates |
| 3 $NiO \cdot 2\ SiO_2 + KCl$‡ | 220 | 5,000 | 24 | few tubes, v. fine particles |
| 3 $NiO \cdot 2\ SiO_2 + KCl$‡ | 450 | 10,000 | 24 | good tubular crystals |
| 3 $NiO \cdot 2\ SiO_2$‡ | 325 | 5,000 | 26 | v. fine plates, some poor tubes |
| 3 $NiO \cdot 2\ SiO_2$‡ | 325 | 5,000 | 190 | v. fine plates |
| 3 $NiO \cdot 2\ SiO_2$‡ | 500 | 10,000 | 90 | platy |
| 3 $NiO \cdot 2\ SiO_2$‡ | 400 | 8,000 | 215 | platy |
| 3 $NiO \cdot 2\ GeO_2$‡ | 300 | 10,000 | 144 | v. fine-grained platy |
| 3 $NiO \cdot 2\ GeO_2 + KCl$‡ | 230 | 5,000 | 24 | fairly large hexag. plates |
| 5 $MgO \cdot 1\ Al_2O_3 \cdot 3\ SiO_2$§ | 515 | 23,000 | 384 | good hexag. plates |
| 5 $MgO \cdot 1\ Al_2O_3 \cdot 3\ SiO_2$† | 515 | 23,000 | 384 | fairly good hexag. plates |
| 5 $MgO \cdot 1\ Al_2O_3 \cdot 3\ SiO_2$§ | 605 | 10,000 | 384 | good hexag. plates |
| 57 $MgO \cdot 1\ Al_2O_3 \cdot 40\ SiO_2$† | 450 | 10,000 | 276 | v. thin plates, possibly few tubes |

* Abbreviations used: v. = very, hexag. = hexagonal, xls = crystals.

† Mixtures of C.P. oxides.

‡ Co-precipitated gels.

§ Nitrate-ethyl silicate type mixture.

relatively small amount of $Al^{3+}$ should be required to cause a good fit. Most of the other feasible substitution in the brucite layer of $Ni^{2+}$, $Zn^{2+}$, $Mn^{2+}$, $Co^{2+}$, etc., should retain or increase the misfit.

2. *Experimental results*. The results of the experiments relating to morphology are summarized in Table 1, and are described briefly below; *x*-ray data for the serpentine phases formed are given in Table 2.

TABLE 2. *X*-RAY DATA FOR SYNTHETIC SERPENTINE PHASES*

| Aluminian Serpentine $5\,MgO\cdot Al_2O_3\cdot 3SiO_2\cdot 4\,H_2O$ | | Magnesia-Germania $3\,MgO\cdot 2\,GeO_2\cdot 2\,H_2O$ | | Nickel-Germania $3\,NiO\cdot 2\,GeO_2\cdot 2\,H_2O$ | | Nickel-Silica $3\,NiO\cdot 2\,SiO_2\cdot 2\,H_2O$ | |
|---|---|---|---|---|---|---|---|
| *d*(Å) | *Int.* | *d*(Å) | *Int.* | *d*(Å) | *Int.* | *d*(Å) | *Int.* |
| 7.17 | s | 7.46 | vs | 7.49 | vs | 7.26 | vs |
| | | 4.70 | m | | | | |
| 4.59 | ms | 4.62 | mw | 4.62 | s, br | | |
| | | 4.50 | m | | | 4.2 | vvw |
| | | 4.34 | w | | | | |
| | | 4.17 | w | | | | |
| | | 4.02 | vw | | | | |
| 3.574 | vs | 3.73 | vs | 3.680 | vs | 3.629 | s |
| | | 3.13 | w | | | | |
| 2.64 | w | 2.76 | w | | | | |
| | | | | 2.690 | m, br | | |
| 2.50 | mw | | | | | | |
| 2.39 | w | 2.553 | s | 2.540 | vs | 2.50 | ms |
| | | 2.488 | w | | | | |
| | | 2.332 | vw | | | | |
| 2.000 | vw | 2.201 | vw | | | 2.14 | m |
| | | 2.017 | w | | | | |
| | | 1.835 | w | | | | |
| 1.536 | vs | | | | | | |
| 1.502 | w | 1.569 | m | 1.559 | s | 1.52 | m |
| 1.412 | w | | | | | | |

* Powder data obtained on GE-XRD-3 diffractometer using filtered Cu radiation.

(*a*) *Substitution for Si*. The substitution of $Ge^{4+}$ for $Si^{4+}$ yielded a magnesia-germania serpentine, formed easily in euhedral hexagonal plates, which in some instances were even visible in the light microscope. Electron microgrographs, Plate 1 (*g*) show this clearly and the sharp *x*-ray diffraction patterns confirm a plate-like rather than tubular, habit.

(*b*) *Substitution for both $Si^{4+}$ and $Mg^{2+}$*. $Al^{3+}$ was found to enter the serpentine structure, substituting for both $Si^{4+}$ and $Mg^{2+}$, producing an "aluminian serpentine" of composition, $Mg_5Al_2Si_3O_{10}(OH)_8$, which con-

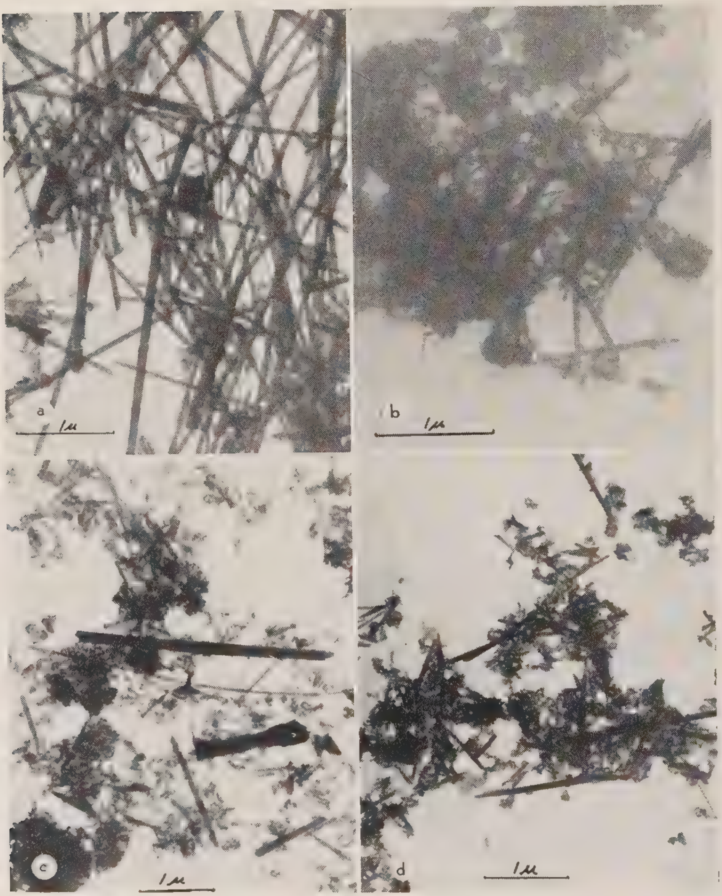

Explanation of Plate I

(*a*) Synthetic Chrysotile, $3MgO \cdot 2SiO_2 \cdot 2H_2O$, formed at 390° C., 10,000 psi, 408 hours.

(*b*) Tubular serpentine, $3NiO \cdot 2SiO_2 \cdot 2H_2O$ formed in presence of NaCl, 445° C., 10,000 psi, 22 hours.

(*c*) $3NiO \cdot 2SiO_2 \cdot 2H_2O$ formed in presence of NaCl, 325° C., 5,000 psi, 48 hours.

(*d*) $3NiO \cdot 2SiO_2 \cdot 2H_2O$ formed in presence of KCl, 450° C., 10,000 psi, 24 hours.

(*e*) $3NiO_2 \cdot 2SiO_2 \cdot 2H_2O$, no NaCl, formed at 325° C., 5,000 psi, 190 hours.

(*f*) $3NiO \cdot 2SiO_2 \cdot 2H_2O$, no NaCl, formed at 500° C., 10,000 psi, 90 hours.

(*g*) $3MgO \cdot 2GeO_2 \cdot 2H_2O$, formed at 500° C., 10,000 psi, 92 hours.

(*h*) $3NiO \cdot 2GeO_2 \cdot 2H_2O$, formed in presence of KCl, 230° C., 5,000 psi, 24 hours.

(*i*) $5MgO \cdot 1Al_2O_3 \cdot 3SiO_2 \cdot 4H_2O$, formed at 600° C., 10,000 psi, 384 hours.

1µ

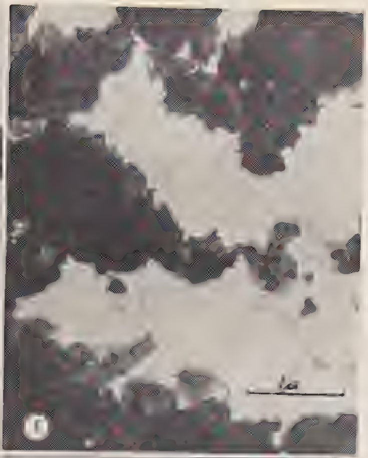
1µ

4
1µ

1µ

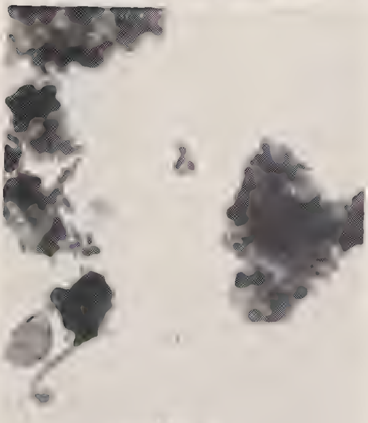
1µ

sistently yields a sharp *x*-ray pattern and forms euhedral platy crystals (Plate 1 (*i*)). This phase is undoubtedly related to that reported in the more qualitative work by Tu (1949) and Bates, Sand and Mink (1950) wherein alumina-containing serpentines were prepared with a platy habit. Tu has referred to these as "antigorite" on the basis of morphology. Indeed, if morphology is the only criterion used to distinguish chrysotile from antigorite, it would be quite possible that natural antigorites should also be characterized by compositional differences such as increased $R_2O_3$ content (over that of chrysotile). The data in the litearture are insufficient to confirm or deny such an hypothesis.

(*c*) *Substitution of divalent ions for* $Mg^{2+}$. Inasmuch as $Mg^{2+}$ is about the smallest divalent ion which exists normally in sixfold coordination, the substitution of $Mn^{2+}$, $Zn^{2+}$, $Co^{2+}$ and $Ni^{2+}$ on the basis of size alone should yield tubular serpentine crystals. $Ni^{2+}$ did yield a serpentine phase, as has been reported before (Voorthuysen and Franzen, 1950*a*, 1950*b*, 1951), but even in the absence of foreign ions—a condition not observed in other investigations. (See Plate 1 (*e*), (*f*).) In distilled water its habit was non-tubular, but no well-formed platy crystals were observed either. The misfit in this case would be expected to be as great or greater than with $Mg^{2+}$ and if greater, perhaps the strain is so large that only very small curved fragments result. $Mn^{2+}$ and $Zn^{2+}$ do not form any layer lattice phase at all with Si, yielding only tephroite or hemimorphite, respectively, at the lowest temperatures (vide infra). The formation of tephroite was an indication that failure to form a serpentine at all cannot be ascribed to oxidation of the $Mn^{2+}$. $Co^{2+}$ did not yield a serpentine-like phase, but this may be the result of failure to react at low temperatures.* Thus, it appears that $Mn^{2+}$, $Zn^{2+}$, and $Co^{2+}$ are either too large or too polarizable to form a serpentine structure at all and that $Ni^{2+}$ represents the largest divalent ion which can replace $Mg^{2+}$ completely in the structure.

(*d*) *Further substitutions.* Inasmuch as a platy serpentine had been formed from $MgO$-$GeO_2$ mixtures, other oxides in combination with $GeO_2$ were tried to further delineate the possible chemical substitutions. $NiO$-$GeO_2$ mixtures yielded a definite 1:1 layer structure with a basal spacing of 7.50 Å (which is very close to that for the $MgO$-$GeO_2$ serpentine). Its habit was definitely non-tubular, but fine-grained platy. $MnO$-$GeO_2$ mixtures failed to yield any hydrous phase, and like in the $MnO$-$SiO_2$ system an olivine type structure (Ge-tephroite) was formed instead. $Ga_2O_3$-$GeO_2$ mixtures did not yield any clay phase—possibly due to the experimental difficulties arising from the enormous differences in solubility; the mixture was made up by three different methods with no improvement in results. $Ga_2O_3$-$SiO_2$ mixtures were tried, in attempt to form a kaolinite type structure which would serve as a possible end-member for substitution in the serpentine structure. No two-layer hydrosilicate was formed; but, a montmorillonite-type phase was synthesized from pure $Ga_2O_3$-$SiO_2$-$H_2O$ mixtures. A close analogy between $Ga^{3+}$ and $Al^{3+}$ containing structures would be expected, since the former is only slightly larger, and should decrease the misfit in the octahedral layer—however it may be just too large to fit in the structure at all. (See Roy and Osborn, 1953, for discussion of Al-montmorillonite.)

---

* Mixtures containing cobalt were prepared only by decomposing cobalt nitrate-ethyl silicate mixtures. It is possible that mixtures made from gels might react better at low temperatures, providing the cobalt remains in the divalent oxidation state.

## B. Influence of Other Factors on Morphology

That the layer-size is not the only and sufficient consideration in the formation of tubular crystals is suggested by the different results obtained by different workers. Noll and Kircher (1952) using a concentrated NaCl solution obtained well-formed tubes whereas in "neutral" water we were unable to do so. It was therefore considered worthwhile to investigate the influence of three other variables usually associated with this work: the temperature of growth, the length of time of growth and the presence of foreign ions. Results of the experiments are summarized in Table 1. The effect of pressure was not investigated extensively, although in only one system, $MgO$-$Al_2O_3$-$SiO_2$-$H_2O$, was there any indication that pressure played a role.*

1. *Presence of foreign ions.* NaCl solutions were added in concentrations up to 10% to the pure Ni-Si end member and the runs repeated. This yields, of course, a very much lower concentration of $Na^+$ and $Cl^-$ than those used by Noll (op. cit.). However, an immediate and distinct difference was made in the habit of the resultant serpentine-phase; the rather poorly formed crystals of the pure end member were replaced by distinct tubes (see Plate 1 (*b*), (*c*)). The reason for this striking change is not at all clear. Whether the $Na^+$ ion acts merely as an "impurity" (such as methylene blue in the case of alums) which modifies the habit, or whether it is actually admitted into the structure, thus enhancing the misfit is not known. KCl additions were used in attempt to clarify this point. Ni-Si serpentine formed as tubular crystals in the presence of KCl (Plate 1 (*d*)); and in the case of Ni-Ge the platy structure was not

---

* Investigation of the polymorphism of the composition $Mg_5Al_2Si_3O_{10}(OH)_8$ (Roy and Roy, 1952) suggested that aluminian serpentine of this composition is metastable at higher temperatures, and yields to clinochlore. High pressures facilitate the conversion and clinochlore was not formed at all at pressures below 10,000 psi.

altered, but improvement in the size and shape of the hexagonal plates was observed (Plate 1 (*h*)).

The data in any case clearly showed the rather surprising influence of the presence of foreign ions on the morphology of these crystals. That the "misfit" is necessary to the formation of curved crystals is shown by the fact that Ni-Ge mixtures did not yield tubes with NaCl additions.

2. *Temperature.* Both pure and NaCl-containing Ni-Si mixtures were treated at successively higher temperatures to see whether the temperature of formation would have any influence on the morphology. No tubes were obtained from the pure member at any temperature, nor was there much evidence for enhancement of crystal size (Plate 1 (*e*), (*f*)). With the NaCl-containing mixtures, tubes were formed at both high and low temperatures in runs of short duration.

3. *Time.* Longer periods of time favored the formation of platy, rather than tubular crystals. In NaCl-containing samples treated for several days very few tubes remained, whereas one- or two-day runs yielded good tubular crystals. This may be the result of removal of $Na^+$ from the system, or may suggest that the tubes are really less stable, eventually yielding to the more stable platy structure.

## C. SYNTHESIS AND STABILITY OF LAYER SILICATES

1. $MgO$-$SiO_2$-$H_2O$. Magnesium silicate serpentine($3MgO \cdot 2SiO_2 \cdot 2H_2O$) was prepared synthetically* by Bowen and Tuttle in their original study of the system $MgO$-$SiO_2$-$H_2O$ and its limit of stability was reported to be 490 ± 10° C. (at 10,000 psi). Our results were in agreement with this value; other relevant data are given elsewhere (Roy and Roy, 1952). The phase thus obtained was tubular. A remarkable "cone-in-cone" habit was noticed in several cases and may be seen in Plate 1 (*a*).

2. $MgO$-$Al_2O_3$-$SiO_2$-$H_2O$. The substitution of Al into the chrysotile structure has been demonstrated to produce a structure which is distinctly platy (see Plate 1 (*i*)), yet having an *x*-ray pattern characteristic of serpentine. As little as 1 mol. per cent alumina produced a distinct tend-

---

* In spite of this synthesis a rather surprising result was reported by Nagy and Bates (1952, 1953) in that an apparent so-called "weight loss" of nearly 20% is reported for natural chrysotile in water, which would of course preclude the possibility of its hydrothermal synthesis. However, chrysotile from Thetford, Que., dried at 110° C. was dispersed as long fibres by blending, re-dried and the weight loss determined after heating in distilled water at 80° C. for 2 hours. Expressed in gms./100 ml. this amounted to 0.16. Another sample (weighing 8 gms.) of chrysotile from Globe, Ariz., was dispersed in a similar manner, dried weighed and boiled at 100° C. with 400 ml. of distilled water. The total loss of weight amounted to 0.65% checked both on the residue and filtrate. This reasonable weight loss was probably due to ferruginous and organic impurities, as shown from the "amorphous to *x*-rays" nature and reddish color of the material obtained by evaporation of the filtrate.

ency toward a platy structure, although in the electron micrographs there was some indication of being mixed in part with tubular crystals. Substitution of 2Al for Mg+Si in the chrysotile formula gives the formula $Mg_5Al(AlSi_3)O_{10}(OH)_8$, which is the same as clinochlore. This composition indeed yielded a serpentine structure, consisting of well-developed hexagonal plates under the electron microscope.

Evidence that substitution of Al may extend even beyond the clinochlore composition is seen in the fact that compositions high in alumina yield an aluminian serpentine with a slightly smaller basal spacing than that of the clinochlore composition. Aluminian serpentine from the 5:1:3 composition had a basal spacing of 7.161; that from 75:15:10 was nearly the same, 7.163; whereas a higher alumina composition 50:30:20 had a spacing of 7.06, indicating further substitution of Al beyond the clinochlore composition, probably extending as far as the amesite composition (4:2:2 $MgO:Al_2O_3:SiO_2$). Electron microscopic examination of these mixtures indicated the absence of any tubular crystals.

Prolonged heating of the 5:1:3 composition at temperatures above 450° C. and pressures of greater than 15,000 psi produced partial conversion of aluminian serpentine to the presumably stable clinochlore structure. The true stability range of aluminian serpentine could not be definitely established, since reaction at low temperatures is very slow. Conditions favoring the stability of aluminian serpentine would no doubt be lower temperatures and relatively low pressures.

3. *$MgO$-$GeO_2$-$H_2O$.* The germanium serpentine, $3MgO \cdot 2GeO_2 \cdot 2H_2O$ is formed easily from intimate mixtures of very fine MgO and the quartz form of $GeO_2$ under conditions similar to those under which the silicon analogue grows. The decomposition temperature was found to be 520 ±15° C. at 10,000 psi. This phase gives a well-defined powder $x$-ray pattern not showing the diffuseness of the chrysotile pattern, and has a basal spacing of 7.47 Å and a mean refractive index for the basal section of 1.600. Above the decomposition temperature the phases which appeared were $Mg_3Ge_4O_{10}(OH)_4$ (germanium talc) and $Mg_2GeO_4$. The former had an $x$-ray pattern similar to magnesia-silica talc, except for the fact that the 001 line is not observed at all, with an expanded cell, whereas the latter was found to be isotropic, and with a spinel-like structure, having a refractive index of 1.76. No reference was found to such a phase in the standard tables or textbooks although it was later found that Goldschmidt (1931) in a study of the crystal chemistry of germanium had found that $Mg_2GeO_4$ has an olivine structure at high temperatures. In a footnote he refers to the fact that he was later able to prepare a spinel-like form at low temperatures with $a_0 = 8.3$. The inversion of the spinel

form to the olivine form was reported to take place (Jander, 1932) at 1065° C. We were able to prepare well-formed single crystals (octahedra) of the spinel form and also of the olivine form. The inversion is very sluggish and by the quenching technique using runs of 12-24 hrs. duration was found to be 1005° C. (see Table 2). *X*-ray measurements yielded a unit cell edge of 8.255 for the spinel form, and $a_0=4.915$, $b_0=10.295$, $c_0=6.020$ for the olivine form. Mason (1952) has noted the possible importance of the increase in density when olivine transforms to spinel as a mechanism for explaining both the second-order discontinuities in seismic data used to obtain information on the earth's structure. A figure of 9% is given (without reference) for the increase in density. From our data a value of 8.16% calculated on the olivine density basis is obtained. However, unless a compositional gradation is assumed it is unlikely that the olivine-spinel inversion could "begin to change—at a depth of 413 km and the change would become complete at a depth of 984 km" as stated by Mason (*loc. cit.*).

4. $NiO$-$SiO_2$-$H_2O$. Garnierite, the nickel-containing serpentine occurs in nature, and the synthetic phase may be regarded as an end-member or pure nickel garnierite. Mixtures were made by coprecipitating gels from weighed amounts of nickel nitrate and sodium silicate solutions, and electrodialyzing to remove the adsorbed $Na^+$. Here also a serpentine structure ($3NiO \cdot 2SiO_2 \cdot 2H_2O$) is formed in a wide range of temperatures and pressures. The decomposition temperature at 10,000 psi was found to be much higher than expected, and indeed exceeded that of the magnesium analogue; a value of 530 ± 15° C. was assigned to this equilibrium temperature. The Ni-serpentine has a basal spacing of 7.35 Å, and on decomposition yields Ni-talc and Ni-olivine. The basal spacing of nickel-talc was 9.50 Å compared to 9.41 for the magnesian member.

Further investigation of the morphology of nickel serpentines revealed that the tubular structure (Noll and Kircher, 1952) was formed only when $Na^+$ was present. Sodium chloride was added to the nickel-silica gel in a ratio of about 1:10, and such mixtures treated hydrothermally for short periods yielded a serpentine structure having tubular crystals. Prolonged heating of similar mixtures, however, yielded no apparent tubes; and the electrodialyzed gels produced a platy, or non-tubular structure (vide supra).

5. $MnO$-$SiO_2$-$H_2O$. This system offered greater experimental difficulties than the ones mentioned earlier due to the easily variable oxidation state of manganese. Mixtures were made by mixing manganous carbonate with finely precipitated silica. No serpentine-like phase was encountered at any time during this study; this does not preclude the existence of such a phase in nature—as it has not been possible to synthesize many

naturally occurring minerals—but since the other serpentine structures form so easily this does indicate that such a structure is unlikely in nature. It was moreover surprising that no other hydrate of manganese and silica was encountered; instead tephroite was found to be stable in the presence of water as low as 250° C.; and no appreciable reaction was obtained at much lower temperatures.

6. *$ZnO$-$SiO_2$-$H_2O$.* Although no layered zinc silicate hydrates are known n nature we hoped to be able to synthesize such a phase. The mixtures were made by evaporating an alcohol-water solution of zinc nitrate and ethyl orthosilicate, and decomposing the product to leave only the oxides. Hemimorphite was the only hydrated phase encountered and this was dentical with the natural mineral. Its decomposition temperature at 10,000 psi was found to be about 200° C., where it is replaced by willem-te + water.

7. *$CoO$-$SiO_2$-$H_2O$.* In this system also no serpentine-like structure was obtained at all, the phase appearing most commonly being the olivine $Co_2SiO_4$, with lattice dimensions very close to that of the magnesium olivine, forsterite. At low temperatures oxidation of $Co^{2+}$ took place, giv-ng rise to the spinel $Co_3O_4$. It is possible that a serpentine phase might still be formed, however, if sufficiently reactive mixtures were used, providing the oxidation state of cobalt could be controlled.

8. *$Ga_2O_3$-$SiO_2$-$H_2O$.* The other family of layered silicates derive from the alumina-silica-water system, and the obvious ion which may be substituted here is $Ga^{3+}$ for $Al^{3+}$. This was done in an attempt to prepare a gallium kaolinite, which in turn might be expected to form solid solutions with one of the serpentine minerals. Mixtures were made by two methods: (1) the coprecipitation of gallium nitrate and sodium silicate solutions, and electrodialyzing the gel and (2) mixing alcohol solutions of gallium nitrate and ethyl silicate and decomposing the evaporate.

No gallium-kaolinite was synthesized under any conditions tried, from 200° to 500° C. and pressures of 6,000 to 10,000 psi. However, a gallium montmorillonite containing essentially no other cations besides $Ga^{3+}$ and $Si^{4+}$ was obtained. This montmorillonite produced a fairly sharp x-ray diffraction pattern, and the basal spacings were expandable with ethylene glycol from 13.2 Å (dried at 110° C.) to 17.0 Å. Under the electron microscope the crystals showed a fairly typical montmorillonite habit, extremely thin plates and fuzzy particles, sometimes rolled around the edges.

9. *$NiO$-$GeO_2$-$H_2O$.* The composition, $3NiO \cdot 2GeO_2$ yielded a platy serpentine-like structure, similar to that in the system $MgO$-$GeO_2$-$H_2O$ system. The mixture was made by coprecipitating $GeO_2$ dissolved in water with a nickel sulfate solution. No appreciable amount of $GeO_2$ was pres-

ent in the filtrate, suggesting quite complete co-precipitation. The presence of KCl did not change the crystal habit, but developed larger plates. This phase was stable up to 358±16° C. at 10,000 psi, above which it decomposed to yield a talc and a spinel phase.

10. *$MnO$-$GeO_2$-$H_2O$.* Inasmuch as $Mn^{2+}$ was apparently too large to form a serpentine phase with $Si^{4+}$, combination with $Ge^{4+}$ was tried instead. $MnCO_3$ and the quartz-form of $GeO_2$ were mixed, and at temperatures as low as 200° C. only an anhydrous orthosilicate resembling tephroite was formed, while below 150° C. no reaction was obtained. Hydrous $Mn^{2+}$ germanates must therefore exist, if at all, only at very low temperatures.

11. *$Ga_2O_3$-$GeO_2$-$H_2O$.* The composition $Ga_2O_3$:$2GeO_2$ was investigated for a possible kaolinite-type end member structure, in the hope that this might serve as a basis for substitution into the serpentine structure. Inasmuch as $Ga^{3+}$ was apparently too large to form a kaolinite-type structure with $Si^{4+}$, it was thought that increasing the size of the four-coordinate ion also might result in a stable structure of this type. Several different methods of making mixtures were tried, but in no case was a hydrous gallium germanate obtained. Gallia gels are rapidly converted to Ga-diaspore (Roy, Hill and Osborn, 1951), which is recrystallized under hydrothermal treatment at relatively low temperatures, while the $GeO_2$ is largely dissolved in the water before sufficient reaction takes place. At higher temperatures (about 415° C.) an apparently anhydrous gallium germanate was obtained, resembling one of the aluminosilicates of the sillimanite family.

12. *$Fe_2O_3$-$SiO_2$-$H_2O$.* Mixtures in this system were made up by coprecipitating gels from potassium silicate and ferric ammonium sulfate solutions, washing, and in one case electrodialyzing the samples. A mica-type phase was formed through hydrothermal treatment of the non-electrodialyzed samples at relatively low temperatures; i.e., about 300° C., due to the presence of $K^+$ as impurity. This phase is therefore a pure $Fe^{+++}$ muscovite, with the $Fe^{+++}$ in both octahedral and tetrahedral coordination. Electrodialyzed samples treated above about 350° C. did not form any compound, but yielded a mixture of cristobalite and hematite. At lower temperatures no crystallinity was observed in runs as long as two weeks.

13. *$Cr_2O_3$-$SiO_2$-$H_2O$.* Mixtures in this system were made up by various methods: coprecipitating gels from potassium silicate and chromium nitrate solutions; and by decomposing an alcohol solution of chromium nitrate and ethyl silicate. The results are only preliminary, like those in the $Fe_2O_3$-$SiO_2$-$H_2O$ system, but no kaolinite type compound or other identifiable layer lattice compound was formed at temperatures as low

as 200° C. CrO(OH) was crystallized from some of the runs between 200° C. and 275° C.

## D. Comparison of Equilibria in the Various Systems

In Fig. 2 are given a series of triangles suggesting equilibria for the systems studied which show a general similarity. The data for $MgO$-$SiO_2$-$H_2O$ are taken from Bowen and Tuttle (1949)* and the other systems are drawn very approximately for comparison, from the data obtained in the present study (see Table 3).

The small triangles denote combinations of three phases in equilibrium, throughout a given temperature range, for a constant water pressure of about 10,000 psi. For example, triangle II of the system $NiO$-$SiO_2$-$H_2O$ shows the following equilibrium assemblages of three phases: Ni serpentine-Ni talc-$H_2O$ and Ni serpentine-Ni forsterite-$H_2O$. At 530° C., with a constant water pressure of 10,000 psi the following four phases are in equilibrium: Ni serpentine$\rightleftarrows$Ni forsterite+Ni talc+$H_2O$. Univariant curves describing the change in temperature of such reactions with change in pressure may be drawn, but the effect of pressure in the range used (between 2000 and 20,000 psi) was so small that this was not considered significant.

Significant transitions include the upper stability temperatures (Triangles II–III) for the serpentines (at 10,000 psi) which are (1) 490° C. for Mg-Si, (2) 520° C. for Mg-Ge, (3) 530° C. for Ni-Si, which are remarkably close; and (4) 360° for Ni-Ge, which is considerably lower. Stability limits for talc, show marked differences. Mg-Si talc is stable up to 780° C., whereas the Mg-Ge talc decomposes at about 600° C., and Ni-Si talc appears to be stable to a much higher temperature, about 850° C. (or slightly higher). The decomposition temperature of Ni-Ge talc was not determined. A comparison is shown in Fig. 2 (triangles III–IV).

The magnesia-silica amphibole, anthophyllite, exists in nature, but was produced only metastably in the hydrothermal studies of Bowen and Tuttle (i.e., it was never formed in equilibrium with excess $H_2O$). No anthophyllite phase was found in the $NiO$-$SiO_2$ system, but with $MgO$-$GeO_2$ a structure similar to anthophyllite was produced, consisting of well-formed long needle-like crystals of this phase. Difficulty in pursuing further the stability relations in the system $MgO$-$GeO_2$-$H_2O$ was encountered because of the high solubility of $GeO_2$ in water at elevated temperatures and pressures.

The similarity among the upper stability temperatures for the ser-

---

* The only modification of the data of Bowen and Tuttle is the temperature for the reaction, brucite$\rightleftarrows$periclase+$H_2O$ (Roy, Roy and Osborn, 1953) which has been lowered from 890° C. to 635° C. at 10,000 psi.

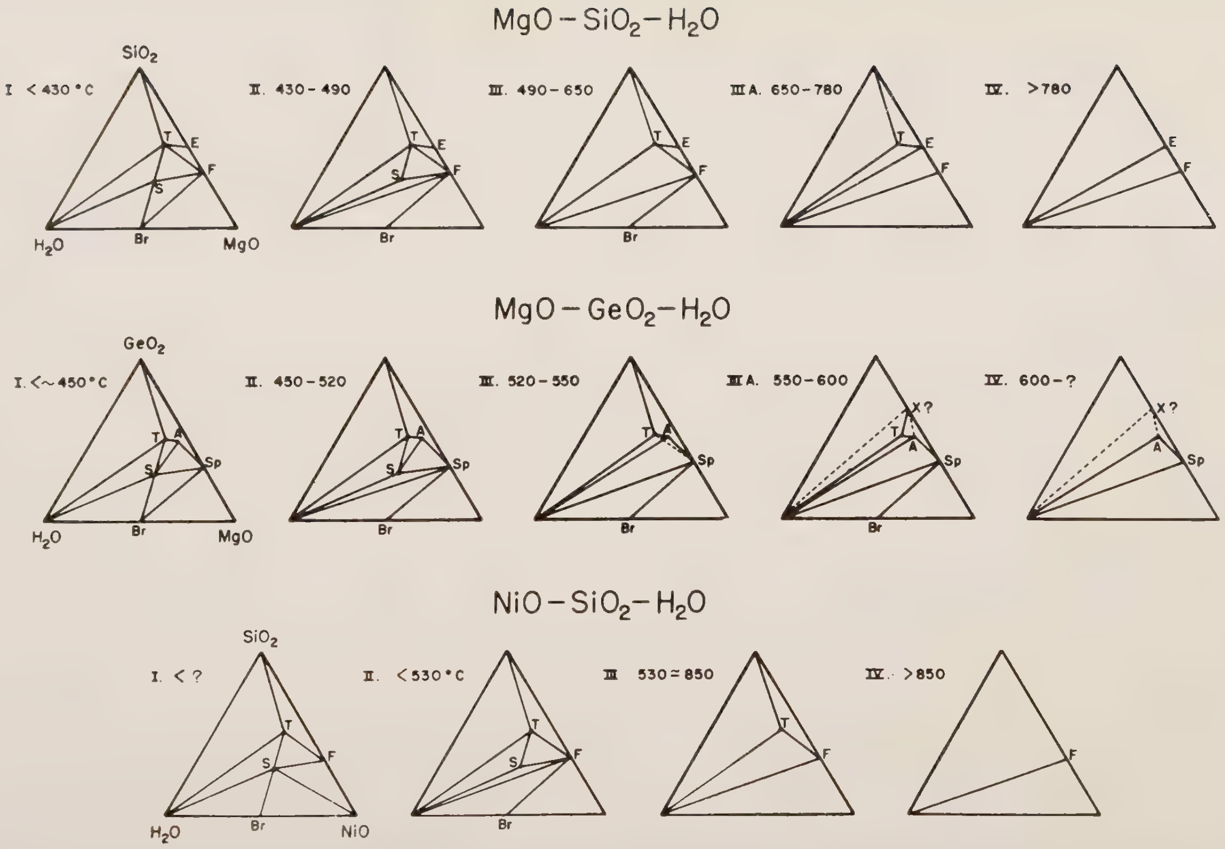

FIG. 2. Comparison of phase equilibria in the systems MgO-SiO$_2$-H$_2$O, MgO-GeO$_2$-H$_2$O and NiO-SiO$_2$-H$_2$O. Abbreviations used:

TABLE 3. PHASE EQUILIBRIUM DATA FOR THE SYSTEMS
$MgO\text{-}GeO_2\text{-}H_2O$, $NiO\text{-}SiO_2\text{-}H_2O$ and $NiO\text{-}GeO_2\text{-}H_2O$

| Composition Mol. Ratio | Temp. ° C. | Press. psi. | Time hrs. | Phases Present* |
|---|---|---|---|---|
| | | $MgO\text{-}GeO_2\text{-}H_2O$ | | |
| 3 MgO:4 $GeO_2$ | 200 | 10,000 | 24 | talc |
| 3 MgO:4 $GeO_2$ | 370 | 4,000 | 24 | talc |
| 3 MgO:4 $GeO_2$ | 500 | 10,000 | 74 | talc+l. serp. |
| 3 MgO:4 $GeO_2$ | 550 | 10,000 | 49 | talc+l. anth. |
| 3 MgO:4 $GeO_2$ | 650 | 10,000 | 24 | anth+? |
| 3 MgO:4 $GeO_2$ | 800 | 5,000 | $\frac{1}{2}$ | spinel-? |
| 3 MgO:2 $GeO_2$ | 500 | 10,000 | 92 | serp. |
| 3 MgO:2 $GeO_2$ | 450 | 20,000 | 120 | serp. |
| 3 MgO:2 $GeO_2$ | 520 | 10,000 | 96 | talc+l. serp. |
| 3 MgO:2 $GeO_2$ | 530 | 10,000 | 96 | spinel+anth. |
| 3 MgO:2 $GeO_2$ | 650 | 10,000 | 24 | anth.+spinel+? |
| 2 MgO:$GeO_2$ | 400 | 10,000 | 18 | serp. mostly |
| 2 MgO:$GeO_2$ | 500 | 10,000 | 74 | spinel+l. serp. |
| 2 MgO:$GeO_2$ | 550 | 10,000 | 49 | spinel+l. anth. |
| 2 MgO:$GeO_2$ | 900 | 2,000 | 1 | spinel |
| 2 MgO:$GeO_2$ | 1003 | | 12 | spinel+olivine |
| 2 MgO:$GeO_2$ (spinel)† | 1003 | | 12 | spinel |
| 2 MgO:$GeO_2$ | 1012 | | 36 | olivine |
| 2 MgO:$GeO_2$ (spinel)† | 1012 | | 36 | olivine |
| 2 MgO:$GeO_2$ | 1030 | | 12 | olivine |
| 2 MgO:$GeO_2$ (spinel)† | 1030 | | 12 | olivine |
| 3 MgO:$GeO_2$ | 400 | 10,000 | 18 | serp.+bru. |
| 3 MgO:$GeO_2$ | 645 | 5,000 | 18 | spinel+per. |
| | | $NiO\text{-}SiO_2\text{-}H_2O$ | | |
| 3 NiO:2 $SiO_2$ | 180 | 5,000 | 29 | serp. |
| 3 NiO:2 $SiO_2$ | 325 | 5,000 | 190 | serp. |
| 3 NiO:2 $SiO_2$ | 400 | 8,000 | 216 | serp. |
| 3 NiO:2 $SiO_2$ | 500 | 10,000 | 90 | serp. |
| 3 NiO:2 $SiO_2$ | 520 | 10,000 | 25 | serp.+talc+NiO ? |
| 3 NiO:2 $SiO_2$ | 525 | 8,000 | 192 | talc+ NiO? +olivine |
| 3 NiO:2 $SiO_2$ | 540 | 7,000 | 48 | talc mostly |
| 3 NiO:2 $SiO_2$ | 650 | 5,000 | 24 | talc+olivine |
| 3 NiO:2 $SiO_2$ | 835 | 5,000 | .5 | talc+olivine |
| 3 NiO:2 $SiO_2$ | 900 | 5,000 | $1\frac{1}{2}$ | olivine+l. talc |
| 3 NiO:2 $SiO_2$ | 1200 | | 14 | olivine+trid. |
| | | $NiO\text{-}GeO_2\text{-}H_2O$ | | |
| 3 NiO:2 $GeO_2$ | 230 | 22,000 | 24 | serp. |
| 3 NiO:2 $GeO_2$ | 318 | 10,000 | 144 | serp. |
| 3 NiO:2 $GeO_2$ | 318 | 10,000 | 24 | serp. |
| 3 NiO:2 $GeO_2$ | 342 | 10,000 | 24 | serp. |
| 3 NiO:2 $GeO_2$ | 375 | 10,000 | 72 | spinel+talc |
| 3 NiO:2 $GeO_2$ | 400 | 10,000 | 24 | talc+spinel |
| 3 NiO:4 $GeO_2$ | 230 | 22,000 | 24 | talc |
| 3 NiO:4 $GeO_2$ | 310 | 10,000 | 24 | talc |

* Abbreviations: l.=little, serp.=serpentine, anth.=anthophyllite, bru.=brucite, per.=periclase, trid.=tridymite.

† Starting material was spinel form; others were mixed oxides.

pentine structures in the $MgO$-$SiO_2$, $NiO$-$SiO_2$ and $MgO$-$GeO_2$ systems was not expected, especially in view of the similarity in decomposition products; i.e., they all give rise to talc+an orthosilicate type (either olivine or spinel type)$+H_2O$. One would naturally expect the higher covalency in the case of Ni to be reflected in a pronouncedly lower stability temperature, and similarly a lower temperature might also be expected for the stability limit of the Mg-Ge phase. Only in the case of $NiO$-$GeO_2$ was the expected lower stability temperature realized. In a very qualitative way this might indicate that the bonds responsible for the break-up of the serpentine structure are not M-OH bonds, but some bond or group common to all the serpentines and influenced only to a minor extent by the octahedrally coordinated ion. In other words, the weakest link in the chain may be the weak interlayer bonds, which are influenced only to a minor extent by the ions within the layers. The strength of the interlayer bonds will undoubtedly be affected by the extent of contrapolarization of the OH or O ions by the cation "within" the layer; but this should be relatively small.

The talc decompositions on the other hand, give rise to different products in each case, and generalizations as to the explanation for differences in maximum stability temperatures would involve very complex considerations, which will not be discussed here.

## SUMMARY

A number of synthetic phases with the serpentine structure have been prepared hydrothermally. A comparison of their morphology suports the thesis that in such structures a "misfit" between layers is the basic cause for the formation of tubular cyrstals.

Other data show the secondary importance of the presence of foreign ions, temperature of formation, and length of run in conditioning this basic requirement.

A series of composition tirangles are presented showing the sequence of phase assemblages stable at various temperatures for the systems $MgO$-$SiO_2$-$H_2O$, $MgO$-$GeO_2$-$H_2O$, and $NiO$-$SiO_2$-$H_2O$. A large number of new phases has been synthesized, and these are described briefly inasmuch as they affect the equilibria.

## REFERENCES

ARUJA, E. (1945), An $x$-ray study of the crystal structure of antigorite: *Mineral. Mag.*, **27,** 65–74.

BATES, T. F., HILDEBRAND, F. A., AND SWINEFORD, A. (1950), Morphology and structure of endellite and halloysite: *Am. Mineral.*, **35,** 463–484.

BATES, T. F., SAND, L. B., AND MINK, J. F. (1950), Tubular crystals of chrysotile asbestos: *Science,* **111,** 512–513.

Bowen, N. L., and Tuttle, O. F. (1949), The system MgO-$SiO_2$-$H_2O$: *Bull. Geol. Soc. Am.*, **60**, 439–460.

Fock, V. A., and Kolpinsky, V. A. (1940), *J. Phys. (USSR)*, **3**, 194.

Goldschmidt, V. A. (1931), Zur Kristallchemie des Germaniums: *Nachr. Gesellsch. d. Wissensch. Göttingen, Math. Phys. Kl., Fachgr.* **IV**, Bd. I, 184.

Hillier, J. (1949), New worlds for study: *Scientific Monthly*, **69**, 161–168.

Jander, W., and Stamm, W. (1932), The inner structure of solid inorganic compounds at higher temperatures. V. Electrical conductivity, diffusion, and reactivity of magnesium orthosilicate and magnesium orthogermanate in the solid state: *Zeit. anorg. Chem.*, **207**, 289–307.

Mason, B. (1952), Principles of Geochemistry. John Wiley and Sons, Inc., New York.

Nagy, B., and Bates, T. F. (1952), Stability of chrysotile asbestos: *Am. Mineral.*, **37**, 1055–1058.

Noll, W. (1950), Zur Morphologie des Chrysotilasbestos: *Naturwiss.*, **37**, 540–541.

Noll, W., and Kircher, H. (1952), Synthese des Garnierites: *Naturwiss.*, **10**, 233–234.

Pauling, L. (1930), The structure of the chlorites: *Pro. Nat. Acad. Sci.*, **16**, 578–582.

Roy, D. M. (1952), Phase equilibria in the system MgO-$Al_2O_3$-$H_2O$ and in quaternary systems derived by the addition of $SiO_2$, $CO_2$ and $N_2O_5$. *Ph.D. Thesis*, The Pennsylvania State University, Jan. 1952.

Roy, D. M., and Roy, R. (1952), Studies in the system MgO-$Al_2O_3$-$SiO_2$-$H_2O$: *Am. Mineral.*, **38**, 358. (Abstract).

Roy, D. M., Roy, R., and Osborn, E. F. (1953), The system MgO-$Al_2O_3$-$H_2O$ and influence of carbonate and nitrate ions on the phase equilibria: *Am. Jour. Sci.*, **251**, 337–361.

Roy, R., Hill, V. G., and Osborn, E. F. (1951), Polymorphism of $Ga_2O_3$ and the system $Ga_2O_3$-$H_2O$: *Jour. Am. Chem. Soc.*, **74**, 719–722.

Roy, R., and Osborn, E. F. (1952), Some simple aids in hydrothermal investigation of mineral systems: *Econ. Geol.*, **47**, 717.

Roy, R., and Osborn, E. F. (1954), The system $Al_2O_3$-$SiO_2$-$H_2O$, *Am. Mineral.*, **39**, 853–885. See also summary in "Problems of Clay and Laterite Genesis," *AIME*, New York (1952)

Roy, R., Roy, D. M., and Osborn, E. F. (1950), Compositional and stability relationships among the lithium aluminosilicates: eucryptite, spodumene and petalite: *Jour. Am. Ceram. Soc.*, **33**, 152–159.

Tu, K. C. (1950), *Ph.D. Thesis*, University of Minnesota, Department of Geology.

Turkevitch, J., and Hillier, J. (1949), Electron microscopy of colloidal systems: *Anal. Chem.*, **21**, 475–485.

Voorthuysen, J. J. B. van Eijk van, and Franzen, P. (1950), Synthesis of nickel hydrosilicates: *Trans. Intern. Congress of Soil Sci., Amsterdam*, **1950**, vol. III, pp. 34–37.

——— (1950*b*), The influence of $SiO_2$ on the activity of nickel catalysts: *Rec. Trav. Chim.*, **69**, 666–667.

——— (1951), The structure and properties of compounds formed during the preparation of nickel-on-silica catalysts: *Rec. Trav. Chim.*, **70**, 793–812.

Whittaker, E. J. W. (1949), Structure of Bolivian crocidolite: *Acta Cryst.*, **2**, 312.

——— (1952), Unit cell of chrysotile: *Acta Cryst.*, **5**, 143.

Yoder, H. S. (1952), The MgO-$Al_2O_3$-$SiO_2$-$H_2O$ system and the related metamorphic facies: *Am. Jour. Sci.* (Bowen vol.), 569–627.

*Manuscript received Oct. 13, 1953.*

# A SINGLE CRYSTAL TEMPERATURE CONTROLLED OVEN FOR AN *X*-RAY SPECTROMETER

R. Lefker, A. deBretteville, Jr., and J. S. Dodd, *Squier Signal Laboratory, Signal Corps Engineering Laboratories, Fort Monmouth, New Jersey.*

## Abstract

An oven was built to heat a single crystal on the end of a goniometer head so that absolute *x*-ray diffraction intensity measurements of the basal plane reflections could be made at various temperatures. The temperature range is 50° C. to 270° C. and the temperature stability is within ±0.1° C. This stability is accomplished by a main winding and a controlled auxiliary winding outside the circumference of the main winding; these windings radiate energy to a copper block in which the crystal is mounted, and so maintain constant crystal temperature.

## Introduction

A high-temperature crystal heater was built for the purpose of obtaining absolute intensity measurements from the basal plane reflections of a crystal. The integrated reflection for a mosaic crystal is determined by either of two methods:[1] the crystal is revolved with angular velocity $\omega$ and the total counts summed; or a point-by-point determination of the counts per second for each angular setting through the range of reflection is made, and the area under the curve that represents these data is determined by a planimeter or by graphical integration. The first method is mathematically expressed by $E\omega/I_0$, where $E$ is the total counts from the line reflection, $\omega$ the angular velocity in radians per second, and $I_0$ the direct beam intensity in counts per second. The second method is defined by the expression

$$\int_{\theta_0-\epsilon}^{\theta_0+\epsilon} \frac{R(\theta)}{I_0}\, d\epsilon,$$

where $\theta_0$ is the Bragg angle and $\theta_0+\epsilon$ and $\theta_0-\epsilon$ the angular limits over which the reflection occurs, $R(\theta)$ the reflected beam intensity in counts per second at angle $\theta$, and $I_0$ is defined as above.

From these absolute intensity measurements the electron density as a function of a particular direction in the crystal may be determined and from the position of the peaks, the atomic parameters determined.

## Requirements

The requirements were as follows: (1) The oven must be light in weight to prevent over-loading of the goniometer to which it is attached; (2)

---

[1] *Internationale Tabellen zur Bestimmung von Kristallstrukturen*, Gebrüder Borntraeger, Berlin, **2**, 560 (1935).

The oven must be thermally insulated to prevent excessive heating of the goniometer head; (3) The temperature to which the oven is set must remain constant within ±0.1° C. for long periods of time and at any temperature setting within the range from 50° C. to 270° C.; (4) The size of the oven must conform to the limited mounting space available in the spectrometer;[2] (5) The crystal face must be on the boundary of the oven to receive the incident *x*-ray beam for diffraction work.

The temperature accuracy is necessary because the oven was built to study ferroelectric barium titanate, the integrated intensity of which changes rather rapidly, i.e., by more than a factor of five for the second order with a change of four degrees of the crystal temperature near the Curie point at 120° C.[3]

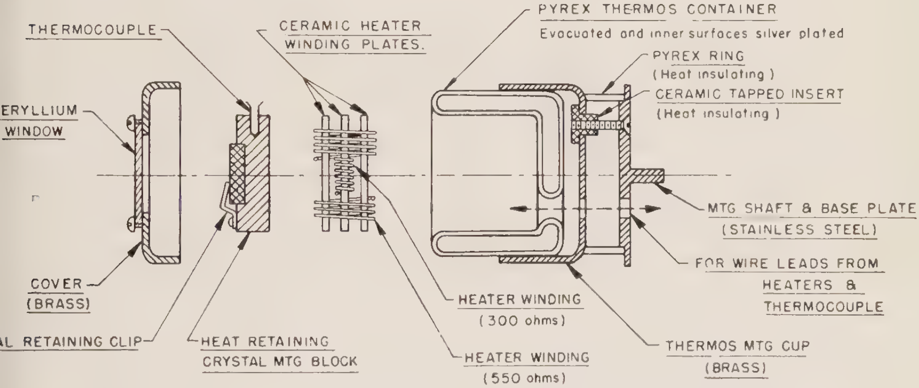
THERMOCOUPLE
CERAMIC HEATER WINDING PLATES.
PYREX THERMOS CONTAINER
Evacuated and inner surfaces silver plated
PYREX RING
(Heat insulating)
CERAMIC TAPPED INSERT
(Heat insulating)
ERYLLIUM WINDOW
MTG SHAFT & BASE PLATE (STAINLESS STEEL)
FOR WIRE LEADS FROM HEATERS & THERMOCOUPLE
COVER (BRASS)
HEATER WINDING (300 ohms)
L RETAINING CLIP
HEAT RETAINING CRYSTAL MTG BLOCK
HEATER WINDING (550 ohms)
THERMOS MTG CUP (BRASS)

FIG. 1. Exploded cross-sectional view of heater.

## MECHANICAL AND ELECTRICAL CHARACTERISTICS

The main body of the oven is a Dewar or "thermos" container, constructed of "pyrex" glass with the space between the inner and outer walls evacuated, and the inner surfaces of the walls silver plated, shown in the exploded drawing (Fig. 1) and the photograph (Fig. 2). This construction satisfies the requirement for a comparatively thin oven wall with high thermal insulating properties, together with the necessity of using a heat-resisting and an electrical non-conducting material.

The "thermos" mounting base consists of a brass cup mounted on a stainless steel base plate. The base plate contains a stud for mounting the assembled oven in the chuck of the goniometer head. The "thermos" container is held in position on the brass mounting cup by a light press

---

[2] Baron, M. L., deBretteville, Jr., A., *Rev. Sci. Inst.*, **21**, 458–461 (1948).

[3] Kanzig, W., *Helv. Phys. Acta*, **24**, 184, 186, 187 (1951).

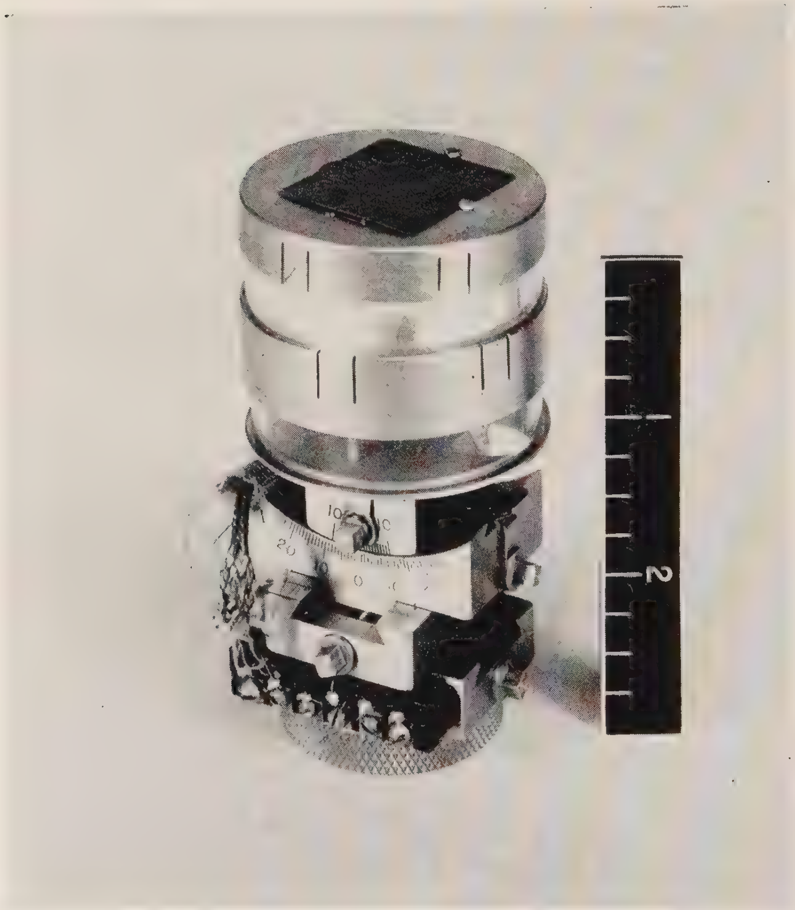

FIG. 2. Single crystal heater on adjustable goniometer head with beryllium cover.

fit. The cup and stainless steel base plate are mounted or coupled together through a "pyrex" stand-off ring; the purpose of the glass ring is to minimize heat conduction between the oven and the oven-mounting stud, and thus to prevent heat absorption by the goniometer head.

Two heater windings of #40 wire are provided. The main winding and the auxiliary one are 300 and 550 ohms, respectively. The main winding is located inside the auxiliary winding. To achieve maximum oven temperature, the main winding uses energy at the rate of some 20 watts. The temperature-stabilizing auxiliary winding operates best when it uses energy at the rate of approximately 7 watts. The concentric arrangement of the windings produces uniform heating of the exposed under-surface of the crystal mounting block. The main winding is connected, directly, to the energy source; the auxiliary winding operates only when needed. The oven may be set at any temperature between 50° and 270° C.; over long periods of time, the oven temperature is maintained within ±0.1° C. of the established value.

The crystal mounting block is made of oxygen-free electrolytic copper and is chromium plated. An iron-constantan thermocouple is inserted into a recess in the mounting block. Two spring clips hold the crystal in position.

The crystal mounting block is attached to a brass cover which slips over the "thermos" container with a light press fit. A beryllium window, 0.016 cm. thick, is mounted on the cover. The beryllium window provides thermal insulation for the crystal under study, and is transparent to iron and copper K radiations.

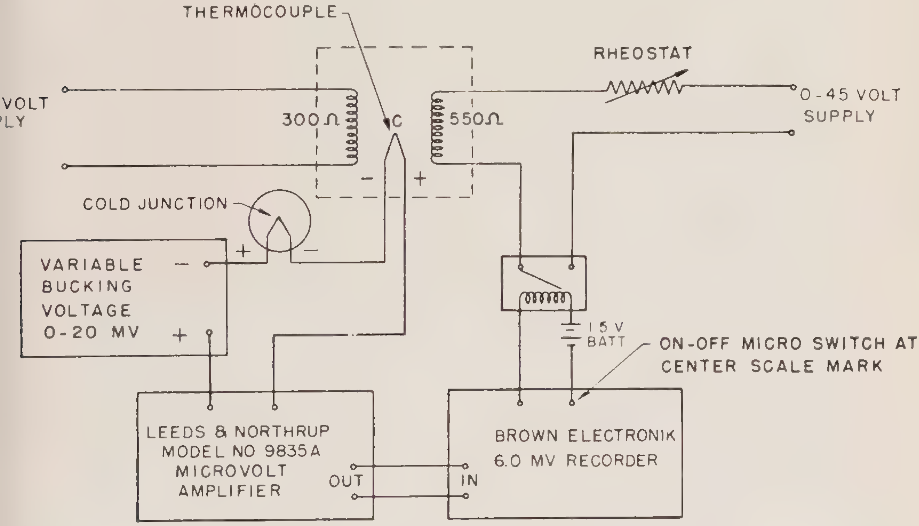
THERMOCOUPLE
RHEOSTAT
VOLT
LY
300Ω
C
550Ω
0-45 VOLT SUPPLY
−
+
COLD JUNCTION
+
−
VARIABLE BUCKING VOLTAGE 0-20 MV
−
+
1.5 V BATT
ON-OFF MICRO SWITCH AT CENTER SCALE MARK
LEEDS & NORTHRUP MODEL NO 9835A MICROVOLT AMPLIFIER
OUT
IN
BROWN ELECTRONIK 6.0 MV RECORDER

FIG. 3. Block wiring diagram of heater control circuits.

The electrical connections are shown in Fig. 3. The thermocouple is in series with the reference ice (cold) junction; to obtain the variety of possible oven temperatures, a bias voltage of 0–20 mv. is provided. The bias voltage output is applied to a Leeds and Northrup Amplifier No. 985-A; the amplifier output, made positive and set at approximately 150 microvolts, is connected to a 6 millivolt Brown Recorder—one that has a time constant of 1 second. This arrangement adjusts the pen of the recorder to the midscale position; the recorder is provided with a microswitch—one that closes whenever the scale reading is less than 3 milli-

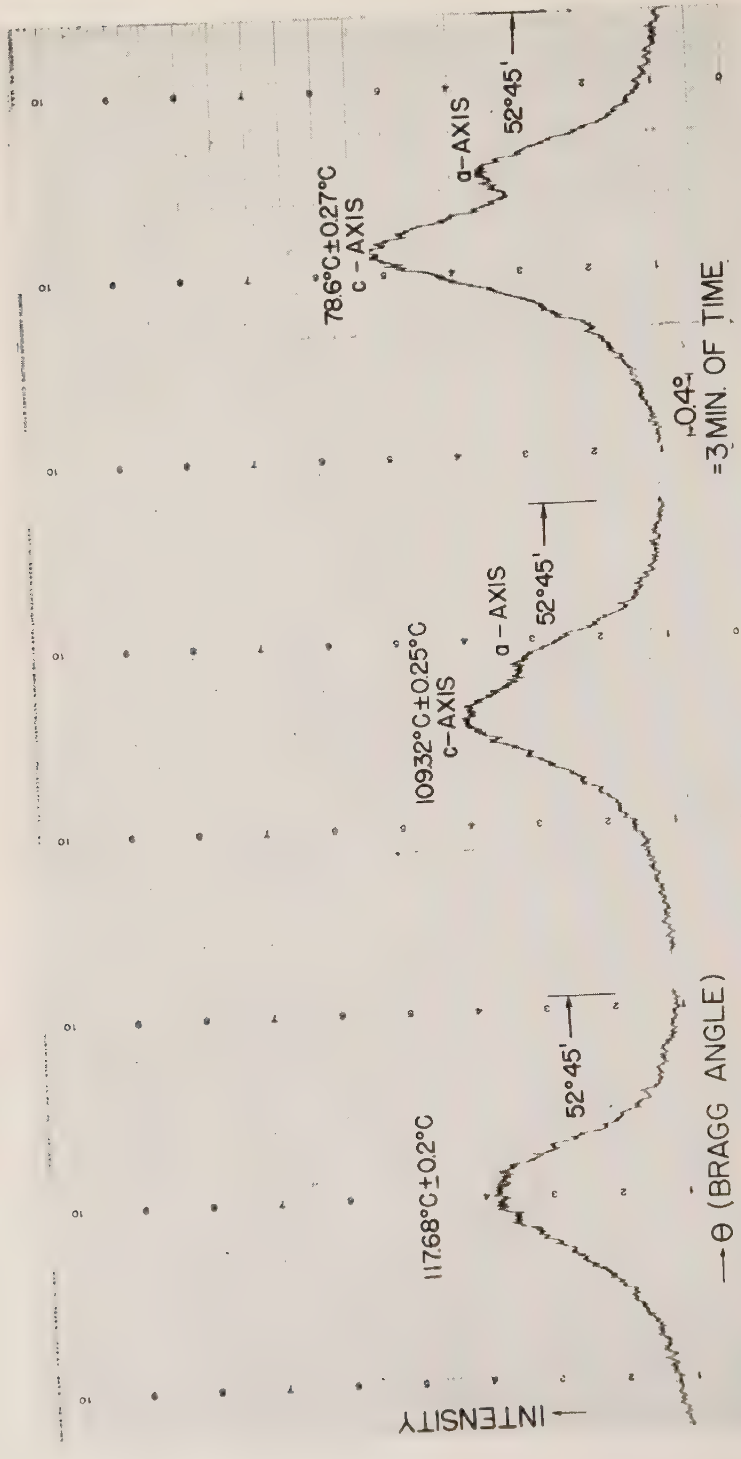

FIG. 4. X-ray intensities as a function of angle for single crystal oven. The 4th order reflection of $BaTiO_3$ tetragonal to cubic phase change for Cu K radiation is used to check the crystal vs. thermocouple temperature.

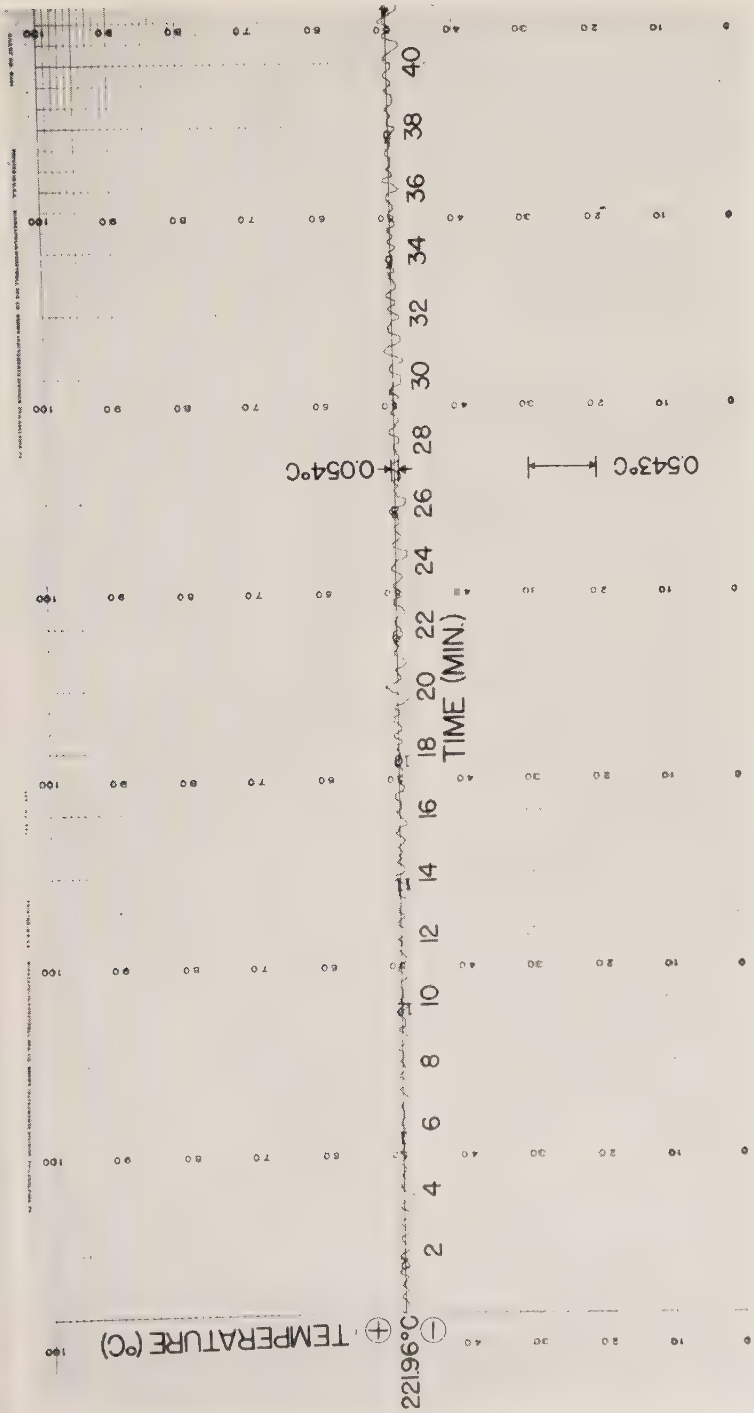

FIG. 5. Temperature vs. time chart for 221.96° C.

volts, and opens when the reading is 3 millivolts or greater. The microswitch actuates a relay that controls the energy supplied to the auxiliary winding of the heater.

The oven here described is intended, primarily, for flat crystal surfaces, 4 millimeters on a side and a few millimeters thick; the oven is not designed for rod-shaped crystals.

*X*-ray diffraction data are used to check temperature at the crystal; these data show the phase transition, known to occur at approximately 120° C., of a multi-domain single crystal of $BaTiO_3$. Figure 4 shows recordings of these data; above 120° C. (the Curie temperature) the cell structure is cubic, and hence a single reflection peak occurs; below the Curie temperature the cell structure is tetragonal, and so there are two reflection peaks—one corresponding to the *a* and one to the *c* axis. Figure 4 also shows a shift in the reflection peaks; such a shift may be used to calculate the coefficient of thermal expansion of the barium titanate.

Figure 5 is a recording of oven temperature over a 40-minute test period. The inherent stability of the temperature-control system is indicated by the recorded temperature variations—approximately ±0.054° C. during most of the test period.

## CONCLUSIONS

The oven described maintains a constant temperature, within the range 50° to 270° C. with an accuracy of ±0.1° C. The particular design of this oven was determined by its use on an *x*-ray spectrometer; the small size and weight were necessary in order to mount the oven on the end of a goniometer head, so that the crystal could be positioned near the outer surface of the oven, thus permitting optical alignment and measurement of the intensity of reflected *x*-rays. Variation in oven design is possible, without impairing the precision control of temperature.

## ACKNOWLEDGMENTS

The authors are indebted to Messrs. E. Limper, K. Wright, and G. Drouard, of the Squier Signal Laboratory Shop—to the first two for unusual skill and care in the construction of the oven, and to the last for the able construction of the Dewar container.

*Manuscript received Aug. 10, 1953.*

# ZIRCONS AS PROVENANCE INDICATORS

MICHAEL WYATT, *Stanford University, Stanford, California.*

## ABSTRACT

Study of a Scottish granite intruded into Moine "granulites" showed that although most of the granite was magmatic, there was considerable granitization near the contact in some areas. Examination of accessory zircon showed that in the granite it is idiomorphic and in the Moine it is well-rounded. Furthermore zircon from contaminated granite is very elongated, and zircon from granitized Moine is recrystallized and idiomorphic, but quite distinct from that in the granite. It is suggested that this technique may have wider uses in similar studies.

## INTRODUCTION

In a recent examination of a granitic intrusion and the associated contact relations, a statistical study of the form of zircon provided clear confirmatory evidence of the extent of granitization of the contact rocks adjacent to the instrusion, although the behavior of zircon in this instance, under both regional and thermal metamorphism, was not entirely in agreement with the findings of others (Poldervaart and Von Backstrom, 1950).

The Monadhliath granite,* situated in the Grampian Highlands of Scotland about twenty miles South of Inverness, is approximately circular and covers an area of about thirty-two square miles, and all the evidence indicates that it is mainly a normal intrusive magmatic granite. It is remarkably uniform mineralogically—a quartz-monzonite in which orthoclase is usually slightly more abundant than plagioclase (oligoclase), and biotite is the only ferromagnesian constituent; neither hornblende nor muscovite were found. The texture is usually coarse and non-porphyritic, but finer porphyritic and aplitic types are common in some areas.

The granite cuts metamorphic rocks of the Moine series, which are mainly a monotonous succession of typical Moine "granulites"—uniform massive rocks showing little or no banding or segregation of dark and light constituents. The granulites consist essentially of quartz, orthoclase, oligoclase or andesine, and some biotite. Pelitic schists, found in some areas, frequently contain much garnet, staurolite and sillimanite, and belong to the sillimanite zone (Barrow, 1893); and there are also a few quartzite bands.

Adjacent to the contact the Moines have been recrystallized, with the formation of andalusite and cordierite in the pelitic types; and many transgressive veins and apophyses from the granite cut this contact region. Sometimes extensive granitization accompanies this veining, producing augen-gneisses, banded gneisses, or "granite-looking rocks," depending on the original composition.

---

* The area will be described in detail in a forthcoming paper.

The intrusion contains some inclusions of diorite and granodiorite showing varying degrees of modification by the enclosing granite, which is itself contaminated in their vicinity, but contamination of granite by Moine, or inclusion of Moine xenoliths in granite, is very rare—this circumstance is confined to some of the granite apophyses in the Moine near the margin of the granite.

Normal granite and granitized Moine can usually be differentiated with reasonable certainty, but it was thought that a statistical study of the form and elongation of the zircon in these rocks might supply an additional criterion for differentiating between similar-looking types of different origin, since zircon behaves as a highly refractory mineral under conditions of normal metamorphism. Accordingly it was thought that zircon from granitized Moine might show features characteristic of zircon from sediments, in which case it would probably be distinct from zircon in the granite. The refractory behavior of zircon is well known (Harker, 1932, pp. 12, 71), and zircon has been shown to retain a detrital form even in quartzite which has undergone intense thermal metamorphism and metasomatism (Reynolds, 1936), and in rocks which have been subjected to conditions of strong regional metamorphism (Poldervaart and von Backstrom, 1950; McLachlan, 1951). However there is abundant evidence that zircon does not always behave as a refractory mineral; for instance, in the Kakamas area of South Africa Poldervaart and von Backstrom (1950) show that zircon has recrystallized during ultrametamorphism. Again there are several records of authigenic outgrowths on zircon in unmetamorphosed sandstones (Butterfield, 1936; Smithson, 1937; Bond, 1948), and zircon has also been recorded as a pneumatolytic mineral, produced in limestones near the contact with a granite intrusion (Gillson, 1925). Thus much care must be observed in determining the origin of rocks from the form or habit of their zircon.

The possibility that an examination of the zircon would assist in differentiating rock types of different origin was tested by separating the heavy minerals from a variety of rocks and studying the zircon statistically. All the rocks examined contained zircon, sphene and iron ore and garnet and, less commonly, monazite were present in some types. The long axis of each crystal of zircon, and an axis perpendicular to this, were measured with a micrometer eyepiece (in well-rounded crystals the long axis is not necessarily the *c*-axis), and the elongation of each crystal was calculated; error in measurement is about 0.002 mm. Breakage of crystals during crushing constituted a source of error, but broken crystals were easily recognized, were generally those with an elongation greater than 3, and never formed more than about 5% of the zircons present.

The results were represented by plotting the elongation of 200 zircons from each rock on a histogram, and assemblages of different origin could be distinguished easily on these graphs. This method of representation is independent of the size of the grains, but assemblages of similar origin gave similar histograms, even though the average size of the grains varied greatly from rock to rock. As this method only serves to distinguish short zircons (typical of rounded grains from sediments) from long zircons (typical of idiomorphic grains from igneous rocks), it must be used with caution, since:

TABLE 1. TYPE OF ZIRCON

| Type | Habit | Nature of faces | Zoning | Color | Alteration |
|---|---|---|---|---|---|
| Sedimentary | Well rounded<br>No faces present | — | Absent | Clear. Usually colorless | Fresh |
| Igneous | Idiomorphic; dominant forms: {110}, {111}; small {100}, {311}; rare {101} | Rather dull and pitted | Usually present | Cloudy. Colorless or pale mauve | Metamict zones common, often with reddish stain |
| Contamination | Idiomorphic; very long. Dominant forms: {110}, {111}; others rare | Smooth | Usually present | Usually clear and colorless | Usually fresh |
| Recrystallized | Idiomorphic; dominant forms: {100}, {110}, {311}; small {331}, {111}, {101}; rare {001} | Perfectly smooth and brilliant | Absent | Clear. Usually colorless | Fresh |

(1). In many sediments the majority of zircons are idiomorphic, so would give a histogram of "igneous" type.

(2). In some igneous rocks the zircons may be very short, although they are idiomorphic—this is the case particularly if {001} is present, or if the prism zone is short and the pyramidal faces are rather flat; a histogram for such assemblages would be similar to one for well-rounded grains.

Because of these difficulties a careful examination of the appearance of the grains must accompany a statistical study of the elongation of zircon. In the present study it was found that zircon from different rocks could be divided into four types, which are named according to their typical environment (Table 1).

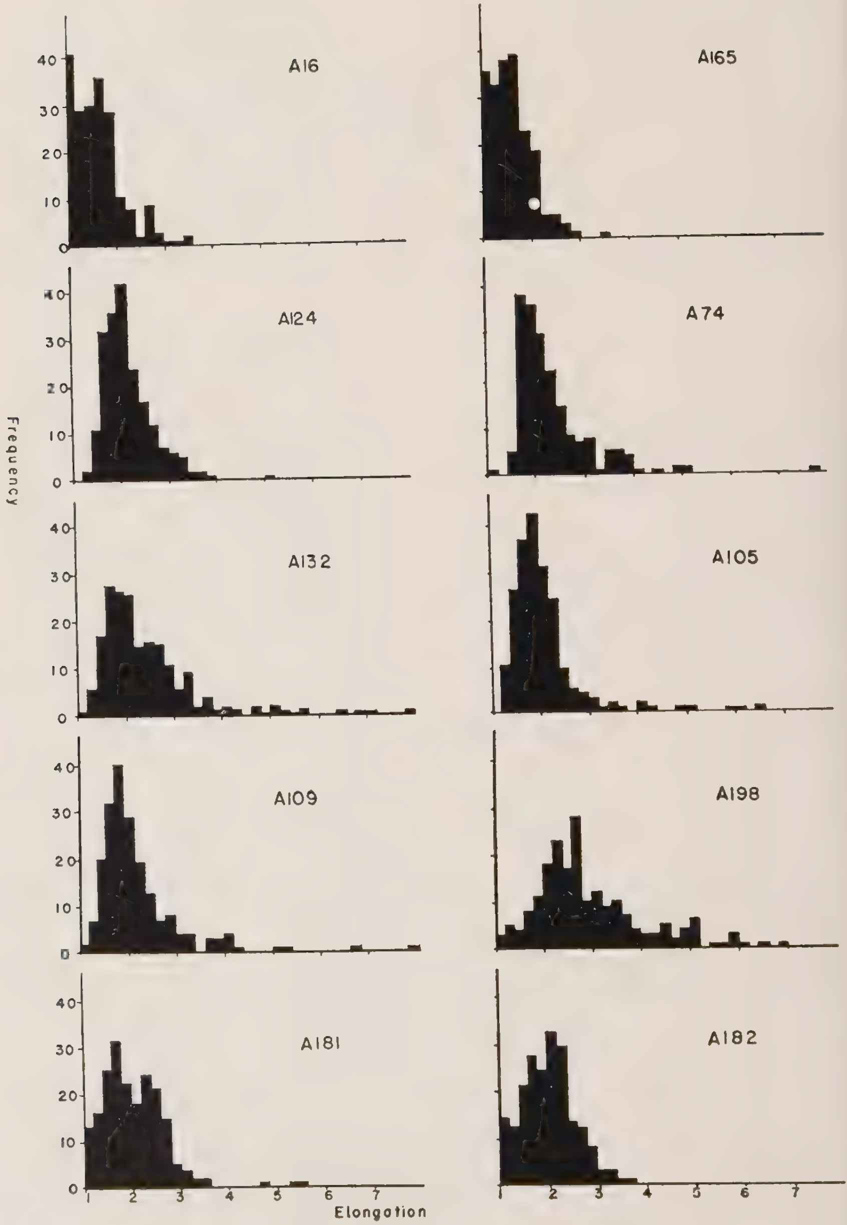

FIG. 1. Frequency-elongation histograms of zircons.

## RESULTS

Zircon was examined from typical Moine types; granite and aplite; xenoliths; contaminated granite; and granitized Moine. The zircon from each of these types showed differences as follows:

### *Moine schists*

Zircon from a typical Moine "granulite" (*A16*)* and a fairly pure quartzite (*A165*) was examined. All the zircon was of "sedimentary" type, and the histograms (Fig. 1) show the very high degree of rounding; the only essential difference between the two assemblages is the size of the grains, for in the quartzite they are 0.06–0.35 mm. long, and in the granulite they are 0.02–0.14 mm. The larger grains in the quartzite are to be expected in a rock which was probably much coarser-grained originally.

An interesting feature is the high degree of rounding of small crystals, since none showed any trace of crystal faces. It is a general observation that grains below a certain size are not effectively rounded by water action, and Hutton (1952) found that crystals smaller than about 60 microns show little if any rounding when they occur in beach sands, so the high degree of rounding in the present case would seem to be due to some factor other than corrasion in water. If this high degree of rounding is a primary feature, it may be due to extensive wind transportation, or possibly the zircon originally crystallized as well-rounded grains; however, the absence of any grains showing crystal faces makes the latter suggestion unlikely. Other possibilities would be either solution or mechanical granulation during metamorphism. Solution seems unlikely, and in the few other areas of intensely metamorphosed sediments where zircon has been studied a mixed assemblage of rounded and idiomorphic crystals is found; and if the rounding were to be attributed to some mechanical cause, then some traces of broken crystals or partially crushed augen would be expected; these were not observed. Accordingly, wind transportation is believed to be the prime factor in the formation of these rocks.

### *Granitic types*

Zircon was examined from a typical coarse granite (*A124*) and from a porphyritic aplite (*A74*). In both instances zircon was of "igneous" type, and the histograms for the two assemblages are very similar—each shows 55% of the zircon with an elongation between 1.6 and 2.2, but the aplite has a slightly higher proportion of stumpy crystals within this range. The only significant difference between the two assemblages is that the zircon from the granite is generally rather larger than that from the aplite, though the actual range in size is similar for both assemblages (0.035–0.35 mm.).

---

* Specimen numbers are field numbers of material in the collection of the Department of Mineralogy and Petrology, University of Cambridge.

### *Contaminated granites*

Zircon was examined from two contaminated granites; one of these (*A 109*) has been contaminated by adjacent xenoliths of more basic material, and as a result is richer in biotite and plagioclase than is the normal granite; the second (*A 198*) is a granite vein in the Moines, which contains many small xenoliths of Moine rocks, and has incorporated some material from them.

The first example (*A 109*) has a zircon assemblage composed mainly of normal "igneous" zircons, with a smaller number of "contamination" zircons, transitional types between typical "igneous" and "contamination" zircons being common. This assemblage is clearly shown in the histogram (Fig. 1) which is similar to that for zircon from the normal granite, except for the larger number of elongated crystals—6% of the crystals have an elongation in excess of 3.8, whereas only 0.5% occur in this region in the normal granite.

The zircon from the vein in the Moine shows a more complex assemblage. About 20% of the crystals are of "sedimentary" type, and the remainder are of "igneous" and "contamination" types, including many transitional between the last two. As a result, the histogram is more complex, and here the proportion of elongated zircons is even higher—20% have an elongation in excess of 3.8. The "sedimentary" zircons are identical with those from the Moines, and are probably due to actual incorporation of Moine schist in the granite, the zircon persisting unchanged. The elongated zircons are of interest—the evidence indicates that very elongated zircon is produced only in granite which has been contaminated, and they supply some evidence of the degree of crystallization of the granite at the time contamination took place. These elongated crystals are commonly zoned, and the zoning is always concentric, so the first-formed portions of the crystals were also elongated. Since zircon is one of the first minerals to start crystallizing, this suggests that at the time the granite was intruded as veins into the Moines, and incorporated some material from them, it was largely or entirely liquid.

### *Xenoliths*

Zircon from two large cognate xenoliths was examined. One of these (*A 132*) is granodiorite, the other (*A 105*) is an albitized biotite-tonalite, and both are veined by contaminated granite. In each of these, zircon is mainly of "igneous" type, but there is a little material of "contamination" type, probably from the veins of contaminated granite. This is reflected in the histograms, which are similar to those for the granite except for the presence of a few elongated crystals. The only other way the zircon from these rocks differs from that in the granite is that the crystals in the xenoliths are rather smaller, the usual size being 0.02–0.2 mm.

### *Granitized Moine*

Zircon from two examples of granitized Moine was examined. One of these (*A181*) is a "granite-looking" rock derived from a rather leucocratic granulite; the other (*A182*) is a coarse micaceous augen-gneiss derived from a pelitic schist. The zircon assemblages in these rocks are complex; the "granite-looking" rock contains a few "igneous" zircons, probably from granite veins which are abundant in the area, and are present in the specimen; the majority of the other crystals in both rocks are of "recrystallized" type, and there are also some which appear to be typical "sedimentary" zircons. These "sedimentary" zircons, however, if examined in detail, show unusual features; in transmitted light they appear to be well-rounded, but under reflected light they are seen to be bounded by numerous small irregularly-developed crystals faces, and from crystals of this type there is every transition to typical "recrystallized" zircons. The process of recrystallization must be solution of material from some parts of a crystal and deposition on others, so that a rounded grain is gradually converted to a perfectly idiomorphic crystal in which no trace of the original form can be detected. Breakdown of one large detrital grain to give an aggregate of smaller grains, such as Poldervaart and von Backstrom (1950) found at Kakamas, is very rare here, but instead this gradual change from a rounded grain to an idiomorphic crystal is the usual process. The average size of the recrystallized zircon is about the same as that of zircon in the original Moine from which these rocks were derived, and this appears to suggest that no material has been subtracted or added to the zircons during recrystallization.

## SUMMARY

The zircon assemblages from the normal igneous types, contaminated igneous rocks, Moine schists, and granitized Moines, are quite distinct, and comparison of the different assemblages was found very useful in confirming the difference between normal granite and granitized schists. A similar comparative study may give useful results in other areas.

## ACKNOWLEDGMENTS

This study was carried out in the Department of Mineralogy and Petrology at the University of Cambridge, while in receipt of a Department of Scientific and Industrial Research grant. The writer is indebted to Professor C. E. Tilley and Drs. S. O. Agrell and S. R. Nockolds for their interest and advice, and to Professor C. O. Hutton for critical reading of the manuscript.

## REFERENCES

BARROW, G. (1893), On an intrusion of muscovite-biotite-gneiss in the south-eastern Highlands of Scotland, and its accompanying metamorphism: *Quart. Jour. Geol. Soc.*, **49,** 330.

BOND, G. (1948), Outgrowths on zircon from southern Rhodesia: *Geol. Mag.*, **85,** 35.

BUTTERFIELD, J. A. (1936), Outgrowths on zircon: *Geol. Mag.*, **73,** 511.

GILLSON, J. L. (1925), Zircon, a contact metamorphic mineral in the Pend Oreille District, Idaho: *Am. Mineral.*, **10,** 187.

HARKER, A. (1939), Metamorphism. London.

HUTTON, C. O. (1952), Accessory mineral studies of some California beach sands: *U.S.A.E.C. Report* **RMO-981**.

McLACHLAN, G. R. (1951), The aegerine-granulites of Glen Lui, Braemar, Aberdeenshire: *Mineral. Mag.*, **29,** 476.

POLDERVAART, A., AND VON BACKSTROM, J. W. (1950), A study of an area at Kakamas (Cape Province): *Trans. Geol. Soc. South Africa*, **52** (for 1949), 433.

REYNOLDS, D. L. (1936), Demonstrations in petrogenesis from Kiloran Bay, Colonsay. I. The transfusion of quartzite: *Mineral. Mag.*, **24,** 367.

SMITHSON, F. (1937), Outgrowths on zircon in the Middle Jurassic of Yorkshire: *Geol. Mag.*, **74,** 281.

*Manuscript received Nov. 6, 1953*

# THE PROBLEM OF BOND TYPE

W. S. Fyfe, *Department of Geological Sciences, University of California, Berkeley, California.*

## Abstract

The difficulties of assessing ionic and covalent contributions to bonds are discussed. It is suggested that one of the best indications of such contributions can be obtained from a consideration of atomic orbital overlap in the linkages. The structures of the bonds in some compounds are discussed from a consideration of the overlap integrals.

## Introduction

Numerous writers (Ahrens (1), Ramberg (2), Gruner (3)) have recently discussed the problems of bond type and its implications in geochemical problems. In a previous paper (4) the writer used the Pauling electronegativity scale to obtain information on bond type. At the present time some doubt must rest on the validity of some of these arguments and the present discussion is directed at focusing attention on what is now becoming accepted as one of the best indications of bond type, namely, the overlapping of atomic orbitals in a bond.

It is generally agreed that the bonds in a crystal or molecule formed between unlike atoms cannot be adequately described by considering only pure ionic or covalent structures, but that the actual structure is some combination of the limiting forms. The emphasis placed on the limiting forms differs considerably between workers. Ahrens (1), for example, prefers to use the ionic approach in most arguments while Pauling (5) considers most bonds as more nearly covalent. The wave function which will describe the state of affairs in a bond will in general have the form:

$$\psi \text{ mol} = \psi \text{ covalent} + k\, \psi \text{ ionic}.$$

The essential problem is to find some suitable means of evaluating the constant in this relation. The importance of the evaluation is obvious for upon it rest the steric properties, energies and lengths, etc., of the bond.

The various electronegativity scales have been directed at providing the necessary information on bond transition and all such scales (Pauling (6), Mulliken (7), Walsh (8)) agree in large part in the direction of such transitions. Thus, all would make cesium fluoride more ionic than lithium iodide. (It may be noted that some quite large differences do occur between the scales of Pauling and Walsh.) Although the data that can be derived from considerations of electronegativity differences between atoms can be invaluable in discussing some problems, there is considerable doubt in relating such differences to the actual *amount* of each contribution. The most important attempt to relate electronegativity to the quantitative evaluation of bond contributions was made by Pauling (6), who used the dipole moments of the hydrogen halides to fix limits to ionic contributions. At the present time considerable doubt must rest on this interpretation due to the complexity of the factors which lead to a molecule possessing a permanent dipole.

To elaborate on this latter difficulty we may consider bonding in the water molecule. At first sight we might expect oxygen with a structure $1s^2 \cdot 2s^2 \cdot 2p^2 \cdot 2p^1 \cdot 2p^1$ to use its two singly occupied "$p$" orbitals to form bonds with the $1s$ orbitals of the two hydrogen atoms. If this represented the true picture, then the lone pairs of electrons of the oxygen atom would remain in orbitals symmetrical about the oxygen nucleus and these would make no contribution to the dipole of the molecule. The bond angle in the water molecule (105°) is not that expected from "$p$" bonding (90°) and is close to the tetrahedral bond angle. This suggests that the oxygen atom may use an $sp^3$ hybrid state similar to the normal quadrivalent carbon atom. If such hybridization occurs, the lone pairs of the oxygen atom are no longer left with a symmetrical distribution and will make a contribution to the dipole moment. The large bond angle in the water molecule is often explained by considering that the normal "$p$" angle is opened slightly by repulsions between the adjacent hydrogens. If this occurred, the covalent bond would be weakened, an effect which is easily overcome by rehybridization of the oxygen orbitals. Confirmation of this hybridization in water has come from considerations of the structure of water and the calculations of hydrogen bond energies by Pople and Lennard-Jones (9) and Fyfe (10). The small moments of the carbon monoxide and nitrogen trifluoride molecules find ready explanation when lone pairs are considered but would not be explicable on the Pauling theory of ionic-covalent resonance. Coulson (11) from calculations of the various contributions to the water dipole has concluded that only a small proportion comes from ionic structures. It is thus clear, that if there is any hybridization of the halogen orbitals in the hydrogen halides, then the dipole moment cannot be a measure of the amount of ionic-covalent resonance. That such hybridization is likely to occur has been shown by Robinson (12). [Cf. Kastler (13)] For a full discussion of the dipole problem see Coulson (14).

From the above discussion it becomes clear that the Pauling relation of electronegativity difference to percentage ionic character of bonds (as used by writer (4)) is not entirely satisfactory. The Pauling relation must tend to place too much weight on ionic contributions. We may summarize by saying that although present electronegativity scales give us an order of bond transition, they can give us no quantitative data.

It should be noted that essentially there is little difference between the approach to bond transition from consideration of electronegativities to the approach via polarizability of Fajans and others which Ahrens uses (1). Consideration of charge and radius effects give an order of bond transition similar to that derived from electronegativities. The chief advantages in using electronegativities in the past has been that these functions are more likely to provide quantitative data.

Recently attention has been focussed on the overlap integral as a quantity capable of giving precise information on bond type and structure. The overlap integral $S$ for overlap between any pair of atomic orbitals is defined by the relation

$$S(\psi_A\psi_B;\, R) = \int \psi_A\psi_B dv.$$

This integral gives a measure of the regions in space where the two atomic orbitals overlap. $\psi_A$, $\psi_B$ represent suitable normalized atomic orbitals of atoms $A$ and $B$ and $R$ is the internuclear distance. This quantity gives us a measure of the amount of classical covalent bonding and for purely ionic bonds should have a value of zero. The value of $S$ depends upon the type of atomic orbital and the internuclear distance. Recently Mulliken (15), McColl (16) and Walsh (17) have made extensive use of overlap integrals in discussing bond properties.

Where possible it is desirable to use full self-consistent field wave functions to represent the atomic orbitals. However, because these are not always available and are rather unwieldy, the simple Slater functions (18) are almost always used. These functions express the outer part of atomic orbitals with considerable accuracy and are adquate for most problems at normal bonding distances. Numerous solutions exist for the necessary integrals; Mulliken (19), Couslon (20), Barnnet and Coulson (21). Recently Mulliken (22) has proposed relations between overlap integrals and bond energies greatly extending the usefulness of such calculations. The values of the overlap integrals for various orbital types also provide leading information on the state of an atom in an actual bond. These may be used along with the guiding principle enunciated by Pauling (6) that "of two orbitals in an atom the one which can overlap more with an orbital of another atom will form the stronger bond with that atom, and, moreover, the bond formed by a given orbital will tend to lie in the direction in which the orbital is concentrated."

Recently Pauling (5) has developed the "neutrality principle" which appears to be a most useful generalization. The principle essentially states that the formal charges on atoms in molecules or crystals probably rarely exceed $\pm\frac{1}{2}e$, and that charges as large as this are only found in bonds between atoms at the extreme ends of the electronegativity scale. Pauling has applied the following type of argument. The electronegativity difference between a cesium and a fluorine atom indicate that the bond in the diatomic molecule has about 9% covalent character. In the CsF crystal as each atom is surrounded by six others, the bond in the crystal may be described as a single bond with as much as 54% covalent character resonating among the six positions. Thus the charge in this extreme ionic case may not exceed $\frac{1}{2}e$. Again, if we consider the hexahydrated ferric ion in aqueous solution, the O-Fe bonds have about 50% covalent character. By the formation of six such bonds the charge on the ferric ion is essentially neutralized, the charge being relayed to the hydrogen atoms of the solvating water molecules. Pauling considers that the oxidation states of aqueous ions are controlled by such factors and not by the ionization potentials alone. The usefulness of the principle in the field of ion solvation has been developed by the writer (23). The principle greatly increases the weight to be given to covalent structures. It is of interest that similar trends are indicated in other work. Pitzer (24) and Mulliken (15) have both attributed repulsion effects to overlap of nonbonding electrons rather than to polarity. Walsh (17) has also demonstrated very clearly that polarity does not increase bond strength, a conclusion which might have been drawn from the original arguments of Pauling (6).

The remainder of this discussion will be concerned with overlap integrals for some typical types of bond and the calculation of bond lengths, etc.

## OVERLAP INTEGRALS AND ELECTRONEGATIVITY DIFFERENCES

Primarily it must be emphasized that a general correlation exists between the amount of covalent bonding determined either from overlap integrals or electronegativity differences. In Table 1 some results for

TABLE 1. OVERLAP INTEGRALS AND ELECTRONEGATIVITY DIFFERENCES FOR Li-X BONDS

| $X$ | $S(ss)$ | $S(sp)$ | $S(ps)$ | $S(pp)$ | $x_a - x_b$ |
|---|---|---|---|---|---|
| F | 0.17 | 0.05 | 0.27 | 0.08 | 3.0 |
| Cl | 0.23 | 0.15 | 0.40 | 0.19 | 2.0 |
| O | 0.20 | 0.07 | 0.31 | 0.10 | 2.5 |
| S | 0.29 | 0.18 | 0.44 | 0.22 | 1.5 |
| N | 0.24 | 0.10 | 0.37 | 0.14 | 2.0 |
| P | 0.33 | 0.23 | 0.46 | 0.26 | 1.1 |
| C | 0.28 | 0.14 | 0.43 | 0.18 | 1.5 |
| Si | 0.37 | 0.28 | 0.50 | 0.29 | 0.8 |

Li-X bonds are summarized. (Note: See Appendix for meaning of terms $S(ss)$, etc. The orbitals always refer to the valence shell electrons.)

In almost all cases the order of increasing overlap of the orbitals concerned is that predicted from electronegativity differences $(x_a - x_b)$. Thus for the $(ss)$ series the order is:

$$\mathrm{Si}>\mathrm{P}>\mathrm{S}>\mathrm{C}>\mathrm{N}>\mathrm{Cl}>\mathrm{O}>\mathrm{F}$$

while from the electronegativity differences we would expect

$$\mathrm{Si}>\mathrm{P}>\mathrm{C}\overset{=}{>}\mathrm{S}>\mathrm{N}\overset{=}{>}\mathrm{Cl}>\mathrm{O}>\mathrm{F}.$$

The differences in the $S$ values are rather smaller than might be expected but small differences in $S$ can lead to relatively large differences in covalent bond energy. Some of the values for lithium fluoride are sufficiently large to suggest that covalent terms in this bond are too large to be neglected. The order of overlapping of the electronegative atoms appears to be almost independent of the metal chosen and similar series have been found for beryllium, magnesium and hydrogen. (Note: The $S$ values have been calculated using Slater functions at a distance corresponding to the covalent radius sum in all cases.)

If the Pauling neutrality principle is to be considered reasonable for classical ionic crystals such as the alkali halides, then, there should be substantial amounts of overlap between atoms in such crystals. To test this, the overlap integrals for some of these bonds have been evaluated and are summarized in Table 2. (Note: In calculating these overlap integrals the screening constants have been evaluated for the neutral atoms, not the ions. Thus for NaCl the overlap is considered between Na $(3s)$ and Cl $(3s \cdot 3p)$, etc. $R$ refers to the internuclear distance in angstroms.)

It will be noticed that in all cases there is substantial overlap, even for RbF. However, in this case the contribution to the bonding energy would be small but could account for the 10% covalent character deduced from

TABLE 2. OVERLAP INTEGRALS FOR ALKALI HALIDES

| *Compound* | $R$ | $S(ss)$ | $S(ps)$ | $S(pp)$ | $S(ps)$ |
|---|---|---|---|---|---|
| LiF | 2.01 | 0.20 | 0.32 | 0.09 | 0.06 |
| LiCl | 2.57 | 0.27 | 0.40 | 0.20 | 0.15 |
| LiI | 3.02 | 0.28 | | | |
| NaF | 2.31 | 0.16 | 0.27 | 0.05 | 0.03 |
| NaCl | 2.81 | 0.31 | | | |
| NaI | 3.23 | 0.28 | | | |
| RbF | 2.82 | 0.08 | | | |
| RbCl | 3.29 | 0.14 | | | |
| RbI | 3.66 | 0.26 | | | |

Pauling's electronegativity differences. It will be noted that the values for sodium chloride are larger than for the iodide, while for lithium chloride and iodide the values are approximately equal. This effect would not be expected either from consideration of electronegativities or polarizabilities. This effect is probably to be attributed to the very different size of the orbitals concerned. If two overlapping orbitals have different quantum numbers such as Li (2) and I (5), the space distributions of the electron clouds about such atoms are very different. Thus, for the "*s*" electrons, although in both sodium and iodine these have spherical distributions the radius of the cloud for iodine is much larger. In such a case it is not possible to obtain large amounts of overlap of the regions in space where these electrons are concentrated. The effect does not occur in the case of rubidium iodide where both metal and non-metal have the same quantum numbers.

In Table 3 values are given for the integrals for M-O and M-S bonds.

TABLE 3. OVERLAP INTEGRALS FOR M-S AND M-O BONDS

| *Bond* | $S(ss)$ | $S(sp)$ | $S(pp)$ | $S(ps)$ | $S(\pi\pi)$ |
|---|---|---|---|---|---|
| C-O | 0.27 | 0.38 | 0.28 | 0.24 | 0.14 |
| C-S | 0.24 | 0.39 | 0.33 | 0.29 | 0.17 |
| Si-O | 0.27 | 0.20 | 0.18 | 0.46 | 0.16 |
| Li-O | 0.20 | 0.31 | 0.10 | 0.07 | 0.10 |
| Li-S | 0.29 | 0.18 | 0.22 | 0.44 | 0.14 |
| Mg-O | 0.23 | 0.38 | 0.12 | 0.09 | 0.10 |
| Al-O | 0.25 | 0.13 | 0.18 | 0.38 | 0.11 |
| Na-O | 0.20 | 0.33 | 0.08 | 0.05 | 0.08 |

From these figures it is apparent that even in linkages such as Na-O and Mg-O covalent contributions to the bond energy may be considerable. For Si-O and Al-O bonds all terms indicate fairly strong overlap. One feature of interest is the fairly large magnitude of the $\pi$ overlap terms in some cases which suggest that double bonding may be important. The bond shortening in Si-O has been attributed to this effect. (Note: For definition of $\pi$ bonds see appendix.)

## BOND ENERGIES AND OVERLAP INTEGRALS

If covalent contributions to a bond are to be considerable it is necessary that the energy from such overlap be reasonably large compared with the total bond energy. From the values of the integrals alone little data of real value can be obtained except of a qualitative nature.

Recently Mulliken (22) has proposed semi-empirical relations between bond energies and overlap integrals. The general form of the relation is as follows:

$$D_0 = \Sigma X_{ab} - 1/2\Sigma Y_{ab} + 1/2\Sigma K_{ab} - P + RE.$$

$D_0$ = dissociation energy of the molecule.
$X_{ab} = AS_{ab}I_{ab}/(1+S_{ab})$ ($S$ for bonding electrons.)
$Y_{ab} = A'S_{ab}^2 I_{ab}$ ($S$ for non bonding electrons.)
$P$ = Promotion energies to the valence state.
$RE$ = Resonance energy of all types (as in benzene).
$I$ = Mean ionization potentials of the electrons.

$A$ and $A'$ are constants determined by fitting the equation to the known bond energies of two molecules. The $Y$ terms which cover repulsions due to overlap of filled shells are of two types, one due to inner shell electrons of $A$ reacting with valence shell electrons of $B$ and overlap of non-bonded electrons such as the two hydrogen atoms in a water molecule. The $K$ terms cover exchange energy between full shells which is small, but not negligible. Mulliken has found that the above relation fitted to two molecules gave dissociation energies within 1–2% of the experimental values for eight others. The relation is extremely useful in obtaining some indication of the energy contributions from particular sets of orbitals. Thus in diatomic RbF the (*ss*) overlap corresponds to an energy of 16 k.cals/mol. while for LiF the (*ss*) overlap gives a bonding energy of about 43 k.cals/mol. The relation can also be applied to obtaining bond lengths. In this case it is necessary to evaluate the energy over a range of atomic distances to obtain maximum bond energy.

## Bonding in the Si-O and C-O Groups

It is well known that the bonds in the Si-$O_4$ and similar groupings are often abnormally short. Pauling (25) has discussed this and similar problems and attributes this shortening largely to the effect of $\pi$ bonding between silicon and oxygen. Pitzer (24) considers that inner shell-outer shell repulsions are probably more important. Another feature of the chemistry of these groups is to explain why there is no $SiO_3^{--}$ group corresponding to a $CO_3^{--}$ group and conversely no $CO_4^{----}$ group corresponding to $SiO_4^{----}$. Generally these effects are vaguely attributed to the influence of size and charge. However, if we are to take the neutrality principle seriously, the effect of polarity must take a less important place. To attempt to find factors influencing these problems some calculations have been made of the principal overlap energies in such bonds. It may be noted that size factors are not controlling, for molecules such as $CI_4$ are quite stable with the iodine atom much larger than oxygen. In Table 4 some of the important overlap integrals and the corresponding energies are recorded. As the $CO_3^{--}$ ion is planar, the bonds are most

Table 4. Overlap Integrals and Energies for C-O Bonds. (R=1.3 Å)

| | $S$ | $E$(e.v) | Notes |
|---|---|---|---|
| $(2s2s)$ | 0.33 | | |
| $(2s2p)$ | 0.42 | | |
| $(2p2s)$ | 0.28 | | |
| $(2p2p)$ | 0.30 | | |
| $(C_{sp^2}O_{sp})$ | 0.664 | 8.24 | Carbon trigonal oxygen digonal hybrids |
| $(C_{sp^3}O_{sp})$ | 0.663 | 8.20 | Carbon tetrahedral oxygen digonal hybrids |
| $(\pi\pi)$ | 0.18 | 4.15 | |
| $(pp)$ | 0.12 | 0.124 | Repulsion adjacent oxygens *S.C.F.* functions |
| $(C_{sp^3}O_{1s})$ | 0.072 | 0.61 | Carbon valence shell oxygen inner shell repulsion |
| $(C_{1s}O_{sp})$ | 0.055 | 0.20 | Oxygen valence shell carbon inner shell repulsion |

probably formed from a carbon $sp^2$ trigonal hybrid. We have considered that oxygen may use an $sp$ linear hybrid which will give maximum overlapping. The inclusion of a large amount of "$s$" character in this bond may not be justified, but certainly in the $SiO_2$ crystal this is justified by the Si-O-Si bond angle. One feature of interest is the very large values of the hybrid overlaps compared with the simple orbital overlaps. As Mulliken (26) says "a little hybridization goes a long way." It is also well established that the amount of overlap increases with "$s$" character of the bond. The remaining carbon "$p$" orbital will lie above and below the plane of the group and can thus form a strong $\pi$ bond with the oxygen "$p$" orbitals. We may thus sum the energies of the two possible structures.

$$E(CO_3) = 3E\sigma + E\pi - 3E(O\text{-}O) - 3E(C_{1s}O) - 3E(O_{1s}C)$$
$$= 26.07 \text{ e.v.}$$
$$E(CO_4) = 4E\sigma - 6E(O\text{-}O) - 4E(C_{1s}O) - 4E(O_{1s}C)$$
$$= 28.60 \text{ e.v.}$$

Thus neglecting any polarity we calculate that the bond energy of the $CO_4$ group is larger. This fact is not as alarming as might be first thought and will be discussed later. (Note. Allowance has been made for the smaller O-O distance in the tetrahedral grouping.)

By applying an exactly similar treatment to the Si-O groupings we arrive at energies of 22.62 e.v. for $SiO_3$ and 25.50 e.v. for $SiO_4$. Once more the four co-ordinated structure is favoured on these arguments.

We may now consider some of the factors indicated from these calculations. Firstly, the internuclear distances appear to be controlled more by inner shell, outer shell repulsions, which are much larger than the O-O repulsions. These latter values should be fairly accurate as *S.C.F.* functions have been used (26). Secondly, the inner shell repulsions are much less for silicon than for carbon. Thus the energy for the overlap of silicon ($2s$) orbitals with oxygen valence is almost negligible while for carbon this is not the case. This effect will favour higher co-ordination with silicon. The O-O repulsions in the silicon structures with larger bond lengths than in the case of carbon are only 25% as great, once more favouring higher co-ordination. Another feature of interest is that the $\pi$ energy terms for C-O are 51% as strong as the $\sigma$ bonds while for silicon this is reduced to 45%.

To obtain some indication of bond lengths, calculations have been made of the variation of energy with internuclear distance. The results are summarized in Table 5.

TABLE 5. VARIATION OF BOND ENERGY WITH BOND LENGTH

$CO_3$ $R=1.4$, $E=25.36$; $R=1.3$, $E=26.07$; $R=1.2$, $E=24.4$
$CO_4$ $R=1.5$, $E=27.92$; $R=1.4$, $E=28.83$; $R=1.3$, $E=28.6$
$SiO_4$ $R=1.7$, $E=23.87$; $R=1.6$, $E=25.50$; $R=1.5$, $E=24.83$

For all groups the calculated distance is close to the observed. It will be noticed that for a $CO_4$ group the calculated length is somewhat longer than for $CO_3$. This effect, with a similar order of magnitude to that indicated is observed with the borates where both co-ordination numbers are observed. (Wells 27.)

The calculations discussed above support the ideas of Pitzer (24) and show that extensive $\pi$ bonding using "$d$" orbitals is not necessary to explain the short Si-O distance. It appears that the state of hydridization and its effect on repulsion energies may play a very important part in determining bond lengths. Thus if the oxygen orbitals in the $SiO_4$ group were not hybridized, the repulsion energies would be at least doubled.

It should be emphasized that only limited conclusions can be drawn from considerations of the grouping alone. For example, the formation of the $SiF_6^{--}$ group is controlled to large extent by the cations associated with it in the structure.

## THE EFFECT OF POLARITY ON THE Si-O AND C-O GROUPS

To this stage we have assumed that the formal charges on the anionic groupings are small, i.e., the bonds between the oxygen atoms and metal atoms are sufficiently covalent to drain away the negative charge on the anion. The bond length calculations to some extent justify this conclusion. However, it is well to consider the conditions if these bonds carry charges as if the metal oxygen bonds were fully ionic. To calculate charge distributions in the groupings the electronegativities and relation to the polarity given by the writer (4) may be used. The charge distributions in the anions are summarized in the diagrams below. It is obvious at a glance that structure $B$ is much less stable than structure $A$ for the

FIG. 1.

CHARGE DISTRIBUTIONS IN C-O
Si-O GROUPINGS.

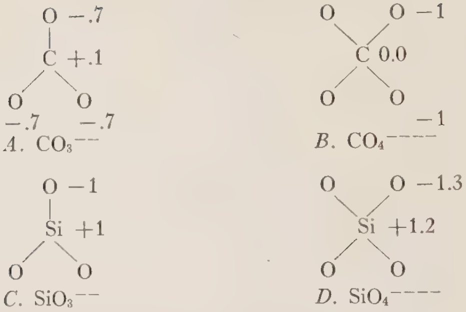

C-O groupings. However, the $SiO_3$ grouping is also electrostatically more stable. It will be noticed however, that the four co-ordinated structure is relatively more stable for silicon than carbon. It can be concluded that the inclusion of much smaller amounts of polarity than above could well adjust the additive effect of the covalent and ionic attractions in the correct direction. Covalently, both four co-ordinated members are more stable and conversely if a large amount of polarity is introduced. However, polarity has a larger effect on the C-O groupings than on the Si-O groupings.

## VALENCE STATE PROMOTION ENERGIES

If an atom such as aluminum is to enter into six co-ordination and form strong covalent bonds, "*d*" orbitals will have to be used. The use of such orbitals requires considerable energy to promote electrons into the higher states, and such promotion energies must control the ease with which an atom may reach a higher state. Promotion energies can be obtained from spectroscopic data and some typical values are given below from Moore (28). It will be noticed that the relative ease of excitation increases greatly from carbon to silicon to aluminum. These spectroscopic excitation energies are possibly too large as has been emphasized by Gillespie (29) particularly when the atom is bound to an extremely

TABLE 6. EXCITATION ENERGIES OF CARBON, SILICON AND ALUMINUM

Carbon ground state to carbon $sp^3 = 9$ *e.v.*
Silicon ground state to silicon $sp^3 = 6$ *e.v.*
Aluminum ground state to aluminum $sp^3 = 3.6$ *e.v.*
Carbon ground state to carbon "*d*" = 18.6 *e.v.*
Silicon ground state to silicon "*d*" = 11.8 *e.v.*
Aluminum ground state to aluminum "*d*" = 7.5 *e.v.*

electronegative atom such as fluorine. They must, however, provide some indication of the relative ease of promotion. There is some correlation with the observation that carbon is not found in six-co-ordination, silicon only with the most electronegative atoms such as fluorine and aluminum very frequently in six.

## Effect of Cations on Oxygen Hybridization

The state of oxygen hybridization might be expected to change with changes in the environment caused by cation distribution. Thus in the forsterite structure, each oxygen as well as being linked to silicon is linked by partially covalent bonds to three magnesium atoms. Thus it is in an almost tetrahedral environment. In such a situation we would expect some change from the *sp* hybrid which has been considered most closely approached in silica. It must be emphasized that all possible hybrids of *s* and *p* electrons are possible between the end members hybrids *sp*, $sp^2$ and $sp^3$. (See Coulson 14.) If in a structure such as forsterite the oxygen hybrids are more nearly $sp^3$, then the Si-O bonds will be considerably weakened. It would also be expected that as Si-O-Si bonds become important in determining the structure, that is, from isolated groups through chains, bands, sheets to three dimensional frameworks, that the Si-O bonds should increase in strength. The amount of *s* character should increase as Si-O bonding becomes more important. Within any single structural type we would expect that as the cation overlaps more with oxygen, the tendency for rehybridization will increase thus weakening the Si-O bonds. Thus in a series such as $Ca_2SiO_4$, $Mg_2SiO_4$, $(MgFe)_2SiO_4$ we would expect to find the strongest Si-O bonds in the calcium member. Similarly in feldspars, we would expect the Si-O bonds in albite to be weaker, although very slightly, than in orthoclase.

Some qualitative agreement with these ideas comes from the infra red studies of Launer (30 See Fig. 13). Here the principal absorbtion bands shift to the short wave length region as Si-O bonding becomes complex and in the orthosilicate series mentioned above the shift to the short wave length region is as expected.

## The Additivity of Radii

It appears to the writer that rather too much weight is placed on values of radii in problems concerned with bond distances. The radius of an atom is by no means a constant quantity. Additivity of radii is only to be expected when the atoms are in very similar environments. The simple fact that we must postulate ionic, covalent, metallic and van der Waals radii, and that there is always some doubt as to which to use is sufficient evidence to demonstrate that radii are not constant. It would be expected that in many cases they should be approximately additive, but recent work, particularly from micro wave spectra, has shown that almost always small deviations occur, even in very similar compounds. These anomalous effects are often explained by postulating double bonding, etc., but surely small differences are to be expected, for a slight change in structure may alter repulsion effects very considerably. The striking effects of hybridization which Coulson and others have emphasized may have more influence on radius than change in bond type. Radii, although always a useful guide to the order of bond length can never possibly give us accurate lengths for a wide variety of compounds even although we may evolve more than one set of radii.

## APPENDIX

(*a*) Slater atomic orbitals have forms of the type

$$\psi(1s) = N_{1s}e^{-cr}, \qquad \psi(2s) = N_{2s}e^{-cr/2} \text{ etc.}$$
$$\psi(2p) = N_{2p}\,Xe^{-cr/2}, \qquad \psi(3p) = N_{3p}\,Xe^{-cr/3} \text{ etc.}$$

The constants $N$ are normalizing factors such that

$$\int \psi^2 dv = 1.$$

The constant $c$ refers to the effective nuclear charge $(Z\text{-}s)$ which refers to the atomic number minus the screening constants of the outer electrons which can be evaluated from the recipes of Slater (18). The overlap integral thus is simply the integral of the products of two such Slater functions. Thus $S(ss)$ is the overlap integral for two $s$ orbitals, etc.

Self-consistent-field functions which are considerably more accurate can be expressed as a series of Slater functions and treated by the solutions mentioned earlier (19, 20, 21).

The $x$ terms in the above relations refer to the angular dependence of the functions. The $s$ orbitals being spherically symmetrical possess no such constant. It is of considerable value to have some picture of the electron distribution corresponding to these functions and illustrations of these are supplied by Coulson (14).

(*b*) The normal covalent bond such as occurs in a hydrogen molecule is referred to as a $\sigma$ bond. The double bond in say ethylene is made of two parts, a normal $\sigma$ bond and a $\pi$ bond. The $\pi$ bond is formed when two adjacent "$p$" orbitals with the same angular dependence ($x$) overlap. (See Coulson for illustrations.)

A hybrid atomic orbital can always be formed by suitable mixing of the simple types. For example a hybrid $sp$ functions can have the form

$$\psi_{hyb.} = a\psi_s + (1 - a^2)^{1/2}\psi_p$$

where the constant "*a*" determines the contribution of each end member. For tetrahedral, trigonal and digonal hybrids $a^2 = \frac{1}{4}$, $\frac{1}{3}$, $\frac{1}{2}$, respectively. A tetrahedral hybrid has four equivalent orbitals directed towards the corners of a regular tetrahedron, a trigonal hybrid has three equivalent orbitals with trigonal symmetry in the one plane and a digonal hybrid has two equivalent orbitals 180° apart. In methane, for example, carbon uses a tetrahedral hybrid, in $C_2H_4$ ethylene, carbon uses a trigonal hybrid (the remaining unhybridized $p$ orbitals forming the $\pi$ bonds) and in acetylene carbon uses a digonal hybrid (the two remaining unhybridized $p$ orbitals form two $\pi$ bonds).

## ACKNOWLEDGMENTS

The writer wishes to acknowledge assistance both from the Office of Naval Research and the Institute of Geophysics of the University of California. Dr. J. Verhoogen of this University has also been most helpful in his criticisms although all responsibility for statements in this work is taken by the author.

## REFERENCES

1. AHRENS, L. H., The use of ionisation potentials: *Geochimica et Cosmochimica Acta*, **3,** 1 (1953).
2. RAMBERG, H., Chemical bonds and distribution of cations in silicates: *J. Geol.*, **60,** 331 (1952).
3. GRUNER, J. W., An attempt to arrange silicates in the order of reaction energies at relatively low temperatures: *Am. Mineral.*, **35,** 137 (1950).
4. FYFE, W. S., Isomorphism and bond type: *Am. Mineral.*, **36,** 538 (1951).
5. PAULING, L., The modern theory of valence: *J. Chem. Soc.*, 1461 (1948).
6. PAULING, L., Nature of the chemical bond: Cornell (1946).
7. MULLIKEN, R. S., A new electroaffinity scale: *J. Chem. Phys.*, **2,** 782 (1934).
8. WALSH, A. D., Factors affecting bond strengths: *Proc. Roy. Soc.*, **207,** 13 (1951).
9. POPLE, J. A., AND SIR JOHN LENNARD-JONES, Molecular association in liquids: *Proc. Roy. Soc.*, **205,** 155 (1951).
10. FYFE, W. S., Conditions for the formation of hydrogen bonds: *J. Chem. Phys.*, **21,** 2 (1953).
11. COULSON, C. A., A critical survey of the method of ionic-homopolar resonance: *Proc. Roy. Soc.*, **207,** 63 (1951).
12. ROBINSON, D. Z., Ionic character and the dipole moment of chemical bonds: *J. Chem. Phys.*, **17,** 1022 (1949).
13. KASTLER, D., Electronic exchange effects in the calculations of dipole moments: *Comt. rend.*, **232,** 2323 (1951).
14. COULSON, C. A., Valence. Oxford (1952).
15. MULLIKEN, R. S., Overlap integrals and chemical bonding: *J. Am. Chem. Soc.*, **72,** 4493 (1950).
16. MCCOLL, A., The principle of maximum overlapping: *Trans. Faraday. Soc.*, **46,** 369 (1950).
17. WALSH, A. D., Factors influencing the strength of bonds: *J. Chem. Soc.*, 398 (1948).
18. SLATER, J. C., Atomic shielding constants: *Phys. Rev.*, **36,** 57 (1930).

19. Mulliken, R. S., Rieke, C. A., Orloff, D., and Orloff, H., Formulas and numerical tables for overlap integrals: *J. Chem. Phys.*, **17,** 1248 (1949).

20. Coulson, C. A., Two centre integrals occurring in the theory of molecular structure: *Proc. Cambridge. Phil. Soc.*, **38,** 210 (1941).

21. Barnett, M. P., and Coulson, C. A., Evaluation of integrals occurring in the theory of molecular structure: *Philosophical Trans. Roy. Soc.*, **243,** 221 (1951).

22. Mulliken, R. S., Structure of bond energies: *J. Phys. Chem.*, **56,** 295 (1951).

23. Fyfe, W. S., Factors influencing the stability of complex ions: *J. Chem. Soc.*, 2018 (1952).

24. Pitzer, K. S., Repulsion forces in relation to bond energies: *J. Am. Chem. Soc.*, **70,** 2140 (1948).

25. Pauling, L., Interatomic distances and bond character in the oxygen acids and related substances: *J. Phys. Chem.*, **19,** 900 (1952).

26. Mulliken, R. S., Overlap and bonding power of 2*s*, 2*p* hybrid orbitals: *J. Chem. Phys.*, **19,** 900 (1951).

27. Wells, A. F., Structural Inorganic Chemistry: Oxford (1950).

28. Moore, Charlotte E., Atomic energy levels: *Circular* **467,** *National Bureau of Standards* (1949).

29. Gillespie, R. J., The use of 3*d* orbitals in certain valency states of carbon: *J. Chem. Soc.*, 1002 (1952).

30. Launer, P. J., Regularities in the infra red absorption spectra of silicate minerals: *Am. Mineral.*, **37,** 764, 1952.

*Manuscript received Nov. 26, 1953*

# A NEW SYNTHETIC HYDRATE OF ALUMINUM ARSENATE*

Gerald Katz and Horst Kedesdy, *Signal Corps Engineering Laboratories, Fort Monmouth, New Jersey.*

## Abstract

In an attempt to grow large crystals of aluminum orthoarsenate ($AlAsO_4$) by the hydrothermal method, a dense polycrystalline product resulted. The aggregate was in the form of fibrous crystallites in parallel arrangement which readily parted into fine, clear needles. Thermal decomposition analyses, chemical analysis, and powder and single crystal $x$-ray diffraction studies indicate this material to be a new hydrate of aluminum arsenate. The oxide formulation as determined by chemical analysis is:

$$Al_2O_3 \cdot 3As_2O_5 \cdot 10H_2O.$$

An orthorhombic unit cell was established from rotation and Weissenberg studies as follows:

$$a = 12.30\text{Å} \qquad b = 4.64\text{Å} \qquad c = 8.61\text{Å}.$$

The systematically absent reflections indicate a body-centered unit cell; the possible space groups are:

$$D_{2h}^{25} - I_{mmm}, \qquad C_{2v}^{20} - I_{mm2}, \qquad D_2^{8} - I_{222}.$$

Two molecules per unit cell gives a calculated density $\rho = 3.27$. The pycnometric density is 3.21.

## Introduction

One part of the research program of the Signal Corps Engineering Laboratories has been directed toward the synthesis of substitutes for piezoelectric quartz. In this connection, the growth and properties of aluminum orthoarsenate ($AlAsO_4$) have been studied because of its marked isomorphism with the natural piezoelectric quartz.[1] This compound has been shown to be isostructural with $\alpha$-quartz with the three silicon atoms of the elementary cell of quartz statistically substituted in a 1:1 ratio by $Al^{+3}$ and $As^{+5}$ cations. The $c$-axis is doubled in order to distribute properly the $Al^{+3}$ and the $As^{+5}$ ions. In the course of an attempt to increase the size of aluminum orthoarsenate crystals grown by the hydrothermal method, changes were made in the normally used temperature gradient and ratio of $Al_2O_3$, $As_2O_5$, and $H_2O$ of the feed materials. Instead of obtaining a single crystal with the usual well developed morphology, a dense polycrystalline product resulted. This aggregate was in the form of fibrous crystallites, in parallel arrangement, which readily parted into exceedingly fine, clear needles of a fibrous nature.

Figure 1 shows the gross character of the polycrystalline product. The overall height of this cross-sectional view is approximately 1.5 cm. The

---

* Presented at June 1953 meeting of American Crystallographic Association, Ann Arbor, Michigan.

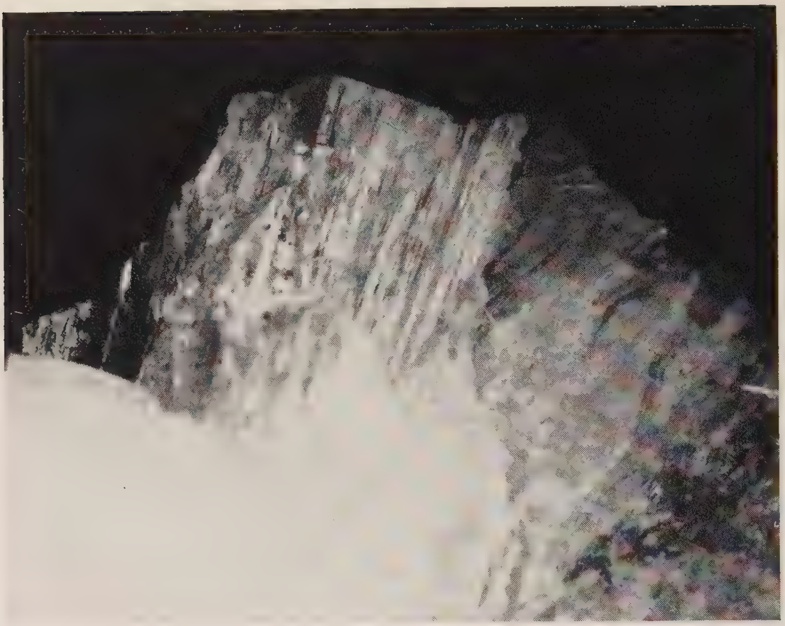

FIG. 1. Cross-sectional view of polycrystalline aggregate. Mag. 5×

electron micrograph (Fig. 2) shows the needle-like nature of the crystallites. The crystallites are generally triangular in cross-section and frequently have a characteristic cleavage at their tip, making an angle of approximately 110° with the needle axis.

## THERMAL ANALYSES

As an initial step, the $x$-ray diffraction powder pattern made from selected clear crystals was compared with a reference pattern of aluminum orthoarsenate. The comparison disclosed at once that the material under study was not of the $\alpha$-quartz structure (see Fig. 5). Since spectrochemical analysis showed aluminum and arsenic to be the only cations present in structurally significant amount, the possibility was considered that the material might be a hydrate of aluminum arsenate. In order to check this, a decomposition study was made of this compound using the differential thermal analysis method. The sample was heated from room temperature to 1,000° C. at a rate of 13° C./min. (Fig. 3). The *DTA* curve showed several endothermic peaks and a very small exothermic one. Such a *DTA* curve is not uncommon for hydrous compounds such as the hydrous aluminum phosphates.[2] The endothermic reactions at low temperature indicate the loss of water of crystallization; those at higher temperatures are correlated with the loss of water due to hydroxyl

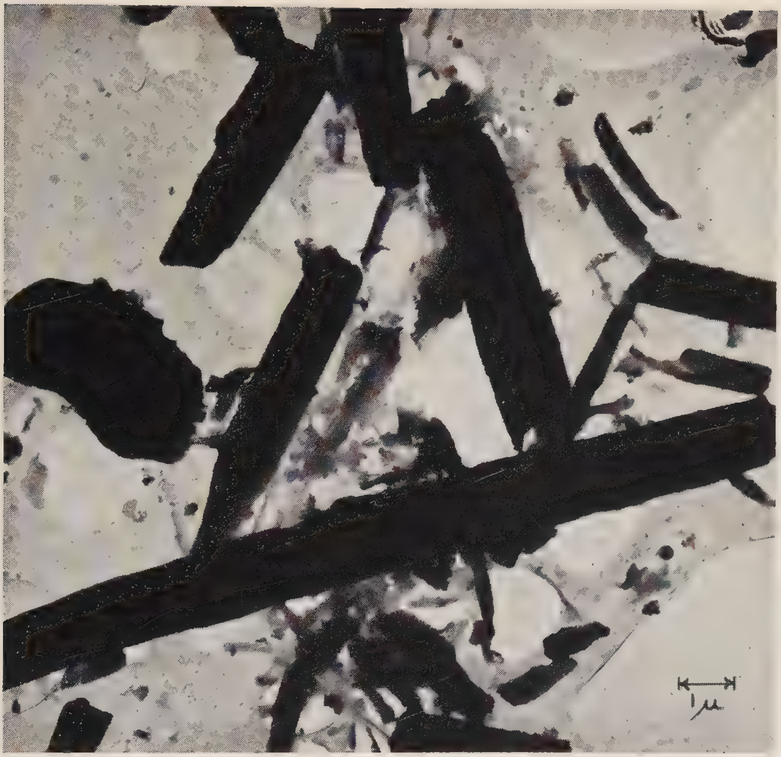

FIG. 2. Electron micrograph of crystallites showing their acicular nature and characteristic cleavage at the end of needles. Mag. 7,500×

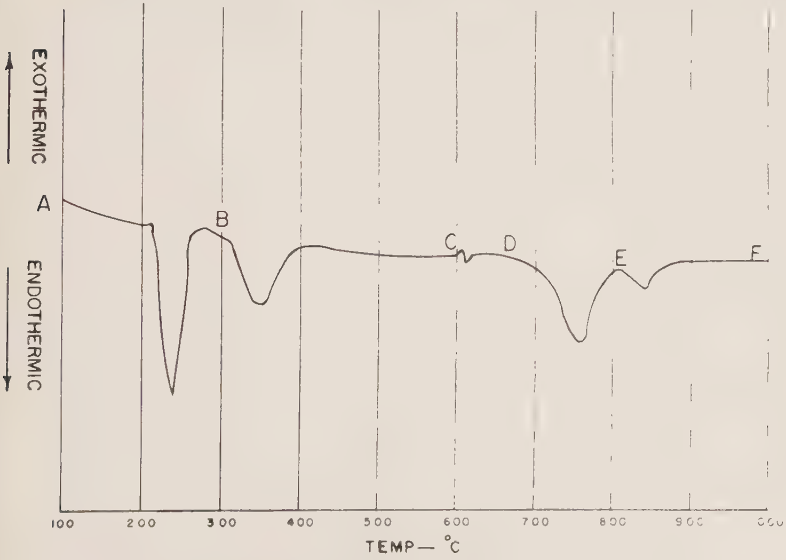

FIG. 3. Differential thermal analysis curve, heating rate—13° C./min.

groups in the structure. Recrystallization is indicated by exothermic reaction peaks.

As will be shown from the chemical analysis, this structure is believed to have a total of 10 waters per unit cell. A rough comparison was made of the area under each of the major endothermic peaks in order to explain the various steps of the conversion to the anhydrate. The first sharp peak at 240° C. appears to be the loss of all the water of crystallization. This water is bonded by van der Waals' forces and may be expected to be the first to leave the structure. This would mean that all the waters of crystallization would leave at 240° C. and the remaining 6 waters, due to hydroxyl groups, would be distributed among the other three endothermic peaks according to their relative areas; namely, 3 waters at 355° C., 2 waters at 765° C., and 1 water at 835° C.

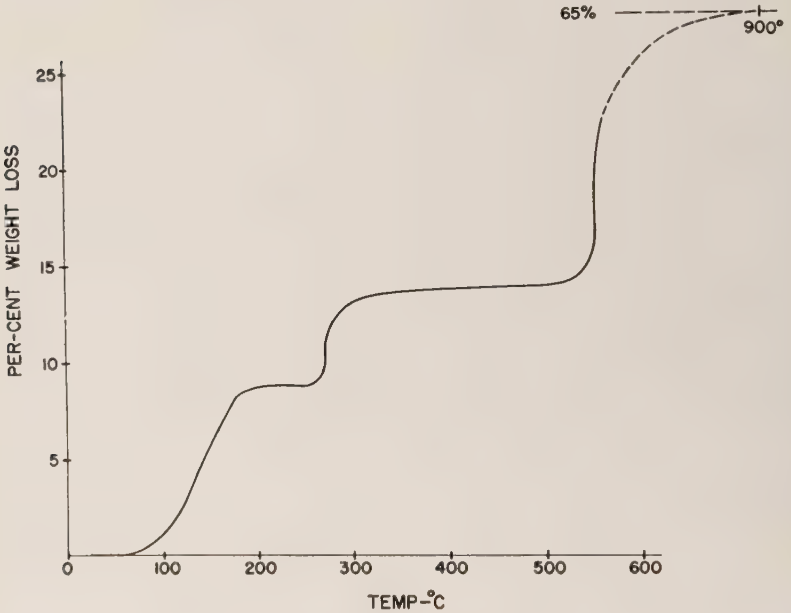

Fig. 4. Static loss-in-weight curve.

In order to check the *DTA* results concerning the water loss, a loss-in-weight study of a heated sample of this aluminum arsenic compound was made (Fig. 4). A powdered sample was heated at progressively higher temperatures; the specimen being held at each temperature for a three-hour period. The two steps in the curve below 300° C., which correspond to the first two endothermic peaks of the *DTA* curve, indicate

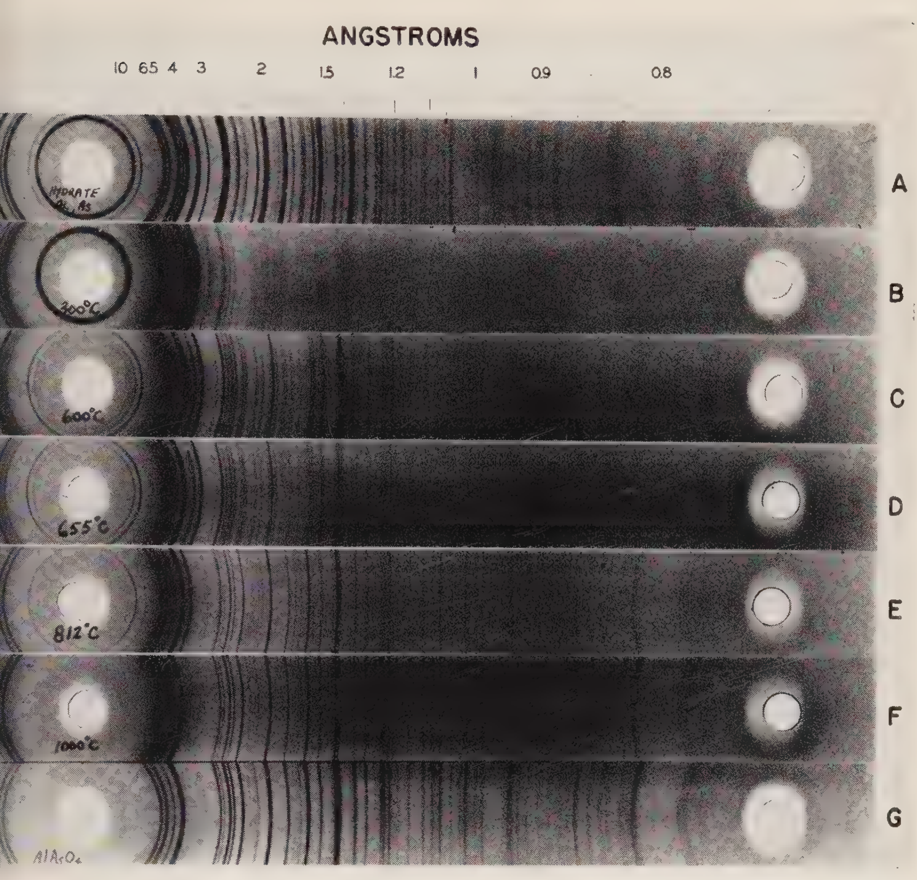

FIG. 5. *X*-ray powder patterns taken using CuK radiation $\lambda = 1.5418$ Å; camera radius 57.3 mm. All patterns taken at room temperature. *A*—Hydrate of aluminum arsenate—unheated. *B*—Hydrate after air-quenching from 300° C. *C*—Hydrate after air-quenching from 600° C. *D*—Hydrate after air-quenching from 655° C. *E*—Hydrate after air-quenching from 812° C. *F*—Hydrate after air-quenching from 1000° C. *G*—Aluminum orthoarsenate—pattern made from ground single crystal.

a loss-in-weight of about 14%. This compares very well with the calculated losses of $4H_2O$ between 100°–170° C. and $3H_2O$ in the vicinity of 270° C. which give a theoretical cumulative loss of 13%, 1% difference is attributed to adsorbed water. Above 600° C. there was a marked increase in the weight-loss accompanied by the evolution of $As_2O_3$ and $O_2$ from the sample. Since no differentiation could be made between the water loss and the loss due to $As_2O_3$ and $O_2$, the loss-in-weight measurements were discontinued.

## *X*-Ray Diffraction Powder Analysis

To further monitor the decomposition study, Debye-Scherrer powder patterns were made of samples after being heated in the *DTA* unit to temperatures bracketing each reaction peak as indicated by the lettered points in Fig. 3. Each of the samples was heated at the same rate of 13° C./min., as in the *DTA* run, to the desired temperature and then immediately air-quenched. The powder patterns in Fig. 5 were obtained from air quenched specimens corresponding to the lettered points in the *DTA* curve (Fig. 3). While the patterns of each of the quenched specimens have not been completely identified, the patterns which bracket the *DTA* peaks indicate phase transitions, some probably representing mixtures of two or more phases. It is interesting to note from the diffraction patterns that a marked change occurs in the heating interval between room temperature and 300° C.; after the evolution of the water of crystallization, the sample exhibits broader diffraction lines. Between 300° C.–600° C. there is another noticeable change reflected in the diffraction patterns. The characteristic 6 Å and 7Å lines of the original material re-appear with a reversal in their relative intensity. At the same time, the first appearance of the strongest characteristic lines of $AlAsO_4$ are detected, at 3.45 Å, 2.18 Å, 1.88 Å, 1.42 Å, 1.41 Å. It is surprising to note that before reaching the last decomposition step the final phase has already appeared. Its intensity shows that only a small amount has been converted. However, an attempt to complete the formation of $AlAsO_4$ by heating this compound for four days at 500° C. was unsuccessful. At 655° C. there is a more noticeable appearance of the final $AlAsO_4$ phase with a gradual diminution in the intensity of the intermediate phase represented by the 6 Å and 7 Å lines. A slight shift is noted in the 5 Å line changing to 5.2 Å. At 812° C. only the 6.5 Å, 5.5 Å, and 2.79 Å lines are detectable in addition to those of the $AlAsO_4$ pattern. At 1000° C. the material is completely converted to $AlAsO_4$; its pattern can be seen to be identical to that made from a pure $AlAsO_4$ single crystal (see Fig. 5, pattern G).

These results led us tentatively to designate this material as a hydrate of aluminum arsenate. A literature study of the arsenates and phosphates has indicated the existence of a number of mineral hydrates of the phosphates and arsenates. Table 1 summarizes various reported hydrates found in nature. Among these is a di-hydrate of aluminum orthoarsenate called mansfieldite, ($AlAsO_4 \cdot 2H_2O$) reported by V. T. Allen, J. J. Fahey, and J. M. Axelrod.[3] However, no crystallographic data were given other than that the powder pattern of the material, which was intimately intergrown with kaolinite and quartz, was similar to that of scorodite

($FeAsO_4\cdot 2H_2O$). A comparison of the powder pattern made from a sample of mansfieldite supplied by the authors with the powder pattern of this material under investigation established them to be different compounds; yet mansfieldite may well be $AlAsO_4\cdot 2H_2O$. In all the hydrates reported in Table 1, there is a 1:1 atomic ratio of the metal cations.

TABLE 1. ISOSTRUCTURAL α-QUARTZ COMPOUNDS AND MINERAL DI-HYDRATES OF PHOSPHATES AND ARSENATES

| Formula | Name | $a_0$ | $b_0$ | $c_0$ | $\beta$ | $\rho_x$ | $\rho_{s.g.}$ |
|---|---|---|---|---|---|---|---|
| $SiO_2$ | Quartz | 4.90 Å | — | 5.39 Å | — | 2.65 | — |
| $AlAsO_4$ | Aluminum ortho-arsenate[1] | 5.03 Å | — | 2x 5.61 Å | — | 3.34 | 3.30 |
| $AlPO_4$ | Aluminum ortho-phosphate | 4.93 Å | — | 2x 5.47 Å | — | 2.56 | — |
| $FePO_4\cdot 2H_2O$ | Phosphosiderite[4] | 5.30 Å | 9.79 Å | 8.67 Å | 90°36′ | 2.74 | 2.76 |
| $FePO_4\cdot 2H_2O$ | Phosphosiderite[5] | 5.28 Å | 9.75 Å | 8.71 Å | 90°36′ | — | 2.76 |
| $FePO_4\cdot 2H_2O$ | Strengite[5] | 10.06 Å | 9.85 Å | 8.65 Å | — | 2.89 | 2.86 |
| $FeAsO_4\cdot 2H_2O$ | Scorodite[6] | 8.88 Å | 10.26 Å | 9.98 Å | — | 3.35 | 3.41 |
| $FeAsO_4\cdot 2H_2O$ | Scorodite[7] | 10.42 Å | 8.96 Å | 10.15 Å | — | 3.24 | 3.27 |
| $AlPO_4\cdot 2H_2O$ | Variscite[4] | 9.85 Å | 9.55 Å | 8.50 Å | — | 2.61 | 2.5 |
| $AlPO_4\cdot 2H_2O$ | Metavariscite[4] | 5.15 Å | 9.45 Å | 8.45 Å | ~90° | 2.53 | 2.54 |
| $AlAsO_4\cdot 2H_2O$ | Mansfieldite[3] | — | — | — | — | — | 3.03 |

## CHEMICAL ANALYSIS

A chemical analysis was made in order to compare the composition of the hydrate under investigation with those shown in the table. The following result was obtained:

| | *Analysis Wt. %* | *Postulated Formula* | *Calculated Wt. %* |
|---|---|---|---|
| $Al_2O_3$ | 11.7 | $1\cdot Al_2O_3$ | 10.5 |
| $As_2O_5$ | 69.8 | $3\cdot As_2O_5$ | 71.0 |
| $H_2O$ | 18.0 | $10\cdot H_2O$ | 18.5 |
| | 99.5% | | 100.0% |

This indicates a 1:3 ratio of Al: As. The total loss-in-weight of the sample, including the loss of water and of other volatile decomposition products, when ignited at 900° C., was found to be 64.6%. From this it can be assumed that a decomposition has taken place with the liberation of $As_2O_3$ and $O_2$ as well as water. Taking 18% from the loss as the amount of liberated water the remainder of the loss would correspond to two moles of $As_2O_5$.

From these results the following formula for this hydrate of aluminum arsenate was proposed:

$$Al(H_2AsO_4)_3 \cdot 2H_2O.$$

Using this formula, it can be assumed that the following decomposition takes place:

$$2[Al(H_2AsO_4)_3 \cdot 2H_2O] \rightarrow 2AlAsO_4 + 2As_2O_3 \uparrow + 2O_2 \uparrow + 10H_2O \uparrow$$

## SINGLE CRYSTAL ANALYSIS

As described earlier, no difficulty was encountered in obtaining a fine, clear needle of the material suitable for single-crystal *x*-ray studies.

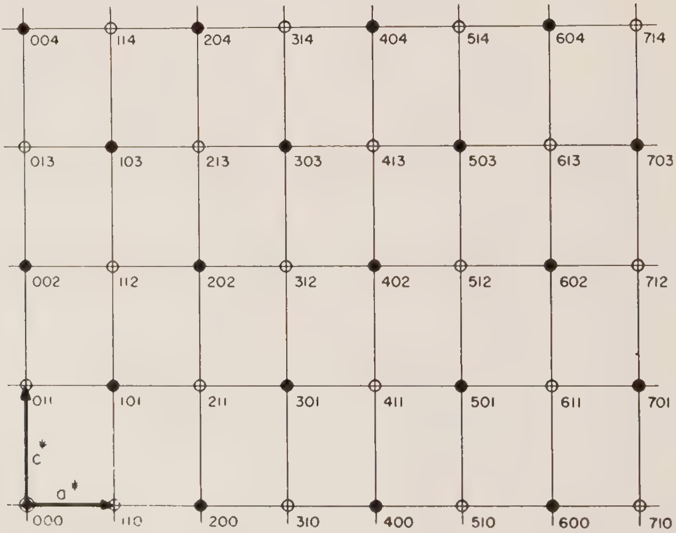

FIG. 6. Zero and 1st level of the reciprocal lattice from *b*-axis rotation. ●—zero level. ○—1st level.

Uniformly parallel optical extinction between crossed Nicols along the needle or fiber axis indicated this direction to be a crystallographic axis. Rotation photographs were taken of this crystal; the crystal being rotated about the fiber axis. The identity period, as determined from the rotation photograph, is 4.64 Å. In addition, Weissenberg photographs were taken for the zero, first, and second layer lines. Figure 6 represents the reciprocal lattice drawn to scale as found from the evaluation of the Weissenberg photographs. The dots represent the zero level, the circles the first layer line. The two reciprocal axes chosen lie 90° apart giving an

TABLE 2. *X*-RAY POWDER DATA—HYDRATE OF ALUMINUM ARSENATE—
$Al_2O_3 \cdot 3\,As_2O_5 \cdot 10\,H_2O$
Orthorhombic: $a=12.30$ Å, $b=4.64$ Å, $c=8.61$ Å; $Z=2$
Possible Space Groups: $D_{2h}^{25}$—$I_{mmm}$, $C_{2v}^{20}$—$I_{mm2}$, $D_2^8$–$I_{222}$
Radiation: Cu-Ni filter $\lambda=1.5418$ Å

| *I* | *d*(meas.) | *hkl* | *d*(*calc*)* |
|---|---|---|---|
| VS | 7.09 | 101 | 7.04 |
| M− | 6.10 | 200 | 6.15 |
| VS | 4.33 | 110 | 4.34 |
| | | 002 | 4.31 |
| M | 4.08 | 011 | 4.08 |
| VS | 3.69 | 301 | 3.70 |
| M | 3.54 | 202 | 3.53 |
| VS | 3.39 | 211 | 3.40 |
| VS | 3.06 | 400 | 3.08 |
| | | 310 | 3.07 |
| | | 112 | 3.06 |
| M | 2.81 | 103 | 2.80 |
| S | 2.51 | 312 | 2.50 |
| | | 402 | 2.49 |
| M+ | 2.44 | 411 | 2.46 |
| | | 013 | 2.44 |
| VW | 2.31 | 501 | 2.37 |
| | | 303 | 2.35 |
| | | 020 | 2.32 |
| M | 2.27 | 213 | 2.27 |
| VW | 2.20 | 121 | 2.20 |
| M− | 2.17 | 510 | $2.17_3$ |
| | | 220 | $2.17_1$ |
| | | 004 | 2.15 |
| M | 2.04 | 600 | 2.05 |
| | | 022 | 2.04 |
| | | 204 | 2.03 |
| M, B | 1.963 | 321 | 1.966 |
| M+ | 1.944 | 512 | 1.940 |
| | | 222 | 1.938 |
| M− | 1.925 | 114 | 1.929 |
| | | 413 | 1.918 |
| W | 1.860 | 503 | 1.868 |
| W | 1.845 | 420 | 1.852 |
| | | 602 | 1.851 |
| W, B | 1.833 | 611 | 1.832 |
| M | 1.785 | 123 | 1.785 |
| S | 1.766 | 404 | $1.763_4$ |
| | | 314 | $1.762_9$ |
| M | 1.708 | 105 | 1.705 |
| | | 422 | 1.701 |
| VW, B | 1.652 | 521 | 1.656 |
| | | 323 | 1.651 |
| M− | 1.640 | 710 | 1.643 |
| M− | 1.622 | 015 | 1.614 |
| M− | 1.593 | 305 | 1.588 |
| M | 1.570 | 024 | 1.578 |
| | | 613 | 1.570 |

* Calculated *d* spacings taken from indices of zero, 1st, and 2nd level Weissenberg photographs, *b*-axis rotation CuK radiation.

TABLE 2—*continued*

| *I* | *d*(meas.) | *hkl* | *d*(calc.)* |
|---|---|---|---|
| M | 1.560 | 424 | 1.567 |
| | | 215 | 1.561 |
| M+ | 1.534 | 800 | 1.537 |
| | | 620 | 1.536 |
| | | 712 | 1.535 |
| | | 514 | 1.529 |
| | | 224 | 1.528 |
| M | 1.519 | 604 | 1.515 |
| M | 1.493 | 703 | 1.499 |
| VW, B | 1.470 | 523 | 1.455 |
| M | 1.446 | 802 | 1.448 |
| | | 622 | 1.447 |
| W | 1.437 | 811 | 1.437 |
| | | 006 | 1.435 |
| | | 413 | 1.429 |
| M, B | 1.410 | 505 | 1.411 |
| M | 1.370 | 125 | 1.374 |
| | | 901 | 1.367 |
| M | 1.360 | 116 | 1.363 |
| W, B | 1.309 | 910 | 1.311 |
| | | 325 | 1.310 |
| | | 714 | 1.306 |
| | | 813 | 1.301 |
| | | 406 | $1.300_3$ |
| | | 316 | $1.300_1$ |
| VW | 1.275 | 820 | 1.282 |
| M, B | 1.268 | 615 | 1.268 |
| M, B | 1.248 | 912 | 1.254 |
| | | 804 | 1.251 |
| | | 624 | 1.250 |
| M, B | 1.229 | 903 | 1.234 |
| | | 1000 | 1.230 |
| | | 705 | 1.229 |
| | | 822 | 1.228 |
| | | 107 | 1.224 |
| M, B | 1.203 | 525 | 1.205 |
| | | 516 | 1.198 |
| | | 226 | 1.197 |
| VVW | 1.187 | 017 | 1.189 |
| | | 1002 | 1.183 |
| M, B | 1.176 | 1011 | 1.178 |
| | | 307 | 1.177 |
| | | 606 | 1.176 |
| M, B | 1.153 | 035† | 1.151 |
| W+ | 1.139 | 426 | 1.134 |
| W | 1.122 | 914 | 1.120 |
| W, B | 1.115 | 815 | 1.113 |
| | | 417 | 1.109 |
| | | 1101 | 1.109 |
| W, B | 1.098 | 824 | 1.101 |
| | | 507 | 1.100 |
| | | 1013 | 1.098 |
| W, B | 1.084 | 1110 | 1.087 |
| | | 1020 | $1.086_7$ |
| | | 725 | 1.084 |
| | | 127 | 1.083 |
| | | 716 | 1.081 |
| W, B | 1.069 | 905 | 1.071 |
| | | 1004 | 1.068 |
| | | 208 | 1.060 |
| M, B | 1.053 | 1112 | 1.054 |
| | | 327 | 1.050 |
| | | 806 | 1.049 |
| | | 626 | $1.048_6$ |

† Reflection outside sphere of reflection for *b* axis rotation. B broad diffraction line.

orthorhombic real unit cell. The unit cell dimensions were determined to be:

$$a = 12.30\text{A}$$

$$b = 4.64\text{Å}$$

$$c = 8.61\text{Å}$$

Table 2 is an evaluation of the powder pattern using the lattice parameters obtained from the rotation and Weissenberg data. The indices for the calculated $d$ spacings were obtained from the zero, 1st, and 2nd level Weissenberg photographs. The $d$ spacings for indices outside the sphere of reflection for $b$-axis rotation using Cu/Ni filtered radiation were not calculated.

Using the previously postulated chemical formula of $Al(H_2AsO_4)_3 \cdot 2H_2O$ together with the unit cell dimensions, the density can be calculated

$$\rho_x = \frac{M \cdot Z \cdot 1.65}{V}$$

M = Mol. weight

Z = Moles per unit cell

V = Unit cell volume in Å$^3$

assuming Z = 2, we get:

$$\rho_x = \frac{485.70 \times 2 \times 1.65}{12.30 \times 4.64 \times 8.61} = 3.27.$$

Due to the characteristic fibrous nature of the crystals, it was necessary to powder the material in order to obtain accurate density measurements. The pycnometric density determined using toluene was 3.21.

Figure 7 shows the indexing of the reciprocal lattice of the zero and 1st level directly on the Weissenberg photographs. The 2nd level was a repetition of the zero level.

The following reflections were found to be systematically absent:

$hkl$ with $h + k + l = 2n + 1$
$00l$ with $l = 2n + 1$
$h00$ with $h = 2n + 1$
$h0l$ with $h + l = 2n + 1$
$0kl$ with $k + l = 2n + 1$

This indicates a body-centered unit cell. Considering the assumed chemical formula of the compound and the extinction rules found, the possible space groups are: $D_{2h}{}^{25} - I_{mmm}$, $C_{2v}{}^{20} - I_{mm2}$, $D_2{}^8 - I_{222}$.[8]

---

[8] R. Pepinsky, private communication April 20, 1954, Penn. State University, hydrate of aluminum arsenate found to be clearly piezoelectric. This data, which is in agreement with the detection of optical activity and triboluminescence, eliminates the centrosymmetric space group $D_{2h}{}^{25}$—$I_{mmm}$.

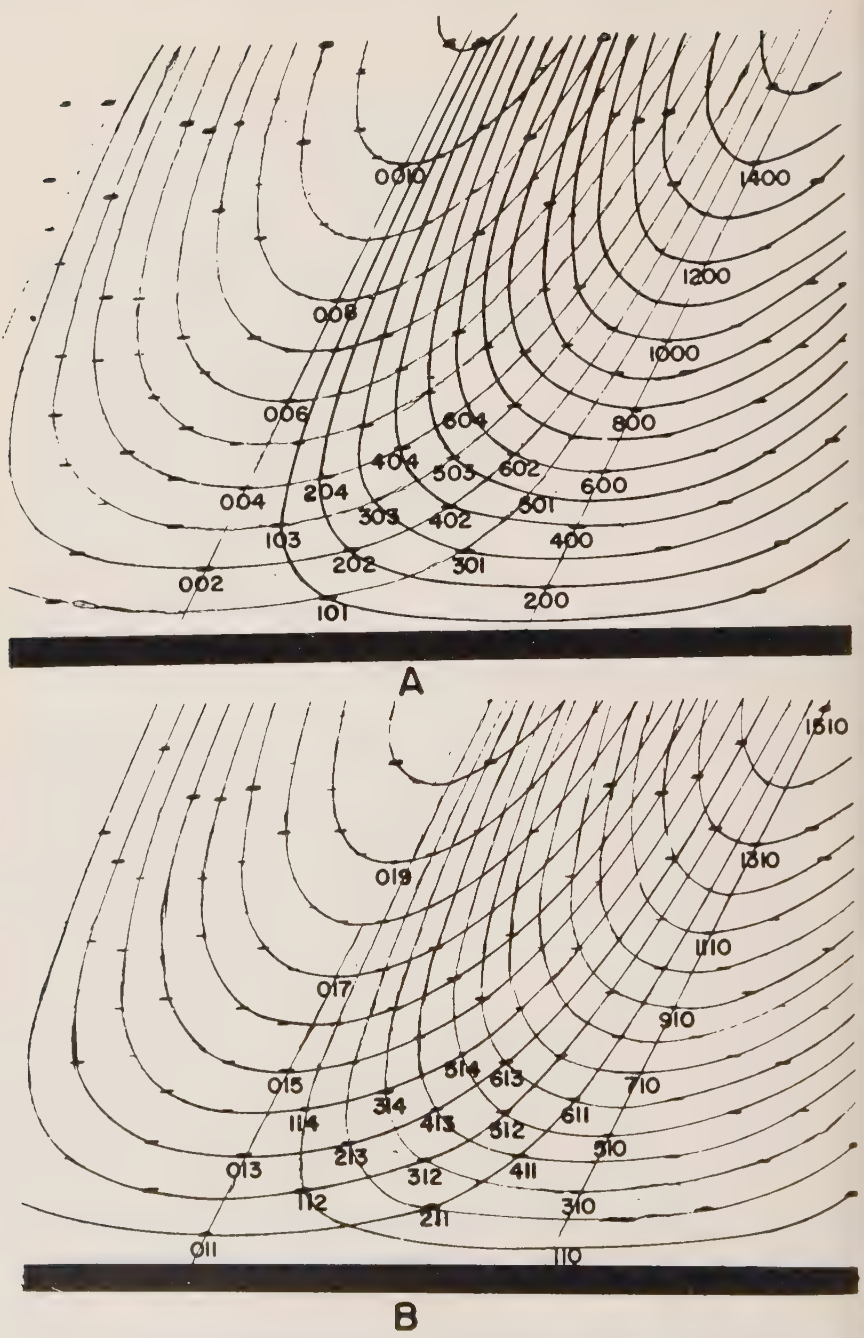

FIG. 7. Indexed Weissenberg photographs. *A*—zero level. *B*—1st level.

This paper has described the identification and characterization and preliminary structure postulation of a new synthetic hydrate of aluminum arsenate. A complete structure determination has been started.

## ACKNOWLEDGMENTS

The authors wish to express their indebtedness to the following: Mr. J. M. Stanley for growing the sample; Mr. S. delVecchio for performing the chemical analysis; Mr. L. Toman for obtaining the *DTA* data; Mr. R. Clarke for the density measurement.

## REFERENCES

1. MACHATSCHKI, F., The crystal structure of aluminum arsenate $AlAsO_4$: *Zeit. Krist.*, **90,** 314–321 (1935).
2. MANLY, R. L., JR., The differential thermal analysis of certain phosphates: *Am. Mineral.*, **35,** 108–115 (1950).
3. ALLEN, V. T., FAHEY, J. J. , AND AXELROD, J. M., Mansfieldite, a new arsenate, the aluminum analogue of scorodite, and the mansfieldite-scorodite series: *Am. Mineral.*, **33,** 122–134 (1948).
4. MCCONNELL, D., Clinobarrandite and isodimorphous series, variscite-metavariscite: *Am. Mineral.*, **25,** 719–725 (1940).
5. STRUNZ, H., AND SZTRÓKAY, K. V., Isomorphism between metavariscite, variscite, phosphosiderite, and strengite: *Zentral. Mineralogie, Geol., Palaont.*, **A,** 272–278 (1939).
6. KOKKOROS, P., *Extr. Prakt. Acad. Athenes*, **13,** 337 (1938).
7. KIRIYAMA, R., AND SAKURAI, K., The crystal structure of scorodite: *X-Sen* (Rays), **5,** 85–88 (1949).

*Manuscript received Aug. 31, 1953*

# NOTES AND NEWS

## STUDIES OF URANIUM MINERALS (XVI): AN ALTERATION PRODUCT OF IANTHINITE[1]

Judith W. Frondel and Frank Cuttitta, *U. S. Geological Survey, Washington 25, D. C.*

A specimen from Katanga labeled ianthinite and consisting of purple-colored minute needles and laths was sent by J. F. Vaes to the Harvard University mineral collection several years ago. The mineral resembles ianthinite in the hand specimen, but chemical analysis gave only a trace of $UO_2$ and a formula of $UO_3 \cdot 2H_2O$ (Table 1), although ianthinite reportedly contains only quadrivalent uranium and has a formula of $2UO_2 \cdot 7H_2O$ (Schoep, 1930). The mineral probably is an alteration product of ianthinite in which the $U^4$ is almost completely oxidized to $U^6$; it may be epiianthinite, inadequately described by Schoep and Stradiot (1947). The purple color of the mineral is due to the trace of $UO_2$. Although epiianthinite is yellow, the optical properties of the alteration product are more like those of epiianthinite than those of ianthinite (Table 2).

Table 1. Chemical Analyses of Ianthinite and of an Alteration Product of Ianthinite

| | 1 | 2 | 3 | 4 |
|---|---|---|---|---|
| $UO_2$ | <0.1 | — | — | — |
| $UO_3$ | 87.83 | 88.64 | 88.60 | — |
| $U_3O_8$ | — | — | — | 82.90 |
| $H_2O-$ | 1.06 | | | 15.85 (ignition loss) |
| $H_2O+$ | 11.26 | 11.36 | 11.40 | — |
| $Fe_2O_3$ | — | — | — | 1.25 |
| Total | 100.15 | 100.00 | 100.00 | 100.00 |

1. Alteration production of ianthinite; analyst, Frank Cuttitta.
2. Analysis 1 recalculated to 100 after deducting $H_2O-$.
3. Theoretical composition $UO_3 \cdot 2\ H_2O$.
4. Ianthinite (Schoep, 1930).

The *x*-ray powder pattern (Table 3) of the alteration product is distinctive and cannot be confused with that of schoepite, which has practically the same chemical composition. Authentic *x*-ray powder data are lacking for ianthinite and epiianthinite. *X*-ray Weissenberg study, using copper radiation, gave sharp lattice patterns with $a_0 = 7.17$ Å, $b_0 = 11.46$ Å,

---

[1] Contribution from Harvard University, Department of Mineralogy and Petrography, No. 349. Publication authorized by the Director, U. S. Geological Survey.

TABLE 2. OPTICS OF IANTHINITE, EPIIANTHINITE, AND ALTERATION PRODUCT OF IANTHINITE

| Ianthinite[1] | Epiianthinite[2] | Alteration product of ianthinite |
|---|---|---|
| $\alpha=1.674$ | 1.70 | 1.695 |
| $\beta=1.90$ | 1.79 | 1.730 |
| $\gamma=1.92$ | 1.793 | 1.790 |
| 2V (−) small | (−) Small) | (−)∼50° |
| $a$=colorless | $X=c$, pale yellow | $X=c$, pale pink |
| $c$=violet | $Y=b$, yellow | $Y=b$, brownish orange |
| $b$=dark violet | $Z=a$, deep yellow | $Z=a$, dark reddish purple |
| Orthorhombic | Orthorhombic | Orthorhombic |

[1] Schoep (1930).

[2] Schoep and Stradiot (1947).

TABLE 3. *d*-SPACINGS FOR ALTERATION PRODUCT OF IANTHINITE

(Copper radiation, nickel filter, in $\lambda=1.5418$Å)

| *d* | *I* | *d* | *I* |
|---|---|---|---|
| 7.63 | 10 | 1.673 | 4 |
| 5.37 | 2 | 1.632 | 2 |
| 4.13 | 4 | 1.615 | 2 |
| 3.78 | 9 | 1.595 | 2 |
| 3.60 | 3 | 1.574 | 5 |
| 3.36 | 7 | 1.541 | 1 |
| 3.20 | 8 | 1.510 | 1 |
| 2.96 | 6 | 1.470 | 1 |
| 2.67 | 5 | 1.436 | 3 |
| 2.60 | 1 | 1.405 | 1 |
| 2.51 | 5 | 1.380 | 1 |
| 2.38 | 4 | 1.343 | 2 |
| 2.29 | 2 | 1.313 | 4 |
| 2.24 | 2 | 1.256 | 2 |
| 2.14 | 5 | 1.226 | 3 |
| 2.06 | 2 | 1.168 | 1 |
| 2.03 | 3 | 1.158 | 1 |
| 1.978 | 2 | 1.139 | 3 |
| 1.950 | 2 | 1.127 | 3 |
| 1.915 | 2 | 1.115 | 2 |
| 1.889 | 4 | 1.102 | 1 |
| 1.833 | 2 | 1.086 | 3 |
| 1.783 | 3 | 1.067 | 2 |
| 1.756 | 1 | 1.027 | 4 |
| 1.734 | 2 | 1.009 | 1 |

and $c_0=15.20$ Å; $a_0:b_0:c_0=0.6257:1:1.311$. The measured specific gravity is slightly less than 3.5 (minute needles of the mineral rose very slowly to the surface of Clerici solution of sp. gr. $=3.503$), and the calculated specific gravity is 3.467, assuming 8 formula units of $UO_3 \cdot 2H_2O$ per unit cell.

This study is part of a program undertaken by the Geological Survey on behalf of the Division of Raw Materials of the Atomic Energy commission.

### References

Schoep, A. (1930), Les minéraux du gîte uranifère du Katanga: *Ann. Musée du Congo Belge*, Serie 1, **Tome 1,** 9–13.

Schoep, A., and Stradiot, S. (1947), Paraschoepite and epiianthinite, two new minerals from Shinkolobwe (Belgian Congo): *Am. Mineral.*, **32,** 344–350.

## ANALYSES AND INDICES OF REFRACTION OF TOURMALINE FROM FAULT GOUGE NEAR BARSTOW, SAN BERNARDINO COUNTY, CALIFORNIA[1]

Henry Kramer and Robert D. Allen, *U. S. Geological Survey, Claremont, California.*

Blue cryptocrystalline tourmaline is the principal mineral in massive, pale-blue fault gouge[2] 3.5 miles north of Barstow, California. T. W. Dibblee, Jr., of the U. S. Geological Survey, collected samples from the north side of a low ridge in the SE$\frac{1}{4}$ sec. 18, T. 10 N., R. 1 W., San Bernardino base and meridian (lat. 34° 57′ N., long. 117° 00′ W.). According to Dibblee (personal communication) the blue tourmaline rock, a lenticular mass roughly 30 feet long and 10 feet wide, occurs in a local shear zone in fine-textured, poorly bedded, greenish-brown lime-silicate rock within a thick series of dark-gray biotite-hornblende-feldspar schists.[3]

An *x*-ray diffraction pattern of purified material is in close agreement with standard tourmaline patterns cited by the American Society for Testing Materials. Spacings of $d/n(A)$ calculated from the hexagonal unit-cell dimensions $a_0=15.96$ Å, $c_0=7.16$ Å (Buerger and Parrish, 1937) are in reasonable accord with experimental values found on Barstow tourmaline.

Microscopically, this tourmaline is gray-green and cryptocrystalline with chalcedony-like fibrous to radiating structure. Associated minerals are quartz and calcite, the former included as minute doubly terminated prismatic crystals in polycrystalline tourmaline aggregates. Indices of refraction, determined with sodium light, are as follows: $\epsilon = 1.638 \pm 0.002$; $\omega = 1.645 \pm 0.002$. To the writers' knowledge, the birefringence ($0.007 \pm 0.004$) is less than any previously reported for tourmaline. The mineral is faintly pleochroic and has wavy extinction.

---

[1] Publication authorized by the Director, U. S. Geological Survey.

[2] Pale blue 5B 6/2, Rock-Color Chart, *Geol. Soc. Am.* (1951).

[3] Subsequently, two other occurrences of blue tourmaline rock similar to that described above were found on the same ridge, one about 300 feet to the southeast and the other about 1200 feet to the west. In both these localities the tourmaline rock occurs at the contact between the metamorphic rocks and a small andesite body capping the hill.

The chemical analysis of Barstow tourmaline is compared with two analyses quoted by Hamburger and Buerger (1948) of colorless and black tourmalines from De Kalb, New York, and Andreasberg, Harz, Germany, respectively.

|  | *Blue*<br>Barstow, Calif. | *Colorless*<br>De Kalb, N. Y. | *Black*<br>Andreasberg, Harz |
|---|---|---|---|
|  | (per cent) | (per cent) | (per cent) |
| $SiO_2$ | 33.41 | 36.72 | 34.01 |
| $TiO_2$ | 1.08 | 0.05 | 0.61 |
| $B_2O_3$ | 9.68 | 10.81 | 10.89 |
| $Al_2O_3$ | 32.46 | 29.86 | 28.80 |
| $Fe_2O_3$ | 3.25 | — | 4.37 |
| FeO | 6.39 | 0.22 | 13.57 |
| MnO | trace | — | 0.12 |
| CaO | 0.23 | 3.49 | 0.58 |
| MgO | 6.40 | 14.92 | 0.42 |
| $Na_2O$ | 2.71 | 1.26 | 2.03 |
| $K_2O$ | 0.69 | 0.05 | 0.20 |
| $Li_2O$ | nil | — | 0.10 |
| PbO | 0.09 | — | — |
| SnO | 0.10 | — | — |
| $V_2O_3$ | 0.06 | — | — |
| $H_2O(+)$ | 3.33 | 2.98 | 2.92 |
| F | nil | 0.93 | 0.71 |
| Total | 99.88 | none given | none given |
| Analysts: | Henry Kramer | S. L. Penfield and H. W. Foote | M. Dittrich and F. Noll |

Barstow tourmaline is intermediate between the others with respect to $Fe_2O_3$, FeO, MgO, and MnO. In contrast, Barstow tourmaline is higher than the others in $TiO_2$, $Al_2O_3$, $Na_2O$, $K_2O$, and $H_2O$; it is lower in $SiO_2$, $B_2O_3$, and CaO. Other characteristics are (1) the absence of $Li_2O$ and F, and (2) the presence of PbO, SnO, and $V_2O_3$.

Purification of tourmaline was accomplished by (1) acid leaching to remove calcite, and (2) bromoform separation to reduce the amount of quartz. It was not possible, however, to rid the tourmaline of included finely crystalline quartz. By means of the proportion $B/Si = \frac{1}{2}$ (Hamburger and Buerger, 1948; Donnay and Buerger, 1950), the amount of excess $SiO_2$ was calculated. All oxides were then recalculated to nullify the sample dilution by excess $SiO_2$.

The spectrographic analysis, in per cent, is tabulated below.

| | |
|---|---|
| Si | XX.O |
| Al | XX.O |
| Fe | X.O |
| Mg | X.O |
| Na | X.O |
| B | X.O |
| K | O.X |
| Ca | O.X |
| Ti | O.X |
| V | O.X |
| Pb | O.OX |
| Sn | O.OX |
| Ga | O.OX |
| Cu | O.OOX |
| Sr | O.OOX |
| Cr | O.OOX |
| Mn | O.OOX |
| Ni | O.OOX |
| Co | O.OOX |

The formula for the blue tourmaline calculated from the above analysis is:

$$(\mathrm{Na, K, Ca, Pb})_{1.08}(\mathrm{Ti, Mg, Fe''}, \mathrm{Fe'''}, \mathrm{Sn, V})_{3.06}\mathrm{B}_{2.81}\mathrm{Al}_{6.47}\mathrm{Si}_{5.62}\mathrm{O}_{27.00}(\mathrm{O, OH})_{4.00}.$$

This formula is patterned after one proposed by Berman (1937):

$$(\mathrm{Na, Ca})(\mathrm{Mg, Fe''}, \mathrm{Fe'''})_3\mathrm{B}_3\mathrm{Al}_3(\mathrm{Al}_3\mathrm{Si}_6\mathrm{O}_{27})(\mathrm{O, OH})_4.$$

In our analysis the Al/Si ratio is 1.15. Thus, boron, aluminum, and silicon fail to yield integral subscripts in the Barstow tourmaline formula. It is possible that aluminum substitutes for silicon and boron in this structure.

X-ray diffraction data were supplied by Arthur Chodos, Department of Geology, California Institute of Technology. The tourmaline was independently identified by Fred A. Hildebrand of the U. S. Geological Survey. The spectrographic analysis was made by Hal W. Johnson, Pacific Spectrochemical Laboratory, Los Angeles, California.

## REFERENCES

BERMAN, H. (1937), Constitution and classification of the natural silicates: *Am. Mineral.*, **22,** 342–408.

Buerger, M. J., and Parrish, W. (1937), The unit cell and space group of tourmaline (An example of the inspective equi-inclination treatment of trigonal crystals): *Am. Mineral.*, **22**, 1139–1150.

Dibblee, T. W., Jr. (1953), Personal communication.

Donnay, G., and Buerger, M. J. (1950), The determination of the crystal structure of tourmaline: *Acta Cryst.*, **3**, 379–388.

Hamburger, G. E., and Buerger, M. J. (1948), The structure of tourmaline: *Am. Mineral.*, **33**, 532–540.

---

## DERIVED DIFFERENTIAL THERMAL CURVES*

A. F. Frederickson, *Washington University, St. Louis, Missouri.*

Under certain routine conditions where, for example, original grain size of particles, the presence of other mineral constituents, and certain chemical impurities are known, differential thermal techniques can be applied in a semi-quantitative manner. Greatest accuracy is obtained by measuring the area under portions of the curve representing certain kinds of reactions: loss of absorbed or other kinds of water, decomposition, inversion from one polymorphous form to another, and recrystallization. Ordinarily, the loss of water (and perhaps atomic oxygen) as well as decomposition reactions do not start at a sharply defined temperature, but are first represented by a gradual departure of the differential thermal curve from baseline. This gradual drift from baseline often grades imperceptibly into the portion of the curve representing the important part of the reaction which is used for quantitative measurement. If the operator cannot accurately select the point where the important part of the reaction started, it is impossible to accurately position a baseline from which to delimit the area under the curve. Small changes in the positioning of the baseline result in large changes in the measured area under the curve so, under these conditions, the technique degenerates to only a rough, semi-quantitative procedure.

Baseline drift can often be controlled, when carbonate minerals or rocks are being investigated, by the use of a $CO_2$-atmosphere in the furnace (Rowland and co-workers, 1951 and 1952). This technique, however, does not help in systems where carbonate minerals are not present: when clay and other silicate systems are being investigated.

The purpose of this note is to call attention to a technique long used by the metallurgist to help resolve this difficulty. The metallurgist employs heating or cooling curves to help construct equilibrium diagrams and, in particular, to locate inversion temperatures in steels and other systems. They also have applied the differential thermal method to their problems.

---

* Contribution number 172 of the Department of Geology, Washington University, St. Louis, Missouri.

The first derivative of a differential thermal curve often provides very useful information. Slight changes in the slope of a gradually drifting curve, or reversals in slope, are represented by sharp changes in the direction of a curve representing the first derivative of the differential thermal curve. To avoid using the word "differential" twice, this second curve might best be called a derived differential thermal curve. The use of derived differential thermal curves was proposed by Walter Rosenhain and is described in detail by Foote, Fairchild and Harrison (1921, pp. 200–203).

In Fig. 1, *B* represents the differential thermal curve for a typical kaolinite; curve *A* is the first differential or derived differential thermal curve for the same kaolinite specimen.

A derived differential thermal curve can be graphically constructed in approximately 10 minutes after a little practice. If a galvanometer

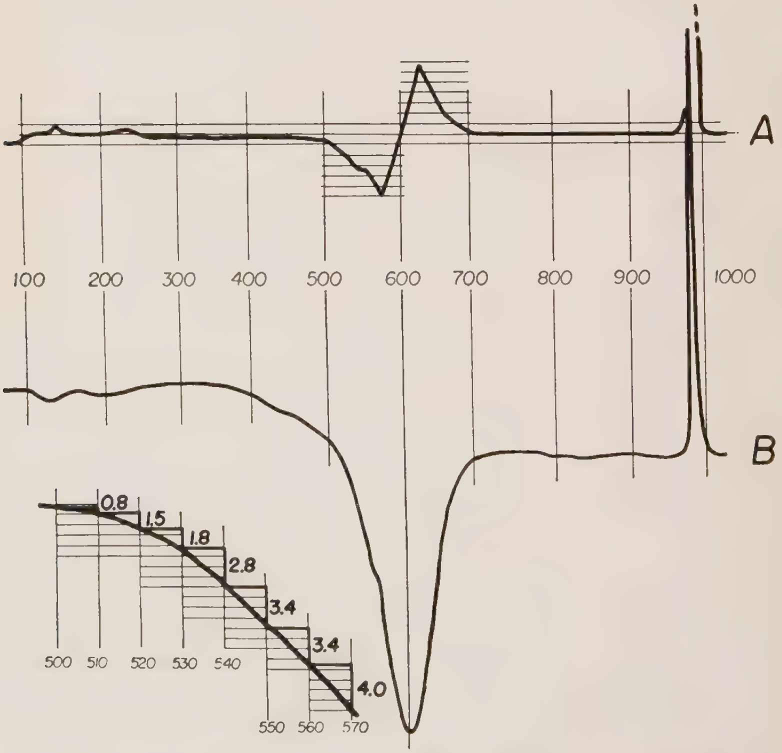

FIG. 1. Differential thermal curve (*B*) of a sample of kaolinite; (*A*) represents the first derivative or the derived differential thermal curve for the same sample.

record is obtained (instead of one traced by an electronic recorder on graph paper) it is most convenient to first transfer it to some convenient graph or ruled paper.

The method of obtaining the derived curve consists of observing successive values of change of temperature $(T-T')$ for equal increments of $T$. A convenient increment is 10° C. This is expressed as $\Delta(T-T')/\Delta T$ where $\Delta T$ is taken as 10° C. The derived differential is the graph obtained by plotting the temperature differences against $T: d(T-T')$ vs. $T$.

The inset in Fig. 1 represents an enlargement of a portion of curve $B$. The differences in temperature (represented by any convenient unit) between the kaolinite sample and the standard, on heating from 500 to 570° C., are 0.8, 1.5, 1.8, 2.8, etc., units for each 10° increase in temperature. These values are plotted against 500, 510, 520, 530° C., etc., respectively.

The slight "bump" on the large endothermic peak (curve $B$) plots as a straight horizontal line (between 550 and 560° C.) in the derived curve. The base line under the two peaks of the derived curve can be objectively drawn with precision. Apparently the important part of the reaction starts at 500° C. The area to be measured under this peak can be delimited by extending the straight-line portion of the derived curve (from 500–550° C.) back to the base line.

Two independent operators can select a base line and duplicate the measured areas under the curve within 3 per cent. Usually the differential curve obtained from two portions of the same sample check rather closely, consequently, when suitable samples are chosen to construct an area vs. quantity-of-mineral-present curve, the derived differential technique greatly improves the accuracy of the method.

### REFERENCES

FOOTE, P. S., FAIRCHILD, C. O., AND HARRISON, T. R. (1921), Pyrometric Practice: *U. S. Bureau of Standards, Technologic Paper No. 170.*

ROWLAND, R. A., AND LEWIS, D. R. (1951), Furnace atmosphere control in differential thermal analysis: *Am. Mineral.*, **36,** 80–91.

---

## THE ST. PETER SANDSTONE-GLENWOOD SHALE CONTACT

W. G. ERNST, *Carleton College, Northfield, Minnesota.*

### INTRODUCTION

Between Northfield and Cannon Falls, Minnesota, some 40 miles south of St. Paul, on State Highway 19, mesas rise to heights of 60 feet or more above the preglacial Cannon River Valley flood plain (1). These prominences, when traced by aerial photographs, are seen to pass southward into undissected tableland. Figure 1 reveals that simple headward stream erosion has been responsible for the topography. The hills are capped by the Spechts Ferry and McGregor limestone members of the Middle Ordovician Platteville formation (2). Below these resistant layers are the readily weathered Glenwood shale member of the Platteville, and the friable Middle Ordovician St. Peter sandstone (3). Figure 2 exhibits the stratigraphic relationship, while also showing a secondary mesa-forming horizon between the Glenwood above, and the St. Peter below. This horizon owes its superior resistance locally to abundant limonite cement. Solution etching indicates the presence of carbonates. This intermediate bed will be called the "transition zone," and will be found to be a reworked phase of the underlying sandstone.

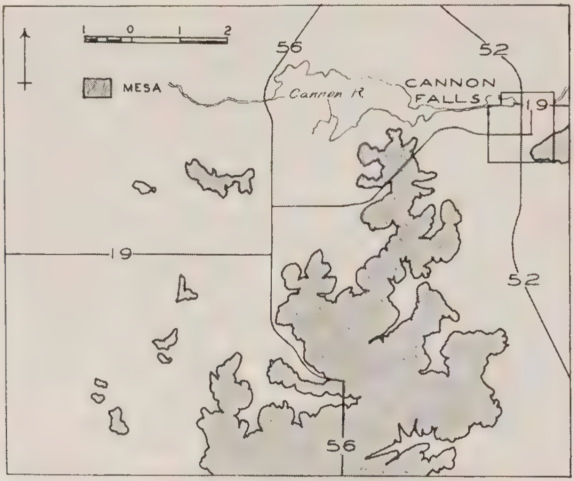

FIG. 1. Location of mesas in the Cannon River Valley.

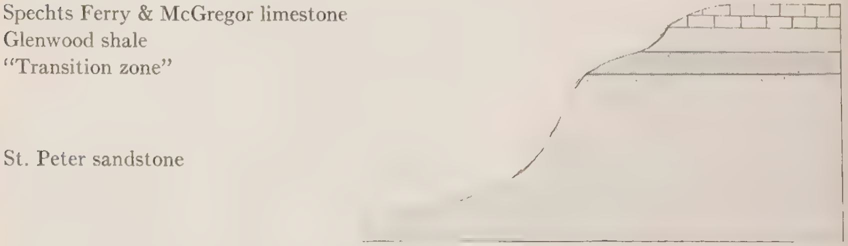

FIG. 2. Stratigraphic Section.

## THE PROBLEM

Thiel states that the upper five to ten feet of the St. Peter sandstone contain heavy mineral grains, especially garnet, foreign to the formation as a whole, but quite similar to the assemblage in the overlying Glenwood beds; considering this he deduces that this zone represents reworked sandstone of Mohawkian age, and should be classified as an early stage of Glenwood sedimentation (4, 5). Following Thiel's suggestion,the writer analyzed the heavy mineral content of a vertical section of 35 feet, from the base of the McGregor limestone member down into typical St. Peter sandstone. The channel samples were taken at road cuts one-tenth of a mile east of U. S. Highway 52 at the south city limits of Cannon Falls. Characteristic St. Peter material was then compared with Upper St. Croixian series Jordan sandstone just below its contact with the overlying Oneota dolomite.

## METHOD OF ANALYSIS

Samples approximately two pounds in weight were taken at every lithologic and textural change in character of the beds. The shales were then dried and pulverized by abrasion between a steatite table surface and a block of soft wood. The sandstone samples were friable enough to be broken down into individual grains between the fingers. The samples were then screened by hand, using U. S. standard sieves. Grains retained were divided into three diameter sizes: (1) between .420–.250 millimeters; (2) between .250–.125 millimeters; and (3) less than .125 millimeters. Heavy mineral separation tests were then run using acetylene tetrabromide (sp. gr. 2.95 at 20 degrees Centigrade). Samples were placed in a funnel containing the heavy medium, and after a sufficient time, the high density grains were drained off by means of a petcock. The acetylene tetrabromide was then neutralized by the addition of benzene. Finally, the minerals were mounted in canada balsam. In all, fifty-seven slides were analyzed. Very few grains were present in the .420–.250 millimeter size, so percentage figures there may be distorted. No attempt was made to record the percentages of the original samples which were retained as heavy grains.

## DESCRIPTION OF THE SAMPLES

All samples, *A1–A6*, are from Cannon Falls. Horizons *A1* through *A3* are Glenwood shale and horizons *A4* through *A6* are St. Peter sandstone.

*Horizon A1.* The first sample is a greenish brown shale taken two feet below the contact with McGregor limestone. It is a fairly blocky layer, exhibiting little pyrite, the coloring being due to a great deal of limonite, which tends to coat the quartz grains to such an extent that they sink with the heavy minerals. Much of this quartz shows secondary bipyramidal enlargements. Epidote and minor amounts of chlorite may also be partially responsible for the color. Garnet and zircon are noted. Most of the sand grains are between .250–.125 millimeters diameter with very few grains in the smallest size.

*Horizon A2.* Five to six feet below the base of the McGregor is found a somewhat arenaceous shale, of alternating blue, brown, and green layers. Here again there is much limonite. Epidote is absent and garnet and zircon are relatively abundant. Staurolite is present in great quantities in both *A1* and *A2* horizons and is apparently a local flood mineral, since its presence has not been reported elsewhere. Again the .250–.125 millimeter size is most productive of minerals in number and variety.

*Horizon A3.* One foot below horizon *A2* is an argillaceous, gray-green sandstone, of which 60 per cent of the grains have greater diameter than .420 millimeters. Quartz shows little secondary growth and there is less hydrated iron "ore." There is a general paucity of heavy minerals, kaolin, etc., apparently making up most of the fines. Garnet suggests Middle Ordovician sedimentation.

*Horizon A4.* Seven to ten feet down from the contact between limestone and shale, alternating layers of brown and white sandstone are observed. In some areas, this sandstone forms "shoulders" on the otherwise uniformly descending flanks of mesas. The re-

Table 1. Grains Counted

| Horizon | Size of grains in mm. | Almandite | Zircon | Schorlite | Staurolite | Magnetite | Ilmenite | Leucoxene | Rutile | Pistacite | Chlorite | Pyrite | Indicolite | Hornblende | Ceylonite |
|---|---|---|---|---|---|---|---|---|---|---|---|---|---|---|---|
| *A1* | .420–.250 | 4 | 1 | | 4 | 10 | 2 | 1 | 3 | 2 | | | | 1 | |
| | .250–.125 | 15 | 14 | 1 | 37 | 25 | 7 | 10 | 7 | 37 | 7 | 3 | 3 | 4 | |
| | .125–.000 | 3 | 2 | | 3 | 2 | | | | 1 | | | | 1 | |
| *A2* | .420–.250 | 2 | 1 | | 1 | 2 | 1 | 1 | | | | | | | |
| | .250–.125 | 12 | 9 | 1 | 7 | 4 | | 5 | | 1 | 2 | 3 | 1 | | |
| | .125–.000 | 6 | 4 | | 1 | 1 | | | | 1 | | | 1 | | |
| *A3* | .420–.250 | 1 | | | | 2 | | | | | | | 1 | | |
| | .250–.125 | 1 | 3 | 1 | | 2 | | 3 | 1 | | | | 1 | | |
| *A4* | .420–.250 | 1 | 1 | | | | | | | | | | | | |
| | .250–.125 | 10 | 17 | 7 | 2 | 8 | 1 | 1 | 1 | | | | | | |
| *A5* | .420–.250 | | 1 | 1 | | 2 | | | | | | 2 | 1 | | |
| | .250–.125 | | 49 | 13 | 10 | 11 | 3 | 6 | 2 | | | 9 | 1 | 1 | |
| | .125–.000 | | 99 | 1 | 4 | 2 | | | | 1 | | 7 | | | |
| *A6* | .420–.250 | | 4 | | | 1 | | | | | | | | | |
| | .250–.125 | | 4 | 9 | | 6 | | | 1 | | | | | | |
| | .125–.000 | | | 2 | | 1 | | | | | | 1 | | | |
| *B1* | .250–.000 | 80 | 7 | 3 | 9 | 8 | | | 1 | | | 12 | | 3 | |
| *B2* | .250–.000 | 32 | 4 | 1 | 71 | 4 | 1 | 1 | 1 | | | 1 | | | 1 |

TABLE 2. INDIVIDUAL GRAIN PERCENTAGES

| Horizon | Size of grains in mm. | Almandite | Zircon | Schorlite | Staurolite | Magnetite | Ilmenite | Leucoxene | Rutile | Pistacite | Chlorite | Pyrite | Indicolite | Hornblende | Ceylonite |
|---|---|---|---|---|---|---|---|---|---|---|---|---|---|---|---|
| *A1* | .420–.250 | 14 | 4 | | 14 | 36 | 7 | 4 | 10 | 7 | | | | 4 | |
| | .250–.125 | 9 | 8 | 1 | 22 | 15 | 4 | 6 | 4 | 22 | 4 | 2 | 2 | 2 | |
| | .125–.000 | 25 | 17 | | 25 | 17 | | | | 8 | | | | 8 | |
| *A2* | .420–.250 | 25 | 13 | | 13 | 25 | 13 | 13 | | | | | | | |
| | .250–.125 | 27 | 20 | 2 | 15 | 9 | | 11 | | 2 | 4 | 7 | 2 | | |
| | .125–.000 | 43 | 28 | | 7 | 7 | | | | 7 | | | 7 | | |
| *A3* | .420–.250 | 25 | | | | 50 | | | | | | | 25 | | |
| | .250–.125 | 8 | 25 | 8 | | 17 | | 25 | 8 | | | | 8 | | |
| *A4* | .420–.250 | 50 | 50 | | | | | | | | | | | | |
| | .250–.125 | 21 | 36 | 15 | 4 | 17 | 2 | 2 | 2 | | | | | | |
| *A5* | .420–.250 | | 14 | 14 | | 29 | | | | | | 29 | 14 | | |
| | .250–.125 | | 48 | 12 | 9 | 10 | 3 | 6 | 2 | | | 8 | 1 | 1 | |
| | .125–.000 | | 87 | 1 | 4 | 2 | | | | 1 | | 6 | | | |
| *A6* | .420–.250 | | 80 | | | 20 | | | | | | | | | |
| | .250–.125 | | 20 | 45 | | 30 | | | 5 | | | | | | |
| | .125–.000 | | | 50 | | 25 | | | | | | 25 | | | |
| *B1* | .250–.000 | 65 | 6 | 2 | 7 | 6 | | | 1 | | | 10 | | 2 | |
| *B2* | .250–.000 | 27 | 3 | 1 | 61 | 3 | 1 | 1 | 1 | | | 1 | | | 1 |

sistance and color is due to abundant limonite. Garnet is still present, but otherwise it is similar to the St. Peter sandstone below. Like horizon *A3*, it probably represents a reworked deposit of Mohawkian seas.

*Horizon A5*. At a distance of twelve feet below the base of the McGregor member, pure, white, fairly well cemented sandstone is observed. Zircon is the predominant heavy mineral, garnet is absent. There is an anomaly in the presence of staurolite. This horizon, according to Thiel, represents the final stage of Chazyan time. No garnet is noted in the underlying Ordovician sandstone.

*Horizon A6*. Pure sandstone is definitely noted here, 35 feet below the contact between shale and limestone. It is massive and poorly cemented. There is a scarcity of heavy grains. Zircon, tourmaline, and magnetite predominate; no garnet was observed.

Compared to the heavy mineral assemblage of typical St. Peter sandstone, two analyses of Jordan sandstone are presented.

*Horizon B1*. At an elevation of approximately 685 feet above sea level, drill cuttings from the Carleton well, Northfield, Minnesota, show a typical Jordan sandstone; this is 15 feet below its contact with the Oneota dolomite. The heavy mineral content is principally garnet, with minor amounts of zircon, magnetite, and staurolite.

*Horizon B2.* Eighteen feet below the first sample, another was examined. It shows a good deal of garnet, but in addition, there is an amazing increase in amount of staurolite. The general percentages agree with the work of James F. Anderson, Carleton College, who in 1941 prepared, but did not publish, a petrographic log of the Owatonna, Minnesota, New City Water Well. However, it must be admitted that the staurolite count in the above work is much lower in both St. Peter and Jordan sandstones than this writer noted at Cannon Falls and Northfield. (Tables 1 and 2.)

## CONCLUSIONS

(1) The channel samples seemed to substantiate the aforementioned work of Thiel. Garnet, so typical of the Mohawkian deposition, is present only in the "transition zone," or upper few feet of the St. Peter; this zone is mineralogically more closely related to the overlying shale than to the underlying sandstone (Fig. 3).

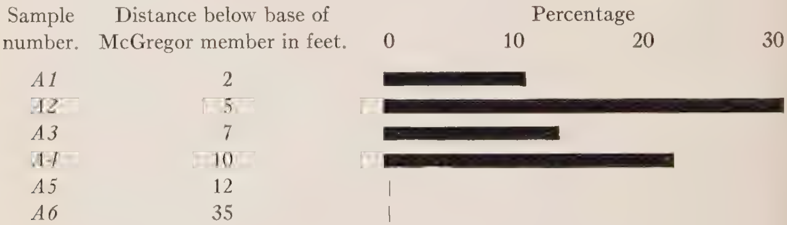

FIG. 3. Percentage distribution of garnet in channel, .420–.000 mm.

(2) The positive occurrence of large amounts of staurolite in the channeled material may be explained as local flooding. The source of the staurolite may have been in metamorphic rocks which were above sea level for some time, inasmuch as the Upper Cambrian Jordan sandstone exhibits it as well as the St. Peter and Glenwood beds, of Lower and Middle Ordovician respectively; more likely, the staurolite of Mohawkian age was derived from older strata which had been locally uplifted at this time.

(3) Ignoring local flood granules, widespread heavy minerals lend themselves to correlation of well-sorted clastic horizons.

## ACKNOWLEDGMENTS

The writer is indebted to Dr. Duncan Stewart of Carleton College, whose assistance made this paper possible, as well as to Dr. G. A. Thiel of the University of Minnesota, who suggested the topic.

## REFERENCES

1. LEVERETT, FRANK, AND SARDESON, F. W. (1919), Surface formations and agricultural conditions of the south half of Minnesota: *Minn. Geol. Surv., Bull.* **14,** 109.
2. STAUFFER, C. R., AND THIEL, G. A. (1941), Paleozoic, and related rocks of southeastern Minnesota: *Minn. Geol. Surv., Bull.* **29,** 70.

3. *Ibid.*, p. 66.
4. Thiel, G. A. (1935), Sedimentary and petrographic analysis of the St. Peter sandstone: *Geol. Soc. Am., Bull.* **46,** 612–613.
5. Thiel, G. A. (1937), Petrographic analysis of the Glenwood beds of southeastern Minnesota: *Geol. Soc. Am., Bull.* **48,** 120.

### Bibliography on Uranium in Colorado and Utah

The Geological Society of America published the following article in the June, 1954, issue of its Bulletin: "Bibliography and Index of Literature on Uranium and Thorium and Radioactive Occurrences in the United States. Part 3: Colorado and Utah," by Margaret Cooper of the Division of Raw Materials, U. S. Atomic Energy Commission. Since this 124-page bibliography may prove helpful to both geologists and laymen interested in uranium prospecting, the Society has prepared reprints for public sale at 50 cents per copy. Remittance must accompany orders, which should be sent to:

*The Geological Society of America*
*419 West 117 Street*
*New York 27, New York*

Dr. A. N. Winchell is preparing a third edition of his "Microscopic Characters of Inorganic Substances" and will welcome data on compounds not included in previous editions as well as more up-to-date data on compounds already listed. This book will cover data on inorganic solids other than natural minerals. Information on compounds of commercial nature will be included if possible, provided satisfactory evidence of exact composition is given. Any other suggestions should be forwarded to Dr. Winchell, 88 Vineyard Road, Hamden, Connecticut.

The Arizona Bureau of Mines has published Bulletin No. 163 of Mineral Technology Series No. 47, entitled "Minerals and Metals of Increasing Interest-Rare and Radioactive Minerals," by Richard T. Moore. Price 30 cents (free to residents of Arizona). Address University of Arizona, Tucson, Arizona.

A conference on silicosis and occupational chest diseases jointly sponsored by the McIntyre Research Foundation of Toronto, Canada, and the Saranac Laboratory of Saranac Lake, New York, has been arranged for Monday, Tuesday, and Wednesday, February 7, 8, and 9, 1955, in the Town Hall at Saranac Lake. The papers to be presented in the five full sessions will all report on original work conducted or sponsored by either the McIntyre Research Foundation or the Saranac Laboratory. In addition there will be papers presented by guest lecturers.

The business arrangements including reservations will be handled by Norman R. Sturgis, Jr., and the treasurer will be Clarence L. Wagner, both of the Trudeau-Saranac Institute staff. All communications concerning the conference should be addressed to Mr. Sturgis, Saranac Laboratory, Saranac Lake, New York.

Bulletin No. 164 of the Arizona Bureau of Mines—Mineral Technology Series No. 48, entitled "Exploration and Development of Small Mines," by H. E. Krumlauf, is now available. Price 25 cents (free to residents of Arizona). Address University of Arizona, Tucson, Arizona.

# BOOK REVIEWS

THE PHYSICAL CHEMISTRY OF THE SILICATES, by Wilhelm Eitel. The University of Chicago Press, Chicago, Illinois, 1954, xvii+1592 pages, $6\frac{3}{4}\times 9\frac{5}{8}$ inches. Price, $30.00.

William Eitel is eminently, perhaps uniquely, qualified to write on the physical chemistry of the silicates. He has had broader all-around experience in performing and directing silicate research, and in teaching and writing about silicate systems, technology, and theory than anyone else in the world.

The nucleus around which the present impressive volume grew, however, was formulated by another man, while Eitel was still much more concerned with studying books than with writing them. In 1915 H. E. Boeke had come to realize the great importance that physical chemical research was having, and would have, in interpretative petrology. In his classic work published that year, *Grundlagen der physikalisch-chemischen Petrographie*, he emphasized fundamental studies of silicate melts, transformation points, and other properties of silicates, and used the few silicate systems that had already been worked out as examples in his discussion of the groups of igneous rock-forming minerals.

In the early 1920's Eitel went to study with Boeke and was eventually given the responsibility of preparing a second edition of Boeke's book. In the meantime many more silicate systems had been worked out; and the second edition, Boeke-Eitel, 1923, although following the general outline of the first edition closely, reflects the new work in one important innovation: the 80-page treatment of igneous mineral groups in the first edition is reduced to 25 pages in the second, and a new section of more than 100 pages is devoted to artificial systems.

Eitel then made a trip to the United States, where he gained firsthand knowledge of the work of the Geophysical Laboratory and other American research centers in silicate chemistry. On his return to Germany he was charged with organizing and directing the Kaiser Wilhelm Institut für Silikatforschung, which was to do for silicate technology what the Geophysical Laboratory has done for experimental petrology.

It was at once apparent that the workers at the new institute needed a summary of the current status of silicate science. Eitel's 1923 revision of Boeke's book contained much useful information, but it was primarily a textbook and contained much extraneous material on techniques, mineral groups, and treatments of sedimentary and metamorphic rocks. The result of this need was the first edition (1929) of Eitel's *Physikalische Chemie der Silikate.* Although the purpose and emphasis of this book are different, the first five parts are, in subject matter, treatment, and order closely parallel to the *Grundlagen der physikalisch-chemischen Petrographie.* The last three parts of the latter, however, on weathering, sedimentation, and metamorphism, are replaced in Eitel's book by a new section on Die technische Silikatsysteme, in which glass, ceramics, and cement are discussed.

The second edition, 1941, removed most of the remaining textbook aspects—the chapters on elements of $x$-ray diffraction phenomena, mineralogical-optical methods, and the theoretical treatment of 1-, 2-, 3-, and 4-component systems. It became almost a straight reference work, and enough additional data were included to increase the size about 50% (from 552 to 826 pages).

The current encyclopedic treatise is in reality a third edition of the *Physikalische Chemie der Silikate.* It follows the outline of the German editions closely, but many new topics have been added and the size is almost twice that of the 1941 edition. For example, under Constitution of Melts and Glasses, discussions of the following topics have been added to the five previously treated: (*a*) Experimental Results of Structure Investigations on Silicate Glasses; (*b*) Freezing-in Reactions; (*c*) Glass Color and Glass Constitution; Fluorescence As an Indicator Method; and (*d*) The Surface Structure of Glass and Its Properties. Under Colloids a section on Electron Microscopy of Colloids has been added.

In addition to entirely new subjects, some of the old ones have been completely rearranged and rewritten. For example, a 6-page summary of Formation of Clay Minerals from Gel Mixtures in the 1941 edition has been replaced by a 90-page discussion of Clay-Water Systems.

The chapter on the thermochemistry of the silicates has been omitted from the new edition. This material was expanded and published as a separate volume in 1952 (Thermochemical Methods in Silicate Investigations, Rutgers University Press, 132 pages).

In spite of all the changes and additions, the original framework of Boeke's 1915 book is still much in evidence and many of the headings are translations of his topics.

The Physical Chemistry of the Silicates is far and away the most complete and up-to-date reference book on the subject. Emphasis has slipped away from mineralogy and petrology, but for treatment of principles, and especially summary of the results of laboratory work on silicates, no other book approaches it. Perhaps the best way to give an idea of its scope and content will be to list the primary and secondary headings and to indicate the number of pages devoted to each:

| | |
|---|---|
| *A*. The States of the Silicates | |
| I. The Crystalline State | 114 pp. |
| II. Fused and Glassy States | 230 pp. |
| III. Colloids | 210 pp. |
| *B*. Fusion and Polymorphic Equilibria in Dry Silicate Melts | |
| I. General Remarks on Fusion and Polymorphism Phenomena | 57 pp. |
| II. Special Silicate Systems | 214 pp. |
| *C*. Pneumatogenic and Hydatogenic Silicates | |
| I. Silicate systems with Volatile Components | 148 pp. |
| II. Silicate Hydrates of the Zeolite, Permutite Group | 61 pp. |
| *D*. Solid-State Reactions and their Ceramic Use | |
| I. Reactions in the Solid State | 51 pp. |
| II. Reactions in Ceramic Bodies | 70 pp. |
| III. Reactions in Hydraulic Cements | 105 pp. |
| *E*. Silicate Melts as Industrial Glasses and Slags | |
| I. Reactions in Glass Melting; Industrial Glasses, Enamels, and Glazes | 127 pp. |
| II. Industrial Slags | 31 pp. |

Even a volume of this size cannot record *all* of the experimental data now available about the silicates. But where a summary is incomplete, earlier summaries or bibliographies are listed in the copious footnotes; so the original references are easily available. For example, only 31 pages are devoted to hydrothermal syntheses; 4 to techniques and apparatus, and 27 to a summary of experimental work on 6 mineral groups. Reference is made to an earlier summary of all work on hydrothermal syntheses of silicates.

It is gratifying to see a comprehensive reference work like this with indexes that are accurate and adequate both in number and in type of entries. There are 6 separate indexes totaling 142 pages. References are to section and paragraph; in some instances it takes a little longer to find the page this way, but the paragraphs average much less than a page, so once the place is found it is easier to locate the topic than if it had been referred to by page number.

Literature references are handled in an interesting manner. Just preceding the index there is an alphabetical list of 714 "periodicals in silicate research" to each of which is assigned a key number. The titles of the journals are written out in full to avoid confusion.

References from the text are to footnotes giving key number, volume, year, and pages. The author's name is given in the text or footnote, as required.

The University of Chicago Press is to be heartily congratulated, not only on their breadth of vision in undertaking the publication of a work of this nature and its completion in commendable style, but also on the excellent cooperation evidently extended to the author. Much of the late literature is included in the text; and still more recent references, although it was not possible to incorporate tables, illustrations, or extensive summaries from them in the text, are at least given in footnotes. This makes the book about as complete and up-to-date as it is possible to have a comprehensive reference work on such a large field of science.

There is no need to recommend this book. It will be automatically required for reference wherever there is interest in silicates, silicate science, or silicate technology.

EARL INGERSON,
*U. S. Geological Survey, Washington 25, D. C.*

PETROGRAPHIE DES ROCHES SEDIMENTAIRES, by ALBERT CAROZZI (1953); with a preface by EDOUARD PAREJAS. F. Rouge and Cie S. A., Librairie de L'universite Lausanne, 257 pp., 27 figs. Suisse Fr. 23.40.

This volume is one of a science series published by the library of the University of Lausanne. The table of contents at the end of the book—there is no index—lists the following:

Part I: The minerals of sedimentary rocks
  Chapter 1. Detrital and authigenic minerals
Part II: The detrital rocks [including pyroclastics—GJN]
  Chapter 2. Conglomerates and breccias
  Chapter 3. Sandstones
  Chapter 4. Argillites
Part III: The bio-chemical rocks [biochemical and chemical sediments—GJN]
  Chapter 5. Carbonate rocks
  Chapter 6. Siliceous rocks
  Chapter 7. Ferruginous rocks
  Chapter 8. Phosphatic rocks
  Chapter 9. Saline rocks
  Chapter 10. Carbonaceous rocks

The major structure of the classification of sedimentary rocks used in this book is well indicated by the table of contents. The classification is broken down to include further gross details of composition, and the rocks are finally classed according to their mode of formation. The treatment is concerned primarily with the petrology of sediments, their petrography—in the American sense of the word—being limited to short descriptions sufficient to explain the subjects under discussion. Emphasis is placed on environment and mode of deposition and their general significance in terms of stratigraphy. Almost no quantitative aspect of sedimentary geology is included; for instance, not one histogram is to be found in the book.

In a relatively few pages, Carozzi has presented a well-balanced perspective statement of the content and meaning of sedimentary petrology. The book is very well written and provides easy and coherent reading. Bibliographies at the end of each chapter contain a choice assortment of literature on sediments. It is interesting to note that of 298 listings, including repetitions, 177 or 60 per cent of the references are in the English language; French is second in number. This book is to be recommended for its well-organized discussion and definition of sedimentary petrology in broad and meaningful context, uncluttered with digressions into detailed descriptions.

George J. Neuerburg,
*U. S. Geological Survey, North Hollywood, California**

DIE GRUNDLAGEN DER THEORIE DES MIKROSKOPS, by Kurt Michel (1950). Wissenschaftliche Verlagsgesellschaft M. B. H., Stuttgart, xi+314 pages, 160 figures, and 15 tables. DM 27.00.

This brief statement of the nature and contents of Michel's book on optical theory is offered as notice of a book of exceptional value and use to the petrographer, a book not likely in the ordinary course of affairs to come to his attention. This is not a critical review; such is best provided by the physicist: an unusually favorable review is to be found in *Jour. Roy. Micro. Soc.*, Ser. IV, vol. **71**, Pt. 1, pp. 148–149 (1951). I am simply impressed by a dissertation of unusual clarity, completeness, and authority, features generally lacking in the optical texts used by geologists.

The table of contents lists the following major headings:

Part I: The most important laws.
1. Propagation of light, its absorption, reflection, and refraction.
2. The basic laws of geometrical optics (including a comprehensive discussion of aberrations).†
3. The formation of images by lenses according to the wave nature of light.
4. The eye as an optical apparatus and as a receiver of light energy.
5. Other receivers of light energy (photochemistry, the photocell, and the photoelement).

Part II: The theory of optical instruments.
6. The geometrical optical theory (microscopical apparatuses, telescopes, and the camera).
7. The wave-optical theory of the microscope (containing much that has not been found outside of professional journals).
8. Appendix (containing 120 formulae, lists of illustrations and tables, references cited, and errata).

The style is short and lucid; the illustrations, many in color, are unusually clear and helpful. These in connection with the tables and formulae make the book usable even to those who read no German. The book neither illustrates nor describes any given manufactured optical instrument, and even excludes those made by Zeiss-Winkel, the firm with which Michel is associated. The simple, clear, and complete authoritative explanations of the bases of optics relative to microscopy comprise a dissertation such that the book will become, if it is not already, a foremost standard on the subject. It most certainly should be the principal reference used in preparation of any future texts on optical mineralogy, and it is a book that petrographers would do well to add to their working library.

George J. Neuerburg,
*U. S. Geological Survey, Pasadena, California*‡

ERZLAGERSTÄTTEN, by Hans Schneiderhöhn (1949). Kurzvorlesungen zur Einführung und zur Wiederholung, Piscator-Verlag, Stuttgart, xv+326 pages, 2 figures and 26 tables, 2nd edition. DM 14.00.

This book is an outgrowth of a two-semester lecture course on ore deposits, which are described in three sections according to their assignment to the magmatic, sedimentary, or metamorphic sequence (Abfolge). The table of contents is far too imposing for quotation here. Each of the three sections opens with a simplified statement of the ore-forming processes involved in the sequence and of the classification employed. In a few places, brief digressions on matters of genesis are offered. For the most part the book consists of short descriptions of types of ore deposits with fine-print remarks on principal examples of each type. Many of these descriptions are almost barren of usable information because of their brevity, although many odd gems of generally overlooked and interesting observations are to be found.

---

* Publication authorized by the Director, U. S. Geological Survey.

† Statements in parentheses added by reviewer.

‡ Publication authorized by the Director, U. S. Geological Survey.

The book is most notable for its lack of illustrations in treating a subject in which illustrations have become a principle mode of description. Not only are maps and sections lacking, but there is almost no mention of the structural aspect of economic geology. An atlas of illustrations for this book is promised in the foreword to the first edition. I noted no reference to this atlas in this second edition.

Literature citations are few in number, and most of them are to an earlier, more comprehensive text by Schneiderhöhn. Such a brief introduction as this book offers to the subject would be infinitely more useful with an extensive bibliography.

Technical criticism of the ideas expressed in such an elementary text as this can be of little value. Schneiderhöhn has presented in a remarkably succinct and highly readable fashion much observation of a general nature and his notions and opinions concerning the realm of economic geology. It should suffice to say that many, if not most of his ideas are not free of controversy and that to such controversy he rarely gives heed. Despite this single-minded approach and the highly generalized character of the book, Schneiderhöhn's lectures are interesting for the perspective view of the subject that they provide.

It is appropriate to expect the reader of this book to be fully aware that he peruses one man's prejudices, a man who, however, has a remarkable wealth of experience in this field.

George J. Neuerburg,
*U. S. Geological Survey, Pasadena, California**

---

* Publication authorized by the Director, U. S. Geological Survey.

# NEW MINERAL NAMES

## Rabbitite

M. E. Thompson, A. D. Weeks, and A. M. Sherwood, Rabbitite, a new uranyl carbonate from Utah U. S. Geol. Survey Trace Elements Investigation Report **405** (1954), as summarized by A. D. Weeks and M. E. Thompson. Identification and occurrence of uranium and vanadium minerals from the Colorado Plateaus: *U. S. Geol. Survey, Bull.* **1009-B** (1954).

Rabbitite occurs as fibrous or finely acicular microscopic crystals, elongated parallel to (001). Color pale greenish yellow, luster silky, fluorescence weak, G. approximately $2\frac{1}{2}$, soft. Monoclinic, cleavage (001); the strongest lines of the $x$-ray pattern in Å. are 8.1 S, 11.1 m, 4.37 m. Analysis by A. M. Sherwood gave CaO 10.6, MgO 9.2, $UO_3$ 37.4, $CO_2$ 17.8, $H_2O$ 24.5; total 99.5%, corresponding to $Ca_3Mg_3(UO_2)_2(CO_3)_6(OH)_4 \cdot 18\ H_2O$. It is biaxial, positive (?), with large 2V, $\alpha = 1.502 \pm 0.005$, $\beta = 1.508 \pm 0.005$, $\gamma = 1.525 \pm 0.003$, $Y = b$, $Z \wedge c = 15°$. Slowly soluble in water, effervesces with HCl. It occurs at the Lucky Strike No. 2 mine, San Rafael district, Utah, as an efflorescent coating on the mine wall, and is associated with gypsum, cobaltocalcite, bieberite, and uranium sulfates.

The name is for John C. Rabbitt, geologist, U. S. Geological Survey.

Michael Fleischer

## Unnamed New Black Uranium Mineral; Coffinite

A. D. Weeks and M. E. Thompson, *op cit.*, pp. 31–32.

The mineral is black, opaque, translucent in very thin fragments. Tetragonal, strongest lines of $x$-ray patterns, which is very similar to that of thorite, in Å, 3.48 S, 4.62 Ms, 2.64 m, 1.80 m. Analyses show as much as 61% U and varying amounts of Si, As, and V. It may be $USiO_4$ with OH substituting for Si, or it may be a hydrated oxide. No analysis of pure material is yet available. G. greater than 3.3. It has been found with uraninite, a new V oxide, carbonaceous material, and pyrite, impregnating sandstone and replacing wood, at 9 mines in Colorado, Utah, and New Mexico.

This mineral is referred to as "coffinite" by Rosenzweig, Gruner, and Gardiner, *Econ. Geol.*, **49,** 356 (1954).

M. F.

## Metatyuyamunite

A. D. Weeks and M. E. Thompson, *op. cit.*, pp. 37–38.

The name is for a lower hydrate of tyuyamunite with formula $Ca(UO_2)_2(V_2O_4)_2 \cdot 5-7\ H_2O$ (tyuyamunite has 7–$10\frac{1}{2}$ $H_2O$). Resembles tyuyamunite; properties variable with water content. G. = 3.81–3.93. Optically biaxial, neg., $\alpha = 1.67$ (calculated), $\beta = 1.835$, $\gamma = 1.865$, $2V = 44°$. The strongest lines of the $x$-ray pattern, in Å., are 8.4 S, 4.21 m, 3.24 m, 3.04 m.

M. F.

## Two Unnamed New Vanadium Oxides

A. D. Weeks and M. E. Thompson, *op cit.*, p. 54.

The first mineral is nearly black with bronze tint, opaque, adamantine luster, occurring in massive, fibrous, radial aggregates, in veinlets along grain of mineralized wood. One perfect cleavage. G. = 3.25. Strongest lines of $x$-ray powder pattern, in Å., 4.72 S, 2.47 S, 3.88 M, 3.17 m. No analysis of pure material yet available, probably a hydrated $V^3$, $V^4$ oxide. Occurs with new U mineral (above) and new V oxide (below) at La Sal No. 2 mine, Mesa County, Colorado, with clausthalite and pitchblende at Corvusite mine, Grand County, Utah, at the Mi Vida mine, San Juan County, Utah.

The second mineral is known only from the *x*-ray powder pattern and single crystal *x*-ray data on a few microscopic crystals. It is orthorhombic and the formula, according to *x*-ray data of H. T. Evans, is probably $V_2O_3 \cdot V_2O_4 \cdot H_2O$. The *x*-ray intensities are consistent with an atomic arrangement that contains elements of the montroseite structure and the rutile-type structure of $VO_2$.

M. F.

### Unnamed Sodium Analogue of Hewettite

A. D. Weeks and M. E. Thompson, *op cit.*, pp. 57–58.

Analysis by A. M. Sherwood gave $V_2O_5$ 77.17, $V_2O_4$ 1.56, $Na_2O$ 9.17, $K_2O$ 1.35, CaO 0.12, insol. in acid 0.31, $H_2O^-$ 1.83, $H_2O^+$ 7.86; total 99.37%, corresponding to $Na_2V_6O_{16} \cdot 3\,H_2O$. The mineral is monoclinic, bladed or acicular or botryoidal; color deep red, brownish red on exposure, luster adamantine to dull on exposure, fluorescence none. The strongest lines of the *x*-ray pattern, in Å., are 7.97 VS, 3.13 S, 2.27 S. Optically biaxial, neg., $\alpha = 1.797 \pm 0.003$, $\beta$ and $\gamma$ above 2.0, 2V medium, $Z = b$, pleochroic with X yellow, Y orange-yellow, Z orange-red. Occurs with steigerite coating a fracture in the roof of the Cactus Rat mine, Grand County, Utah.

M. F.

### Kahlerite

Heinz Meixner, Kahlerit, ein neues Mineral der Uranglimmergruppe, aus der Huttenberger Erzlagerstatte. *Der Karinthin*, **23**, 277–280 (1953).

In 1939, Meixner observed that "autunite" from Huttenberg, Austria, did not fluoresce under ultraviolet light. Qualitative tests at that time showed the presence of U, As, and $H_2O$ and the absence of P; the mineral was supposed to be troegerite. New microchemical tests show the presence of Fe, which is in accord with its occurrence associated with scorodite, symplesite, and pitticite on altered loellingite. The mineral is therefore probably the arsenate analogue of bassetite and its formula is probably $Fe(UO_2)_2(AsO_4)_2 \cdot nH_2O$ ($n = 8$?). It occurred as a rarity in tabular lemon-yellow crystals 2 mm. in size. Tetragonal with excellent basal cleavage, forms are *t* (111), *i* (021), *y* (012), *P* (011), and *n* (010). Optically negative, nearly uniaxial to biaxial, $\beta = 1.632 \pm .005$, $\gamma$ $1.634 \pm 0.005$, $2V = 9$ to 33°. The name is for Dr. F. Kahler, geologist of the Carinthian Landesmuseum, Klagenfurt.

M. F.

### Laueite

H. Strunz, Laueit, $MnFe_2^{III}(OH)_2(PO_4)_2 \cdot 8\,H_2O$, ein neues Mineral. *Naturwissenschaften*, **41**, 256 (1954).

Triclinic crystals up to 2 mm. occur on rockbridgeite at the Hagendorf pegmatite, eastern Bavaria. Space group $Ci^1 - P^1$. $a_0$ 5.28, $b_0$ 10.66, $c_0$ 7.14 Å., alpha 107°55′, beta 110°59′, gamma 71°07′, $Z = 1$. Cleavage perfect (010), very brittle. Color honey-brown, hardness 3, G. 2.44–2.49. Most common forms are *a* (100), *b* (010), *m* (110), *M* $(1\bar{1}0)$, *k* $(0\bar{1}1)$, and *f* (011). Analysis: $P_2O_5$ 26.47, CaO 0.23, MnO 11.06, FeO 1.34, MgO 0.52, $Fe_2O_3$ 27.54, $Al_2O_3$ 1.76, $H_2O$ 30.84%. Laueite is isotypic with gordonite (MgAl) and paravauxite (Fe″Al). No optical data are given.

The name is for Max von Laue.

M. F.

## REDEFINITION OF NAMES

### Riversideite, Tobermorite, Plombierite

J. D. C. McConnell, The hydrated calcium silicates riversideite, tobermorite, and plombierite. *Mineralog. Mag.*, **30**, 293–305 (1954).

Recent work by Claringbull and Hey (Abst. in *Am. Mineral.*, **39**, 407 (1954)) showed tobermorite (Heddle, 1880) to be a valid species, probably $CaSiO_3 \cdot H_2O$. Taylor (Abs. in *Am. Mineral.*, **39**, 405 (1954)) showed that crestmoreite and riversideite were mixtures of tobermorite and wilkeite. In a recent study of artificial preparations, H. F. W. Taylor, *J. Chem. Soc. London*, 163–171 (1953) showed that three distinct calcium silicate hydrates could be distinguished on the basis of their 002 spacings.

The data follow:

| *Compound* | *Approx. molar ratio* $H_2O:SiO_2$ | *002 spacing* | α | β | γ |
|---|---|---|---|---|---|
| *A* | 0.5 | 9.6 Å | 1.600 | 1.601 | 1.605 |
| *B* | 1.0 | 11.3 | 1.570 | 1.571 | 1.575 |
| *C* | 2.0 | 14.6 | — | 1.550 | — |

Examination of these compounds is made difficult by the ease of re-hydration of the lower hydrates. It is believed that this happened to Eakle's samples of riversideite, which now contain only small amounts of *A*, the 9.6 Å hydrate. It is suggested that the name riversideite be reserved for *A*, should this be found and preserved in the unhydrated state.

The name tobermorite is to be used for *B*, the 11.3 Å. hydrate. New *x*-ray, *D.T.A.*, and optical data are given for this mineral from Ballycraigy, Larne, Antrim County, Ireland. An analysis gives the formula $5CaO \cdot 6SiO_2 \cdot 5H_2O$, assuming that drying at 105° drives off water in excess of the 11.3 Å hydration stage.

*X*-ray data and a chemical analysis are given of gelatinous material from Ballycraigy that corresponds to *C*. The analysis is very close to that of plombierite (Daubrée, 1858), but Daubrée's material is not available for *x*-ray study. *C* is therefore provisionally named plombierite.

M. F.

## ERRATUM

Unfortunately the author's name (Kedesdy) was misspelled on the cover and also in connection with the title of the paper on page 750 of the September–October issue of the Journal.

# ave time and money with ON-THE-SPOT ANALYSES

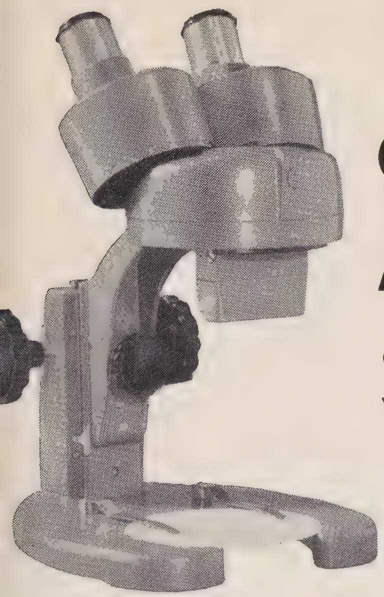

**Get complete data faster, *in the field,* with a Bausch & Lomb Stereomicroscope**

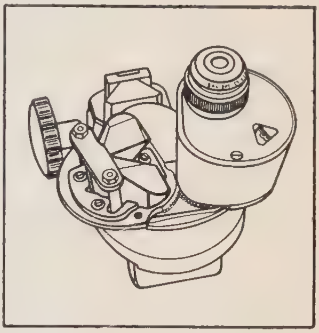

**SHOCKPROOF — for lifetime dependability**

Ready whenever you need it, because prisms *can't* jar loose despite rough rides in the field, despite the punishment of year-after-year practical use. Double support locks them into lifelong alignment . . . clamps at the top, gibs at the bottom.

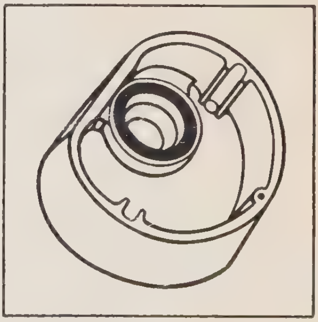

**DUSTPROOF — for bright, detailed views**

Even in dust-swept terrain you get "laboratory clean" images of samples. Patented Neoprene ring inside prism housing fits flush on prism surface, seals out dust . . . one of the reasons why B&L Stereomicroscopes are *dustproof for life!*

BAUSCH & LOMB
SINCE B&L 1853

**WRITE** for Catalog D-15 and demonstration. Bausch & Lomb Optical Company, 67635 St. Paul St., Rochester 2, New York.

**STEREOMICROSCOPES**

# OPTICAL "TOOLS"
## for Mineralogists

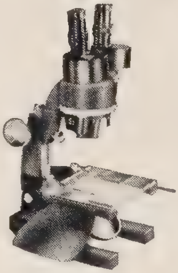

### AO STEREOSCOPIC MICROSCOPES

For examining surface characteristics of specimens large and small, nothing surpasses the life-like, three dimensional image and wide field of view provided by these instruments. Image is right side up unreversed. Many different models available, magnifications from 6.3X to 144X.

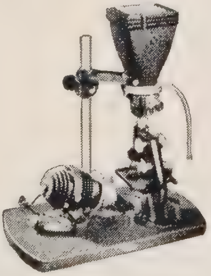

### AO PHOTOMICROGRAPHIC CAMERAS

The answer to the demand for a sturdy precise camera that is convenient and rapid to operate. Camera swings easily in and out of position over the microscope without disturbing settings. Provides quick changeover from 4″ x 5″ to 35mm film.

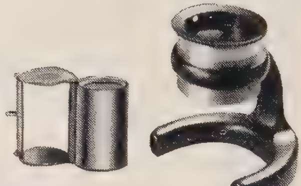

### AO MAGNIFIERS

For those who require the finest, AO magnifiers provide good working distance, and clear, undistorted images. Doublet and triplet pocket magnifiers, 6X to 15X, in plain or folding mounts. Large field 4.5X triplet in convenient horseshoe focusing mount.

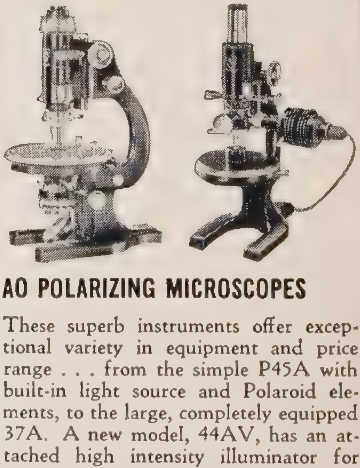

### AO POLARIZING MICROSCOPES

These superb instruments offer exceptional variety in equipment and price range . . . from the simple P45A with built-in light source and Polaroid elements, to the large, completely equipped 37A. A new model, 44AV, has an attached high intensity illuminator for studying polished opaque minerals.

Choose AO scientific instruments and *invest* in enduring quality, exceptional performance and readily available service. See your AO distributor or write Dept. L7.

American Optical
INSTRUMENT DIVISION
BUFFALO 15, NEW YORK

# LEITZ GEOLOGICAL MICROSCOPES

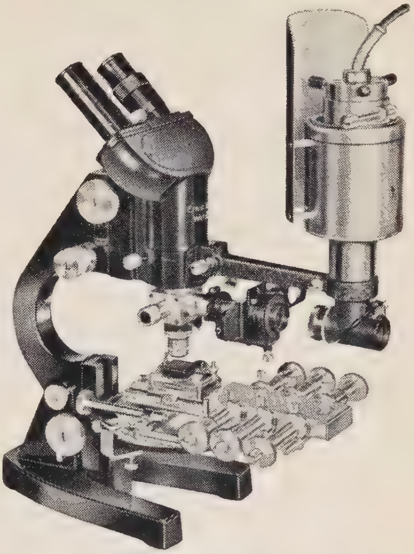

**Leitz Coal Petrography Microscope KPM**

*Functions of this versatile instrument include monocular examination by reflected polarized light, microscopical measuring and binocular observation in ordinary light. A special stage is provided for profile measurement. The KPM is adaptable to all photomicrographic cameras.*

**Leitz Ultropak Ore Dressing Microscope**

*Permits study with a combination of transmitted and reflected light on the same specimen. It is equipped with the Leitz Variocolor which varies the color of the transmitted background light for blending or contrasting. The Ultropak illuminator for incident light allows magnifications from the lowest to the highest powers.*

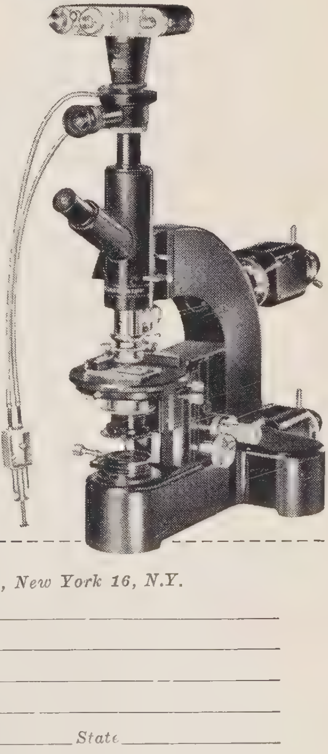

**E. LEITZ, INC.**

*Distributor of the world-famous products of Ernst Leitz, Wetzlar, Germany*

Leitz

**microscopes**
**binoculars**
**Leica cameras**
**lenses**

**E. Leitz, Inc.,** *Dept. AM, 468 Fourth Avenue, New York 16, N.Y.*

Please send me your brochure on the ____________________

*Name* ____________________

*Company* ____________________

*Street* ____________________

*City* ____________________ *State* ____________________

*New American*

**PEAT AND MARL SAMPLER**

The instrument embodies the essential features of a design by Professor Davis of the Geographical Survey. It consists of a jacketed plunger with a sharpened end. As the instrument is pressed into the ground, it remains closed. When the proper depth has been reached for taking the sample, the instrument is drawn up about 6 or 8 inches; at this point an internal locking device holds the plunger fast in the upper part of the jacket. This instrument is again forced downward, cutting and retaining the desired sample. Complete with illustrated head, 9 four foot lengths of extension rod and case; catalog number 76-432 sells for $75.00.

SCIENTIFIC INSTRUMENTS & APPARATUS

Eberbach CORPORATION

ANN ARBOR, MICH. ESTABLISHED 1843

---

W. HAROLD TOMLINSON

**Petrographic Laboratory**

260 N. ROLLING RD., SPRINGFIELD, PA.

ROCK SECTIONS ORIENTATED MINERAL SECTIONS

---

Minerals From All Over The World

*Most Complete Stock*

*Write for Catalogue*

ECKERT MINERAL RESEARCH

*110 East Main St., Florence, Colorado*

---

**PRACTICAL REFRACTOMETRY**

*By Means of the Microscope*

By Roy M. Allen, Sc.D.

A text on the Immersion Method of Microscopy. For elementary and advanced workers

(With listings of other products for mineralogists)

Price $1.00 (Discounts on six or more for student use)

Write for a copy on approval. To be sent on publication

Published by:

R. P. CARGILLE LABORATORIES, INC., 117 Liberty Street, New York 6, N.Y.

*McGraw-Hill presents . . . . . .*

## MINERALS IN WORLD INDUSTRY

By
WALTER H. VOSKUIL
University of Illinois
In press

A logical, interesting, up-to-date treatment by the man who is probably the top U. S. authority on the subject, with statistics and historical background skillfully employed in leading the student into appreciation of modern products and practices. The book covers the part played by minerals in economics productivity, the establishment and maintenance of a high standard of living, and the international political aspects of mineral resources. Discussion begins with the study of iron, as the core of the productive society based on minerals, then pursues the topic of fuels —coal, petroleum, natural gas, and "alternative fuels," describing the distinctive use of each metal and mineral in the productive economy and its relationship to iron as the basic material.

---

Other McGraw-Hill Books for Geologists

### MINERALOGY: An Introduction to the Study of Minerals and Crystals

By EDWARD H. KRAUS, WALTER F. HUNT, and L. S. RAMSDELL, University of Michigan. Fourth edition. 664 pages, $8.00

Here is a well-known college text used in geology departments and for reference by practicing geologists. It has always been popular for its extensive use of halftone cuts of crystal models to supplement the conventional line drawings of crystals which many students have difficulty in visualizing correctly. Photographs and short biographical sketches of distinguished mineralogists are another feature of this book.

### CLAY MINERALOGY

By RALPH E. GRIM, University of Illinois. "McGraw-Hill Series in Geology." 384 pages, $9.00

A distinguished text by a world authority based on the increased research activity of the past twenty-five years. The book presents all available data on the atomic structure, composition, physical characteristics, origin, and occurrence of clay minerals. It is carefully prepared, clearly presented, and well illustrated with drawings and tables of data.

### FIELD GEOLOGY Fifth Edition

By FREDERIC H. LAHEE, Sun Oil Company. 883 pages, $8.50

The subject of geology is treated from the field standpoint and is intended for use both as a text and manual. Full attention is given to all new developments in such areas as geophysics, well-logging, and air photography. The text's broad coverage and concise definitions make it a consistent leader in the field.

*Send for copies on approval*

**McGRAW-HILL BOOK COMPANY, INC.**

330 West 42nd Street New York 36, N.Y.

*Our Specialty is*
SELECTED MINERAL SPECIMENS
FROM WORLD-WIDE LOCALITIES FOR COLLECTORS AND MUSEUMS
we also carry a complete line of
MINERALIGHTS, DETECTRON GEIGER COUNTERS, ESTWING PROSPECTOR PICKS, MINERALOGICAL BOOKS, ETC.
*Send for free current bulletin*

SCHORTMANN'S MINERALS
**6 McKinley Avenue** **Easthampton, Massachusetts**

---

FILER'S
CRYSTALS CRYSTALLIZED MINERALS
ORE MINERALS RARE MINERALS

*Send for free catalog. University orders welcomed.*

**NOTE:** We are interested in purchasing or exchanging for crystals and uncommon minerals, especially from foreign sources. Correspondence is invited.

FILER'S
***1344 Highway 99, San Bernardino, California***

---

SYMPOSIUM ON QUARTZ OSCILLATOR-PLATES

This popular number of the *American Mineralogist* for May-June, 1945, has just been reprinted for the third time. Fourteen authoritative articles in 264 pages, illustrated.

*Price $3.00, postpaid*

Send orders to the Treasurer

**Dr. Earl Ingerson,**
**U. S. Geological Survey**
**Washington 25, D.C.**

---

FOR SALE
AMERICAN MINERALOGIST
Complete set (vols. 1-38) unbound
Also run of vols. 5-12, bound
Inquire: **Duncan McConnell,** Department of Mineralogy
The Ohio State University, Columbus, Ohio

# *NOTICE*

## CHANGE IN SUBSCRIPTION PRICE OF THE AMERICAN MINERALOGIST

***Effective with 1955 Subscriptions***

The price of the annual subscription to *The American Mineralogist,* Journal of the Mineralogical Society of America, beginning with Volume 40, 1955, will be $6.00 U. S. funds. This rate applies to subscriptions for *libraries, colleges, institutions, companies, and similar organizations.* The usual 10% discount will be continued for dealers and agents who remit the subscription payment WITH the order. No discount will be allowed when an invoice is requested. All orders, checks, and drafts are to be made payable in U. S. dollars to the Mineralogical Society of America, and sent to *Earl Ingerson, Treasurer, Mineralogical Society of America, c/o U. S. Geological Survey, Washington 25, D.C.* Please note that subscriptions are accepted for the calendar year (January-December) ONLY. For orders placed after the first of the year, back numbers to January are supplied.

Membership dues, $4 annually, and Fellowship dues, $5 annually, applicable to *individuals only,* remain unchanged except where a membership is maintained to provide the Journal for institutional use. In such cases, the new subscription rate will apply.

**MINERALOGICAL SOCIETY OF AMERICA**
**Earl Ingerson, Treasurer**
**U. S. Geological Survey, Washington 25, D.C.**

# AMERICAN MINERALOGIST
# BACK ISSUES

The following rates for back issues of the AMERICAN MINERALOGIST, Journal of the MINERALOGICAL SOCIETY OF AMERICA, are now in effect. These rates apply to both the regular edition and the microtext edition of out-of-print issues. Postage is charged unless otherwise indicated.

| Volume | Year | Volume Price | Single Issue Price (except special issues) |
|---|---|---|---|
| 1–9 | 1916-1924 | $3.00 | $ .50 |
| 10–19 | 1925-1934 | 4.00 | .50 |
| 20– | 1935- | 6.00 | .80 (monthly issue) |
| | | | 1.60 (bimonthly issue) |

Out of print issues in microtext edition

| Vol. | Year | Vol. | Year |
|---|---|---|---|
| 1-5 complete volume only | 1916-1920 | 29, nos. 1-4 | 1944 |
| 26, nos. 1, 2, 3, 6-8 | 1941 | 30, nos. 1-4 | 1945 |
| 27, nos. 1-9 | 1942 | 31, nos. 1-4 | 1946 |
| 28, nos. 1-8 | 1943 | 32, nos. 1-2 | 1947 |

## Special issues

| Volume | Number | Month | Year | Issue | Price |
|---|---|---|---|---|---|
| 10 | 9 | September | 1925 | Michigan | $1.00 |
| 10 | 11 | November | 1925 | Harvard | 1.00 |
| 12 | 4 | April | 1927 | Harvard | 1.00 |
| 13 | 7 | July | 1928 | Harvard | 1.00 |
| 15 | 8 | August | 1930 | Harvard | 1.00 |
| 17 | 7 | July | 1932 | Harvard | 1.00 |
| 22 | 5 | May | 1937 | Palache Volume | 3.00 |
| 23 | 11 | November | 1938 | Harvard | 1.50 |
| 30 | 5–6 | May-June | 1945 | Quartz Symposium | 3.00 postpaid |
| 35 | 9–10 | Sept.-Oct. | 1950 | Larsen Volume | 2.50 |
| 38 | 1–2 | Jan.-Feb. | 1953 | Hunt Volume | 2.00 |
| 38 | 11–12 | Nov.-Dec. | 1953 | Ross-Schaller Volume | 3.00 |

Index to Vols. 1-20, $2.00; $1.00 to members and subscribers; postpaid

Index to Vols. 21-30, $3.00; $2.00 to members and subscribers; postpaid

***Send all orders to***

**MINERALOGICAL SOCIETY OF AMERICA**
**Earl Ingerson, Treasurer**
**U. S. Geological Survey, Washington 25, D.C.**

# *Notice*

## MICROTEXT EDITION OF OUT OF PRINT ISSUES

All out of print issues of the American Mineralogist are now available in microtext edition as indicated below. The microtext is furnished on 3x5-inch cards, each card containing 48 pages of text material. A heading on each card in regular size type indicates the volume, number, pages, and date. All orders that include out of print issues will be filled with the microtext edition unless it is specifically stated that it is not desired. The cost of the microtext edition is the same as the cost of the regular issue. The following issues are available

| Volume | Number | Year |
|---|---|---|
| 1-5 | complete volume only | 1916-1920 |
| 26 | 1, 2, 3, 6-8 | 1941 |
| 27 | 1-9 | 1942 |
| 28 | 1-8 | 1943 |
| 29 | 1-4 | 1944 |
| 30 | 1-4 | 1945 |
| 31 | 1-4 | 1946 |
| 32 | 1-2 | 1947 |

Send all orders to

**MINERALOGICAL SOCIETY OF AMERICA**
**Earl Ingerson, Treasurer**
**U. S. Geological Survey**
**WASHINGTON 25, D.C.**

# HOW OLD ARE URANINITES?

Many answers to this important question have been revealed and confirmed by studies carried on at the Department of Physics, University of Toronto, Canada. (Collins, C. B., Farquhar, R. M., and Russell, R. D. "Isotopic constitution of radiogenic leads and the measurement of geologic time." *Geol. Soc. Am. Bull.*, vol. 65, no. 1, pp. 1-22, 1954.)

Of particular interest is age data given for several uraninites, pitchblendes, and an Ontario Fergusonite, specimens of which are currently available in Ward's stock.

1. Lake Athabasca, Saskatchewan (pitchblende): 1730 ± 100 my
2. Eldorado Mine, Great Bear Lake, Northwest Territories (pitchblende): 1400 ± 50 my
3. Wilberforce, Ontario (uraninite): 1030 my
4. Madawaska, Ontario (fergusonite): 960 ± 50 my
5. Ruggles Mine, near Grafton Center, New Hampshire (uraninite): 455 ± 160 my
6. Mitchell County, North Carolina (uraninite): 355 ± 40 my
   (my = million years)

### Special Offering of Radioactive Minerals

A suite of 8 specimens from the above 6 localities including species listed, plus secondary uranium minerals: $30.00.

## *Announcing*

WARD'S NEW GEOLOGY CATALOG—September 1954
Contents include the following:

Mineral and Rock Collections
Fossil Collections
Charts and Models
Crystallographic aids
Minerals, Rocks and Soils by weight
Color Slides
Field and Laboratory Equipment
Storage and Display Equipment
Lapidary (and Thin Section) Equipment
Instruments for Gemology
Petrographic Equipment
Fluorescence Equipment
Radiation Equipment

If you have not received this catalog, please write today on your university or business letterhead.

### OTHER CATALOGS AND PRICE LISTS:

FM 7 Mineral specimens, for research, study, private collections, museum display. One of a kind items, and suites. Nov. 1954.

Ward's Geology Newsletter. Contains items of current interest. Issued 5 x yearly.

Ward's Natural Science Bulletin. Issued 5 x per year, September through May . . . . $1.00

WARD'S *NATURAL SCIENCE ESTABLISHMENT, INC.*
3000 RIDGE ROAD EAST · ROCHESTER 9, N.Y.

GEORGE BANTA PUBLISHING COMPANY, MENASHA, WISCONSIN